Molecular cloning of Human T-cell leukaemia virus type I (HTLV-I) proteins and the role of HTLV-I infection in multiple drug resistance (MDR)

Thesis submitted for the degree of

Doctor of Philosophy

at the University of Leicester

By

Alan Lau BSc (Leeds)

Department of Microbiology and Immunology

University of Leicester

January 1997

UMI Number: U088010

UMI

Dissertation Publishing

ProQuest

Abstract

To facilitate the structural and functional analysis of Human T-cell leukaemia virus type-I (HTLV-I) a recombinant proviral expression system was to be employed in which viral protein expression is uncoupled from the inefficient process of infection. Several molecular genomic HTLV-I proviral clones were isolated and used to express viral proteins. However, none of these molecular HTLV-I proviral clones were found to be fully competent for virus expression and did not allow the further development of the expression system. HTLV-I is etiologically linked to a rapidly progressing T-cell malignancy known as adult T-cell leukaemia (ATL) and a degenerative neurological disorder called HTLV-I associated myelopathy/tropical spastic paraparesis (HAM/TSP). These diseases are noted for their poor response and high resistance to chemotherapy. Clinical drug resistance has been associated with the overexpression of the mdr-1 gene and its protein product P-glycoprotein (PGP). The presence of multiple drug resistant (MDR) cell phenotypes in peripheral blood mononuclear cells (PBMC) from HTLV-I infected patients was assessed and enhanced mdr-1 mRNA expression and PGP drug efflux activity was observed. MDR phenotypes were found in nine out of ten HTLV-I infected subjects tested. Development of MDR was independent of disease type or status with significant MDR activity being found in ATL, lymphoma type ATL, TSP/HAM and asymptomatic individuals. Furthermore the demonstration of stimulation and trans-activation of the mdr-1 gene suggests potential molecular mechanisms for the development of drug resistant cell phenotypes induced by HTLV-I infection.

Publications

Haddrick, M., Liu, ZH., **Lau, A.**, Heaphy, S., Cann, AJ. (1996). Production of non-infectious human immunodeficiency virus-like particles which package specifically viral RNA. *J. Virol. Meth.* **61**. 89-93.

Acknowledgements

Contents

CHAPTER 1. Introduction

CHAPTER 2. Materials and methods

Contents

CHAPTER 3.   The molecular cloning of HTLV-I and expression of recombinant HTLV-I proteins

Contents

Abbreviations

AA	Amino acid
ABC	ATP-binding cassette
AIDS	Acquired immune deficiency syndrome
amp	Ampicillin
AMV	Avian myeloblastosis virus
APS	Ammonium persulphate
ATF	Activating transcription factor
ATL	Adult T-cell leukaemia
ATP	Adenosine triphosphate
BSA	Bovine serum albumin
BPV	Bovine papilloma virus
cam	Chloramphenicol
cAMP	Cyclic adenosine monophosphate
CAT	Chloramphenicol acetyl transferase
CD	Cluster of differentiation
C/EBP	CAAT/enhancer binding protein
CIAP	Calf intestinal alkaline phosphatase
CMV	Cytomegalovirus
CNS	Central nervous system
CRE	cAMP responsive element
CREB	cAMP responsive element binding protein
G-CSF	Granulocyte-colony stimulating factor
CTP	Cytidine triphosphate
DEPC	Diethyl pyrocarbonate
DMSO	Dimethylsulphoxide
DNA	Deoxyribonucleic acid
ddNTP	Dideoxynucleotide

dNTP	Deoxynucleotide
DTT	Dithiotreitol
E. coli	*Escherichia coli*
ECL	Enhanced chemiluminescence
EDTA	Diaminoethanetetra-acetic acid
EGF	Epidermal growth factor
ELISA	Enzyme linked immunosorbent assay
EtBr	Ethidium Bromide
FACS	Fluorescence activated cell sorting
FCS	Foetal calf serum
FITC	Fluorescein isothiocyanate
GM-CSF	Granulocyte-macrophage-colony stimulating factor
GSH	Glutathione
GTP	Guanosine triphosphate
HAAP	HTLV-I associated arthropathy
HAU	HTLV-I associated uvetis
HFV	Human foamy virus
HIV	Human immunodeficiency virus
HLA	Human leukocyte antigen
HPV	Human papilloma virus
HTLV	Human T-cell leukaemia virus
HRPO	Horse-radish peroxidase
IAA	Isoamyl alcohol
IL	Interleukin
IPTG	Isopropylthio-β-D-galactoside
ISC	Internal standard control
IVDA	Intravenous drug abuser
kDa	Kilodalton
LDH	Lactate dehydrogenate

LFA	Lymphocyte function-associated antigen
LMP	Low melting point
LTR	Long terminal repeat
MAPK	Mitogen activated protein kinase
MDR	Multiple drug resistance
MHC	Major histocompatability complex
M-MLV	Moloney murine leukaemia virus
MOPS	3-[N-morpholino]propanesulfonic acid
MRP	Multidrug resistance-associated protein
Mw	Molecular weight
NCS	Newborn calf serum
OD	Optical density
orf	Open reading frame
PAGE	Polyacrylamide gel electrophoresis
PBL	Peripheral blood lymphocyte
PBMC	Peripheral blood mononuclear cell
PBS	Phosphate buffered saline
PCR	Polymerase chain reaction
PDGF	Platelet derived growth factor
PE	Phycoerythrin
PEG	Polyethylene-glycol
PGP	P-glycoprotein
PHA	phytohaemagglutinin
PI	Propidium iodide
PKC	Protein kinase C
PMSF	Phenyl methyl sulphonyl fluoride
R123	Rhodamine 123
RNA	Ribonucleic acid
RRE	rev responsive element

RSV	Rous sarcoma virus
RT	Reverse transcriptase
RT-PCR	Reverse transcriptase-polymerase chain reaction
R_XRE	rex responsive element
SDS	Sodium dodecyl sulphate
SSC	NaCl-Sodium citrate buffer
SV40	Simian virus 40
TAE	Tris-acetate-EDTA buffer
TBE	Tris-borate-EDTA buffer
TBS	Tris buffered saline
TCR	T-cell receptor
TE	Tris-EDTA buffer
TEMED	N,N,N',N'-Tetramethylethylenediamine
TEN	Tris-EDTA-NaCl buffer
TLC	Thin layer chromatography
TSP/HAM	Tropical spastic paraparesis/HTLV associated myleopathy
TTP	Thymidine triphosphate
UV	Ultraviolet
VLP	Virus-like particle
v/v	Volume by volume
w/v	Weight by volume
X-gal	5-bromo-4-chloro-3-indolyl-β-D-galactoside

List of figures

Chapter 4

List of tables

CHAPTER 1

Introduction

1.1 The family *retroviridae*

The family *retroviridae* are enveloped, single stranded "diploid" RNA viruses. They are called "retroviruses" because they uniquely reverse transcribe their RNA into a double stranded DNA, a process which opposes the "central dogma" or normal flow of genetic information from DNA to RNA to protein. Retroviral double stranded DNA becomes integrated into the host cells' chromosomes where it may remain dormant for many years or become expressed to produce more virus particles. Retrovirus particles (virions) are around 100 nm in diameter with an icosahedral nucleocapsid enveloped by a lipid bilayer derived from the host cell membrane. All retroviruses encode at least three genes; gag (nuclear core proteins), pol (reverse transcriptase/integrase/protease) and env (envelope proteins) (figure 1.1). The retroviral genomes are between 7 to 12 kb long and are flanked at both 5' and 3' ends by long terminal repeat (LTR) regions which confer enhancer/promoter and other regulatory functions (Coffin, 1990).

The first retrovirus to be identified was Rous sarcoma virus (RSV) in 1911 which caused sarcomas in chickens (Rous, 1911). Examination of the retroviruses discovered in animals showed clear associations between virus infection and cancer. These observations led to the development of the "proto-oncogene" hypothesis for cellular transformation. Subsequently several classes of proteins have been identified which are involved in retroviral oncogenesis such as tyrosine kinases (*src*) and G-proteins (*ras*). The search for human retroviruses led to the discovery in 1971 of Human foamy virus (HFV) which is non-transforming and non-pathogenic (Achong *et al.*, 1971). In the early 1980s the second human retrovirus was discovered, the Human T-cell leukaemia

1

virus type 1 (HTLV-I) and was etiologically linked to the T-cell malignancy adult T-cell leukaemia (Poiesz *et al.*, 1980; Yoshida *et al.*, 1982). HTLV-I was the first human retrovirus to be linked to disease and for a short time was known as adult T-cell leukaemia virus (ATLV) in Japan (Watanabe *et al.*, 1984). Study of HTLV-I also led to the discovery of the first retroviral regulatory protein, tax (Sodroski *et al.*, 1984) and the concept of "complex" or trans-activating retroviruses. However, over the last decade much attention has been focused at the human immunodeficiency virus (HIV) which was the third human retrovirus to be isolated (Barre-Sinoussi *et al.*, 1983; Popovic *et al.*, 1984), and is the etiologic agent of acquired immune deficiency syndrome (AIDS).

Figure 1.1. A schematic representation of the structure of a HTLV-I retrovirus particle. Mature HTLV-I particles consists of two strands of genomic RNA in addition to reverse transcriptase and integrase enzymes all surrounded in a central core of the structural gag proteins (p15, p24, p19). The nucleocapsid core is itself enveloped by a lipid bilayer derived from the host cell membrane. The viral envelope proteins (gp46, gp21) are embedded in the lipid bilayer and observed as projections on the surface of the retrovirus particle.
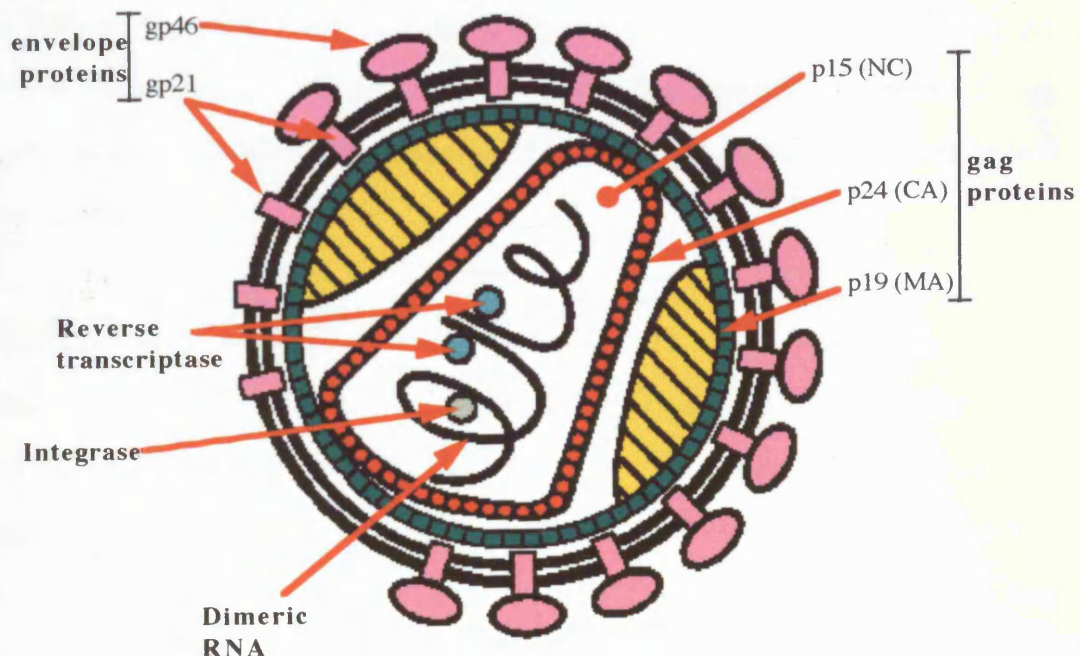
1.2 The human T-cell leukaemia viruses (HTLV)

Human T-cell leukaemia virus (HTLV) is a transforming retrovirus which belongs to the distinct HTLV-BLV group of *retroviridae*. Two variants of HTLV exist, HTLV types I and II, which although distinct from each other are serologically and genetically related. HTLV-I was first isolated from T-lymphoblastoid cell lines derived from patients with cutaneous T-cell lymphoma (Poiesz *et al.*, 1980) and adult T-cell leukaemia (Yoshida *et al.*, 1982). HTLV-II was isolated from T-cell lines derived from a patient with hairy T-cell leukaemia (Kalyanaraman *et al.*, 1982). At the nucleotide level HTLV-I and -II share around 70 % sequence homology (Shimotohno *et al.*, 1985). Clear etiological links for HTLV-I have been established, but evidence for an etiologic role of HTLV-II has been far less consistent although links to atypical hairy T-cell leukaemia have been suggested (Rosenblatt *et al.*, 1987). Disease induction by HTLV is thought to be due, in a large part, to the oncogenic potential of the viral protein tax which can activate a large number of cellular oncogenes and growth factors. Aberrant growth gene expression ultimately gives rise to malignant transformation of T-cells. One mathematical theoretical model applied to HTLV-I describes a "multistep theory of carcinogenesis" relating age to ATL. It demonstrates a model of age dependency by ATL which is the end result of cumulative somatic genetic mutations (Okamoto *et al.*, 1990).

HTLV-I is endemic Japan, the Caribbean, Central and south America, Africa and Melanesia. The number of HTLV-I infected individuals in these areas are estimated to be around 10 to 20 million (De Thé *et al.*, 1993). HTLV can also be found in the USA and Europe, but only usually in afro-Caribbean immigrants or high risk groups such as intravenous drug abusers (IVDAs). Also HTLV-II seems far more prevalent than HTLV-I in these areas (but not worldwide) and has a much higher incidence in IVDA populations (Manns *et al.*, 1991) with around 84 % of IVDA HTLV seropositives in the USA being due to HTLV-II infection (Khabbaz *et al.*, 1992). Epidemiological analysis of HTLV-I isolates has separated it into three major genetic types based upon nucleotide

sequence and geographical location. The major HTLV-I type is the "cosmopolitan" HTLV-I variant which demonstrates high nucleotide sequence conservation between isolates (around 98 %) but is located in geographically diverse regions such as the USA, West Africa, Japan and Europe (Gessain et al., 1992 and 1994). It is suggested that the cosmopolitan type may have originated from a single region, probably West Africa, and recently spread to the rest of the world through the slave trades (Gallo et al., 1983; Gessain et al., 1992). HTLV-I isolates clustered around equatorial Zaire and Gabon comprise the "Central African" type which differs from the cosmopolitan HTLV-I subtype by around only 3 % at the nucleotide sequence level (Fukasawa et al., 1987; Gessain et al., 1992). The third HTLV-I type is distinct from the previous two HTLV-I variants and differs by around 8 % at the nucleotide sequence level. It is known as the "Australo-Melanesian" variant and contains isolates found in remote populations from Melanesia and Papua New Guinea and in Aborigines from Australia (Bastian et al., 1993; Gessain et al., 1991 and 1993). It is thought that this variant diverged at a much earlier period than the split between cosmopolitan and Zaire types. HTLV-II is related but distinct from HTLV-I and HTLV-II isolates can be subgrouped into variants A and B (Hall et al., 1992). HTLV-II differs from HTLV-I by around 30 % at the nucleotide sequence level (Shimotohno et al., 1985).

HTLV-I is transmitted through direct cell to cell contact between infected cells and non-infected target cells with transmission of HTLV-I not being observed for cell free blood plasma (Inaba et al., 1989; Sandler et al., 1991). Transmission occurs through HTLV-I infected cells and is most commonly associated with the vertical transmission from mother to child, infected blood products, sexual intercourse and from contaminated needles (Blattner et al., 1989 and 1994; Manns et al., 1991). In endemic areas such as Japan the major route seems to be through mother to child transmission, accounting for around 25 to 30 % of all cases (Hino, 1990). Breast feeding was found to be the primary source of maternal transmission (Kinoshita et al., 1984; Takahashi et al., 1991) with a low incidence of in utero placental transmission (Katamine et al., 1994).

Transmission of HTLV-I occurs efficiently via contaminated blood products containing cells, with transmission rates as high as 60 % (Sato *et al.*, 1986; Inaba *et al.*, 1989; Sandler *et al.*, 1991). The efficiency of sexual transmission of HTLV-I is found to be low but occurs far more frequently from males to females (Miyamoto *et al.*, 1985; Murphy *et al.*, 1989a; Stuver *et al.*, 1993) with transmission rates of around 60 % compared to only 0.4 % from females to males over a ten year period (Take *et al.*, 1993). Preventative practices in high endemic areas have included avoidance of breast feeding in Japan (Ichimaru *et al.*, 1991) and the routine screening of blood products in Japan, parts of the West Indies, USA, Canada and France (Nishimura *et al.*, 1989; Sandler *et al.*, 1991; Couroucé *et al.*, 1993).

1.3 HTLV-I associated disease

HTLV-I is the etiologic agent of a rapidly progressing T-cell malignancy called adult T-cell leukaemia (ATL) (Blattner *et al.*, 1982; Hinuma *et al.*, 1982; Robert-Guroff *et al.*, 1982) and a neurological degenerative syndrome known as HTLV-I associated myelopathy or tropical spastic paraparesis (HAM/TSP) (Gessain *et al.*, 1985; Osame *et al.*, 1986; Roman *et al.*, 1988). HTLV-I is also implicated in a wide spectrum of other syndromes (Table 1.1) such as arthropathy (Ijichi *et al.*, 1990; Nishioka *et al.*, 1993), chronic respiratory disease (Kimura *et al.*, 1986; Sugimoto *et al.*, 1987), infectious dermatitis (Lagrenade *et al.*, 1990), lymphadenitis (Ohshima *et al.*, 1992), immunosuppression (Murai *et al.*, 1990), polymyositis (Morgan *et al.*, 1989) and uvetis (Mochizuki *et al.*, 1992). The estimated cumulative lifetime risk of developing a life threatening or dehabilitating disease as a consequence of HTLV-I infection is about 5 % and if all other syndromes associated with HTLV are included this figure rises to around 10 % (De Thé *et al.*, 1993). Infected individuals with no clinical manifestations are known as asymptomatic carriers and as disease develops in less than 10 % of all HTLV-I infected individuals the vast majority are asymptomatic carriers (Gotoh *et al.*, 1982).

Table 1.1. Diseases and clinical manifestations associated with HTLV-I infection.

Adult T-cell leukaemia (ATL)
    aggressive leukaemia of T-cells
    hypercalcaemia
    pulmonary infections
        leukaemic pulmonary infiltration's
        interstitial pneumonitis
        bronchial infection
    hepatosplenomegaly
    arthropathy
    dermal lesions
        infiltrative leukaemia
        Kaposi's sarcoma
    encephalopathy
    immunodeficiency

Tropical spastic paraparesis/HTLV-I associated myleopathy (TSP/HAM)
    neurological abnormalities
    demyelination

HTLV-I associated arthropathy (HAAP)
    hyperimmune responsivity to HTLV-I

HTLV-I associated uveitis (HAU)

Polymyositis

Eosinophilia

Infective dermatitis

1.3.1 Adult T-cell leukaemia (ATL)

Adult T-cell leukaemia (ATL) is an aggressive malignancy of mature predominantly CD4$^+$ T-lymphocytes and is one of the major diseases linked to HTLV-I infection. The first documented case of ATL was in 1974 and was characterised by chronic leukaemic cells of T-cell origin (Yodoi *et al.*, 1974). Evidence that HTLV-I is the causative agent of ATL is based upon findings that virtually all ATL patients have anti-HTLV-I serum antibodies (Hinuma *et al.*, 1981 and 1982; Blattner *et al.*, 1982; Robert-Guroff *et al.*, 1982), HTLV-I can be found monoclonally integrated in leukaemic cells derived from all ATL patients (Yoshida *et al.*, 1984) and that HTLV-I infected cells can transform other T-cells *in vitro* (Ishii *et al.*, 1978; Myoshi *et al.*, 1981).

In endemic areas such as Japan an estimated 1.2 million HTLV-I carriers are found annually and approximately 700 new cases of ATL are diagnosed each year with most being centred in the south western regions (Araki et al., 1988; Tajima et al., 1990). A similar rate of incidence of ATL was also found in Jamaica (Murphy et al., 1989b). The overall lifetime risk of a HTLV-I infected individual developing ATL was also estimated at around 1 to 5 % in these countries. Due to a long disease free period of several decades the mean age at development of ATL is around 57 years with large increases in incidence occurring after the age of 40 (Araki et al., 1988; Tajima et al., 1990). However, if ATL develops then the prognosis is extremely poor and less than 9 months median survival time is predicted (Kwano et al., 1985; Murphy et al., 1989b; Tajima et al., 1990).

Disease symptoms often include general malaise, fevers, abdominal fullness and pain, jaundice, thirst, drowsiness and constipation. Elevated calcium or hypercalcaemia is often associated with ATL and is consistent with symptoms of thirst and constipation. Physical signs often aid diagnosis and include swelling of the lymph nodes, skin lesions, jaundice and ascites. Leukaemic T-cell infiltrates into other tissues of the body are thought to be responsible for a large part of the disease manifestations seen in ATL. Leukaemic infiltrates in dermal and sub-cutaneous tissues cause the skin lesions often found in ATL patients. Infiltrates into the liver can cause general liver dysfunction such as hyperbilirubinemia, elevated serum alkaline phosphatase and transaminase levels. Lung or pulmonary abnormalities in ATL patients can also be attributed to invasive T-cells. Often leukaemic cells from ATL patients can also be characterised by the appearance of morphologically varied cells in peripheral blood smears. The presence of flower like or abnormally sized and shaped cells in peripheral blood lymphocytes (PBLs) from ATL patients are often seen. In addition to leukaemic T-cells ATL is often further complicated by the development of opportunistic infections and are reported to be the cause of death of around half of all ATL patient fatalities. Most commonly these infections are pneumonia's from bacterial, fungal (aspergillus) or viral

(cytomegalovirus) origins. Approximately 80 % of deaths caused by these infections is due to pneumonia (Kwano *et al.*, 1985). The high incidence of these infections can be explained by a mechanism of immunodeficiency in ATL patients (Murai *et al.*, 1990).

Treatment of ATL patients has traditionally consisted of combination chemotherapy but this approach has shown limited clinical improvement. Four generations of increasingly aggressive combination chemotherapies have shown an increase in remission rates rise from 11 to 21 % then to 41 % but a corresponding improvement in overall or disease free survival time was not observed (Shimoyama *et al.*, 1979, 1982, 1988 and 1992; Minato *et al.*, 1991). Traditional or old type chemotherapy was comprised of either of cyclophosphamide, vincristine, prednisolone (COP) and vincristine, cyclophosphamide, 6-mercaptopurine, prednisolone (VEMP) regimes. First generation combination chemotherapy regimes included vincristine, cyclophosphamide, prednisolone, adriamycin (VEPA), VEPA + methotrexate (VEPA-M) and cyclophosphamide, adriamycin, vincristine, prednisolone (CHOP). Second and third generations of combination chemotherapy usually consisted of alternating the different regimes and the use of methotrexate, adriamycin, cyclophosphamide, vincristine, prednisolone, bleomycin (MACOP-B) combinations. Several other novel treatments have similarly not shown clinical improvements and includes bone marrow transplantation (Asou *et al.*, 1985; Sobue *et al.*, 1987), total body irradiation (Timura *et al.*, 1983) and treatment with interferon β and γ (Timura *et al.*, 1987). Limited clinical improvements have been reported using Deoxycoformycin (DCF), an adenosine deaminase inhibitor (Dearden *et al.*, 1991), MST-16, a topoisomerase II inhibitor (Ohno *et al.*, 1993), and anti-Tac antibodies (Waldmann *et al.*, 1993). Improved remission rates have also been reported within a small study group using α-interferon and AZT in combination (Gill *et al.*, 1995; Hermine *et al.*, 1995). Generally, it can be noted that ATL is highly resistant to traditional chemotherapeutic strategies, of which none can confer significant clinical improvement. This observation may be suggestive

that ATL cells have innate drug resistance, a phenotype which could be a result of HTLV-I induced gene deregulation and transformation.

Upon the onset of disease ATL can be split into four clinical subtypes which reflect the various degrees of disease progression. These are known as smouldering, chronic, lymphoma and acute types of ATL (Shimoyama *et al.*, 1991; figure 1.2). Acute ATL seems to encompass the majority (55 %) of ATL patients and unfortunately also shows the greatest rates of mortality with mean survival times estimated at only 6.2 months. However, the overall prognosis for all ATL subtypes is poor. The median survival rate is only 9 months with survival rates of just 26.8 % at 2 years and 10.3 % at 4 years.

Figure 1.2. Clinical subtypes of ATL. The four clinical subtypes of ATL are shown relating the severity of disease with time. Smouldering and chronic types of ATL may eventually progress to the more severe lymphoma and acute types. (Modified from Yamaguchi *et al.*, 1993).
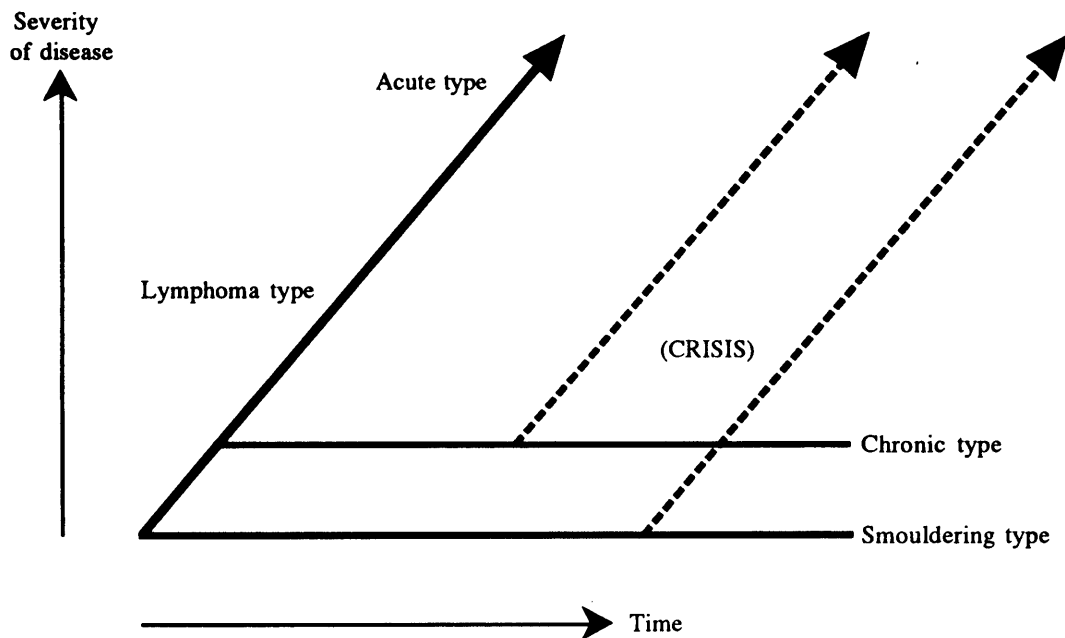
Smouldering ATL

Smouldering ATL is characterised by normal peripheral blood lymphocyte (PBL) levels (normal range: 1.5 to 3.5 x10^9 cells/L; Eastman, 1984) of which less than 5 % of lymphocytes are abnormal with only occasional flower like appearances. The serum lactate dehydrogenate levels (LDH) are <1.5 times the normal upper limit with no signs of hypercalcaemia, lymphadenopathy, ascites or pleural effusion. Occasional skin or lung tumour lesions may be present. Smouldering ATL represents around only 5 % of all ATL cases with a high survival rate of 77.7 % after 2 years, decreasing to 62.8 % after 4 years.

Chronic ATL

Here the PBL levels are greater than the normal upper range limit 3.5x10^9/L (normal range: 1.5 to 3.5 x10^9 cells/L), more than 5 % abnormal lymphocytes or proven tumour lesions with only occasional flower-like cells. Serum LDH levels are up to 2 times the upper normal limit with no signs of hypercalcaemia, no ascites or pleural effusion. Lymphadenopathy, hepatomegaly, spenomegaly and skin or lung tumours may be present. Chronic ATL comprises around 20 % of all ATL cases with a mean survival time of 24.3 months. Survival rates are relatively good at 52.4 % at 2 years, dropping to only 26.9 % after 4 years.

Lymphoma type ATL

This stage is generally characterised by lymph node enlargement, lymphadenopathy, shows no signs of leukaemic manifestations with normal PBL levels (1.5 to 3.5 x10^9 cells/L) and less than 1 % abnormal cells. Dysfunctions related to lung, lymph node, liver, spleen, central nervous system and bone may be observed. Patients also usually have elevated serum LDH and IL-2Rα levels. Renal dysfunctions are also observed in around 15 % of all lymphoma type cases. Lymphoma type ATL constitutes around 20 % all ATL cases. Mean survival time is poor at 10.2 months with survival rates at 21.3 % at 2 years and only 5.7 % after 4 years.

Acute ATL

Acute ATL types comprise the largest single group of ATL patients at around 55 % of all cases and is also known as the "prototypic" type of ATL. This group includes ATL patients with leukaemic manifestations and tumour lesions but do not fall into any of the other three ATL types. Typically, PBL levels, serum LDH and IL-2Rα are elevated and greater than 5 % of lymphocytes are abnormal. Liver and renal dysfunctions are observed in around 60 % and 30 % of all acute ATL cases respectively. The prognosis for acute ATL patients is very poor, the mean survival time being only 6.2 months. As a result survival rates are equally low at only 16.7 % at 2 years and 5.0 % at 4 years.

1.3.2 Tropical spastic paraparesis/HTLV associated myleopathy (TSP/HAM)

TSP/HAM is a slowly progressing neurological degenerative disorder which is characterised by paraparesis and spasticity of the lower extremities and is the second major disease linked to HTLV-I infections (Imamura *et al.*, 1988; Sarin *et al.*, 1989). A disease known as tropical spastic paraparesis (TSP) was first associated with the presence of HTLV-I in 1985 (Gessain *et al.*, 1985). Myleopathies associated with HTLV-I were independently demonstrated in 1986 (Osame *et al.*, 1986) and were known as HTLV associated myleopathies (HAM). Comparative studies in 1988 showed that TSP and HAM were identical and has been known since as TSP/HAM (Roman *et al.*, 1988).

The cumulative lifetime risk of a HTLV-I infected individual developing TSP/HAM is lower than for ATL at only around 0.25 % (Kaplan *et al.*, 1990). The mean age at disease onset is 43 (Osame *et al.* 1990). However, the period of latency between infection and onset of disease is much shorter than for ATL, being measured in months to years as opposed to decades. The involvement of HTLV-I in TSP/HAM patients has been demonstrated by the presence of HTLV-I antibodies in serum and cerebrospinal fluid (CSF), increased circulating abnormal and activated lymphocytes (Itoyama *et al.*, 1988a and 1988b; Jacobson *et al.*, 1988 and 1990) and the detection of HTLV-I

11

replication (Jacobson *et al.*, 1988). As with ATL, the presence of infiltrative HTLV activated lymphocytes can be seen as a major contributing factor for disease progression, by causing general nervous system damage. Magnetic resonance imaging demonstrated lesions in various regions of the brain (Tournier *et al.*, 1987) and autopsies have shown significant spinal cord abnormalities with lymphocytic infiltrates (Akizuki *et al.*, 1987) and non-specific cell type damage (Iwasaki *et al.*, 1993). Although the exact mechanisms of disease progression are unclear a number of suggestions have been put forward. It has been noted that HTLV-I may be able to directly infect the CNS and influence neurologic disease (Liberski *et al.*, 1988; Saida *et al.*, 1988; Kira *et al.*, 1992). Chronic inflammatory reactions have been demonstrated in the peripheral nerve roots in TSP suggesting a mechanism of disease elicited by an anti-HTLV-I auto-immune response (Sonada, 1990). The bystander tissue damage of the CNS by invading activated lymphocytes has also been suggested (Ijichi et al., 1993) which would result in general non-cell type specific CNS damage. Disease manifestations of TSP/HAM are profound spastic paraparesis of the lower limbs, bladder dysfunction, hyperreflexia, exaggerated jaw jerk, peripheral sensory loss and is also sometimes associated with a number of other neurologically related abnormalities (Brew *et al.*, 1988; Molgaard *et al.*, 1989).

1.3.3 Other HTLV-I associated diseases

HTLV-I associated arthropathy (HAAP)

HAAP is defined as an arthopathy that develops in HTLV-I infected individuals. It was considered to be a new disease entity in its own right in 1993 (Nishioka *et al.*, 1993) but can also be a clinical complication associated with TSP/HAM and sometimes ATL (Nishioka *et al.*, 1989; Sato *et al.*, 1991). Sufferers are commonly found in HTLV-I endemic areas. Observations that HTLV-I provirus is detectable (Kitajima *et al.*, 1991) and high levels of tax expression are observed in the joints and synovial fluids of HAAP patients (Nakajima *et al.*, 1993) are strongly suggestive of HTLV-I involvement. Suggestions for HAAP development include raised inflammatory cytokine or synovial

cell growth factor production by tax trans-activation or immunologic perturbation by autoimmunity to HTLV-I infection.

HTLV-I associated uvetis (HAU)

HAU is characterised by inflammatory lesions of the iris, ciliary body, choroid and adjacent tissues. HTLV uveitis was associated with certain types of uveitis by observations of HTLV-I proviral DNA in infiltrating cells of the eye and a high prevalence of HTLV-I antibodies in patient sera (Mochizuki *et al.*, 1992 and 1994). Due to the association of HTLV-I with certain types of uvetis HAU was proposed as a new clinical entity in 1992.

1.4 The molecular biology of HTLV

The complete proviral genomes of both HTLV-I and HTLV-II have been cloned and sequenced (Seiki *et al.*, 1983; Shimotohno *et al.*, 1985). The HTLV-I genome is similar to other retroviruses in that it has a 5'-*gag-pol-env*--3' gene orientation flanked by two long terminal repeat (LTR) regions (Seiki *et al.*, 1982 and 1983). In addition HTLV-I also encodes two other major non-structural regulatory proteins tax (p40^{tax}) and rex (p27^{rex}) encoded on two exons positioned at the 3' end of the genome (Black *et al*, 1990). The tax gene encodes a protein which is involved in the transcriptional regulation of viral gene expression via the LTRs. The rex gene is involved in mediating post-transcriptional processing and transport of the structural genes. The 3' region of HTLV encoding the tax and rex genes is traditionally known as the pX region. Initially this region had open reading frames (orf) of unknown function and was named the "X" region. This region contains four open reading frames (orf-I to -IV) which is now thought to encode several proteins in addition to tax and rex through alternative RNA splicing events. These putative proteins from the pX region have been designated p12^I, p13^{II}, p21^{rex}, rof and tof (or p30^{II}) but the exact roles and functions of these proteins

remain unclear (Furukawa *et al.*, 1991; Orita *et al.*, 1991; Ciminale *et al.*, 1992; Berneman *et al.*, 1992; Koralnik *et al.*, 1992).

Expression of the major HTLV-I genes occurs from three different mRNA transcripts derived from three exons; gag, pro and pol from full length genomic RNA, env and tax/rex from two spliced sub-genomic RNAs (figure 1.3). All HTLV mRNA transcripts start from the U3-R junction in the 5' LTR (nucleotide 352) and end at the R-U5 junction or polyadenylation site (nucleotide 8856) in the 3' LTR. An unspliced 8.5 kb mRNA transcript encodes the structural proteins gag, protease and polymerase. Unlike other groups of retroviruses the protease gene (pol) is not encoded within the same reading frame as either gag or pol but expressed by a ribosomal frameshift which skips the gag termination codon to give a gag/pro precursor. Similarly polymerase arises from a second ribosomal frameshifting event across the protease termination. Between gag, pro and pol three different reading frames are employed for their expression (Nam *et al.*, 1988 and 1993). A single splicing event from the 5' splice donor in the 5' LTR R region (exon 1; nucleotide 471) to the 3' a splice acceptor at the start of exon 2 (nucleotide 4993) generates a 4.2 kb subgenomic mRNA which encodes the envelope proteins.

A doubly spliced 2.1 kb mRNA transcript is generated from splicing between exon 1 and exon 2 (as above) then from a second 5' splice donor (190 nts from the start of exon 2; nucleotide 5183) to exon 3 (nucleotide 7302) in the 3' pX region. This doubly spliced transcript encodes both the tax and rex proteins but in alternative reading frames (orf IV and III respectively) which utilise different initiation codons in exon 2. The initiation codon for both tax and env proteins are shared (but on different mRNA transcripts) whilst the rex initiation codon is located 56 nucleotides further upstream. The tax initiation codon forms part of a consensus kozak translation initiation sequence which enhances the translation efficiency from that codon (Kozak, 1987). The result is preferential expression of the tax protein from the tax/rex mRNA transcript.

14

Figure 1.3. Organisation of the HTLV-I proviral genome, mRNA species and encoded proteins. The HTLV-I DNA provirus is 9032 bp in length. Expression of HTLV-I yields three major mRNA species encoding gag/pro/pol, envelope and tax/rex proteins. At least five minor mRNA species derived from alternative RNA splicing in the pX region encode putative proteins designated p12^I, p13^{II} (orf-2), p21^{rex}, rof and tof (p30^{II}). All numbering starts at base 1 of the 5' LTR and is based on the HTLV$_{ATK-1}$ provirus nucleotide DNA sequence (Seiki *et al.*, 1983).

15
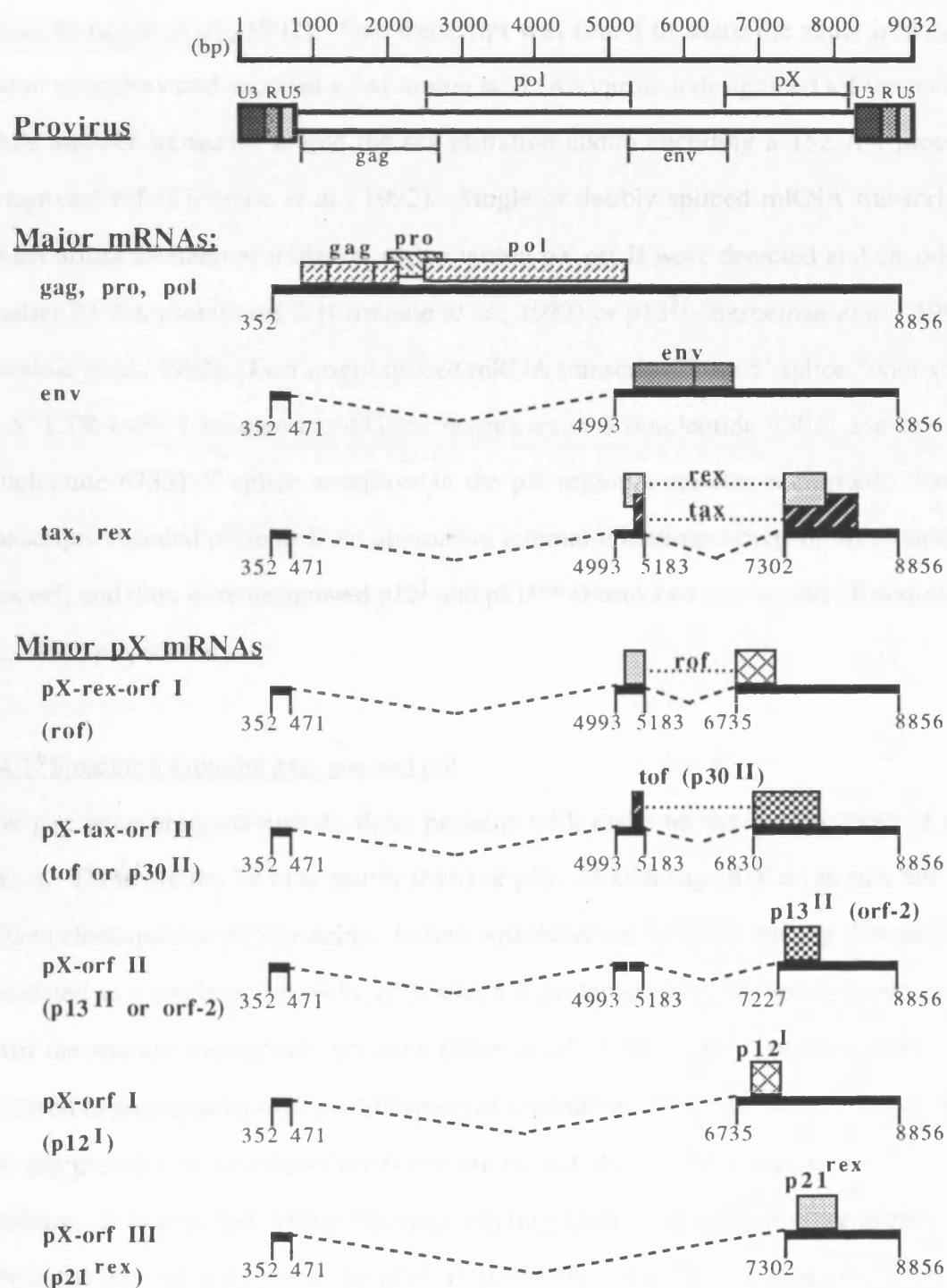
Three other doubly spliced mRNA transcripts were found to be expressed from the pX region of a molecular clone and in HTLV-I infected cells by alternative splicing from the spliced tax/rex exon 2 (nucleotide 5183) to three alternative 3' splice acceptor sites in the pX region upstream of the normal tax/rex splice acceptor of exon 3 (Ciminale *et al.*, 1992; Koralnik *et al.*, 1992). One transcript was found to share the same initiation codon as tax/env and encoded a 241 amino acid (AA) protein designated tof (or p30^{II}) while another transcript shared the rex initiation codon encoding a 152 AA protein designated rof (Ciminale *et al.*, 1992). Single or doubly spliced mRNA transcripts which utilise an internal initiation codon within pX orf II were detected and encode a smaller 87 AA protein orf-2 (Ciminale *et al.*, 1992) or p13^{II} (Berneman *et al.*, 1992; Koralnik *et al.*, 1992). Two singly spliced mRNA transcripts from 5' splice donor sites of 5' LTR exon 1 (nucleotide 471) to tax/rex exon 3 (nucleotide 7302) and the rof (nucleotide 6735) 3' splice acceptors in the pX region were also identified. These transcripts encoded proteins from alternative internal initiation codons of orfs I and III (rex orf) and thus were designated p12^{I} and p21^{rex} (Furukawa *et al.*, 1991; Koralnik *et al.*, 1992) respectively.

1.4.1 Structural proteins gag, pro and pol

The gag gene products encode three proteins with make up the nuclear core of the virion. These are the 19 kDa matrix (MA) or p19, 24 kDa capsid (CA) or p24 and 15 kDa nucleocapsid or p15 proteins. In line with other retroviruses the gag proteins are translated as a single polyprotein, p53, which is proteolytically cleaved by protease to form the mature constituent proteins (Nam *et al.*, 1988). The protease protein is involved in post-translational modifications of several viral proteins, namely cleavage of the gag proteins to their functional derivatives and also self-cleavage to give mature protease. It is encoded within the same reading frame as gag and is translated via ribosomal frameshifting event (Le *et al*, 1991; Coffin, 1990) from a 'slippery' sequence in the 3' end of gag. The pol gene encodes the polymerase protein, which in turn has a variety of functional regions involved in viral replication. The N terminal most region is

thought to contain reverse transcriptase activity while the intregrase and RNase H functions are found further C terminal. Several molecules of both protease and polymerase proteins are packaged within infectious virions.

1.4.2 Structural envelope glycoproteins

HTLV envelope glycoproteins proteins are encoded on the singly spliced sub-genomic mRNA. The env gene product initially gives rise to a 68 kDa precursor protein. As with other retroviruses the precursor is then proteolytically cleaved and glycosylated in the golgi apparatus by cellular enzymes to give mature proteins of 46 kDa and 21 kDa. These glycoproteins are known as gp46 and gp21 respectively; gp46 is the surface glycoprotein (SU) and gp21 is the transmembrane glycoprotein (TM). Unlike other retroviruses, HTLV-I encodes relatively short envelope proteins which show high degrees of amino acid sequence conservation between different isolates (Daenke et al, 1990; Seiki et al, 1983). This observation seems remarkable in that viral envelope proteins are believed to be under great selective pressure in order to escape host defence systems and thus thought subject to rapid mutation rates. However, mutations generated along the HTLV-I env gene are not readily tolerated as in other retroviruses and the result is a non-functional protein. These observations suggest a high degree of host adaptation and low virus turnover (Pique et al, 1990). The transmembrane glycoprotein gp21 is responsible for anchoring the envelope complex and also in mediating the fusion process between viral and target cell membrane. The surface glycoprotein gp46 is involved in recognition and attachment to an as yet unidentified target cell receptor. However, the cellular receptor has been mapped to human chromosome 17 (Somerfelt et al., 1988; Fan et al., 1992) and a study using an anti-HTLV monoclonal antibody have indicated several candidate proteins of 31, 45, 55 and 70 kDa (Gavalchin et al., 1993). It was also suggested that gp46 is a T-cell mitogen and that this cellular activation activity may be involved in the early stages of productive infection and contributes toward HTLV-I cell transformation (Merl et al., 1984; Duc Dodon et al., 1987; Gazzolo et al., 1987), possibly via the CD2 T cell signalling

pathway (Kimata *et al.*, 1991). However recent reports have contradicted these early findings, maintaining that gp46 is not itself mitogenic but that the mitogenic activity observed for HTLV is restricted to infected T-cells and conferred by other surface bound viral antigen(s) or by virally induced modification of cell receptor pathways (Wucherpfennig *et al.*, 1992; Kimata *et al.*, 1993 and 1994a).

1.4.3 Regulation proteins tax and rex

The regulatory proteins tax and rex are critical for HTLV replication and are also responsible for the complex interactions between HTLV and the host cell. In common with other "complex" retroviruses the expression of tax and rex regulatory proteins gives HTLV a two step or "biphasic" life-cycle (figure 1.4).

The early phase sees the low-level basal transcription of all viral RNAs, but only the fully spliced *tax*/rex mRNA is efficiently exported to the cytoplasm for translation and no structural proteins are produced. As both tax and rex proteins accumulate to sufficient levels the "late" phase is initiated. Here the tax protein enhances overall viral RNA production by activating in trans the expression from the HTLV promoter/enhancer elements within the 5' LTR. Rex then alters the distribution of the viral RNAs in the nucleus and cytoplasm, allowing significant levels of cytoplasmic gag/pol and env transcripts to accumulate and be translated. The "late" phase than sees the expression of the viral structural proteins and ultimately virion production.

Figure 1.4. A schematic representation of the HTLV-I life cycle. The major events in the HTLV-I life cycle are numbered in step-wise order from 1 to 5. 1) HTLV-I infection and chromosomal integration. 2) Basal viral gene transcription occurs but only fully spliced tax/rex mRNAs are efficiently exported to the cytoplasm. 3) The "Early" expression phase is initiated with regulatory tax and rex proteins becoming expressed. 4a) Tax enhances the transcription from the viral LTR and cellular gene promoters. 4b) Rex alters the subcellular distribution of viral RNAs allowing $R_X RE$ containing RNAs to accumulate in the cytoplasm. 5) Upregulation of viral structural gene expression initiates the "late" expression phase where gag, protease, polymerase and envelope proteins become expressed.
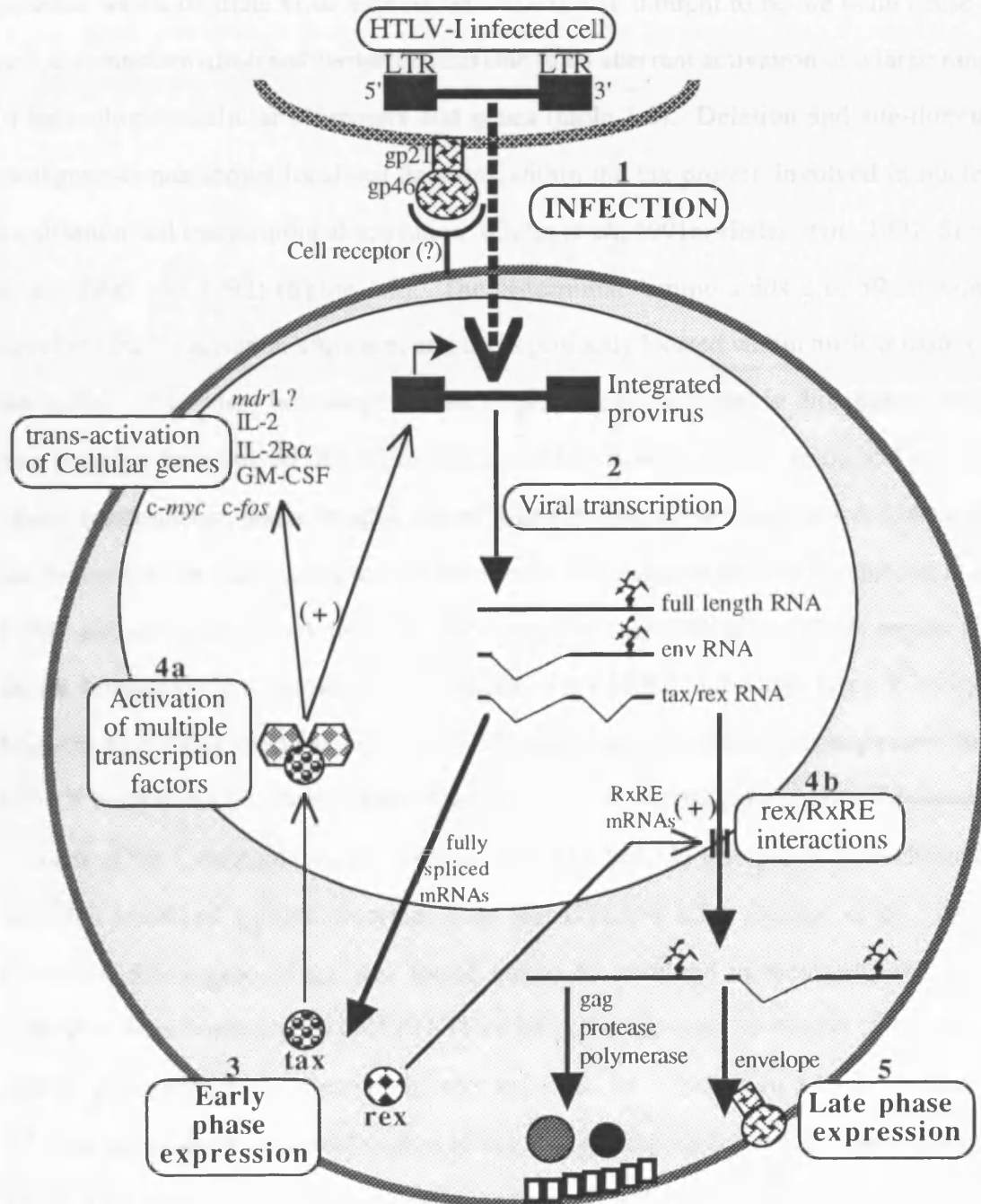
tax

The trans-activator protein tax is a 40 kDa (353 AA) nuclear protein and is encoded on the doubly spliced sub-genomic mRNA from the pX region of HTLV. It is a positive trans-activator of both viral and cellular transcription and its discovery in 1984 led to observations that HTLV-I, in common with all known human retroviruses, encode proteins which regulate virus expression. Tax is also thought to be the main cause of cellular transformation and tumorigenesis due to its aberrant activation of a large range of heterologous cellular promoters and genes (table 1.2). Deletion and site-directed mutagenesis has shown localised domains within the tax protein involved in nuclear localisation and transcriptional activation (Gitlin *et al.*, 1991a; Heder *et al.*, 1991; Smith *et al.*, 1990 and 1992) (figure 1.5). The N-terminal amino acids 2 to 59 contain a novel nuclear localisation sequence, and tax is primarily located within nuclear matrix of the nuclei. Also some homology to zinc finger motifs are found in this region, which may possibly be involved in protein binding or tax dimerisation. The middle of tax is mostly hydrophobic, and a "leucine zipper" like element can be found at AA 124 to 146. Such elements are common to several families of transcription factors (Landshultz *et al.*, 1988) and also may be involved in mediating tax trans-activation. This region also shares homology to adenovirus E1a domain, HPV16 E7 and SV40 large T-antigen. Mutants within this region at AAs 137 to 138 seems to abolish tax trans-activation from NF-κB responsive promoters and suggest a possible activation domain. Mutational analysis of the C-terminal region between AAs 285 and 330 also provided evidence for domains involved trans-activation from the HTLV-I LTR (Heder *et al.*, 1991). However, this region of tax was found not to be involved in mediating the trans-activation from heterologous CREB/ATF or NF-κB responsive promoters (Smith *et al.*, 1990). Activation from these promoters seems to be impaired in a large number of mutants not in the C-terminal region of tax, suggesting multiple functional domains and/or a very strict protein structure (Fujisawa *et al.*, 1991; Fujii *et al.*, 1992; Conner *et al.*, 1993; Tsuchiya *et al.*, 1994). The mechanism of tax transactivation seems to be indirect, interacting with and activating cellular transcription factors rather than by

binding DNA to enhance transcription directly. Such transcription factors include the cAMP-responsive element binding protein/activating transcription factor (CREB/ATF), NF-κB and serum response factor (SRF) families (see section 1.5.2). Thus a whole host of cellular genes become activated upon tax expression and this is thought to be the basis for HTLV-I cellular transformation and pathogenesis.

Figure 1.5. Structure and functional domains of the HTLV-I tax protein. The tax protein is a 353 amino acid, 40 kDa nuclear protein involved in the trans-activation of viral and cellular gene promoters by modulating the activities of normal cellular transcription factors.
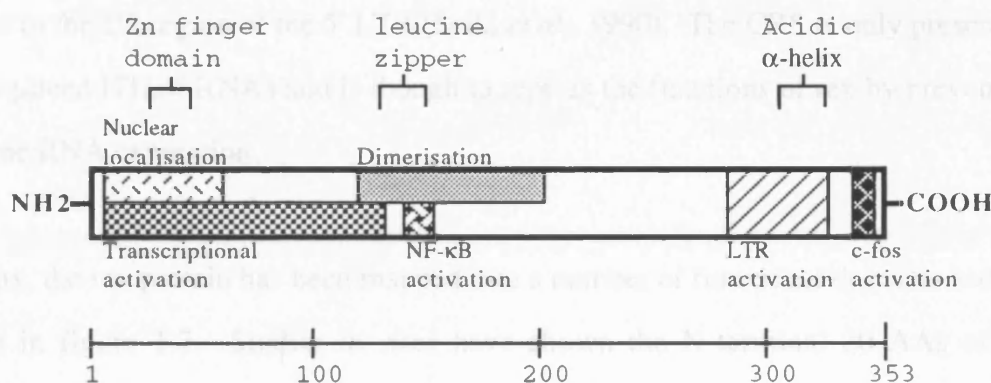
rex

Rex is the second non-structural phospho-protein involved in the regulation of HTLV-I expression. It is a 27 kDa protein encoded on the same doubly spliced mRNA as tax, but utilises a different initiation codon 59 nucleotides upstream. The presence of rex is absolutely required for viral replication and is implicated in post-transcriptional regulation and expression of HTLV gag/pol and env structural mRNAs. This regulatory activity of rex and of similar proteins in other retroviruses is the definitive characteristic the for "complex" retroviruses (Cullen, 1991). Studies have shown that rex is a positive regulator of expression for HTLV unspliced or singly spliced structural mRNAs but a negative regulator for HTLV transcription at high concentrations (Hidaka *et al.*, 1988). Rex seems to function by modulating the proportion of all three HTLV mRNA species between the nucleus and cytoplasm of the cell. It is thought to act as a

mediator of HTLV structural mRNA transport out of the nucleus, increasing the ratio of intron containing gag/pol and env transcripts whilst decreasing fully spliced tax/rex mRNAs in the cytoplasm (Inoue *et al.*, 1991). Rex specifically targets HTLV mRNAs for transport by recognising and directly interacting with a specific RNA stem-loop structural motif present in the 3' LTR of HTLV-I (Hanly *et al.*, 1989) and in both 5' and 3' LTRs of HTLV-II (Bar-Shira *et al.*, 1991; Kim *et al.*, 1991). These *cis*-acting RNA stem-loop motifs are known as rex responsive elements or R_XREs (figure 1.6). Another regulatory element known as the "cis-acting repressive sequence" or CRS is present in the U5 region of the 5' LTR (Seiki *et al.*, 1990). The CRS is only present on the unspliced HTLV RNAs and is though to repress the functions of rex by preventing genomic RNA expression.

Like tax, the rex protein has been mapped into a number of functional domains and are shown in figure 1.7. Studies *in vitro* have shown the N-terminal 20 AAs of rex contains a nuclear localisation signal and an arginine rich R_XRE binding domain (Nosaka *et al.*, 1989; Grassmann *et al.*, 1991; Hammes *et al.*, 1993). The RxRE binding site seems to recognise and bind a small 20 nucleotide (10 bp) sequence found in a region of double stranded RNA within the R_XRE motif (Bogerd *et al.*, 1991). A number of activation domains have also been proposed for rex between AAs 22 to 32 and 79 to 99 (Weichselbraun *et al.*, 1992). Within the activation domain a leucine motif was identified between AAs 82 to 93 and has been suggested to be a nuclear export signal (Malim *et al.*, 1991; Bogerd *et al.*, 1995) (figure 1.6).

The 3' R_XRE is also seems important for efficient polyadenylation of HTLV-I transcripts and is independent of the rex protein. The 255 nucleotide R_XRE is present between the polyadenylation signal sequence and polyadenylation site and brings both these elements in close proximity to allow polyadenylation to proceed (figure 1.6; Ahmed *et al.*, 1991).

Figure 1.6. The predicted RNA stem loop structure of the HTLV-I rex responsive element (R_XRE). The R_XRE is composed of 255 nucleotides spanning the U3-R junction of the HTLV-I 3' LTR. It is present at the 3' end of HTLV-I mRNAs and in association with the rex protein mediates viral mRNA export from the nucleus. The presence of the R_XRE motif also allows efficient processing of viral RNAs as it brings the polyadenylation signal sequence and polyadenylation site into close proximity for RNA polyadenylation.
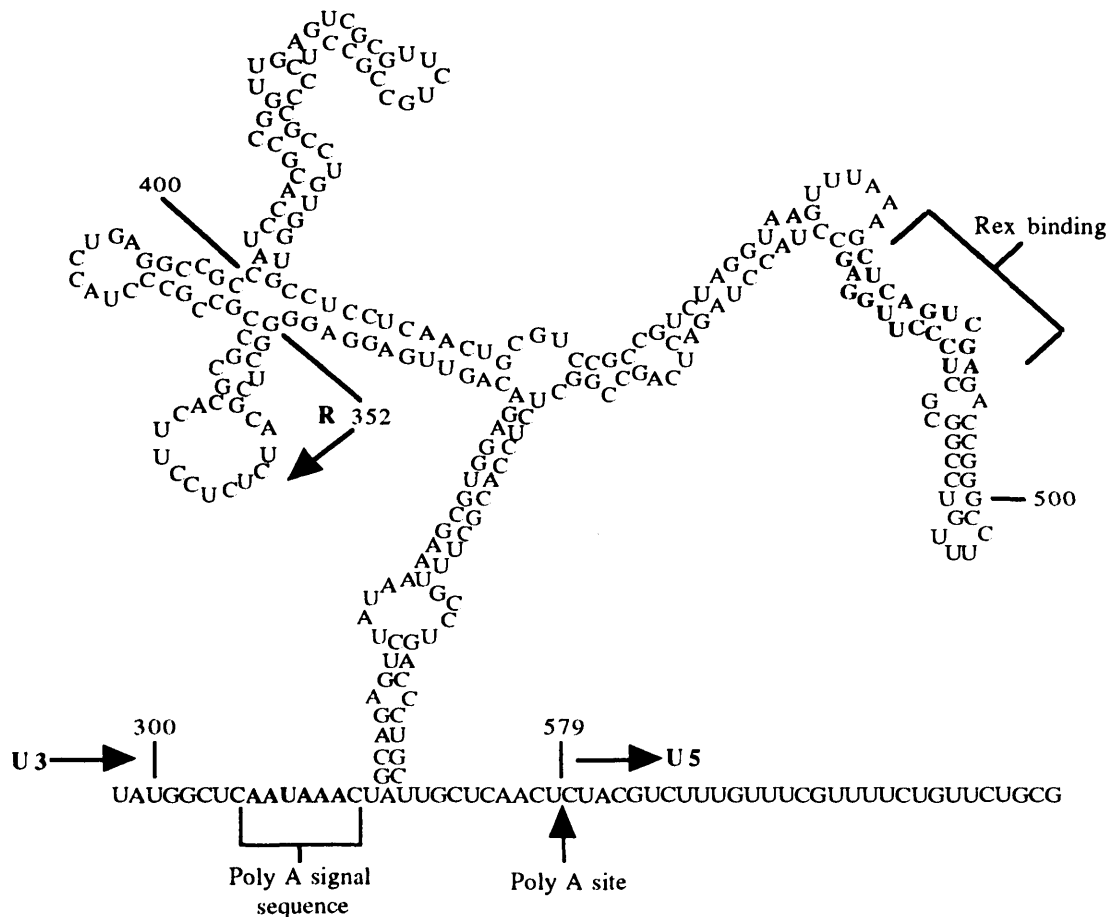
Much is known of the effects of rex but the mechanisms by which rex acts upon viral mRNAs still remain unclear. It has been suggested that rex acts by affecting export of viral mRNAs from the nucleolus to the cytoplasm (Kalland *et al.*, 1991). Another suggestion is that rex binds viral RNA and increases its stability, significantly increasing viral mRNA half-lives and thus accumulating HTLV transcripts in both the nucleus and cytoplasm (Inoue *et al.*, 1991).

Figure 1.7. Structure and functional domains of the HTLV-I rex protein. The rex protein is a 189 amino acid, 27 kDa nuclear RNA binding protein involved in mediating the subcellular redistribution of viral RNAs through interactions with the $R_X RE$ RNA stem loop motif of HTLV-I mRNAs.
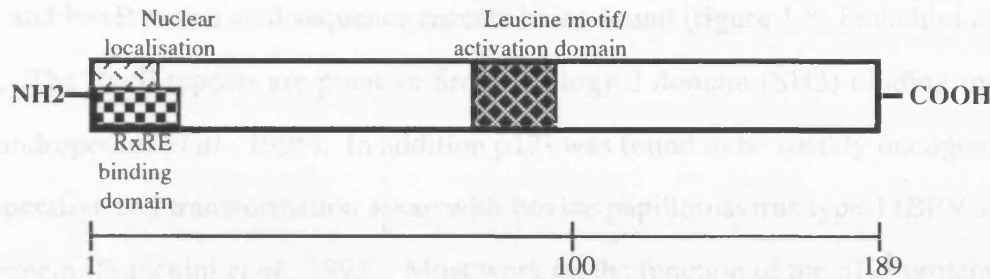
1.4.4 Other HTLV proteins of the pX region

The pX region of HTLV contains at least four open reading frames (orf). Two of these, orf III and IV, encode the essential HTLV-I non-structural regulatory proteins rex and tax. However by alternative RNA splicing events from the 5' LTR (exon 1) and tax/rex (exon 2) splice donors to alternative 3' splice acceptors in the pX region HTLV-I was found generate a number of different mRNA species and increase its protein coding capacity (figure 1.3; Berneman *et al.*, 1992; Ciminale *et al.*, 1992; Koralnik *et al.*, 1992). Several alternatively spliced RNA species which encode putative proteins designated p12^I, p13^{II}, p21^{rex}, rof and tof (p30^{II}) have all been identified by RT-PCR or northern blotting in either HTLV-I infected cell lines or primary cells from HTLV-I asymptomatic, ATL and TSP/HAM patients (Furukawa *et al.*, 1991; Orita *et al.*, 1991; Berneman *et al.*, 1992; Ciminale *et al.*, 1992; Koralnik *et al.*, 1992). However the actual expression of these five proteins *in vivo* has not been demonstrated and their involvement or relevance to HTLV-I replication or disease is unclear.

pX orf I encoded proteins - p12^I and rof

The protein p12^I is a 99 AA 12 kDa membrane associated protein encoded on pX-orf I which is derived from alternative RNA splicing to a 3' splice acceptor at nucleotide 6735 (figure 1.3). The protein is thought to be weakly oncogenic and may play a role

in the process of IL-2 independent cellular transformation of T-cells. Amino acid sequence analysis suggests the protein contains two putative transmembrane spanning domains and is rich in hydrophobic proline and leucine residues with four conserved LLFL and PxxP amino acid sequence repeats being found (figure 1.8; Franchini *et al.*, 1993). The PxxP repeats are putative Src homology 3 domain (SH3) binding motifs (Alexandropoulos *et al.*, 1995). In addition p12^I was found to be weakly oncogenic in a co-operative cell transformation assay with bovine papillomavirus type-I (BPV-I) E5 oncoprotein (Franchini *et al.*, 1993). Most work on the function of the p12^I protein has focused on comparisons with the BPV-I E5 oncoprotein as they share structural and functional similarities. The suggestion is that like BPV-I E5, HTLV-I p12^I may be involved in the processes of transformation and immortalisation of infected cells. Both proteins are found to localise on cellular endomembranes (Koralnik *et al.*, 1993) and interact with the 16 kDa subunit of a H$^+$ vacuolar ATPase (Franchini et al., 1993) which mediates the acidification of membrane bound organelles such as lysosomes, endosomes and Golgi vesicles. In the case the of the BPV-I E5 oncoprotein interactions with the 16 kDa H$^+$ ATPase subunit have been suggested to potentiate cellular transformation by increasing the recycling of cytokine receptors to the cell surface through enhanced breakdown of receptor-ligand complexes within acidified vesicles (Finbow *et al.*, 1991). However the binding sites to the 16 kDa H$^+$ ATPase sub-unit were found to differ between p12^I and E5 oncoproteins and transformation defective mutants of p12^I were not significantly altered in their ability to bind the 16 kDa H$^+$ ATPase sub-unit (Koralnik *et al.*, 1995). Mulloy *et al.*, 1996 recently demonstrated the specific binding and stabilisation of IL-2 receptor β and γ chains in the pre-Golgi compartment of cells by p12^I. The IL-2R β chain is known to associate with p56^{lck} tyrosine kinase and mediate associated cellular kinase cascades in response to IL-2 activation. The Jak-STAT mitogen activated protein (MAP) kinase IL-2 intracellular signalling pathway is also found to be constitutively activated in HTLV-I infected and transformed cells (Migone *et al*, 1995; Xu *et al.*, 1995). This interaction suggested a mechanism of IL-2 ligand independent modulation of the IL-2/IL-2R intracellular

signalling and T-cell activation pathways by p12^I which may all contribute toward cellular transformation.

Figure 1.8. Structure and functional domains of the HTLV-I p12^I protein. The p12^I protein is a 99 amino acid, 12 kDa putative transmembrane protein which localises in cellular endomembranes. The protein has weak oncogenic potential and may interfere with IL-2/IL-2R signalling pathway.
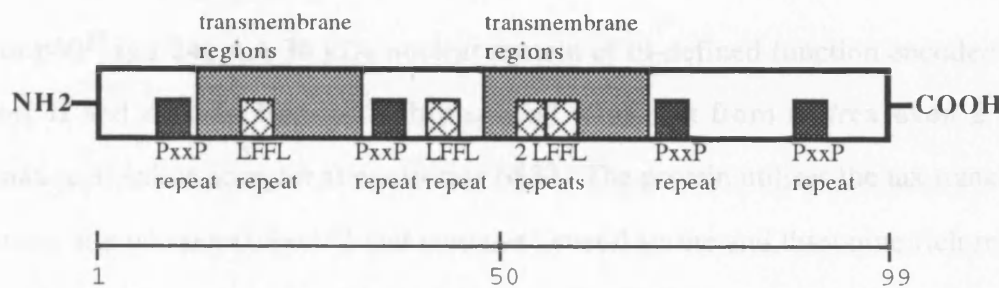
Rof is a 152 AA 27 kDa hydrophobic protein of unknown significance encoded on pX-orf I derived from a doubly spliced transcript from tax/rex exon 2 to an alternative splice acceptor site at nucleotide 6735. The protein utilises the translation initiation start site of rex on tax/rex exon 2 and contains the rex arginine rich R_XRE binding and nuclear localisation domains. However expression of rof cDNA was found not to confer rex-like activity or interfere with the normal actions of rex (Ciminale *et al.*, 1992). The actual expression of the 27 kDa rof protein *in vivo* is also undetermined as the protein was originally generated by *in vitro* translation of rof cDNAs (Ciminale *et al.*, 1992) but the transfection of rof cDNA expression constructs into Hela cells failed to produce whole rof proteins (Koralnik *et al.*, 1992 and 1993). Instead expression from these constructs yielded a 12 kDa major protein product, suggested to be p12^I, which rof overlaps.

pX orf II encoded proteins - p13^{II} (orf-2) and tof (p30^{II})

p13^{II} or orf-2 is a 87 AA protein of unknown function encoded on pX orf-II derived from both singly and doubly spliced transcripts using a 3' splice acceptor site at

nucleotide 7227. Koralnik *et al.*, 1992 identified the singly spliced pX-orf II RNA transcript and Ciminale *et al.*, 1992 identified a doubly spliced transcript from HTLV-I infected cells which were found to encode the same protein designated $p13^{II}$ and orf-2 respectively. This protein was found to be a nuclear protein residing in the nuclear matrix (Koralnik *et al.*, 1993) and its function is currently undetermined.

Tof or $p30^{II}$ is a 241 AA 30 kDa nuclear protein of ill-defined function encoded from pX-orf II and derived from a doubly spliced transcript from tax/rex exon 2 to an alternative 3' splice acceptor at nucleotide 6830. The protein utilises the tax translation initiation site on tax/rex exon 2 and contains several serine and threonine rich regions which are similar to the activation domains found in OCT-1, -2 and pit-1 transcriptional activator proteins. Hence it was suggested that tof may be a trans-activator protein but tof was found not to be able to activate transcription from the HTLV-I LTR promoter or modulate tax or rex activity (Ciminale *et al.*, 1992).

The roles of both $p13^{II}$ and tof proteins remain unclear but the expression of other HTLV-I genes were found not to be significantly influenced by orf-II (tof or $p13^{II}$) protein expression (Roithmann *et al.*, 1994).

pX orf III encoded proteins - p21^{rex}

p21rex is a 111 AA 21 kDa protein of unknown function encoded by 3' rex orf-III derived from a singly spliced RNA transcript utilising the tax/rex splice acceptor at nucleotide 7302. The single spliced RNA transcript does not contain tax/rex exon 2 and an alternative translation initiation codon found internally on rex orf-III is used (Berneman *et al.*, 1992; Koralnik *et al.*, 1992). The protein is found in the cytoplasm of cells and encodes the C terminal region of rex (Furukawa *et al.*, 1991) which lacks a complete rex R_XRE binding domain and nuclear localisation signal but does contain the putative nuclear export signal or leucine motif of rex (Malim *et al.*, 1991). A function of this protein is yet to be defined but has been suggested to be an antagonist of rex

function (Furukawa *et al.*, 1991). Recently it has been suggested that p21^{rex} may play a role in negatively regulating the export of viral RNAs from the nucleus by interfering with rex protein function. Co-expression of rex with p21^{rex} showed a dose dependant increase in accumulation of the rex protein in the nucleus of cells and suggested that p21^{rex} may act as a competitive substrate for nuclear export through their nuclear export signal/leucine motifs (Kubota *et al.*, 1996).

1.5 HTLV-I and cellular transformation

The ability of HTLV-I to immortalise and transform resting T-lymphocyte cells (Miyoshi *et al.*, 1981b; Chen *et al.*, 1983; Popovic *et al.*, 1983b) forms the basis of its pathogenesis. Uncontrolled T-cell growth and activated T-cell infiltrates into other tissues of the body seems to be the main cause of cancers and related disorders associated with HTLV-I. For example, in HAM/TSP large numbers of activated blood T-cells and high levels of spontaneous proliferation are observed. This suggests a significant role of HTLV-I in the development of neurological diseases as only activated T-cells can cross the blood-brain barrier (Wekerle *et al*, 1985). HTLV-I differs from other oncogenic viruses in that it does not integrate proviral DNA at specific sites within the chromosome (Seiki *et al.*, 1984) or carry a cellularly derived oncogene. Other transforming retroviruses, such as RSV, carry oncogenes which are mutant forms of cellular genes involved in regulation of cell growth. These oncogenes were picked-up by a process of illegitimate recombination and carried along "accidentally" by the virus and have no direct involvement in viral replication. However, transformation of infected T-cells by HTLV-I is thought to be a consequence of its natural method of replication. HTLV shows remarkably low genetic variability (Komurian *et al.*, 1991; Gessain *et al.*, 1992) and only low levels of viral gene expression can be detected in freshly isolated ATL cells (Kinoshita *et al.*, 1989; Franchini *et al.*, 1984; Shinzato *et al.*, 1993). Also, the main method of transmission seems to be via direct cell to cell contact and not virus particle production as cell free infected blood plasma is non-infectious (Inaba *et al.*, 1989; Sandler *et al.*, 1991). These observations are in direct contradiction

with other classic retroviruses such as HIV where mutation rates are high (especially in the env gene) due to immunological selective pressure, high levels of virus expression are observed and the main mode of transmission is by virus particle release and infection. Instead it is proposed that HTLV-I replicates via a more covert approach, by clonal expansion. HTLV-I replicates in the provirus (chromosomally integrated) form by cellular transformation of infected cells rather than virion production. HTLV-I transformed cells will spontaneously divide and the provirus becomes passed onto the progeny cells. In this way the number of HTLV-I infected cells has increased. Observations that HTLV has low genetic variability, low viral expression in the peripheral blood of HTLV infected individuals, long periods of latency stretching into decades and only a small percentage of those infected actually develop disease (Araki *et al.*, 1988; Murphy *et al.*, 1989b; Tajima *et al.*, 1990) all support this model of infection and replication. The apparent latency of HTLV may also stem from immune surveillance in which low HTLV expressing cells effectively escape but high expressing cells are eliminated. When PBMCs from HTLV infected subjects are cultured *in vitro* a marked increase in viral expression occurs (Hoshino *et al.*, 1983; Franchini *et al.*, 1984) suggesting that these cells harbour a potentially active provirus but only low expressing cells are maintained *in vivo* due to immune surveillance. In addition early in infection a polyclonal transformed cell population is observed but over time a single dominant clone is eventually selected and may develop into tumour cells (Kimata *et al.*, 1991). Several mechanisms for latency have been proposed such as DNA methylation (Cassens *et al.*, 1994) and basal transcription factor instability (Brauweiler *et al.*, 1995) of the viral LTR promoter.

The induction of cell proliferation by HTLV-I is believed to be conferred on at least two levels. The first being at the cell surface occurring independently of viral infection through mitogenic stimulation of cells by contact with HTLV infected cells (Gessain *et al.*, 1987). The observations that inactivated HTLV-I virions can retain their mitogenic ability (Duc Dodon *et al*, 1989), antibodies directed against gp46 can neutralise

mitogenicity (Gazzolo *et al*, 1987), formation of syncytia (Tanaka *et al*, 1991) and that gp46 could induce proliferation via a T-cell specific antigen CD2 (Duc Dodon *et al* 1989) strongly suggested gp46 was a T-cell mitogen. However, recent evidence has suggested that the mitogenic activity of HTLV may not be due to gp46 but through cellular adhesion molecules (Wucherpfenning *et al.*, 1992; Kimata *et al.*, 1993 and 1994a) Second, after infection, the tax protein as well as enhancing viral gene expression also indirectly trans-activate many cellular genes including IL-2, IL-2Rα, GM-CSF, c-*fos*, c-*myc*, NF-κB and led to suggestions of T-cell activation due to loss of cell growth control and deregulation of cellular gene expression (table 1.2). The trans-activation of both IL-2 and IL-2Ra by tax also suggested a possible autocrine growth loop mechanism for T-cell proliferation (Arima *et al.*, 1986; Maruyama *et al.*, 1987). Thus a model exists whereby stimulation at the cell surface and aberrant gene expression induced by tax in the nucleus may co-operate to induce cellular proliferation (Kimata *et al.*, 1991).

The oncogenic potential of tax has been demonstrated in several studies. The pX region of HTLV-I when introduced into primary human T-cells using recombinant herpesvirus saimiri vectors was found to be able to transform cells (Grassmann *et al*, 1989) and that tax was necessary and sufficient to mediate this effect (Grassmann *et al*, 1992). However, it was unclear as to whether herpesvirus vector proteins may have contributed or co-operated with tax in mediating transformation. Tax has also been shown to immortalise NIH-3T3, RAT-1 and RAT-2 cells *in vitro* in a growth factor dependent manner (Tanaka *et al.*, 1990) and transform fibroblasts in co-operation with the ras oncogene (Pozzatti *et al.*, 1990). It should be noted that the study by Pozzatti *et al*, 1990 could not demonstrate tumorigenesis using tax alone, suggesting the co-operation with other factors for transformation. Transgenic mouse models have similarly shown the oncogenic potential of tax, which was able to induce neurofibromas (Hinrichs *et al.*, 1987), mesenchymal tumours (Nerenberg *et al.*, 1987) and fibroblastic

tumours (Nerenberg *et al.*, 1991). However, none of these mice developed tumours of lymphoid origin.

Primary T-cells isolated from HTLV infected patients typically demonstrate an immortalised IL-2 dependent growth phenotype in cell culture (Hollsberg *et al.*, 1992) and express high levels of IL-2Rα (Uchiyama *et al.*, 1985; Umadome *et al.*, 1988). Upon long term co-culture clonal selection occurs and a transformed or leukaemic clone is derived which can grow in the absence of exogenous IL-2 (Popovic *et al.*, 1983b; Yoshida *et al*, 1982; DeRossi *et al.*, 1985). However, the change from IL-2 dependent to IL-2 independent growth cannot be attributed solely to the tax protein. Although tax is oncogenic, it alone has been suggested to be insufficient to directly confer IL-2 independent transformation of T-cells (Akagi *et al*, 1993) and indicates the involvement of other viral proteins (possibly $p12^I$) or further abrogation of critical growth control processes. Hence, a mechanism of malignant transformation can be envisaged whereby HTLV-I infection provides the initial "step", disrupting normal growth control and inducing IL-2 dependent cell proliferation. Indeed, this can be supported by the observation that tax mRNA can only be detected at low levels in uncultured ATL cells (Franchini *et al.*, 1984), suggesting tax is not required for maintaining a leukaemic (IL-2 independent) state. Continual cell proliferation and repression of the DNA repair enzyme β-polymerase (Jeang *et al.*, 1990) within HTLV infected cells may lead to the accumulation of genetic abnormalities and ultimately to malignant cell transformation (figure 1.9). Mathematical modelling of the age specific onset of ATL led the proposal of a "multistep" model of carcinogenesis by Okamato *et al.*, 1990. The long periods of disease latency and the higher incidence of ATL with age (Araki *et al.*, 1988; Tajima *et al.*, 1990) suggested an time related mechanism of carcinogenesis, resulting from the accumulation of a number of critical somatic mutations.

Figure 1.9. A schematic representation of the mechanisms of cellular transformation and immortalisation by HTLV-I. (Adapted from Franchini *et al.*, 1995a and 1995b).
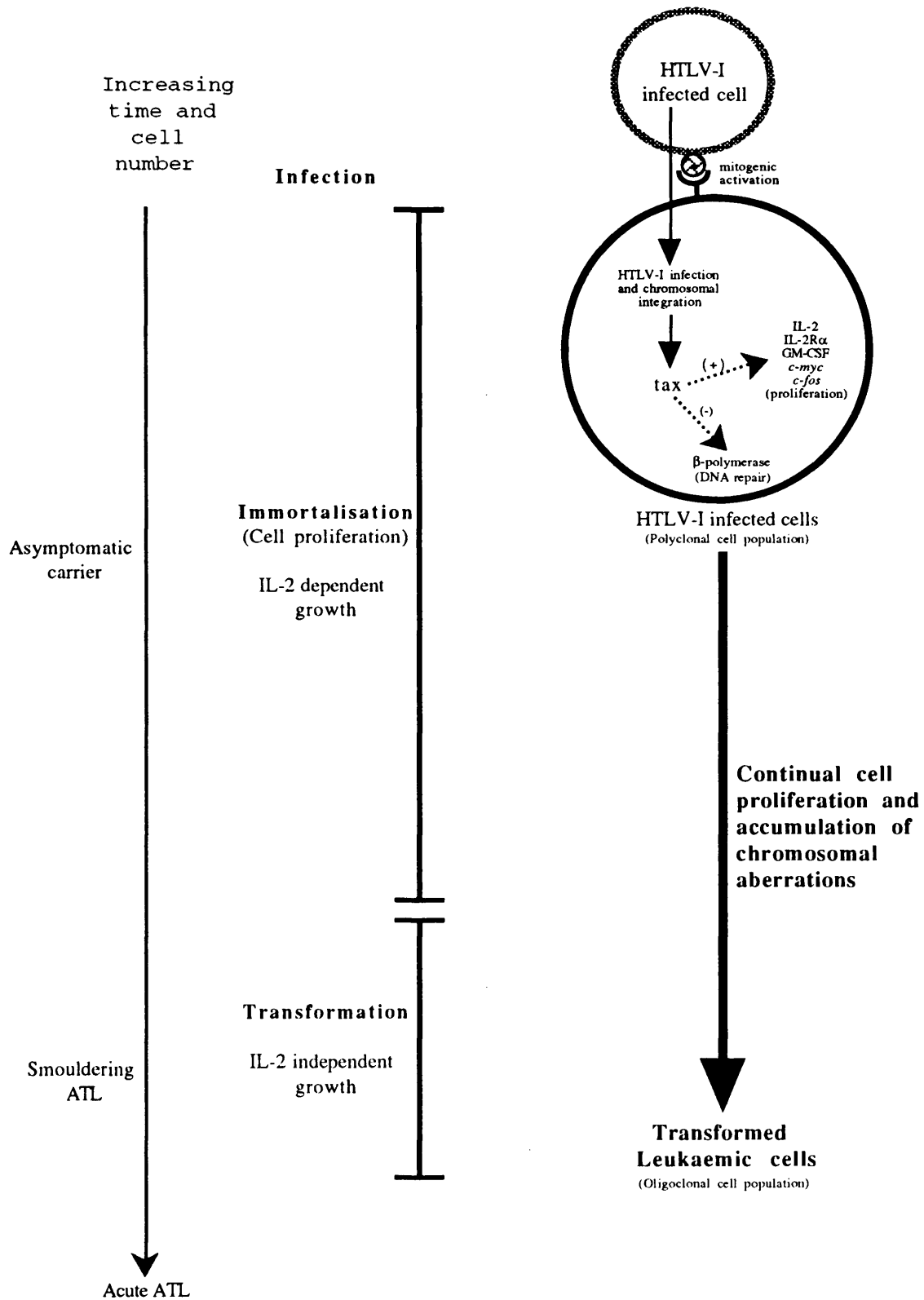
1.5.1 Mitogenic stimulation by HTLV-I

Retrovirus envelope glycoproteins play essential roles in viral replication, being responsible for cell receptor binding, cell membrane fusion and viral entry. In addition the HTLV envelope glycoproteins have also been implicated in novel steps in infection and cellular transformation. Initial observations that inactivated HTLV virions and only cell to cell contact were sufficient to stimulate resting T-cells led to suggestions that HTLV envelope proteins, probably gp46 (SU), are mitogenic for T-cells (Duc Dodon *et al.*, 1987; Gazzolo *et al.*, 1987; Zack *et al.*, 1988; Cassé *et al.*, 1994). Again this mitogenic ability was thought to be deliberate as the activation of target cells may be required for the establishment of a productive infection. Over 95 % of T-cells in the body are in an inactive or quiescent state but studies have shown that retroviruses are generally blocked from productive infection unless the cell has traversed through S-phase of the cell cycle (Merl *et al.*, 1984). Hence HTLV may need to activate the quiescent T-cells to allow a productive infection to occur. However, mitogenic stimulation alone was found not to be sufficient for transformation. Also some experiments have demonstrated that gp46 alone was not sufficient to elicit a mitogenic response (Kimata *et al.*, 1993; Cassé *et al.*, 1994) and that gp46 may, in fact, not be a mitogen but that virally induced or modified cell surface antigens on HTLV cells are responsible for its mitogenic effects (Wucherpfennig *et al.*, 1992; Kimata *et al.*, 1993; Kimata *et al.*, 1994a). These studies indicated that mitogenic ability was restricted to only HTLV infected T-cells (and not free virus as first suggested) via direct cell to cell contact, that stimulation could occur in the absence of virus infection and proliferation was mediated through the CD2/LFA-3 activation pathway with the possible involvement of the (TCR)/CD3 receptor complex. A mitogenic model was suggested in which a cell surface presented viral or virally induced antigen, not env or gag, would interact with CD2/CD3 receptors to co-stimulate activation. In any case a mitogenic model for HTLV can be suggested whereby stimulation of a T-cell receptor(s) leads to spontaneous cell proliferation and, in-conjunction with the intracellular effects of tax, may ultimately lead to cellular transformation.

1.5.2 HTLV-I tax and gene trans-activation

Tax is well established as a potent transcriptional activator of both viral and cellular gene expression. The trans-activating ability of tax contributes greatly to cellular transformation and leukemogenesis.

HTLV directed trans-activation

Much of the knowledge on the mechanisms of tax trans-activation has come from studies upon viral gene expression from the HTLV LTR. The HTLV-I LTR can be split into three regions, 353 bp U3, 225 bp R and 177 bp U5. The U3 region contains the major promoter sequences and enhancer elements responsible for directing HTLV-I RNA synthesis. The U3-R boundary is defined as the mRNA initiation site. Three 21bp repeat sequences within the U3 region have been identified as elements critical for trans-activation and are found in all members of the HTLV/BLV family (Shimotohno *et al.*, 1986; Sodroski *et al.*, 1984; Paskalis *et al.*, 1986; Brady *et al.*, 1987; Seiki *et al.*, 1988). Another tax responsive region has also been identified, located between the second and third 21 bp repeats, and contains binding sites for a number of transcriptional enhancer proteins (Nyborg *et al.*, 1990; Marriott *et al.*, 1989; Bosselut *et al.*, 1990 and 1992; Gitlin *et al.*, 1991b and 1993; Clark *et al.*, 1993). However, it was found that tax does not directly interact with these *cis*-responsive elements but rather sequesters cellular transcription factors to direct transcription (Giam *et al.*, 1989).

Several members of the cAMP response element binding protein/activating transcription factor (CREB/ATF) family of cellular transcription factors have been implicated as 21 bp repeat binding proteins and targets for tax activation. At least four CREB/ATF proteins that bind the 21 bp repeats have been cloned (Yoshimura *et al.*, 1990; Tsujimoto *et al.*, 1991) and two members, ATF-2 and CREB, have been shown to specifically mediate tax trans-activation (Franklin *et al.*, 1993). The defining characteristics of CREB/ATF transcription factors is that they regulate cAMP responsive gene expression (e.g. c-*fos*), bind to an eight nucleotide palindromic DNA sequence

called the cAMP response element (CRE) and contain an alpha-helical basic amino acid DNA binding domain adjacent to a leucine zipper protein dimerisation domain. This basic DNA binding-leucine zipper domain has recently become commonly known as "bZIP" and proteins with these domains are sometimes referred to as bZIP proteins (Lee *et al.*, 1993). Binding of CREB/ATF proteins to the HTLV LTR can also be further supported by the presence of CRE-like sequences within the 21 bp repeats. The structure of the HTLV-I LTR promoter and its major transcriptional control elements are shown in figure 1.10.

The 21 bp repeat sequences are absolutely required for transcriptional activation of viral genes by the action of tax and CREB/ATF proteins. The 21 bp repeat sequence can confer tax trans-activation to a heterologous promoter and function independently of orientation or position (Paskalis *et al.*, 1986). Each 21 bp repeat can be divided into three 7 bp elements; A, B and C, of which domain B contains the first five bases of the eight base CRE (*TGACG*TCA). Domain B, in conjunction with either domain A or C, is absolutely required for trans-activation by tax (Yin *et al.*, 1995). Several members of the CREB/ATF family of proteins seems to interact with domain B (Nyborg *et al.*, 1990; Yoshimura *et al.*, 1990; Tsujimoto *et al.*, 1991). These include CREB-1, ATF-1, -2 , -4 and a number of other unidentified proteins with bZIP and trans-activation domains similar to c-fos, c-jun and C/EBP. The cellular transcription factor HEB1 is also thought to be important, interacting with the 21 bp repeats and mediating tax binding (Montagne *et al.*, 1990; Béraud *et al.*, 1991). Jun/AP-1 and AP-2 transcription factor binding sites are also present, overlapping the 21 bp repeat elements (figure 1.10; Jeang *et al.*, 1991).

Figure 1.10. The HTLV-I long terminal repeat (LTR) structure and U3 sequence. The HTLV-I LTR is 755 base pairs in length and contains three regions designated U3, R and U5. The U3-R junction (base 352) is the transcriptional start site. The 5' splice donor for spliced mRNAs occurs at base 471. The R-U5 junction (base 579) is the polyadenylation site. Transcriptional control elements are present in the R region and are contained in three 21 bp repeats (i to iii) and a 46 bp region. The sequence of the R region is shown and transcription factor binding elements involved in mediating LTR transcription are indicated.
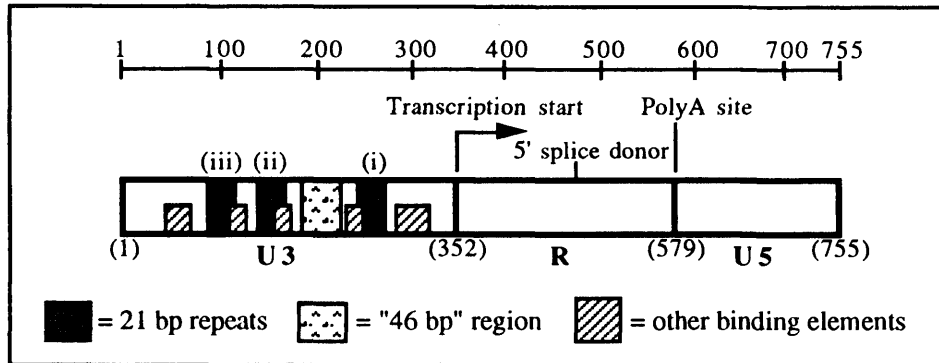

```
                                          myb
TAGAGCCTCCCAGTGAAAAACATTTCCGAGAAACAGAAGTCTGAAAAGGT
                     Ets-1
```

21 bp repeat (iii)
```
                                     AP-2
CAGGGCCCAGACTAAGGCTCTGACGTCTCCCCCCGGAGGGCAGCTCAGCA
                 CREB/ATF, HEB1/2
```

21 bp repeat (ii)
```
                               AP-2
CCGGCTCGGGCTAGGCCCTGACGTGTCCCCCTGAAGACAAATCATAAGCT
               CREB/ATF, HEB1/2
```

46 bp region
```
                        myb
        r - - - - - - - - - - - - - - - - - - -1
        r       SP-1              SP-1         l
CAGACCTCCGGGAAGCCACCAAGAACCACCCATTTCCTCCCCATGTTTGT
l                           Ets-1                  l
L- - - - - - - - - - - - - - - - - - - - - - - - - -J
                        TIF-1
```

21 bp repeat (i)
```
     AP-2
CAAGCCGTCCTCAGGCGTTGACGACAACCCCTCACCTCAAAAAACTTTTC
               CREB/ATF, HEB1/2
```

```
                        myb
ATGGCACGCATATGGCTCAATAAACTAGCAGGAGTCTATAAAAGCGTGGA
     NF-1
```

Transcription start
```
          ┌──▶
◄──────U3 region │ R region ──────▶
GACAGTTCAGGAGGGGGCTCGCATCTCTCCTTCACGCGCCCGCCG
```

A 46 bp region located between the first and second 21 bp repeats contains binding sites for a number cellular proteins including transcription factor SP-1, c-*ets*-1 proto-oncogene protein ets-1 and myb (figure 1.10; Bosselut *et al.*, 1990; Marriott *et al.* 1990; Nyborg *et al.*, 1990; Gitlin *et al.*, 1991b). Distinct ets-1 binding sites are located within this 46 bp region and upstream of the first 21 bp repeat. Ets-1 is constitutively expressed in T-cells (Bhat *et al.*, 1990) and is apparently able to trans-activate the HTLV-I LTR in the absence of tax (Bosselut *et al.*, 1990; Gitlin *et al.*, 1991b) aiding basal transcription.

The involvement of CREB/ATF transcription factors in directing HTLV gene expression is well documented but the exact mechanism in which this occurs is still unclear. It is known that tax does not directly bind the viral promoter sequence but is absolutely required for enhanced viral gene expression. This suggests a mechanism by which tax modulates the interaction of CREB/ATF transcription factors with the 21 bp repeats to direct viral transcription.

One mechanism is that tax stimulates the DNA binding activity of CREB/ATF proteins by increasing the number of active CREB/ATF dimers in solution (Zhao *et al.*, 1991 and 1992; Matthews *et al.*, 1992; Armstrong *et al.*, 1993). Dimerised CREB/ATF proteins or "bZIP" dimers are activated forms of the protein and enhance transcription from responsive promoters (Wagner *et al.*, 1993). Hence tax may modulate CREB/ATF protein dimerisation leading to increased numbers of "active" transcriptional enhancers and ultimately an overall increase in gene transcription. It is suggested that tax interacts with the leucine zipper domains of CREB/ATF proteins resulting in stabilisation of dimers. CREB/ATF protein deletion mutants which only contain the bZIP binding domains can be bound and dimerised by tax (Franklin *et al.*, 1993; Wagner *et al.*, 1993).

Another suggestion for the mechanism of tax trans-activation is one in which the CREB/ATF protein plays a passive role, simply acting as a DNA anchor to stabilise DNA bound tax/CREB/ATF protein complexes so that tax itself can enhance transcription via a putative transcriptional activation domain. Supporting evidence includes activated expression from a yeast GAL4 reporter plasmid using only the yeast GAL4 protein binding domain fused with the tax protein (Conner *et al.*, 1993; Tsuchiya *et al.*, 1994) and that tax mutants in this GAL4 fusion can alter reporter plasmid trans-activation (Fujisawa *et al.*, 1991; Fujii *et al.*, 1992). Here the suggestion is that tax must confer a transcriptional activity and a stable DNA bound tax/CREB/ATF protein complex must assemble.

Although a large body of data exists for both proposed mechanisms, it does not mean both are mutually exclusive. It could be that both mechanisms are active and compliment each other. Tax may increase DNA binding of CREB/ATF to responsive DNA elements by both stabilisation of dimers in solution and then stabilise the 21 bp repeat DNA bound complexes to significantly enhance transcription. Indeed, DNA binding studies have shown that tax can not only increase both CREB and ATF-2 protein dimerisation but also increase DNA binding affinities (Anderson *et al.*, 1994), indicating the second mechanism is more likely. Moreover, two recent studies have shown a stabilisation of the tax/CREB protein-DNA complex to be a result of tax interactions with the DNA binding element of bZIP domains, but still requires the leucine zipper for activity. In addition to modulating protein dimerisation, tax may also alter DNA binding site selectivity/affinity in a sequence-specific manner (Baranger *et al.*, 1995; Perini *et al*, 1995). Tax protein dimerisation in the tax/CREB protein-DNA bound complex was found to be required for transcriptional activation and a domain between amino acids 123 to 204 was identified to mediate these interactions (Tie *et al.*, 1996).

The exact details involved in trans-activation from HTLV LTRs is unclear but it seems certain that complex molecular interactions between tax and the CREB/ATF cellular transcription factors are critically involved. In addition, the presence of other transcriptional enhancer elements within the LTR region, such as the AP-1, NF-1, myb, SP-1, ets-1 binding sites (figure 1.10), suggests a complex interaction of all such factors with the general aim to maximise the up-regulation of HTLV-I gene transcription. It can be noted that activation of CREB alone is not sufficient to up-regulate all CRE containing cellular promoters, indicating the involvement of flanking DNA sequences and other nuclear factors to modulate its effects. Indeed, transcription factor HEB1 is thought to mediate HTLV-I LTR transcription in conjunction with CREB (Montagne et al., 1990).

Trans-activation of cellular genes

One characteristic of tax is its ability to not only trans-activate viral genes but also a large number of cellular genes, the ultimate effect being a deregulation of cellular gene expression and cell transformation. As noted above tax is able to indirectly trans-activate its own promoter in association with the CREB/ATF family of transcription factor via 21bp repeats containing a cAMP responsive element (CRE) like motif. In addition to activating CREB/ATF proteins tax has also been implicated in activating other unrelated transcriptional enhancer proteins of the NF-κB and serum response factor (SRF) families, enhancing expression of NF-κB or SRF binding element containing promoters (figure 1.11). The combination of all these proteins activating their respective responsive elements within cellular promoters allows a large variety of cellular genes to be expressed (table 1.2). This deregulation of gene control is thought to lead to expression of many growth-factor related or oncogenic genes and stimulate cell division, possibly leading to malignant transformation. However, β-polymerase, a DNA repair enzyme seems to be down-regulated by tax (Jeang et al., 1990) and provides an additional mechanism for tumourgenesis in which DNA repair becomes impaired, leading to development of chromosomal abnormalities and cancer. Additional

evidence for this mechanism comes from the fact that numerous chromosomal aberrations are a characteristic of cells from ATL patients (Ushima *et al.*, 1981; Fukuhara *et al.*, 1983). However, cellular transformation and leukemogenesis probably arise from a combination of both cellular gene activation and β-polymerase repression.

The NF-κB family of transcription factors play a central role in the control of cellular transcription and regulate immunoglobulin gene transcription in lymphoid cells. NF-κB recognises a 11 bp consensus sequence which found in the promoter regions of a number of cellular genes including cytokines GM-CSF (Schreck *et al.*, 1990), IL-2, IL-2Rα (Böhnlein *et al.*, 1988; Leung *et al.*, 1988; Hoyos *et al.*, 1989) and the cytoskeletal growth gene vimentin (Lilienbaum *et al.*, 1990). All of these NF-κB responsive genes can also be activated by tax (figure 1.9).

The action of tax on NF-κB seems to occur via interactions with the inactive p105 NF-κB-IκB complex inducing the dissociation of the inhibitory IκB subunit and resulting in an active NF-κB protein (Ruben *et al.*, 1989; Hirai *et al.*, 1992; Sun *et al.*, 1994; LaCoste *et al.*, 1995; Suzuki *et al.*, 1995). Other additional transcription factors may also be involved in mediating NF-κB trans-activation. Studies on expression of IL-2Rα and IL-2 have shown that SRE/SP-1 like binding elements are required for full activation (Ballard *et al.*, 1989; Hoyos *et al.*, 1989). Again this suggests complex interactions of many transcription factors upon their respective promoters are involved in tax induced gene activation.

Figure 1.11. Examples of cellular gene promoters and their associated transcription factor responsive elements which are trans-activated by the HTLV-I tax protein. The HTLV-I tax protein modulates the DNA binding and transcriptional activities of the cAMP responsive element binding protein/activating transcription factor (CREB/ATF), serum response factor (SRF) and NF-κB families of cellular transcription factors. Responsive elements for AP-1, CREB/ATF (CRE), NF-κB, SRF (SRE) and SP-1 (GC rich regions) transcription factors which are thought to be involved in tax trans-activation are shown.
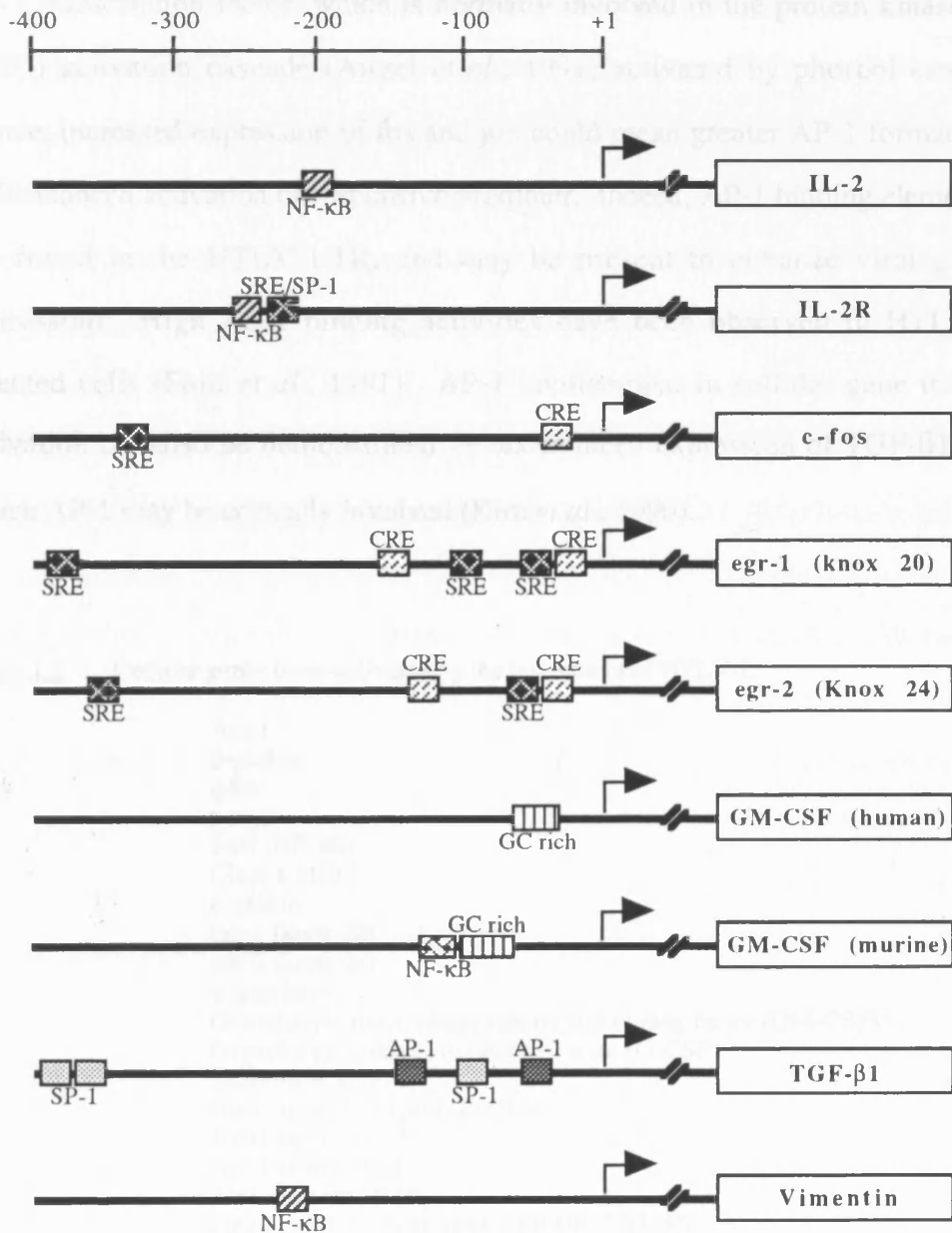
The activation of CREB/ATF proteins by tax leads to a concomitant increase in expression of normal cellular cAMP responsive genes such as c-fos, c-jun and egr-1/-2 or knox-20/-24 (Fujii *et al.*, 1991; Alexandre *et al.*, 1991). Fos in a heterodimeric protein complex with jun associate together and form the active AP-1 transcription factor, which is normally involved in the protein kinase C (PKC) activation cascade (Angel *et al.*, 1991) activated by phorbol esters. Hence, increased expression of fos and jun could mean greater AP-1 formation and enhanced activation of responsive promoter. Indeed, AP-1 binding elements are found in the HTLV LTR, and may be present to enhance viral gene expression. High AP-1 binding activities have been observed in HTLV-I infected cells (Fujii *et al.*, 1991). AP-1 involvement in cellular gene trans-activation can also be demonstrated by tax induced expression of TGF-β1, in which AP-1 may be critically involved (Kim *et al.*, 1990).

Table 1.2.   Cellular genes trans-activated by the tax protein of HTLV-I.

Act-2
β-globin
c-fos
c-myc
c-rel (NF-κB)
Class I MHC
ε-globin
egr-1 (knox 20)
egr-2 (knox 24)
γ-interferon
Granulocyte-macrophage colony stimulating factor (GM-CSF)
Granulocyte colony stimulating factor (G-CSF)
Interleukin 2 (IL-2)
Interleukin 2 receptor (IL-2Rα)
Interleukin 3 (IL-3)
Interleukin 6 (IL-6)
Nerve growth factor
Parathyroid hormone-related protein (PTHrP)
Transforming growth factor-b1 (TNF-β1)
Vimentin

Cellular genes repressed by tax protein of HTLV-1
β-polymerase

Serum response factor (SRF) responses have also been suggested to be modulated by tax protein interactions (Fijii *et al.*, 1992 and 1995). Several genes which contain SRF responsive elements (SRE) can be trans-activated by tax (Alexandre *et al.*, 1991; Fijii *et al.*, 1991b). Such genes include the egr family of zinc finger proteins which are normally activated in response to external cell stimuli such as cytokines, lectins and serum (Gius *et al.*, 1990). Although the egr genes contain both SRE and CRE elements (figure 1.11), tax activation can be demonstrated through both elements (Alexandre *et al.*, 1991) suggesting the involvement of both CREB and SRF transcription factors. The upregulation and modulation of cellular transcription factors and intracellular signalling pathway responses by HTLV-I tax is summarised in figure 1.12.

Extracellular cytokine-like activity of tax

The tax protein is also suggested to possess cytokine-like activities which may contribute to cellular activation and transformation. Soluble tax protein has been found in the extracellular medium of a number of HTLV-I infected and transformed cells (Lindholm *et al.*, 1990; Marriott *et al.*, 1991). Extracellular tax has also been demonstrated to be taken up by cells in culture and enhance NF-κB transcription factor activity and responsive gene transcription in these cells (Lindholm *et al.*, 1990 and 1992). In addition soluble tax was found to stimulate cellular proliferation and gene expression in primary blood lymphocytes at concentrations similar to other cytokines (Marriott *et al.*, 1991 and 1992). It is currently unclear how tax is secreted or taken up by cells but the cytokine-like activity may aid the induction of proliferation in cells in the absence of infection.

Figure 1.12. Modulation of intracellular signalling cascades and their respective transcription factors by the HTLV-I tax protein. The transcriptional activation pathways normally induced in response to phorbol esters, hormones and growth factors are also activated by tax. Tax associates with and alters the activity of a number of cellular transcription factors families which include the cAMP responsive element binding protein/activating transcription factor (CREB/ATF), serum response factor (SRF) and NF-κB. Tax interactions enhance the dimerisation of CREB/ATF and SRF and induces the dissociation of the IκB inhibitory subunit of NF-κB leading to a greater number of active transcription factors. The activation of these transcription factors causes enhanced expression HTLV-I and many cellular genes including cytokines (IL-2), growth factors (GM-CSF, vimentin) and other transcription factors (AP-1, egr 1/2) contributing to cellular activation and transformation.
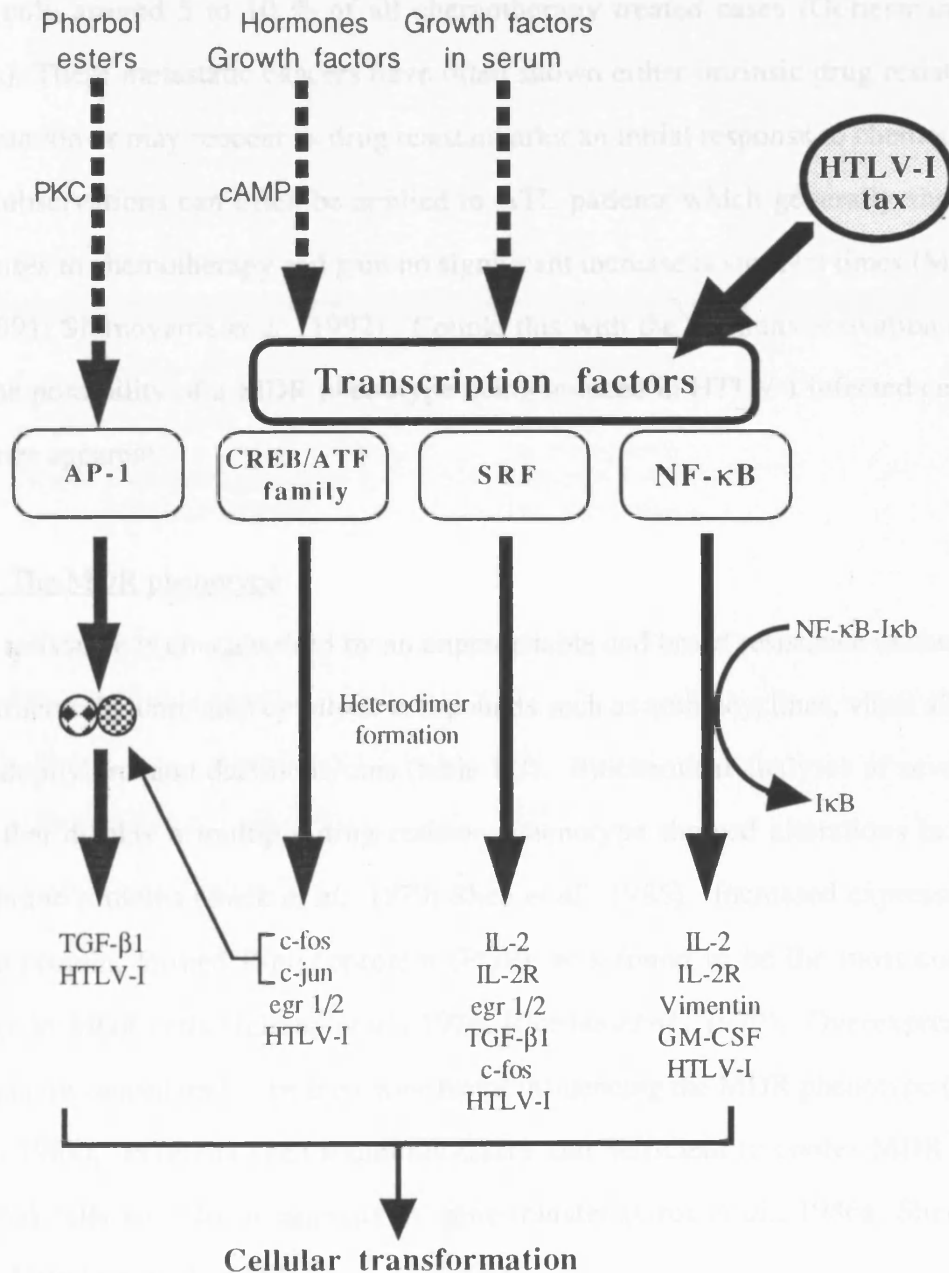
1.6 Multiple drug resistance (MDR)

Multiple drug resistance (MDR) is defined as broad spectrum resistance to chemotherapy in cells. The development of the MDR phenotype may have profound effects in cancer treatments, causing many such chemotherapeutic regimes to fail. Unfortunately systemic cancers such as leukaemias or lymphomas offer very few possible treatments apart from chemotherapy. Improvements in long-term survival form only around 5 to 10 % of all chemotherapy treated cases (Gottesman *et al.*, 1993a). These metastatic cancers have often shown either intrinsic drug resistance at presentation or may reoccur as drug resistant after an initial response to chemotherapy. Such observations can often be applied to ATL patients which generally show poor responses to chemotherapy and gain no significant increase is survival times (Minato *et al.*, 1991; Shimoyama *et al.*, 1992). Couple this with the tax trans-activation activity and the possibility of a MDR phenotype being induced in HTLV-I infected cells then becomes apparent.

1.6.1 The MDR phenotype

Drug resistance is characterised by an unpredictable and broad resistance to chemically and structurally unrelated cytotoxic compounds such as anthracyclines, vinca alkaliods, epipodophylline and dactinomycins (table 1.3). Biochemical analyses of several cell lines that display a multiple drug resistant phenotype showed alterations in plasma membrane proteins (Beck *et al.*, 1979; Shen *et al.*, 1986). Increased expression of a single protein, termed P-glycoprotein (PGP), was found to be the most consistent change in MDR cells (Juliano *et al.*, 1976; Riordan *et al.*, 1979). Overexpression of PGP is now considered to be the major factor influencing the MDR phenotype (Kartner *et al.*, 1985). PGP has been found necessary and sufficient to confer MDR in both cultured cells and also in animals by gene transfer (Gros *et al.*, 1986a; Shen *et al.*, 1986; Deuchars *et al.*, 1987).

Table 1.3. Chemical compounds known to interact with P-glycoprotein (PGP)

Chemotherapeutic agents to which MDR cells become resistant

Anthracyclines	(e.g. doxorubicin)
Epipodophyllotoxins	(e.g. etoposide)
Some antibiotics	(e.g. actinomycin D)
Vinca alkaloids	(e.g. vinblastine)
taxol	
topotecan	
methramycin	

cytotoxic agents to which MDR cells become resistant

Antimicrotubule agents	(e.g. colchicine)
DNA intercalators	(e.g. ethidium bromide)
Protein synthesis inhibitors	(e.g. puromycin)
Toxic peptides	(e.g. valinomycin, gramicidin)
Mitomycin C	

Agents capable of reversing the effects of PGP (chemosensitizers)

Anti-arrhythmics	(e.g. quinidine)
Anti-hypertensives	(e.g. resperpine)
Antibiotics	(e.g. cephalosporins)
Calcium channel blockers	(e.g. verapamil)
Immunosuppressants	(e.g. cyclosporin A)
Modified steroids	(e.g. tamoxifen)

Increased mdr-1 gene expression has also been associated with poor prognosis and drug resistance in acute myeloid leukaemia (AML) and adult lymphoblastoid leukaemia (ALL) (Campos *et al.*, 1991; Marie *et al.*, 1991; Goasguen *et al.*, 1993). However it was demonstrated that in at least one third of clinically drug resistant cancers the presence of mdr-1 RNA or PGP expression could not be detected (Zhou *et al.*, 1992; Hart *et al.*, 1993). The non-PGP mediated drug resistance observed in these cancers was termed atypical MDR and recently found to be linked to the overexpression of the multidrug resistance associated protein or MRP (Cole *et al.*, 1992; Krishnamachary *et al.*, 1993; Zaman *et al.*, 1993).

1.6.2 P-glycoprotein (PGP) and MDR

The most well characterised manifestation of a MDR phenotype is through the broad chemotherapeutic resistance conferred by P-glycoprotein or PGP. PGP is a 170 kDa ATP dependent membrane bound phosphoglycoprotein which acts by pumping cytotoxins out of the cells leading to decreased intracellular drug concentrations (Endicott *et al.*, 1989; Gottesman *et al.*, 1993a). PGP belongs to the family of ABC (ATP binding cassette) transporter proteins and is encoded by the mdr -1 gene which is also part of a larger mdr gene family. In humans only two mdr genes have been identified, these being known as mdr-1 and mdr-2. However only mdr-1, which encodes PGP, has been shown to confer a drug resistance phenotype (Ueda *et al.*, 1987a; Choi *et al.*, 1991). The mdr genes have been mapped to the long arm of chromosome 7 (Trent *et al.*, 1991) and mdr-1 consists of 28 exons spanning more than 100 kb (Chen *et al.*, 1990). PGP is found to be normally expressed in several tissues such as adrenal, liver, colon, renal, endometrium and endothelial cells. Expression in these tissues suggest a normal physiological role of PGP in detoxification and/or steroid transport (Arceci *et al.*, 1988; Cordon-Cardo *et al.*, 1989; Croop *et al.*, 1989; Fojo *et al.*, 1987; Thiebaut *et al.*, 1989). MDR activity and PGP expression has also been detected by sensitive flow cytometric and RNA analysis in fresh peripheral blood lymphocytes and haematopoietic stem cells (Neyfakh *et al.*, 1989; Chaudhary *et al.*, 1991; Coon *et al.*, 1991; Gupta *et al.*, 1992a; Damiani *et al.*, 1993). PGP was found to be expressed preferentially in $CD8^+$ CTL and NK cells and a role in CTL effector function via cytotoxic molecule transport was suggested. However MDR activity and PGP expression was only detected at low levels in a small number of cells (Gupta *et al.*, 1992a) using relatively sensitive techniques and activities were found to be too low to mediate significant drug resistance in normal lymphocytes (Damiani *et al.*, 1993). The over-expression of PGP has been associated with a number of different cancers including leukaemias, lymphomas, myelomas and sarcomas (Bell *et al.*, 1985; Bourhis *et al.*, 1989; Chan *et al.*, 1990; Goldstein *et al.*, 1989 and 1990) suggesting a poor prognosis for chemotherapy.

The mdr-1 gene has been fully cloned and sequenced (Chen *et al.*, 1986). Sequence analysis of mdr-1 and antibody localisation studies (Yoshimura *et al.*, 1989) has shown PGP to contain 1280 AAs with 12 transmembrane domains formed into two homologous halves of 6 domains each. A large intracytoplasmic loop in both halves contain the proposed ATP binding sites. An alternative model for the structure of PGP has also been suggested where transmembrane domains 8 and 9 are extracellular and is based on data from an *in-vitro* translation and translocation system (Zhang *et al.*, 1991). Sequence homologies with the ATP binding sites of other energy dependant transporters (Chen *et al.*, 1986; Gros *et al.*, 1986b; Gerlach *et al.*, 1986) have shown similarities with the ABC ATP binding cassette family (Ames *et al.*, 1986; Higgins *et al.*, 1990). Such family members include the cystic fibrosis transmembrane regulator (CFTR), a peptide mating factor in yeast (STE6), a chloroquine resistance pump in *plasmodium falciparum* (pfmdr), peptide transport proteins TAP 1/2 and a large variety of prokaryotic transporters. The predicted amino acid structure of PGP based upon the primary amino acid sequence, hydropathy profiles and by comparison to other ABC transporters is shown in figure 1.13.

The ability of PGP to transport drugs across cell membranes forms the characteristic of the mdr phenotype. Drug binding and transport by PGP was first demonstrated for vinblastine (Cornwell *et al.*, 1986). Since that time an extremely large and diverse range of drugs have been shown to be substrates for PGP mediated efflux (table 1.3). The exact mechanisms by which PGP can reduce the intracellular drug concentrations in MDR is still unclear. Initially, MDR phenotypes were attributed to reduced cell permeability (Ling *et al.*, 1974) and then by a one way pumping mechanism out of the cell or efflux by PGP (Gottesman *et al.*, 1988). However later evidence suggested a more complicated mechanism involving reduced influx combined with increased efflux (Gros *et al.*, 1986c; Gottesman *et al*, 1993b; Higgins *et al.*, 1992).

Figure 1.13. The predicted amino acid model and topography of the human multiple drug resistance efflux pump P-glycoprotein (PGP). The amino acid model of PGP is based upon amino acid secondary structure and hydropathy profile predictions. PGP is a 170 kDa, 1280 amino acid drug efflux pump which is composed of 12 transmembrane domains. Three N-linked glycosylation sites (spotted lines), four phosphorylation sites (P) and two ATP binding folds are predicted for PGP. (Modified from Gottesman et al., 1993).
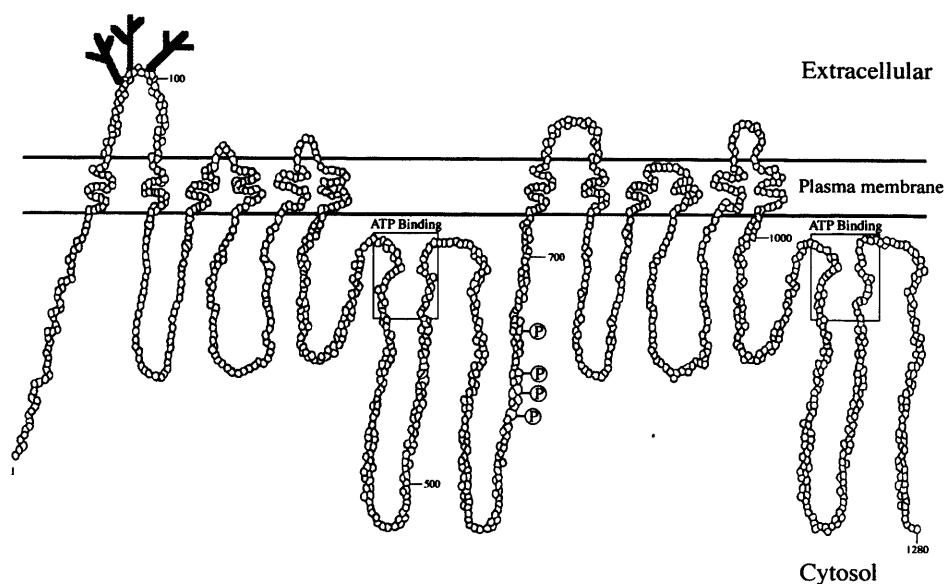
Several models of PGP action exist but the most widely accepted model is the "hydrophobic vacuum cleaner" model (Raviv et al., 1990; Gottesman et al., 1993a) and is supported by the largest body of evidence. Here it is proposed that PGP can recognise and remove drugs directly from plasma membrane, hence the vacuum cleaner analogy, and that transport occurs through a single barrel in the centre of the transporter (figure 1.14). Studies on structurally related drugs have shown relationships between increased hydrophobicity and PGP mediated transport (Zamora et al., 1988; Nogae et al., 1989). In addition efficient substrates must have partition co-efficients greater than 1 suggesting a membrane bound association with drug transport. Several studies have also shown the direct removal of drugs such as rhodamine 123 (R123) and doxorubicin from plasma membranes (Raviv et al., 1990; Weaver et al., 1991). A model of the "pore" like transporter structure of PGP in the plasma membrane is shown in figure 1.12.

Figure 1.14. Diagrammatic model of the structure of P-glycoprotein (PGP) in the plasma membrane showing a "pore" like structure through which drugs are actively exported. The three N-linked glycosylation sites (spotted lines), four phosphorylation sites (P) and two ATP binding folds predicted for PGP are shown. ATP is an absolute requirement for PGP efflux activity. Modifications in PGP phosphorylation have been suggested to alter substrate export activity through the protein. (Modified from Kartner et al., 1993)
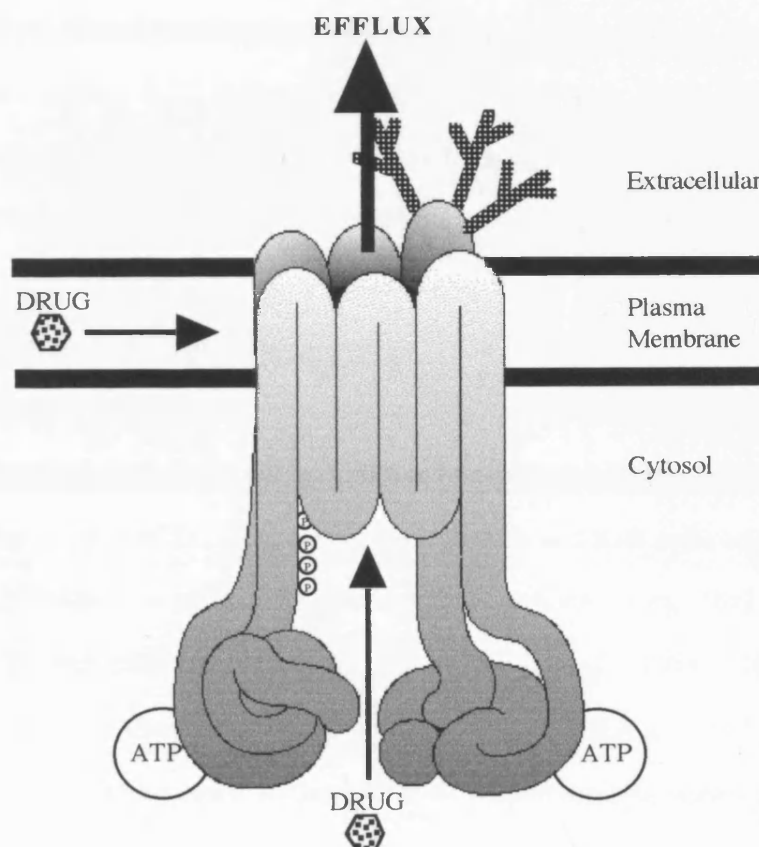
The utilisation of ATP is known to be an absolute requirement of transport activity by PGP and ATP is found to bind with high affinity (Cornwell et al., 1987; Azzaria et al., 1989; Al-Shawi et al., 1993; Sharma et al., 1995). Two ATP binding regions or folds have been identified on intracellular loops on both N-terminal and C-terminal halves of PGP and both are required for proper PGP function (Azzaria et al., 1989). These ATP binding folds are characteristic of the large ABC family of transporters, to which PGP belongs and consists of four consensus elements known as Walker A, Walker B motifs, the centre region and a linker peptide (Walker et al., 1982). The mechanisms of ATP utilisation have included a "waterwheel" model were PGP has a basal ATP requirement

and transports any drug that randomly enters the pumping channel (Sarkadi *et al.*, 1992). Another model is analogous with that of a proton pump, where the motive force for drug transport is provided by a chloride channel activity and ATP usage results from proton pumping (Gottesman *et al.*, 1993a). However it is clear that ATP activity of PGP is intimately related to MDR function and some MDR inhibitors are known which may act by uncoupling ATP utilisation from drug transport. Such chemosensitisers include progesterone which was found not to be a substrate for PGP efflux but did stimulate its ATPase activity (Yang *et al.*, 1990; Ueda *et al.*, 1992).

1.6.3 Regulation of P-glycoprotein expression

Over-expression of PGP in cells shows a direct correlation between decreased intracellular drug accumulation and the MDR phenotype (Gros *et al.*, 1986c; Shen *et al.*, 1986; Deuchars *et al.*, 1987). Overexpression of PGP in MDR cells can be conferred by gene amplification *in vitro* (Roninson, 1992) where up to 1000 times greater resistance to an inducing agent can be seen (Shen *et al.*, 1986). However gene amplification is rarely observed in clinical samples (Michieli *et al.*, 1991) and suggests that it is not of clinical relevance. However PGP expression also seems to regulated at the transcriptional level (Scotto *et al.*, 1986) and modulation of PGP expression is also conferred by protein kinase C (PKC) signalling cascades (Blobe *et al.*, 1993), although it is unclear whether its actions are due to solely to transcriptional upregulation, direct protein phosphorylation or a combination of both.

The control of mdr-1 gene expression still remains unclear. Upstream promoter sequences to the mdr gene have been isolated and sequenced (Ueda *et al.*, 1987b). The mdr-1 promoter does not contain a TATA box, but does contain several distinct regulatory motifs including a CAAT box, two GC rich regions which are putative SP-1 binding sites, a heat shock consensus element (HSE) and an AP-1 like transcription factor binding site. Figure 1.15 shows the immediate 5' upstream sequence and putative transcriptional control elements of the mdr-1 gene promoter. Overall it has

been noted that this promoter region is not dissimilar to many housekeeping genes such as dihydrofolate reductase (Madden et al., 1993). It now seems that control elements downstream of the transcriptional start site are also involved in regulation of mdr-1 transcription as altered expression is observed from mdr-1 promoter deletion mutants linked to a CAT gene (Madden *et al.*, 1993).

Figure 1.15. The 5' upstream nucleotide sequence and putative control elements of the human *mdr-1* gene promoter. Consensus AP-1, NF-IL6 and SP-1 transcription factor binding sequence elements are shown overlined. The consensus stress induced heat shock responsive sequence control elements (HSE) and metallothionein metal responsive control elements are also shown.

```
        AP-1
CAATGATTCAGCTGATGCGCGTTTCTCTACTTGCCCTTTCTAGAGAGGTG
                      |
                     -200


         HSE              NF-IL6
CAACGGAAGCCTGGAAATTCAACCTGTTTCGCAGTTTCTCGAGGAATCAG


      CAAT box  SP-1 (GC rich)
CATTCAGTCAATCCGGGCCGGGAGCAGTCATCTGTGGTGAGGCTGATTGG
           Metallothoinein IIa           |
           metal responsive element    -100


         SP-1 (GC rich)
CTGGGCAGGAACAGCGCCGGGGCGTGGGCTGAGCACAGCCGCTTCGCTCT

             Transcription start (+1)
                      ┌──►
                      |                 HSE
CTTTGCCACAGGAAGCCTGAGCTCATTCGAGTAGCGGCTCTTCCAAGCTC
```

Membrane bound PGP is found to be glycosylated and the role of post-translational glycosylation in mediating MDR activity and expression have been suggested. PGP is initially synthesised as a non-glycosylated precursor, then N-glycosylated on at least three asparagine residues (Asn 91, 94 and 99; Schinkel *et al.*, 1993) on the first extracellular loop in the mature protein (figures 1.13 and 1.14). However, it is thought that glycosylation is not required for sustaining PGP MDR efflux function as glycosylation defective cells were not defective in their ability to become drug resistant (Ling *et al.*, 1983) and tunicamycin treatment of MDR cells over a two day period

showed no decrease in drug resistance activity (Beck *et al.*, 1982). Similarly, a study by Schinkel *et al.*, 1993 demonstrated glycosylation site defective mutants of PGP show an identical pattern of drug resistance to wild type PGP at similar steady-state levels of expression. However, this study also showed that a fully glycosylation defective PGP mutant did not confer drug resistance as efficiently or express PGP at the cell surface at as high a level as wild type PGP, suggesting that glycosylation may play a role in the correct folding or efficient intracellular trafficking of PGP to the cell membrane. Further evidence for a role of PGP glycosylation in translocation to the plasma membrane comes from Kramer *et al*, 1995, who showed that prolonged treatment of an MDR cell line with tunicamycin led to a reduction in cell surface expressed PGP and MDR activity in a time dependent manner. Hence, the glycosylation of PGP may not be directly involved in mediating drug efflux activity but rather in its correct processing and transport to the cell surface.

The mature cell surface expressed form of PGP is found to be phosphorylated on at least four cytoplasmic serine residues (ser-661, -671, -667 and 683; Chambers *et al.*, 1994 and 1995) clustered together within the linker region (figures 1.13 and 1.14) and it has been suggested that phosphorylation of PGP by cellular protein kinases such as PKA and PKC may regulate its activity. Comparisons with the phosphorylation of the R-domain in the CFTR protein have suggested a similar role for the linker region of PGP which was suggested may act as a regulatory domain for drug efflux (Chambers *et al.*, 1993). Protein kinase C α (PKC α) has been shown to phosphorylate PGP *in vitro* and PKC overexpression and PGP phosphorylation was associated with a modulation of drug resistance activity in cells (Yu *et al.*, 1991; Ahmad *et al.*, 1993 and 1994). The use of cellular protein kinase stimulators such as phorbol esters and lectins have also been shown to enhance PGP phosphorylation and MDR activity in cells (Chambers *et al.*, 1992; Gupta *et al.*, 1992a). Consistent with these findings the use of protein kinase inhibitors (e.g. staurosporine) were able to reduce MDR activity of MDR cells (Chambers *et al.*, 1992; Bates *et al.*, 1993). However the use of protein kinase

activators (diacyl glycerol, PHA, TPA) used in many studies are non-specific and lead to multiple changes in cellular activity through activation of intracellular protein kinase signalling cascades. Hence, discrimination between PGP phosphorylation and mdr-1 gene transcriptional regulation in mediating MDR activity is unclear. Often the increase in PGP MDR activity after kinase stimulation is accompanied by enhanced mdr-1 gene transcription (Chaudhary et al., 1992; Gupta et al., 1992a) through phosphorylation activation of associated transcription factors. Similarly the use of the kinase inhibitor staurosporine was found to repress these effects (Chaudhary et al., 1992). In contrast to the earlier reports direct mutational analysis of the major phosphorylation sites of PGP have recently indicated that phosphorylation is not required and dispensable for MDR activity as phosphorylation deficient mutant PGP proteins were found to have identical MDR activity to wild type PGP (Germann et al., 1996). Similarly a study by Scala et al., 1995 showed that decreased phosphorylation of PGP did not correlate with drug efflux activity. Presently it is well documented that protein kinases can modulate the activity PGP mediated MDR but the nature of such mechanisms is unclear due to the complex cellular processes that these protein kinases regulate.

1.6.4 Non P-glycoprotein mediated MDR

An MDR mechanism not involving PGP mediated drug efflux has been proposed involving another similar but distinct transmembrane transporter named the multidrug resistance-associated protein (MRP). In had been noted that at least a third of clinically drug resistant cancers (Zhou et al., 1992; Hart et al., 1993) did not show evidence of mdr-1 or PGP expression and led to the discovery of MRP (Cole et al., 1992; Krishnamachary et al., 1993; Zaman et al., 1993). MRP is a 190 kDa ATP dependent transmembrane drug transporter which can confer resistance to a similar spectrum of chemotherapeutic drugs as PGP. It is structurally similar to PGP and also belongs to the same ATP-binding cassette (ABC) superfamily of transporters but only shows a 15 % amino acid sequence homology to PGP, most occurring in the nucleotide (ATP) binding domains (Walker et al., 1982). The predicted amino acid secondary structure

of MRP has been suggested to be distinct from PGP with a total of twelve transmembrane domains which are asymmetrically distributed with eight clustered in the N-terminal half and four in the C-terminal half (Cole *et al.*, 1992). Like P-glycoprotein MRP is an ATP dependent efflux pump/transporter and can similarly transport amphipathic drugs such as anthracyclines (doxorubicin) and epipodophyllotoxins (etoposide/VP-16) (Krishnamachary *et al.*, 1993; Brock *et al.*, 1995). However, unlike P-glycoprotein MRP is found to preferentially transport substrates which are anionic at physiological pH and modified by conjugation with glutathione (GSH). This suggests MRP plays a role in drug metabolism and detoxification via the GSH system (Mayer *et al.*, 1993; Müller *et al.*, 1994; Zaman *et al.*, 1995). In addition efficient PGP efflux inhibitors or chemosensitisers such as verapamil are found to be poor inhibitors of MRP mediated drug resistance (Cole *et al.*, 1989; Barrand *et al.*, 1993) The gene encoding MRP has been cloned and sequenced (Zaman *et al.*, 1993) and its 5' upstream promoter isolated (Zhu *et al.*, 1994). The MRP gene promoter was found to lack a TATA box like the mdr-1 gene promoter but also lacks a CAAT box. The promoter is GC rich with AP-1, two AP-2 and several SP-1 putative transcriptional binding elements being identified. However, to date little has been documented regarding regulation or expression of MRP gene expression through these elements. The clinical relevance or frequency of MRP in mediating clinical MDR phenotypes is currently uncertain but MRP expression has been identified in a number of tumours, including several leukaemias (Burger *et al.*, 1994; Hart *et al.*, 1994; Nooter *et al.*, 1995).

1.7 HTLV-I and MDR

The involvement of HTLV-I infection in activating an MDR phenotype stems from observations that ATL patients show very poor responses to chemotherapy. The several generations of combination chemotherapies such as COP, VEMP, VEPA, CHOP and MACOP-B have yielded little clinical improvement for patients (see section 1.3.1). The chemotherapeutic drugs cyclophosphamide, vincristine and adriamycin which are used commonly in these therapies are all found to be agents to which MDR

cells are resistant. The presence of MDR leukaemic cells in HTLV infected patients may explain the limited efficacy of such drugs and associated chemotherapies. The tax trans-activation of cellular genes and the many cellular activation strategies employed by HTLV-I provides the basis for several mechanism for mdr-1 gene activation and PGP overexpression. Reports by Kato *et al.*, 1990 and Kuwazuru *et al.*, 1990a first indicated the presence of PGP in HTLV-I induced leukaemia ATL. A preliminary western blot study using the C219 anti-PGP monoclonal antibody on ATL cell membrane fractions from 11 ATL subjects by Kato *et al.*, 1990 indicated the presence of PGP in cells from eight of these patients. Four out of six subjects before chemotherapy and four out of five subjects after relapse tested PGP positive using this method. This suggests that PGP expression is activated in HTLV-I induced leukaemia regardless of chemotherapy treatment. They speculated that chromosomal anomalies commonly found in ATL cells (chromosome 7; Ushima *et al.*, 1981) may be related to PGP enhancement as the mdr-1 gene is also located on the same chromosome (Trent *et al.*, 1991). However the study did not include appropriate non-HTLV-I infected control cell membranes and PGP has subsequently been found to be expressed at low levels on normal lymphocytes (Gupta *et al.*, 1992a and 1992b) and by the use of the C219 antibody (Damiani *et al.*, 1993). In addition mdr-1 gene expression and functional assessment of drug resistance of these ATL cells were not tested.

A report by Kuwazuru *et al.*, 1990a provided a larger investigation into the presence of PGP in ATL cells. They examined 25 ATL subjects for the presence of membrane bound PGP by western blotting using the C219 anti-PGP antibody. One of the relapsed patients was also examined for mdr-1 gene expression by RNA slot blot and semi-quantitative RT-PCR analysis. They demonstrated the presence of membrane PGP in eight of twenty ATL subjects at initial presentation and six out of six ATL patients after clinical relapse. The six relapsed patients were stated to have been PGP western blot negative before chemotherapy treatment. In addition PGP drug binding analysis on a relapsed ATL patient showed a similar pattern of photolabelling to control

MDR$^+$ cells. These data again support HTLV-I induction of PGP expression at initial presentation regardless of chemotherapy although drug treatment can potentiate such effects by possibly selecting for the population of MDR$^+$ leukaemic cells. Mdr-1 RNA was also found to be high in ATL cells from a patient after relapse compared to reference cell lines made drug resistant *in vitro* and demonstrated RNA expression equivalent to cells with between 4 and 123 times the resistance to adriamycin. However this study again did not examine cells from non-HTLV-I infected subjects and the incidence or extent of the enhancement of PGP expression in ATL patients over normal subjects was undetermined. Similarly the apparent upregulation of mdr-1 RNA in ATL cells was unclear as no reference to the constitutive level of mdr-1 RNA expression found in normal healthy lymphocytes was given. It was also undetermined whether the apparent enhancement of mdr-1 RNA occurred as a result of HTLV-I infection/transformation or chemotherapy treatment as the ATL patient studied was in relapse. It should be noted however that at the time of these studies by Kato *et al.* and Kuwazuru *et al.* PGP was not thought to be expressed in normal lymphocyte populations as PGP could not be detected in cells of the lymph nodes (Theibaut *et al.*, 1987; Sugawara *et al.*, 1988; Cordon-cardo *et al.*, 1990).

A third study by Su *et al.*, 1991, using immunostaining (C219 antibody) of frozen tissue sections and northern total RNA blotting of genes expressed by several T-cell malignancies also indicated that the mdr-1 gene was frequently expressed in ATL cells when compared to other non-HTLV-I induced T-cell malignancies. They demonstrated PGP in four out of seven (57 %) ATL tissue sections using C219 anti-PGP antibody and mdr-1 RNA was detected in three of these (43 %). This compared to only three PGP positive (13 %) and two mdr-1 RNA positive (9 %) samples out of twenty-three non-HTLV-I induced leukaemias.

The expression of membrane bound PGP and mdr-1 RNA has been demonstrated in cells from ATL patients by Kato *et al.*, 1990, Kuwazuru *et al.*, 1990a and Su *et al.*,

1991. However these preliminary studies did not examine the role of HTLV-I in mediating the MDR phenotype in MDR cells, only that membrane PGP and mdr-1 RNA could be detected in ATL cells and was enhanced after chemotherapy relapse. The functional activity of PGP in these cells and the relationships to patient disease status was also not addressed. Similarly no evidence for a mechanism of the enhancement of PGP expression in HTLV-I tumours was given. Therefore it was the purpose of the work presented here to confirm and extend these preliminary observations that suggested HTLV-I induced leukaemia is associated with an MDR phenotype mediated by the overexpression of P-glycoprotein. In addition the possible mechanisms for PGP upregulation were also investigated and are outlined in the next few sections.

1.7.1 Trans-activation of the mdr-1 gene by HTLV-I tax

Evidence for trans-activation of the mdr-1 gene comes from observations of differential expression of mdr-1 in normal tissues and cancers in the absence of gene amplification which suggests transcriptional factors are involved (Gottesman *et al.*, 1993a). Similarly, observations that increased mdr-1 RNA and PGP expression can be induced as a result of chemical or physical stress also strongly suggests a mechanism involving trans-activation in the mdr-1 gene (Chin *et al.*, 1990; Uchiumi *et al.*, 1993). Finally, increased CAT expression from mdr-1-promoter CAT reporter plasmids transfected into MDR cells (Kohno *et al.*, 1989) demonstrates transcriptional regulation in *trans*. However, there are few reports of specific nuclear factors interacting with mdr-1 promoter sequences and the mechanisms of mdr-1 gene expression is unclear. NF-IL6 (or C/EBP-β), a bZIP motif containing member of the C/EBP (CCAAT enhancer binding protein) family of transcription factors involved in regulating cytokine IL-6 transcription, has been associated with trans-activation of mdr-1 promoter (Combates *et al.*, 1994). Here, GST/NF-IL6 fusion proteins were found to specifically interact with the mdr-1 promoter, and drive expression from mdr-1 promoter-CAT reporter plasmids through a NF-IL6 like consensus element (Combates *et al.*, 1994). This data provides evidence for a possible mechanism for trans-activation of mdr-1 by the HTLV-I trans-

activator protein, tax. As described earlier tax is capable of modulating the transcription factor CREB through interactions with the basic domain of bZIPs, increasing dimerisation and DNA binding affinities, to increase transcription from CRE containing genes, including the HTLV-I LTR. A similar mechanism could be postulated for NF-IL6, whereby associations with tax via the bZIP domain may lead to increased active NF-IL6 dimers and up-regulation of mdr-1 transcription, overexpression of PGP and development of a MDR phenotype. Although no direct protein associations between tax and the CEBP family of proteins have been reported, tax has been shown to be able to modulate G-CSF expression via a NF-IL6 consensus sequence (Himes *et al.*, 1993). The presence of GC rich elements (putative SP-1 binding sites) and an AP-1 like element in the mdr-1 promoter are also other potential targets for tax trans-activation. Several GC rich elements have been demonstrated to be important for tax trans-activation of GM-CSF and G-CSF (Miyatake *et al.*, 1988; Himes *et al.*, 1993). Also HTLV-I tax up-regulates c-fos (Alexandre *et al.*, 1991), HTLV infected cells show increased AP-1 binding activity (Fujii *et al.*, 1991) and AP-1 induction may be critically involved in other gene trans-activation's such as in TGF-β1 (Kim *et al.*, 1990). Moreover, development of the MDR phenotype in mouse carcinoma cells has been associated with drug inducable, increased c-*fos* expression (Bhushan *et al.*, 1992) suggesting a possible mechanism whereby the induction of AP-1 complexes in-turn stimulates mdr-1 gene expression and MDR. A comparison of the putative 5' promoter control elements regulating mdr-1 gene expression and the transcription factor activities known to be enhanced by HTLV-I tax are shown in figure 1.16. Both of these elements have been implicated in mediating trans-activation by tax protein in other genes. The trans-activation mechanisms known to be active for tax can also be implied for the mdr-1 gene, suggesting a molecular basis for the involvement of HTLV-I infection and MDR development in the resulting cancer. Studies upon tax mediated activation of mdr may also aid in the elucidation of the complex molecular mechanisms involved in normal mdr gene regulation.

Figure 1.16. Comparison of the transcription factor responsive elements in the mdr-1 gene 5' promoter with transcription factors that are activated by the HTLV-I tax protein. The mdr-1 gene promoter contains several consensus AP-1, NF-IL6 and SP-1 transcription factor responsive elements. The mdr-1 gene has been demonstrated to be transcriptionally activated by NF-IL6 and in response to cellular stress (heat shock responsive elements or HSE). AP-1 and SP-1 transcription factor activities are known to be enhanced by the HTLV-I tax protein. Tax may also modulate the activity of the NF-IL6 transcription factor through interactions with their bZIP domains.
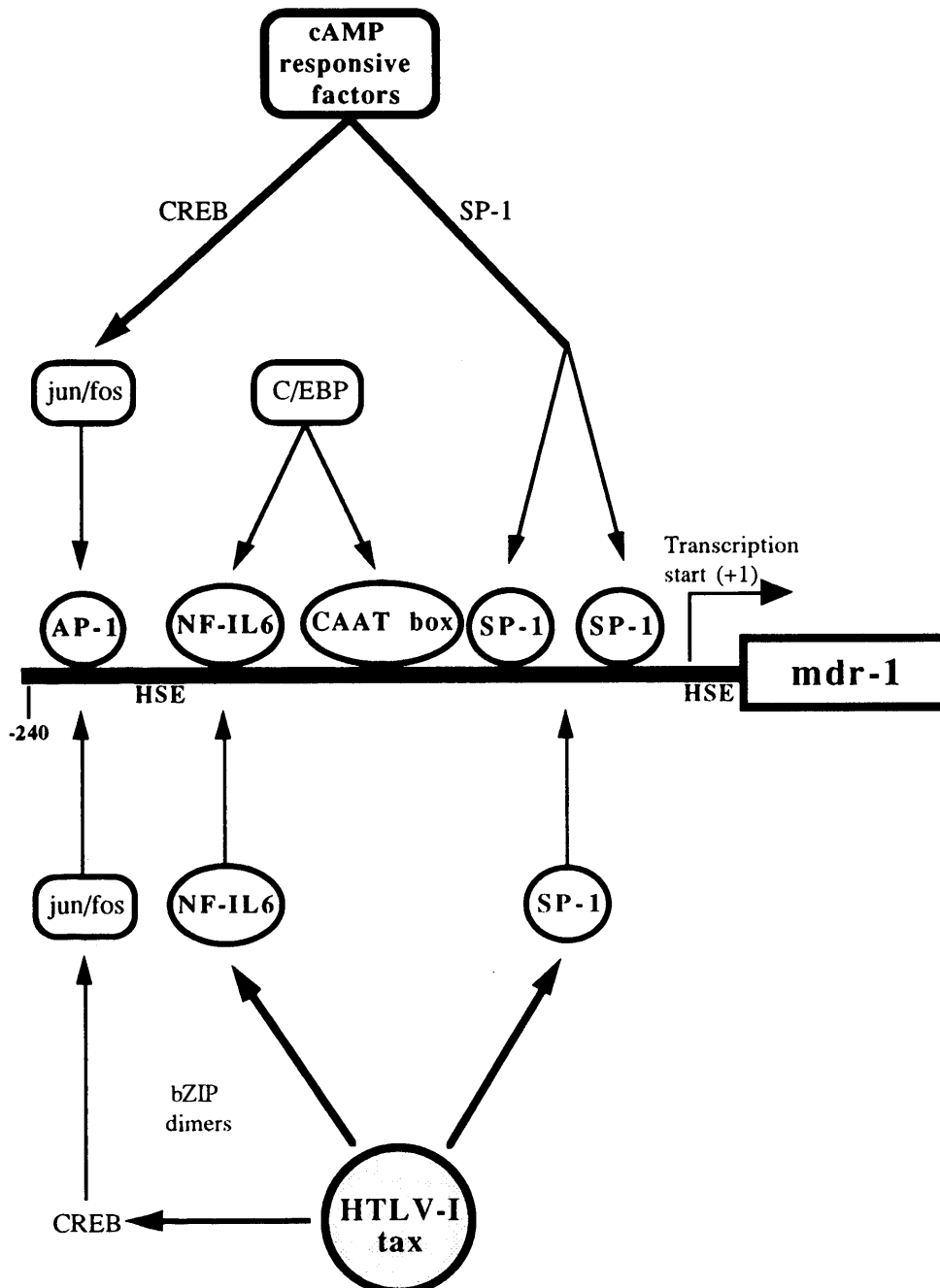
1.7.2 Mitogenic activation of mdr-1 gene expression

The upregulation of PGP mediated MDR activity and mdr-1 gene expression by cellular protein kinases A and C has been long been known and is described in section 1.6.3. Both PKA and PKC are activated in response to extracellular signals such as phorbol esters, lectins, hormones, cytokines and foreign antigens mediated through cell surface receptors. The interaction of such signals with an associated cell surface receptor activates intracellular signalling cascades, PKA and PKC, inducing a large spectrum of cellular changes including enhancement of expression of responsive genes, such as mdr-1 (Chambers *et al.*, 1992; Gupta *et al.*, 1992a; Rohlff *et al.*, 1995). In addition PKCα has been identified to directly phosphorylate membrane PGP which has been suggested to modulate its efflux activity (Yu *et al.*, 1991; Ahmad *et al.*, 1993 and 1994). The modulation of intracellular signalling cascades can be also by postulated for HTLV-I. The mitogenic activity of HTLV-I infected cells on target cells has been well documented and is thought to be mediated through co-stimulation of the CD2/LFA-3 and CD3/TCR cell surface receptor pathways (Kimata *et al.*, 1993 and 1994a). Such pathways are known to activate PKC and associated signalling pathways leading to transcriptional upregulation and activation of T-cells. Hence, a mechanism of mdr-1 gene upregulation and enhancement of MDR activity through known mitogenic stimulation pathways by HTLV-I infected cells can be postulated.

The stimulation of cytokine production by HTLV-I infection is well characterised and the IL-2/IL-2R induced Jak-STAT kinase cascades have recently been found to be constitutively activated in HTLV-I transformed cells, suggesting the modulation of these signalling pathways by HTLV-I (Migone *et al*, 1995; Xu *et al.*, 1995). It has also been demonstrated that other MAP kinases such as the stress-activated protein kinases (SAPKs)/c-jun N-terminal kinases (JNK) are constitutively activated at an early stage in cellular transformation by HTLV-I (Xu *et al.*, 1996). SAPK/JNK activation was not found to directly correlate with tax expression but modulation of these stress induced signalling cascades in HTLV-I infected cells may suggest the enhancement mdr-1 gene

expression by these kinases. HTLV-I infected cells are often found to express high levels IL-2 and IL-2R molecules and a autocrine loop mechanism of continual cellular activation has been long proposed (Arima *et al.*, 1986; Maruyama *et al.*, 1987). The HTLV-I p12^I protein has been found to specifically interact with IL-2β and γ chains and was suggested to interfere the IL-2/IL-2R signalling pathways and may play a role in cellular activation or IL-2 independent transformation (Mulloy *et al.*, 1996). Similarly tax is been demonstrated to display extracellular cytokine-like activities (Lindholm *et al.*, 1990; Marriott *et al.*, 1991) which may act in concert with other secreted cytokines such as IL-2, IL-6 and TNF to stimulate cell proliferation. Hence the stimulation of cellular proliferation induced in HTLV-I infected cells or to bystander cells as a consequence of cytokines released from HTLV-I infected cells may also enhance mdr-1 gene expression and MDR activity.

Overall, the many complex cellular processes involved in the activation, stimulation and ultimate transformation of T-cells by HTLV-I may be intimately associated with the induction of mdr-1 gene transcription, PGP expression and MDR efflux activity. Such enhancement of MDR activity by HTLV-I may be the reason for the poor prognosis often given to individuals with HTLV-I induced disease.

1.8 Aims and Objectives

Expression of recombinant Human T-cell leukaemia virus (HTLV-I) proteins

The initial aim of the project was to clone and express the proteins of HTLV-I with the view to obtaining a molecular clone, which at the time was not readily available. The cloning and expression of HTLV-I is detailed in chapter 3. An infectious molecular clone of HTLV-I would allow the greater understanding of the intricate molecular interactions between HTLV-I, the host cell and disease induction. Usually *in vitro* viral infections are performed by the co-culture of inactivated HTLV infected (donor) cells with permissive non-infected (target) cells (e.g. Miyoshi *et al.*, 1981b; Popovic *et al.*, 1983a; Kuroda *et al.*, 1992; De Revel *et al.*, 1993). However, HTLV infections are

found to be slow and inefficient often taking several months to occur with low viral titres when compared to other retroviruses. Such systems are long, costly and labour intensive requiring maintenance of cell cultures for many weeks with constant monitoring for viral transformation by syncytium formation, viral RT activity, gag protein antigen assays or PCR. In addition, infection and transformation is inefficient with very low rates of transmission (Kuroda *et al.*, 1992) reflecting the inherent difficulty of propagating HTLV *in vitro*. Such infection and transformation systems are also not quantitative and cultures already contain viral protein and nucleic acids from the donor cells making analysis of HTLV difficult and unreliable. The availability of an infectious HTLV-I clone coupled with a high efficiency expression system would circumvent many of these traditional restrictions placed upon HTLV-I study.

To overcome many problems associated with propagation of HTLV in cell culture a recombinant viral expression system would be employed in which viral protein expression is uncoupled from the inefficient process of infection. Efficient viral gene expression and production of large numbers of virus like particles (VLPs) could be induced at higher levels that seen previously. It would allow molecular genetic analysis in the context of whole virus and not just individual viral genes in isolation. Such a system would facilitate structural and functional studies of proteins encoded within the viral genome and provide insights into HTLV virion morphogenesis. A recombinant VLP expression system has been already been successfully developed and employed for the study of HIV-I RNA dimerisation within this laboratory (Haddrick *et al.*, 1996). It was the initial intention of this project to develop a similar system for HTLV based upon this method.

The HIV-I VLP expression system utilised a strong mammalian expression vector to express VLPs from an inserted HIV proviral clone. The expression vector used was based upon the plasmid pBC12/CMV/IL2 which was originally used to overexpress the cytokine IL-2 in mammalian cells (Cullen, 1986). In the HIV VLP expression

construct, pBCCX-CSF the IL-2 gene was replaced by a LTR deleted HIV-I proviral clone JR-CSF and was found to efficiently produce VLPs which specifically packaged viral RNA and were morphologically similar to wild type virions when transiently transfected into COS cells by electroporation (Haddrick *et al.*, 1996). An analogous VLP expression system could thus be envisaged for HTLV were a HTLV proviral clone would be similarly inserted into pBC12/CMV/IL2 and under the control of the CMV IE promoter. Such a construct would be able to express all viral proteins and produce large numbers of HTLV VLPs for its *in vitro* analysis. It was the initial aim of the project to construct and test such a expression system for HTLV based upon the successful recombinant HIV-I VLP expression system. The investigations into the full length cloning and expression of HTLV-I are described in chapter 3.

Another aspect of the work presented here was to identify and functionally map the regions of the HTLV-I envelope proteins responsible for receptor binding, syncytia formation and membrane function. In addition at that time it was believed that the unique mitogenic activity of HTLV-I was conferred, at least in part, by the viral surface envelope glycoproteins (Duc Dodon *et al.*, 1987; Gazzolo *et al.*, 1987). The functional mapping and analysis of these functions of the envelope proteins would have lead to a greater understanding of the HTLV-I life cycle and possibly lead to the development of a vaccine directed against envelope. Indeed the characteristics of HTLV-I such as low genetic variability (Gessain *et al.*, 1992) and that in animal models rats could be protected against HTLV-I by envelope expression vectors (Shida *et al.*, 1987), and rabbits immunised against HTLV-I (Kataoka *et al.*, 1990) suggested the feasibility of such a vaccine. The use of an infectious molecular clone of HTLV-I would have greatly facilitated such a study but at the time one was not available and the envelope genes were cloned and expressed in isolation and on pseudotyped virus particles. Such molecular clones of HTLV-I envelope would be easily mutated or deleted and their effects upon envelope function could be determined allowing a functional map to be

derived. The investigation into the development of a HTLV-I envelope expression system are detailed in chapter 3.

Due to the technical difficulties in manipulating HTLV-I proviral genomes *in vitro* and the complex nature of HTLV-I expression *in vivo*, the production of a molecular HTLV-I clone which was infectious and a working envelope expression system was not obtained. Since the start of the work several infectious molecular clones of HTLV-I have been isolated and characterised (Kimata *et al.*, 1994b; Derse *et al.*, 1995; Zhao *et al.*, 1995). Similarly the functional mapping of the HTLV-I envelope glycoproteins have subsequently been described (Delamarre *et al.*, 1994; Paine *et al.*, 1994). In addition several studies have indicated that the envelope glycoproteins may not actually directly confer mitogenic activity but that other virally induced or modified cell surface markers may be involved (Kimata *et al.*, 1993 and 1994a). Hence the development of similar systems and clones was not pursued. However, the development of several techniques and cloning of several functional HTLV-I proteins during these initial investigations allowed the mechanistic analysis of the involvement of HTLV-I in mediating MDR phenotypes, which is described in chapter 4. The isolation, cloning and expression of HTLV-I proteins is described in Chapter 3.

The role of HTLV-I infection in multiple drug resistance (MDR)

Concurrently with the cloning and expression of HTLV-I proteins investigations were started into the role of HTLV-I in mediating multiple drug resistance (MDR) phenotypes, with a view to clarify the molecular mechanisms and clinical significance to HTLV-I infected individuals. A link between HTLV-I infection and MDR has been previously suggested and a molecular basis for the induction of drug resistance phenotypes in HTLV infected cells seems likely based on evidence outlined above. It was the purpose of the following study to confirm and extend the initial observations of PGP expression in cells from ATL patients (Kato *et al.*, 1990; Kuwazuru *et al.*, 1990a; Su *et al.*, 1991). In addition to the detection of membrane bound PGP a functional

assay of PGP mediated MDR activity was employed based on the sensitive rhodamine 123 (R123) dye efflux from cells (Davies *et al.*, 1996). The R123 dye efflux assay combined with FACs analysis also allows the quantitative analysis of functional MDR cell populations. The range of HTLV-I infected subjects tested was expanded to encompass subjects of different disease status including TSP/HAM and asymptomatic HTLV-I carriers. The level of PGP expression was directly examined by quantitative RT-PCR analysis of mdr-1 mRNA in these subjects. The experiments were also conducted with reference to a panel of non-HTLV-I infected control subjects in order to assess the actual enhancement of PGP expression and activity over normal background levels. Finally investigations into the mechanism of HTLV-I induced MDR activity were examined by assessing the effect of HTLV-I cells and HTLV-I tax trans-activation protein on mdr-1 gene expression and PGP activity.

The investigations into the role in HTLV-I in mediating MDR phenotypes are presented in chapter 4. The study demonstrated the presence of significant MDR activity in circulating fresh PBMCs of the majority of HTLV-I infected individuals tested regardless of disease type or progression. The MDR activity as determined by R123 dye efflux MDR assays and quantitative RT-PCRs was found to be mediated predominantly by PGP and associated with enhanced mdr-1 gene expression. The level of MDR activity found in HTLV-I infected individuals was not found in healthy non-HTLV-I infected control subjects. In addition a mechanism of MDR induction by HTLV-I infection can be suggested as the HTLV-I tax protein and HTLV-I cell co-culture are able to upregulate the expression of the mdr-1 gene.

CHAPTER 2

Materials and methods

2.1 General techniques and protocols

2.1.1 Agarose gel electrophoresis of nucleic acids

Separation of DNA fragments (>300 bp) were performed using 0.8 to 2.0 % agarose (ICN biochemicals, genetic technology grade) melted in 1x TAE buffer containing 0.5 μg/ml ethidium bromide. Molten agarose was poured into slab gel trays and allowed to solidify. DNA samples were mixed with an equal volume of DNA loading dye (0.25 % bromophenol blue, 40 % sucrose) before loading. 0.5 μg λ DNA (*Hind*III cut) or 0.25 μg Φx174 DNA (*Hae*III cut) was also loaded for use as reference DNA size makers (Gibco). Gels were electrophoresed in 1x TAE at 8 V/cm. Separated DNA fragments were then visualised under UV light.

High resolution agarose gel electrophoresis (DNA <300 bp) were performed in 3 % GTG NuSieve agarose (FMC Bioproducts) melted in 1x TBE containing 0.5 μg/ml ethidium bromide. Samples were prepared and gels electrophoresed in 1x TBE as described above.

2.1.2 Purification of nucleic acids by phenol extraction

Nucleic acid purifications by phenol extraction were performed using liquefied phenol (Fisons chemicals) equilibrated with 0.1 M Tris-HCl pH 8. Generally, an equal volume of phenol was added to a sample, mixed by inversion and centrifuged in a microfuge at 13,000 rpm for 5 minutes at room temperature. The upper aqueous phase was carefully removed and transferred to fresh tubes. Samples were then extracted with an equal volume of a 50:50 (v/v) mix of phenol:chloroform and then with

an equal volume of chloroform as described above. After phenol purification nucleic acids were then concentrated by ethanol precipitation (see section 2.1.4).

2.1.3 G-25 Sephadex gel filtration column purification of nucleic acids

Low molecular weight contaminants were removed from high molecular weight nucleic acid samples and short oligonucleotides using G-25 Sephadex gel filtration spin columns. G-25 Sephadex (Sigma) was sterilised by autoclaving in 2-3 times the bed volume of TE buffer. A 1 ml syringe casing (plunger removed) was blocked at the dispensing end with polyallomer wool. The syringe was the packed to the 1 ml mark with G-25 Sephadex by several rounds of packing and centrifugation to 1000 rpm in a Mistral MSE3000i centrifuge. The G-25 Sephadex column was then washed in an appropriate elution buffer (normally TE or H_2O) by addition of 250 μl buffer and centrifugation at 2500 rpm for 30 seconds. A maximum 100 μl volume of sample was applied to the column and the purified eluant collected during centrifugation at 2500 rpm for 1 minute.

2.1.4 Concentration of nucleic acids by ethanol precipitation

Concentration of nucleic acids was routinely performed by ethanol precipitation. Generally 0.1 volumes of 10M NH4Ac and two volumes of 100 % ethanol were added to a given volume of sample and nucleic acids allowed to precipitate either on dry ice/-70°C for 20 minutes or -20°C for at least 1 hour. Nucleic acids were pelleted by centrifugation in a microfuge at 13,000 rpm for 15 minutes. All ethanol was removed and pellets washed by the addition of 100 μl 70 % ethanol and centrifugation in a microfuge for 5 minutes. All ethanol was removed and the nucleic acid pellets dried under a vacuum source for 10 minutes. Pellets were then resuspended in an appropriate volume of desired buffer.

2.1.5 Spectrophotometric quantification of nucleic acids

The concentration of nucleic acid in nucleic acid suspensions were quantified spectrophotometrically by the optical density at 260 nm (OD_{260}). A small aliquot of a nucleic acid suspension was diluted in H_2O and transferred to quartz glass cuvettes (Hellma). The optical density at 260 nm was then measured in an Ultraspec-III spectrophotometer (Pharmacia) blanked against H_2O. Only optical density values within the linear detection range of between 0.1 to 1.0 were accepted and nucleic acid dilutions were adjusted accordingly.

Nucleic acid concentrations were then calculated using the formula,

$$\text{Concentration } (\mu g/ml) = OD_{260} \ (ODu) \times \text{Dilution} \times \text{Constant}$$

Constant = $50 \ \mu g \ ml^{-1} \ ODu^{-1}$ for double stranded DNA

                 $40 \ \mu g \ ml^{-1} \ ODu^{-1}$ for single stranded RNA

                 $37 \ \mu g \ ml^{-1} \ ODu^{-1}$ for single stranded DNA oligonucleotides

Purity of nucleic acid solutions were also assessed by comparison of the optical density of nucleic acid solutions at both 260 nm and 280 nm. An OD_{260}/OD_{280} ratio of between 1.7 and 2.0 was considered to be sufficiently pure for most applications. Nucleic acid suspensions with ratios below 1.7 were deemed impure and typically re-purified by phenol extraction and ethanol precipitation.

2.2   Molecular biology - DNA techniques

2.2.1 Restriction endonuclease digestion of DNA

Most restriction endonucleases used were purchased from Gibco-BRL and digestions performed in the recommended 1x REact buffers (Gibco) using a minimum of 2 U/μg DNA enzyme concentration for 1 hour at an appropriate temperature. Total enzyme added never exceeded 10 % of the total reaction volume in order to prevent star activity

and enzyme inhibition. *Dra*III restriction endonuclease was purchased from New England Biolabs (NEB) and digestions were performed in their recommended buffer as described above. The exact reaction conditions and cleavage sites for the individual enzymes used are shown in table 2.1.

Table 2.1. Restriction endonucleases and reaction conditions

Restriction endonuclease	REact Buffer*	Cleavage site	Temp. of reaction (^{o}C)
*Bam*HI	3	G / GATCC	37°C
*Cla*I	1	AT / CGAT	37°C
*Dra*III	(NEB buffer 3 + BSA)†	GACNNN / GTG	37°C
*Eco*RI	3	G / AATTC	37°C
*Hind*III	2	A / AGCTT	37°C
*Pst*I	2	CTGCA / G	37°C
*Sal*I	10	G / TCGAC	37°C
*Sau*3AI	4	N / GATC	37°C
*Sma*I	4	CCC / GGG	30°C
*Sst*I	2	GAGCT / C	37°C
*Xba*I	2	T / CTAGA	37°C
*Xho*I	2	C / TCGAG	37°C

*1x REact buffers supplied by Gibco-BRL;

REact 1 = 50 mM Tris-HCl pH 8, 10 mM MgCl$_2$.

REact 2 = 50 mM Tris-HCl pH 8, 10 mM MgCl$_2$, 50 mM NaCl.

REact 3 = 50 mM Tris-HCl pH 8, 10 mM MgCl$_2$, 100 mM NaCl.

REact 4 = 20 mM Tris-HCl pH 7.4, 5 mM MgCl$_2$, 50 mM KCl.

REact 10 = 100 mM Tris-HCl pH 7.6, 10 mM MgCl$_2$, 150 mM NaCl.

†1x NEB buffer 3 + BSA;

= 50 mM Tris-HCl pH 7.9, 10 mM MgCl$_2$, 1 mM DTT, 100 mM NaCl.

Reactions were supplemented with 100 μg/ml BSA.

2.2.2 Nuclease BAL-31 exonuclease digestion of DNA ends

Nuclease BAL-31 possesses both 3' and 5' exonuclease activities which is able to degrade DNA in both 3' and 5' directions from a restriction endonuclease cut. It was used to create non-specific partial deletions in plasmids from both sides of a defined restriction endonuclease digestion.

Typically, 2.5 units of nuclease BAL-31 (NEB) was incubated with 5 μg restriction endonuclease digested plasmid DNA in the supplied 1x nuclease BAL-31 buffer (20 mM Tris-HCl pH 8, 0.6 M NaCl, 12 mM $MgCl_2$, 12 mM $CaCl_2$, 1 mM EDTA) in a final volume of 500 μl at 30°C. Incubation times were varied in order to produce exonuclease deletions of varying lengths with longer incubation periods producing larger deletions. Nuclease digestions were performed between 1 and 15 minutes at 30°C with 100 μl reaction aliquots being removed after 1, 2, 4, 8 and 15 minutes. The removed reaction aliquots were immediately inactivated by the addition of an equal volume of phenol. All aliquots were purified by standard phenol extraction and DNA concentrated by ethanol precipitation. Each aliquot produced deletions of increasing size with around 100 bp being removed per minute incubation.

2.2.3 Dephosphorylation of 5'-DNA ends

The 5'-phosphates of DNA ends were removed from plasmid vectors prior to ligation to DNA inserts by treatment with calf intestinal alkaline phosphatase (CIAP). The moles of ends of linearised DNA of a given length (bp) was calculated by the formula;

$$\text{Moles DNA ends} = \frac{2 \times (\text{g DNA})}{(\text{number bp}) \times (660 \text{ daltons/bp})}$$

Typically, 0.1 U CIAP (Gibco) per pmol recessed DNA ends were incubated in the supplied 1x phosphatase buffer (50 mM Tris-HCl pH 8.5, 0.1 mM EDTA) at 37°C for 30 mins. For blunt DNA ends, 1 U CIAP per pmol DNA ends was incubated in 1x

phosphatase buffer at 50°C for 1 hour. After dephosphorylation CIAP was removed by phenol extraction and DNA concentrated by ethanol precipitation.

2.2.4 Ligation of DNA fragments

Typically DNA inserts were ligated into dephosphorylated plasmid vectors at a 3:1 molar ratio of insert:vector using T4 DNA ligase (Gibco). Cohesive end ligations were performed at 30 fmol plasmid vector DNA ends and 90 fmol insert DNA ends at 20°C for 2 hours. Blunt end ligations were performed at 60 fmol plasmid vector DNA ends and 180 fmol insert DNA ends at 14°C for 24 hours. All ligations were performed in 10 μl reaction volumes containing 1x Ligation buffer (50 mM Tris-HCl pH 7.6, 10 mM $MgCl_2$, 1 mM ATP, 1 mM DTT, 5 % (w/v) PEG-8000) and 0.5 U T4 DNA ligase.

2.2.5 Purification of DNA fragments by extraction from agarose gels

a) Large scale plasmid gel purification

The following gel purification method was used for DNA fragments over 3.0 kb in length or when quantity of DNA to be recovered exceeded 2 μg. DNA samples to be extracted were prepared and electrophoresed as described in section 2.1.1 but adjusting the well size such that approximately 1μg of the desired DNA fragment spanned 1 cm of well. Gels were visualised under UV and the desired fragment cut out using a sterile scalpel. The gel slice was then placed into dialysis tubing containing 1 ml of 0.1x TAE and DNA electroeluted in 0.1x TAE at 200 V for 60 to 90 minutes. The current was reversed for 1 minute and the buffer removed from the dialysis tubing. The tubing was rinsed several times with 1 ml fractions of TE and each fraction combined. Pooled fractions were extracted with equal volumes of isobutanol until the sample volume reduced to approximately 500 μl. The samples were then extracted at least three times with equal volumes of phenol and once with an equal volume of chloroform. DNAs were precipitated by the addition of 0.1 volumes of 10M NH4Ac and two volumes of 100 % ethanol at -20°C for a minimum of 1 hour. Precipitated DNAs were pelleted in a microfuge at 13,000 rpm for 15 minutes, washed in 70 % ethanol and vacuum dried

for 10 mins. DNA pellets were then resuspended in an appropriate volume of TE and the concentration determined spectrophotometrically by the optical density at 260 nm. Typically yields of around 50 % DNA recovery were achieved.

b) High yield LMP agarose gel purification

DNA fragments less than 3 kb in length or low abundance DNA (i.e. PCR products) were extracted from low melting point (LMP) agarose gels based on a modified freeze/thaw extraction procedure (Qian *et al.*, 1991). A maximum of 1 μg DNA fragment was electrophoresed in a 1 cm well of a 1-2 % LMP agarose (Ultra Pure, Gibco) gel in 1x TAE buffer containing 50 μg/ml EtBr at 7 V/cm. The DNA fragment was visualised under UV light and the 1 cm strip cut from the gel using a sterile scalpel. The 1 cm DNA fragment was cut into small pieces and transferred into a 1.5 ml microfuge tube. 1 ml of TE was added and agarose was melted by heating at 70°C for 10 minutes. Agarose was precipitated by snap freezing in a dry ice/ethanol bath for 5 minutes and thawing gently to room temperature. The agarose was then pelleted by centrifugation at 13,000 rpm for 5 minutes in a microfuge. The DNA containing supernatant was transferred to fresh tubes, phenol extracted and ethanol precipitated as described in sections 2.1.2 and 2.1.4. DNAs were resuspended in an appropriate volume of TE and the concentration determined spectrophotometrically by the optical density at 260 nm. Typically yields of around 70-90 % DNA recovery were achieved.

2.2.6 Transformation of Bacterial cells

a) CaCl2 transformations

CaCl2 competent cell preparation

From the frozen glycerol stocks, *E. coli*. cells were streaked out to single colonies on 2TY agar plates and grown at 37°C for 14-18 hours. A single colony was then inoculated into 10 ml 2TY broth and grown at 37°C with shaking (200 rpm) for 14-18 hours. The 10 ml starter culture was then inoculated into 500 ml pre-warmed 2TY broth and grown rapidly at 37°C with shaking (200 rpm) until OD_{600} = 0.6 to 0.7.

Cells were transferred to cold centrifuge pots and chilled on ice for 10 minutes. Cells were pelleted at 5000 rpm, 4°C for 5 minutes in a pre-chilled Sorvall GS-3 rotor and RC5B centrifuge. The cells were then resuspended in 125 ml cold 30 mM $CaCl_2$ and chilled on ice for 20 mins. Cells were pelleted at 5000 rpm, 4°C for 5 mins in a pre-chilled rotor and centrifuge and then resuspended in 20 ml cold 30 mM $CaCl_2$ + 10 % glycerol. The competent cells were aliquot in 500 µl volumes and rapidly frozen in a dry ice/ethanol bath. Competent cells were stored at -70°C for a maximum of 6 months.

$CaCl_2$ transformation

Frozen $CaCl_2$ competent cells were allowed to thaw gently on ice before use. 10-200 ng DNA in a maximum volume of 5 µl was added to 100 µl $CaCl_2$ competent cells and incubated on ice for 1 hour. Cells were heat shocked at 42°C for 2 minutes and then incubated on ice for a further 5 minutes. 900 µl 2TY was added and the cells and incubated at 37°C with rapid shaking (>200 rpm) for 1 hour. Cells were pelleted by centrifugation at 13,000 rpm for 5 minutes in a microfuge and resuspended in 100 µl 2TY medium. All the cells were plated on 2TY agar plates containing an appropriate antibiotic and grown up at 37°C for 14-18 hours.

b) Electro-transformation of bacterial cells

High efficiency transformation of bacterial cells by electroporation was done in an Invitrogen Electroporator-II using modified versions of the recommended protocols provided. This method was used routinely in standard cloning experiments.

Electro-competent cell preparation

From the frozen glycerol stocks, *E. coli.* cells were streaked out to single colonies on 2TY agar plates and grown at 37°C for 14-18 hours. A single colony was then inoculated into 25 ml 2TY broth and grown at 37°C with shaking (200 rpm) for 14-18 hours. The 25 ml starter culture was then inoculated into 500 ml pre-warmed 2TY

74

broth and grown rapidly at 37°C with shaking (200 rpm) until OD$_{550}$ = 0.5 to 0.6. Cells were transferred to cold centrifuge pots and chilled on ice for 30 minutes. Cells were pelleted at 3500 rpm, 0°C for 15 minutes in a pre-chilled Sorvall GS-3 rotor and RC5B centrifuge. Cells were washed by gentle resuspension in 125 ml cold H$_2$O and then pelleting at 3500 rpm, 0°C for 15 minutes. Cells were washed again in 75 ml H$_2$O and pelleted at 3500 rpm, 0°C for 15 minutes. Cells were gently resuspended in 5 ml cold 10 % glycerol (in H$_2$O) and pelleted at 5800 rpm, 0°C for 15 minutes. Finally the cells were resuspended in 1 ml cold 10 % glycerol (in H$_2$O) and snap frozen in a dry ice/ethanol bath in 40 μl aliquots. Competent cells were stored at -70°C for a maximum of 6 months.

Electro-transformation of cells

Frozen electro-competent cells were allowed to thaw gently on ice before use. 0.01-1 ng supercoiled DNA in a maximum volume of 1 μl or 1 μl of a ligation reaction was mixed with a 40 μl aliquot of electro-competent cells. The DNA/cells mix was transferred into chilled electroporation cuvettes (0.1 cm gap, Invitrogen) and electroporated at 1500 V, 50 μF, 150 Ω using an Invitrogen electroporator-II. Electroporated cells were immediately plunged back onto ice. 1 ml SOC medium was added and cells incubated at 37°C with rapid shaking (>200 rpm) for 1 hour. Cells were pelleted by centrifugation at 13,000 rpm for 5 minutes in a microfuge and then resuspended in 100 μl SOC medium. Cells were then plated at 1 %, 10 % and 89 % of the total volume and grown at 37°C for 14-18 hours.

2.2.7 Klenow fragment fill-in of recessed 5'-DNA overhangs

Restriction enzyme digested double stranded DNA which generated recessed 5'-overhangs could be "filled-in" in order to create blunt-ends using the large fragment of DNA polymerase-I (Klenow fragment). This practice was used in order to facilitate cloning between normally incompatible recessed and blunt DNA ends generated by restriction enzyme digestion. 1 μg of recessed 5'-overhang DNA was incubated in 1x

75

REact 2 buffer (See section 2.2.1) with 16.6 µM each dNTP and 0.5 U large fragment of DNA polymerase-I (Gibco) in a final reaction volume of 30 µl at 20°C for 15 minutes. DNA was purified by phenol extraction and recovered by ethanol precipitation.

2.2.8 Mung bean nuclease digestion of 3'-DNA overhangs

Restriction enzyme digested double stranded DNA which generated recessed 3'-overhangs could be made blunt-ended by digestion of the single stranded overhangs with mung bean nuclease. This was used in order to facilitate cloning between two normally incompatible recessed DNA ends generated by restriction enzyme digestion. 1 µg of 3'-overhang DNA was incubated in 1x mung bean nuclease buffer (10 mM NaOAc pH 5.0, 50 mM NaCl, 0.1 mM ZnOAc, 1 mM L-cysteine, 5 % (v/v) glycerol, 0.5 mg/ml calf thymus DNA) and 50 U mung bean nuclease (Gibco) in a final volume of 200 µl at 37°C for 15 minutes. DNA was purified by phenol extraction and recovered by ethanol precipitation.

2.2.9 Small scale Triton-boil mini-preparation of plasmid DNA

Single colonies of plasmid containing *E. coli* cells were inoculated into 1.5 ml 2TY medium containing an appropriate antibiotic and grown up at 37°C with shaking (200 rpm) for 14-18 hours. Cells were pelleted by centrifugation at 13,000 rpm for 5 minutes in a microfuge. Cells were then resuspended in 200 µl cold STET buffer (8 % (w/v) sucrose, 50 mM Tris-HCl pH 8, 50 mM EDTA , 0.5 % Triton X-100, 1 mg/ml lysozyme). The cell suspensions were boiled for 2 minutes then immediately incubated on ice for 10 minutes. Cell debris was pelleted by centrifugation at 13,000 rpm for 10-15 minutes in a microfuge and discarded. Nucleic acids were recovered from the supernatants by ethanol precipitation. Pellets were resuspended in a final volume 20 µl TE buffer containing 50 µg/ml RNase A. Typically, 1-2 µl of DNA was sufficient for endonuclease restriction digestion.

2.2.10 Large scale CsCl maxi-preparation of plasmid DNA

Plasmid containing *E. coli*. cells were streaked out to single colonies on 2TY agar plates containing an appropriate antibiotic and grown at 37°C for 14-18 hours. A single colony was then inoculated into 5 ml 2TY broth + antibiotic and grown at 37°C with shaking (200 rpm) for 14-18 hours. The 5 ml starter culture was then inoculated into 500 ml 2TY broth + antibiotic and grown at 37°C with shaking (200 rpm). Non-HTLV containing plasmids were grown until OD_{600} = 0.7 to 0.9 (typically 3-5 hours) then chloramphenicol was added to a final concentration of 150 µg/ml then left overnight at 37°C with shaking (200 rpm).

Cells were harvested on ice and pelleted for 10 minutes at 5000 rpm, 4°C in a Sorvall GS3 rotor and RC5B centrifuge. The supernatants were decanted off and the cell pellet resuspended in 2.5 ml ST buffer (25 % (w/v) sucrose, 50 mM Tris-HCl pH 8). 1 ml of a 20 mg/ml lysozyme solution was added and incubated on ice for 10 minutes. 1.5 ml of 0.5 M EDTA pH 8 was added and incubated on ice for 10 minutes. Finally 2.5 ml Triton lysis mix (1.5 % (v/v) Triton X-100, 50 mM Tris-HCl pH 8, 50 mM EDTA pH 8) was added and gently mixed by inversion. The cells were then immediately centrifuged for 45 minutes at 20,000 rpm, 4°C in a Sorvall SS-34 rotor and RC5B centrifuge. Supernatants were decanted into fresh 15 ml graduated tubes and 1 g CsCl was added per ml of supernatant. CsCl was completely dissolved by incubation at 37°C for 5 minutes. Partial gradients were formed by low speed centrifugation for 10 minutes at 2500 rpm, room temperature in a MSE3000i centrifuge. The lower aqueous phase was transferred to several Beckman 3.9 ml heat seal tubes containing 25 µl 10 mg/ml Ethidium bromide using a Pasteur pipette. The tubes were heat sealed and centrifuged for either 5 hours at 100,000 rpm or for 15-18 hours at 80,000 rpm at 20°C in a Beckman TLN-100 rotor and Optima TL ultracentrifuge.

Plasmid bands were extracted using 20g x 1" needles and 5 ml syringes and transferred to fresh 15 ml graduated tubes. Ethidium bromide was removed by extraction at least

three times with equal volumes of $CsCl/H_2O$ saturated isopropanol. Plasmids were diluted with three volumes of TE and precipitated by addition of two volumes of 100 % ethanol with incubation at -20°C for at least 3 hours. Plasmids were pelleted by centrifugation for 15 minutes at 2500 rpm, room temperature in a MSE3000i centrifuge. DNA pellets were washed in 70 % ethanol for 5 mins at 2500 rpm, room temperature in a MSE3000i centrifuge and vacuum dried for 10-20 minutes. Plasmids were resuspended in appropriate volumes of TE buffer and the concentration determined spectrophotometrically by the optical density at 260 nm.

Large scale preparation of HTLV-I insert containing plasmids

Due to the instability and relative toxicity of retrovirus containing plasmids within bacterial cells (Cunningham *et al.*, 1993; Peden, 1992) large scale preparations could not be performed using the standard CsCl protocol outlined above. Throughout this project it has been observed that larger culture volumes (>50 ml) are prone to deletion of HTLV-I gene inserts in plasmids but small culture volumes HTLV plasmids are far more stable. Therefore large quantity HTLV-I plasmid preparations were performed combining the grow-up and isolation steps of the Triton-boil mini-preparations and a CsCl gradient purification step.

Briefly, a single colony was picked from a streak plate and inoculated into a large volume of 2TY + antibiotic media. This culture was then split into multiple 1.5 ml fractions and grown up at 37°C with shaking (200 rpm) for 14-16 hours. Cells were pelleted, lysed in STET buffer and crude nucleic acid containing supernatants isolated (but not ethanol precipitated) as described for Triton-boil mini-preparations (section 2.2.9). All cell supernatants were combined and 1 g per ml CsCl was added. Plasmids were purified by ultracentrifugation as described for the large scale CsCl plasmid preparations (section 2.2.10). Plasmids were resuspended in appropriate volumes of TE buffer and the concentration determined spectrophotometrically by the optical density at 260 nm.

2.2.11 M13 phage manipulations

JM103 cells were used as standard hosts for M13 phage and were routinely grown on minimal media agar plates at 37°C for 24-48 hours in order to maintain the F' pilus.

a) M13 DNA transformation and phage stocks

5 µl of M13 RF DNA or M13/insert ligations were added to 100 µl CaCl$_2$ competent JM103 cells and transformed by heat shock at 42°C (section 2.2.6a). Heat shocked cells were then mixed with 3 ml molten soft top 2TY agar containing 50 µl 2 % X-gal and 25 µl 2.5 % IPTG and poured onto 2TY agar plates. The soft top agar was allowed to set and the plates incubated at 37°C for 14-16 hours. Recombinant M13 phages were identified as clear plaques and removed using a Pasteur pipette tip then expelled into 1 ml 2TY media. Phage was eluted for at least 1 hour before use and these stocks stored at 4°C.

b) Single stranded M13 DNA preparation (Template preparation)

JM103 cells were streaked out to single colonies on minimal media agar plates and grown at 37°C for 24-48 hours. A single colony was then inoculated into 1 ml 2TY media and grown up at 37°C with shaking (200 rpm) for 14-18 hours. 1 ml 2TY media was inoculated with 50 µl of the overnight JM103 culture and 10 µl of a phage stock (see above). The culture was incubated at 37°C with rapid shaking (>200 rpm) for 5 hours. Cells were pelleted out at 13,000 rpm for 5 minutes in a microfuge. Phage containing supernatants were transferred to fresh tubes and 200 µl PEG solution (10 % (w/v) PEG-8000, 2.5 M NaCl) was added. Phage was precipitated at room temperature for 45 minutes and pelleted at 13,000 rpm for 15 minutes in a microfuge. Pellets were resuspended in 100 µl 1M NaOAc pH 7. 100 µl phenol:CHCl$_3$:IAA (50:50:1) was added, mixed and centrifuged at 13,000 rpm for 5 minutes. The upper aqueous phase was removed, mixed with 100 µl CHCl$_3$:IAA (50:1) and centrifuged at 13,000 rpm for 5 minutes. The upper aqueous phase was removed and mixed with 200 µl 100 % ethanol. Nucleic acids were then precipitated at -20oC overnight then pelleted by

centrifugation at 13,000 rpm for 15 minutes. Pellets were washed in 100 μl 70 % ethanol at 13,000 rpm for 5 minutes and vacuum dried for 10 minutes. Single stranded template DNA was then resuspended in 20 μl TE.1 (10 mM Tris-HCl pH 8, 0.1 mM EDTA). Typical DNA concentrations of 200 to 400 ng/μl were obtained and verified by agarose gel electrophoresis.

c) Double stranded M13 DNA preparation (RF preparation)

JM103 cells were streaked out to single colonies on minimal media agar plates and grown at 37°C for 24-48 hours. A single colony was then inoculated into 1 ml 2TY broth and grown up at 37°C with shaking (200 rpm) for 14-18 hours. 1 ml 2TY media was inoculated with 50 μl of the overnight JM103 culture and 10 μl of a phage stock. The culture was incubated at 37°C with rapid shaking (>200 rpm) until the OD_{600} = 0.5 to 0.6 (approximately 3-4 hours). This 50 ml culture was then inoculated into 500 ml 2TY broth and incubated at 37°C with shaking (200 rpm) for 14-18 hours. Cells were pelleted at 5000 rpm, 4°C for 5 minutes and double stranded M13 RF DNA purified as described for large scale CsCl plasmid purifications in section 2.2.10.

2.2.12 Manual 35S-dATP DNA sequencing

All manual sequencing was performed using reagents contained in the Sequenase v2.0 sequencing kit (except primers and radioactivity) from Amersham by modified versions of their recommended protocols. All sequencing reactions were electrophoresed on 6 % polyacrylamide TBE gradient gels.

a) Single stranded DNA sequencing

A 1.5 kb *Sph*I (5122) to *Pst*I (6729) fragment containing the env region of HTLV-I was digested with *Sau*3AI and cloned into the *Bam*HI site of M13 phage RF DNA for complete env gene sequencing (See chapter 3, section 3.4.5). Single stranded M13 templates were then prepared as described in section 2.2.11.

To 5 µl single stranded template M13 DNA, 1 µl 10 µM primer and 2 µl 5x Sequenase buffer (200 mM Tris-HCl pH 7.5, 100 mM MgCl2, 250 mM NaCl) was added and the volume made up to 10 µl. Primers were annealed by heating at 65°C for 2 minutes and slowly cooling to room temperature over a 15 to 30 minute period. 10 µl ^{35}S-dATP labelling mix (0.1x Labelling nucleotide mix (0.15 µM dCTP, dGTP and dTTP), 5 mM DTT, 5 µCi α-^{35}S dATP, 3.0 U Sequenase v2.0) was added and incubated at room temperature for 5 minutes. 3.5 µl aliquots were transferred to 4 wells of a 96 well round-bottomed microtitre plate and 3.5 µl of an appropriate termination nucleotide mix (80 µM each dNTP, 50 mM NaCl and one of either 8 µM ddATP, ddCTP, ddGTP or ddTTP) was added to each well. Termination reactions were incubated at 37°C for 5 minutes and then stopped by addition of 4 µl stop solution (95 % formamide, 20 mM EDTA, 0.05 % bromophenol blue, 0.05 % xylene cyanol FF). Sequencing reactions were denatured at 80°C for 15 minutes in a dry air oven prior to loading on PAGE gels.

b) Double stranded DNA sequencing

All double stranded template DNAs and plasmids were sequenced using the following method. Double stranded template DNAs were diluted to 1 µg/µl in a 9 µl volume (9 µg DNA total). Templates were denatured by the addition of 1 µl 2M NaOH and incubation at 37°C for 20 minutes. 1 µl of 10 µM primer, 1 µl 3M NaOAc pH 5.2 and 30 µl 100 % ethanol was added and DNAs precipitated on dry ice, 10 minutes. DNAs were pelleted by centrifugation at 13,000 rpm for 15 minutes in a microfuge, washed in 70 % ethanol and vacuum dried for 10 minutes. DNAs were resuspended in 8.5 µl 1x Sequenase buffer (40 mM Tris-HCl pH 7.5, 20 mM MgCl2, 50 mM NaCl). 8.5 µl ^{35}S labelling mix (0.25x Labelling nucleotide mix (0.375 µM dCTP, dGTP and dTTP), 5 mM DTT, 5 µCi α-^{35}S dATP, 3.25 U Sequenase v2.0) was added and incubated at room temperature for 5 minutes. 4 µl aliquots were transferred into 4 wells of a 96 well round-bottomed microtitre plate and 2 µl of an appropriate termination nucleotide mix (80 µM each dNTP, 50 mM NaCl and one of either 8 µM ddATP, ddCTP, ddGTP or ddTTP) was added to each well. The termination reactions were

incubated at 37°C for 5 minutes and stopped by the addition of 4 µl stop solution (95 % formamide, 20 mM EDTA, 0.05 % bromophenol blue, 0.05 % xylene cyanol FF). Sequencing reactions were denatured at 80°C for 15 minutes in a dry air oven prior to loading on PAGE gels.

c) Polyacrylamide gel electrophoresis (PAGE)

All polyacrylamide gel solutions were prepared from dilutions of a 40 % acrylamide stock solution. Gradient gels were formed by using 6 % acrylamide solutions containing of differing ionic strengths (0.5x TBE and 2.5x TBE). All solutions were stored in the dark at room temperature.

The 40 % acrylamide stock solution was prepared by dissolving 280 g acrylamide (BDH) and 20 g bis-acrylamide (BDH) in 1 l H_2O. This solution was de-ionised by the addition of 10 g Duolite MB 6113 mixed resin (BDH) and gentle mixing for 1 hour. The mixed resin was then removed by gravity filtration through Whatman 3MM filter papers.

0.5x TBE 6 % acrylamide top solution was prepared by dissolving 430 g urea and 150 ml 40 % acrylamide stock in 750 ml H_2O. The solution was de-ionised as described above. 50 ml 10x TBE was added and the solution made up to a final volume of 1 litre.

2.5x TBE 6 % acrylamide bottom solution was prepared by dissolving 430 g urea, 150 ml 40 % acrylamide stock and 25 g sucrose in 600 ml H_2O. The solution was de-ionised as described above. 250 ml 10x TBE and 50 mg bromophenol blue was added and the solution made up to a final volume of 1 litre.

PAGE gels were prepared by cleaning 20 x 50 cm glass sequencing plates with IMS and acetone. The sequencing plates were assembled with 0.4 mm spacers in between and the edges sealed with tape. 40 ml 0.5x TBE top solution was mixed with 0.5 %

ammonium persulphate and 0.04 % TEMED. 10 ml 2.5x TBE bottom solution was mixed with 10 % ammonium persulphate and 0.04 % TEMED. 15 ml 0.5x TBE top solution was drawn up into a 25 ml pipette followed by 10 ml 2.5x TBE bottom solution. Several air bubbles were passed through the solutions in the pipette forming the TBE gradient and the resulting solution poured slowly between the sequencing plates. The plate sandwich was then topped up to full with the remaining 0.5x TBE top solution. A 36 well (3 mm) comb was inserted and the gels allowed to set. Sequencing gels were clamped into vertical electrophoresis apparatus with a diffuser plate. Sequencing reactions were heated to 80°C for 15 minutes in a dry air oven and 2-4 µl of sequencing reaction was loaded. Gels were run in 1x TBE at a constant power of 0.045 W/cm^2 (45W). After electrophoresis gels were soaked in fixative (10 % IMS, 10 % glacial acetic acid) for 10 minutes. Gels were transferred onto Whatman 3MM filter paper and dried under vacuum at 80°C for 1 hour. Gels were then exposed to film (Hyperfilm-MP, Amersham) at room temperature for 14-16 hours. Films were developed in an Agfa-Gaevert automatic film developer.

2.2.13 Phosphorylation of oligonucleotide primers

All oligonucleotide primers were synthesised by the Protein and nucleic acid chemistries (PNAC) laboratory at Leicester University and were un-modified. Primers were phosphorylated when their 5'-ends were to be used as substrates for subsequent ligations (T4 ligase), e.g. in blunt end cloning of PCR products. 1 µg of oligonucleotide primer was incubated in 1x forward reaction buffer (70 mM Tris-HCl pH 7.6, 100 mM KCl, 10 mM MgCl$_2$, 1 mM 2-mercaptoethanol) with 1 mM ATP and 10 U T4 polynucleotide kinase (Gibco) in a final reaction volume of 20 µl at 37°C for 1 hour. Enzymes were inactivated by heating at 70°C for 10 minutes and oligonucleotides recovered by ethanol precipitation.

2.2.14 PAGE gel extraction purification of oligonucleotide primers

Denaturing PAGE purifications were performed on long oligonucleotides (>30 nts) and oligonucleotides used for long PCR work. Typically the oligonucleotides used were separated on 10 % polyacrylamide gels containing 8M Urea. The 10 % gels were prepared by mixing 125 ml 40 % acrylamide stock solution (see 2.2.12c) with 50 ml 10x TBE and 240 g urea in a final volume of 500 ml. 400 μl 10 % ammonium persulphate and 25 μl TEMED was added to 50 ml of the 10 % gel solution, poured between thick spaced (2 mm) 20x20 cm gel plates and a comb with 4 cm wells inserted. Gels were allowed to completely set before use.

75 μg of an Oligonucleotide was diluted to a final volume of 40 μl in TE buffer. 40 μl of formamide dye solution (95 % formamide, 10 mM EDTA, 0.02 % bromophenol blue, 0.02 % xylene cyanol FF) was added and boiled for 2 minutes. The oligonucleotides were loaded onto 4 cm wells and electrophoresed in 1x TBE buffer at a constant power of 20 W. Gel plates were disassembled and the gel wrapped in cling film. Oligonucleotide bands were visualised by UV shadowing whereby the gel was placed onto a TLC plate and illuminated from above with UV light. Oligonucleotide bands were cut from the gel using a sterile scalpel. The gel slice was cut into small pieces and transferred to a 1.5 ml microfuge tube. 1 ml elution buffer (10 mM Tris, pH 8, 0.3 M NaOAc, 1 mM EDTA, 0.5 % SDS) was added and oligonucleotides eluted by incubation at 37°C with gentle agitation at overnight. Acrylamide pieces were removed by centrifugation at 13,000 rpm for 5 minutes and the supernatant transferred to fresh tubes. An equal volume of 100 % ethanol was added and oligonucleotides precipitated on dry ice for 20 minutes. Oligonucleotides were pelleted by centrifugation at 13,000 rpm for 15 minutes, washed in 70 % ethanol and vacuum dried for 10 minutes. Pellets were resuspended in 50 μl H_2O and the concentration determined spectrophotometrically by the optical density at 260 nm. Typically around 40 to 50 % recovery of oligonucleotide was achieved.

2.2.15 Polymerase chain reaction (PCR) amplifications

a) PCR precautions and procedures

All PCR work was designed and carried out in such a way that contamination would be minimised. Typically, this involved using reagents and preparing solutions specifically isolated for PCR work, i.e. were not used for any other purpose. Separate work areas were designated for PCR work and surfaces covered with fresh aluminium foil every time before use. No glassware or autoclaved materials were used. All PCR reagents and buffers were aliquoted into small single use vials whenever possible and stored isolated in PCR only areas. Separate pipettes and tips were kept isolated and used solely for PCR work.

PCR amplification reactions always included a negative control reaction (No template DNA) to gauge any contamination. Whenever possible positive control reactions containing a known PCR template were included.

b) Long PCR reactions

Long PCR protocols were used to amplify products greater than 2 kb in length. Several enzymes from different manufacturers were used to perform long PCR amplifications by variations of their recommended protocols. Taq extender long PCR additive (Stratagene), Vent DNA polymerase (NEB) and Pfu DNA polymerase (Stratagene) were used in the long PCR reactions. Typically all long PCR reactions were performed in 50 μl reaction volumes overlaid with 50 μl of mineral oil and reactions 'Hot started' to reduce mis-priming (Cheng *et al.*, 1994; Hengen, 1994). All amplifications were performed in a Techne PHC-1 programmable dry block with CH-5 chillier/pump unit.

All PCR reactions were prepared as a 1x PCR reaction mix consisting of the appropriate 1x PCR buffer (supplied with enzyme), 0.5 mM each dNTP, 100 ng of each gel purified primer, additional $MgSO_4$ (as necessary) and made up in a final volume of 45 μl <u>minus</u> the volume to enzyme to be added. All reactions were overlaid in 50 μl

mineral oil. A 5 μl volume of template DNA was added (200 to 500 ng total cell DNA) and the PCR mix denatured at 90°C for 2 minutes. PCRs were then hot started by the addition of an appropriate volume of enzyme whilst the reaction mixes were still hot (90°C) and then immediately starting the thermocycling profile. PCR products were visualised under UV light after electrophoresis of 10 % of the completed PCR reaction on standard 0.8 % agarose gels in the presence of 0.5 μg/ml ethidium bromide.

Taq extender PCR additive (Stratagene)

Taq Extender was added in addition to normal *taq* DNA polymerase to extend the reliability and length of normal PCR amplification products. Taq extender was added at an equal unit concentration to *taq* DNA polymerase (Promega). Typically 1 U of each enzyme was added per kb to be amplified and reactions performed containing 1x Taq Extender buffer (20 mM Tris-HCl pH 8.8, 10 mM KCl, 10 mM $(NH4)_2SO_4$, 2 mM $MgSO_4$, 0.1 % Triton X-100, 0.1 mg/ml BSA). The supplied reaction buffer contained a final $MgSO_4$ concentration of 2 mM and the supplementation of these PCR reactions with additional Mg^{2+} was found to be unnecessary. Typical cycling parameters were denaturation at 94°C for 30 seconds, annealing at 55-68°C for 30 seconds and extension at 72°C for 40 seconds per kb to be amplified. Amplifications were performed for 25-30 cycles with a final cycle of 72°C for 10 minutes.

Vent DNA polymerase (NEB)

Vent DNA polymerase was used in several long PCR amplifications due to its high fidelity (4.5×10^{-5} errors per bp, Ling *et al.*, 1991) conferred by the 3'-5' proofreading activity. Vent DNA polymerase was added at 0.5 U per kb to be amplified and performed in reaction mixes containing 1x ThermoPol reaction buffer (20 mM Tris-HCl pH 8.8, 10 mM KCl, 10 mM $(NH4)_2SO_4$, 2 mM $MgSO_4$, 0.1 % Triton X-100) supplemented with between 1 to 4 mM additional $MgSO_4$. Typical cycling parameters were denaturation at 94°C for 30 seconds, annealing at 50-68°C for 30 seconds and

extension at 72°C for 1 minute per kb to be amplified. Amplifications were performed for 30-35 cycles with a final cycle of 72°C for 10 minutes.

Pfu DNA polymerase (Stratagene)

Pfu DNA polymerase was used in some long PCR amplifications due to its 3'-5' proofreading activity and higher fidelities (1.6×10^{-6} errors per bp, Lundberg *et al.*, 1991). Cloned Pfu DNA polymerase was added at 1.0 U per kb to be amplified and performed in 50 μl reaction volumes containing 1x cloned Pfu buffer (20 mM Tris-HCl pH 8, 10 mM KCl, 10 mM $(NH_4)_2SO_4$, 2 mM $MgSO_4$, 0.1 % Triton X-100, 0.1 mg/ml BSA). The supplied reaction buffer contained a final $MgSO_4$ concentration of 2 mM and the supplementation of these PCR reactions with additional Mg^{2+} was found to be unnecessary Typical cycling parameters were denaturation at 94°C for 30 seconds, annealing at 45-68°C for 30 seconds and extension at 72°C for 1.5 minutes per kb to be amplified. Amplifications were performed for 30-35 cycles with a final cycle of 72°C for 10 minutes.

2.2.16 Extraction of total genomic DNA from eukaryotic cells

Extractions were typically performed to obtain total cell DNA for PCR amplification and as such all extractions were performed using PCR quality reagents and procedures. Eukaryotic cells were grown in cell culture and washed in 1x PBS prior to DNA extraction. Cells were resuspended at 1×10^6 cells/ml in HIRT buffer (10 mM Tris-HCl pH 7.4, 20 mM EDTA, 0.5 % SDS). Proteinase K solution (2 mg/ml proteinase K (Sigma), 10 mM Tris-HCl pH 7.4, 15 mM NaCl) was added to a final concentration of 100 μg/ml and incubated at 37°C for 14-16 hours. 5 M NaCl was added to a final concentration of 100 mM and the whole solution mixed with an equal volume of phenol. The upper aqueous phase was extracted with equal volumes of phenol only until the interface was clean (typically 3-4 times). Nucleic acids were then ethanol precipitated at -20°C overnight. Nucleic acids were pelleted by centrifugation at 2500 rpm for 15 minutes in a MSE3000i centrifuge, washed in 70 % ethanol and vacuum

dried for 10 minutes. Nucleic acids pellets were resuspended in an appropriate volume of TE buffer. Nucleic acids isolated consisted of both DNA and RNA. RNAs were removed by addition of RNase A to a final concentration of 50 µg/ml and incubation at $37^{\circ}C$ for 30 minutes. The sample was phenol extracted and ethanol precipitated using standard protocols. Total cell DNA was resuspended in an appropriate volume of TE buffer and the concentration determined spectrophotometrically by the optical density at 260 nm. Typically, 2 to 4 µg DNA were recovered per 1×10^6 cells initially extracted.

2.3 Molecular Biology - RNA techniques

2.3.1 Precautions employed for RNA work

All RNA work was performed using precautions and lab procedures that would minimise ribonuclease contamination. Separate work areas were designated for RNA work and surfaces de-contaminated by washing with 3 % H_2O_2 before and after use. All H_2O used for RNA work was treated with 0.1 % (v/v) DEPC overnight and then autoclaved. Solutions were prepared from high purity RNA grade reagents in DEPC treated H_2O and sterilised by filtration through 0.2 µm filters (Gelman Sciences). All reagents and solutions used were specifically isolated for RNA work and prepared in sterile, disposable plasticware. Pipettes tips and microfuge tubes were soaked in a 0.1 % (v/v) DEPC solution overnight, autoclaved and then baked at $80^{\circ}C$ overnight before use. All electrophoresis apparatus and blotting equipment were de-contaminated by soaking in 3 % H_2O_2 for at least 15 minutes and rinsing several times with np H_2O before use.

2.3.2 Extraction of total cellular RNA for northern Blotting

Eukaryotic cells were grown in cell culture and washed thoroughly in warm 1x PBS. Cells were resuspended at 1×10^6 cells per ml in warm urea lysis buffer (10 mM Tris-HCl pH 8, 7M urea, 2 % (w/v) SDS, 0.35 M NaCl, 1 mM EDTA) and shaken vigorously for 10 seconds. An equal volume of RNA grade phenol was added and shaken vigorously for 10 seconds. A 0.5x volume of $CHCl_3$:IAA (24:1) was added

and shaken vigorously for 10 seconds. The phases were separated by centrifugation at 2500 rpm for 10 minutes in a MSE3000i centrifuge. The upper aqueous phase was transferred to fresh tubes and phenol, CHCl3:IAA extracted as described above for a further two times. 1 g CsCl was dissolved into every 2.5 ml of the remaining aqueous phase. 1.7 ml aliquots were gently layered onto 0.5 ml 5.7 M CsCl cushions in 2.2 ml "Ultra clear' ultracentrifuge tubes (Beckman). RNA was then pelleted through the CsCl cushions by centrifugation at 50,000 rpm for 5 hours in a Beckman TLS-55 swing out rotor and Optima TL ultracentrifuge. Pellets were resuspended in 300 μl DEPC treated H_2O. 90 μl 1M NaOAc and 800 μl 100 % ethanol was added and RNA precipitated at -20°C for 1 hour. Nucleic acids were recovered by centrifugation at 13,000 rpm for 15 minutes in a microfuge, washed in 70 % ethanol, vacuum dried for 10 minutes and resuspended in a small volume of DEPC treated H_2O. Samples were then DNase treated by incubation with 1 U RQ1 RNase free DNase (Promega) in the presence of 20 U RNAsin ribonuclease inhibitor (Promega) at 37°C for 15 minutes in 1x RQ1 DNase buffer (40 mM Tris-HCl pH 8, 6 mM $MgCl_2$, 10 mM NaCl, 10 mM $CaCl_2$, 1 mM DTT) per 1×10^6 cells originally extracted. DNA free RNA was then purified by phenol:chloroform extraction and recovered by ethanol precipitation. RNAs were resuspended in an appropriate volume of DEPC treated H_2O and the concentration determined spectrophotometrically by the optical density at 260 nm. Typically, yields were around 1-2 μg RNA per 1×10^6 cells extracted.

2.3.3 Denaturing agarose gel electrophoresis of RNA

RNAs for northern blotting were denatured and separated by electrophoresis through 0.8 % agarose gels containing formaldehyde. 0.8 g of RNA grade agarose (Pharmacia Biotech) was melted in 62 ml DEPC treated H_2O and allowed to cool to 60°C. 18 ml 30 % formaldehyde solution (Fisons) and 20 ml 5x formaldehyde gel buffer (0.1 M MOPS, 40 mM NaOAc, 5 mM EDTA at pH 7) was added, poured into a 8 cm x 8 cm mini-gel tray and allowed to set. 7 to 10 μg of total cell RNA in 4.5 μl DEPC H_2O was mixed with 2 μl 5x formaldehyde gel buffer, 3.5 μl 30 % formaldehyde solution

(Fisons) and 10 µl de-ionised formamide (Sigma). Samples were heated at 56°C for 15 minutes, mixed with 2.0 µl gel loading buffer (50 % glycerol, 1 mM EDTA, 0.25 % bromophenol blue) then plunged onto ice. Gels were pre-run at 55V for 5 minutes in 1x formaldehyde gel buffer before loading the samples. RNAs were electrophoresed in 1x formaldehyde gel buffer at a constant 50 V.

2.3.4 Electroblotting of RNA onto nylon membranes for hybridisation

After denaturing gel electrophoresis RNAs were immobilised onto nylon membranes for probing. After electrophoresis formaldehyde gels were soaked in 1x electroblot buffer (12 mM NaH_2PO_4, 10.4 mM Na_2HPO_4 at pH 6.5) for 10 minutes. 10 pieces of filter paper (Whatman 3MM) and Hybond N membrane (Amersham) cut to the size of the gel was soaked in 1x electroblot buffer for 10 minutes. A gel 'sandwich' was assembled consisting of 5 filter papers, the gel, Hybond N membrane and the other 5 filter papers. The 'sandwich' was emersed in 1x electroblot buffer and RNAs electro-transferred onto the nylon membranes at 200 mA for 16-18 hours at 4°C. After blotting RNAs were permanently immobilised onto the membrane by UV cross-linking (UV Stratalinker 2400, Stratagene). The membrane was then washed 3 times in 1x electroblot buffer and once in 1 % SDS. Membranes were then stored at 4°C or used immediately for hybridisation.

2.3.5 Preparation of random primed DNA probes for hybridisation

DNA probes were random prime labelled with ^{32}-P using the Rediprime DNA labelling system from Amersham. 20 ng of template probe was diluted to a final volume of 45 µl in H_2O. Template was boiled for 5 minutes then added directly to a Rediprime tube (pre-aliquoted labelling mix containing dATP, dGTP, dTTP, Klenow DNA polymerase and random 9 mer primers). 5 µl ^{32}-P dCTP (10 mCi/ml) was added and incorporated into probes by incubation at 37°C for 10 minutes. Reactions were stopped by addition of 2 µl 0.5 M EDTA. Unincorporated radiolabel and small extension products were removed by gel filtration through G-100 Sephadex (Sigma) columns. A Pasteur pipette

was blocked at the dispensing end with polyallomer wool and packed with G-100 Sephadex (autoclaved in 3 times the bed volume of TE buffer). The column was washed through four times with 150 µl volumes of TE buffer. The crude radiolabel was applied to the top of the column and ten 150 µl fractions were collected. 1 µl of each fraction was added to 5 ml scintillation fluid (OptiSafe fluid, LKB) and ^{32}-P counted in a United Technologies Minaxi Tri-carb 4000 scintillation counter. The first three fractions with the highest counts were pooled (450 µl) and used immediately as the hybridisation probe. Typically, specific activities of 1-2x 10^9 cpm/µg were achieved.

2.3.6 Hybridisation and detection of immobilised RNA

Membranes were blocked by pre-hybridisation in 25 ml pre-hybridisation solution (20 % TP5 solution (250 mM Tris-HCl pH 7.5, 1 % PVP, 1 % BSA, 1 % Ficoll, 0.5 % $Na_2P_2O_7$, 5 % SDS), 50 % de-ionised formamide, 10 % dextran-sulphate, 1M NaCl, 50 µg/ml sonicated salmon testes DNA (Sigma)) at 42°C for at least 2 hours in a rotating hybridising oven (Appligene). The random labelled ^{32}-P probe (450 µl) was mixed with 750 µl de-ionised formamide, 300 µl TP5 solution and boiled for 2 minutes. The probe was then added directly to the membrane/pre-hybridisation buffer. Probes were allowed to hybridise at 42°C for 16-18 hours in a rotating hybridising oven (Appligene). Membranes were rinsed in 2x SSC/1 % SDS. Membranes were then washed in 10 ml 2x SSC/1 % SDS at 42°C for 5 minutes, 2x SSC/1 % SDS at 42°C for 30 minutes, 2x SSC/1 % SDS at 65°C for 30 minutes and 0.2x SSC/1 % SDS at 65°C for 20 minutes. Membranes were air dried, wrapped in cling film and exposed to film with an intensifying screen at -70°C for an appropriate length of time. Autoradiographs were defrosted at room temperature for 15 minutes then developed in an Agfa-Gaevert automatic film developer.

2.3.7 Extraction of total cellular RNA for RT-PCR (RNAzol B)

Total cellular RNA for RT-PCR was extracted from cells using a commercial guanidium isothiocyanate/phenol preparation known as RNAzol B (Biogenesis) and a slightly modified version of their enclosed protocol.

Before extraction cells were washed thoroughly in cold 1x PBS. Cells in suspension were resuspended at 4×10^6 cells/ml directly in cold RNAzol B. Monolayer cells were extracted by direct addition of 3 ml per T80 flask or 1 ml per T25 flask RNAzol B and scraping. Cells were solubilised by passing through a pipette several times and then 1 ml aliquots transferred to fresh microfuge tubes. One tenth volume (100 μl) of RNA grade chloroform was added and mixed by vigorous shaking for 15 seconds. Samples were allowed to stand on ice for 5 minutes then centrifuged for 15 minutes at 13,000 rpm, $4^{\circ}C$ in a microfuge. Approximately 60 to 75 % of the upper aqueous phase was extracted and transferred to fresh tubes. An equal volume of RNA grade isopropanol was added and incubated on ice for at least 20 minutes. RNA was pelleted by centrifugation for 15 minutes at 13,000 rpm, $4^{\circ}C$ in a microfuge. Pellets were washed in 100 μl 70 % ethanol for 5 minutes at 13,000 rpm, $4^{\circ}C$ in a microfuge and vacuum dried for 10 minutes Pellets were resuspended in 96 μl DEPC H_2O and 4 μl 5M NaCl. 200 μl 100 % ethanol was added and RNAs stored at $-70^{\circ}C$ until used. Just prior to use RNAs were pelleted for 15 minutes at 13,000 rpm, washed for 5 minutes at 13,000 rpm in 100 μl 75 % ethanol and then vacuum dried for 10 minutes. RNA pellets were resuspended in an appropriate volume of DEPC treated H_2O and the concentration determined spectrophotometrically by the optical density at 260 nm.

2.3.8 Single tube AMV RT-PCR

100 to 500 ng of total cellular RNA was resuspended in 5 μl DEPC H_2O. 5 μl of 3' primer annealing mix (1x RT buffer (50 mM Tris-HCl pH 8.8, 10 mM KCl, 2.5 mM $MgCl_2$), 30 pmol of 3' or anti-sense primer) was added. Each reaction was then overlaid with 50 μl mineral oil. Primers were annealed by heating at $90^{\circ}C$ for 2 mins

then immediately cooling on ice. 10 μl of AMV-RT supermix (1x RT buffer, 10 mM DTT, 10U RNAsin (Promega), 1 mM dNTP (each) mix and 2U AMV-RT (Promega)) was added to each reaction. Reverse transcription was carried out at 42°C for 1 hour. Enzymes were inactivated by heating at 90°C for 5 mins. 30 μl of 5' primer/taq mix (1x Taq PCR buffer A (Promega), 30 pmols 5' or sense primer, 1.25U Taq polymerase (Promega)) was added to each reaction. Final PCR reaction conditions were 1 mM MgCl$_2$ and 0.2 mM dNTPs carried over from the RT reactions.

PCR amplification was carried out in a Techne PHC-1 programmable dry-block plus CH5 chiller unit for 30-35 cycles with a final cycle at 72°C for 2.5 minutes. Typical RT-PCR cycling parameters were denaturation at 92°C for 30 seconds, annealing at T$_m$ minus 10-20°C and extension at 72°C for 30 seconds. PCR products were visualised under UV light after electrophoresis of 10 % of the completed PCR reaction on 3 % GTG Nusieve agarose gels (FMC Bioproducts) in the presence of 0.5 μg/ml ethidium bromide.

The cycling profiles for detection mdr-1 mRNA expression using the specific human mdr-1 primer pairs hmdr1-2416s and hmdr1-2559as (T. Gant, personal communication and Davies *et al.*, 1996) was denaturation at 92°C for 30 seconds, annealing at 46°C for 60 seconds and extension at 72°C for 30 seconds. PCR reactions were performed at 1 mM MgCl$_2$ final PCR concentration and mdr-1 RNA detected by the presence of a 161 bp product after agarose gel electrophoresis.

2.3.9 Quantitative mdr-1 mRNA AMV RT-PCR assays

A quantitative assay for analysis of mdr-1 RNA expression was described by Davies *et al.*, 1996. Internal standard (ISC) RNA and mdr-1 primers were a kind gift from T. Gant, MRC Toxicology unit, Leicester. Briefly, the mdr-1 primer pair (2416a/2559as) amplifies a 161 bp region from 2416 to 2577 of mdr-1 cDNA (see section 2.10). The internal standard contains the same region of mdr-1 DNA but with an additional 51 bp

insert at an internal *Hind*III site. Thus, this internal standard contains the same mdr-1 primer sites, but amplifies a region 51 bp larger (212 bp) than normal cellular mdr-1. The internal standard DNA was cloned downstream of the T7 promoter of a pGEM vector (Promega) and internal standard RNA was transcribed *in-vitro*.

The quantitative RT-PCR method employed was essentially the same as the single-tube RT-PCR procedure, except that known amounts of internal standard control (ISC) RNA was added in addition to the cellular RNAs. The ISC RNA acts as a competitive template to mdr-1 RNA for reverse transcription and PCR. Amplification of mdr-1 RNA and ISC RNA is thus directly proportional to the relative amounts of each RNA in the reaction. Hence, at the point of equal amplification the amount of mdr-1 RNA is equal to the amount of ISC RNA in the reaction and the mdr-1 RNA concentration in a sample can be calculated.

Five reactions were routinely run containing 0.05, 0.25, 0.5, 1.0 and 2.5 pg ISC RNA with a constant amount total cellular RNA in each reaction. For quantification, the amounts of total cellular RNA (100 to 500 ng) was adjusted such that the experimental data always spanned the 1:1 mdr-1:ISC RNA ratio. ISC RNA was added to cellular RNA before the primer annealing step and RT-PCR reaction performed as described in 2.3.8.

Gel scanning and image manipulation

RT-PCR reaction products were electrophoresed on 3 % GTG Nusieve agarose gels. RT-PCR products were visualised and photographed with standard Kodak Polaroid film and camera under UV light and red filter. Gel photographs were then digitally scanned on an Aries Relysis scanner using Adobe Photoshop (Macintosh v2.5) at 300 dpi in 256 grayscales. Scanned gel images were then saved in a standard TIFF graphics file format. Gel images were analysed and relative area band intensities calculated using the 'Gel plotting' macros of NIH Image software (Macintosh v1.54). Standard desktop

digital imaging and scanning equipment was used for densitometric analyses for convenience and these methods have been found to be comparable in accuracy to traditional dedicated densitometric systems (Shea, 1994).

b) Analysis and quantification of mdr-1 RNA

Quantification of mdr-1 RNA could be determined when the ratio of the amount of ISC and cellular mdr-1 RNA was equal to one. Hence, the ratio of the band area of cellular mdr-1 RNA over the band area of ISC RNA was plotted against the amount of ISC RNA used in the reaction. Linear plots were made on a double log scale using Cricket Graph software (Macintosh v1.3) and the amount of mdr-1 RNA calculated when the ratio cellular mdr-1 RNA over ISC RNA was equal to one ($\log_e = 0$). Results were processed and the expression of mdr-1 RNA calculated as the number of molecules of mdr-1 RNA per pg total cellular RNA.

Expression of mdr-1 RNA was calculated using the following procedures,

The ratio of mdr-1 RNA over ISC RNA was plotted against amount ISC RNA on a double $\log_e$ scale. The line equation was obtained using Cricket Graph in the form,

$$y = mx + c$$

Where, y = ratio of mdr-1 RNA over ISC RNA at a given value of x

x = amount of ISC RNA

m = gradient of the line

c = line constant

To obtain the amount of ISC RNA (x) at a given ratio mdr-1 RNA over ISC RNA (y), the equation was rewritten as,

$$x = \frac{y - c}{m}$$

when the ratio of mdr-1 RNA over ISC RNA are equal to one (amount mdr-1 RNA = amount ISC RNA in pg) the value of y = 0 (i.e. $\log_e$ of 1). Thus,

$$x = \frac{-c}{m}$$

Where, $x = \log_e$ (amount ISC RNA in pg) = $\log_e$ (amount mdr-1 RNA)

Thus, to calculate the amount of mdr-1 RNA in grams per pg total cellular RNA (r),

$$r = \frac{e^x * 10^{-12}}{\text{total cellular RNA (pg) in PCR reaction}}$$

Finally, the number molecules of mdr-1 RNA per pg total cellular RNA =

$$\frac{r * \text{Avagadros number } (6.022 \times 10^{-23})}{\text{molecular weight mdr-1 } (90851.4)}$$

A worked example of the mdr-1 gene mRNA quantification is described in chapter 4 (section 4.2.3).

2.3.10 RT-PCR Cloning

Cloning of mRNA transcripts for gene expression studies was done using reverse transcription and PCR protocols designed to minimise the generation of sequence errors within the amplified products. M-MLV reverse transcriptase was used to produce first strand cDNA from total cellular RNAs in preference to AMV RT due to its lower DNA endonuclease and RNase H activities, and its greater efficiency in synthesising longer cDNAs of up to 10 kb in length (Maniatis *et al.*, 1976; Roth *et al.*, 1985). First strand cDNA products were then PCR amplified using the high fidelity thermostable *pfu* DNA

polymerase and molecularly cloned into suitable plasmid vectors for propagation and expression.

Total cellular RNA was extracted from appropriate cells using RNAzol B. Polyadenylated mRNAs from 200 to 400 ng of total cellular RNA was then reverse transcribed in 1x first strand reaction buffer (50 mM Tris-HCl pH 8.3, 75 mM KCl, 3 mM $MgCl_2$), 10 mM DTT, 0.5 mM each dNTP, 200 ng oligo $(dT)_{12-18}$ primer and 200 U M-MLV RT (Gibco) in a 20 μl reaction volume at 37°C for 1 hour. Enzymes were heat inactivated at 70°C for 10 minutes and first strand cDNA purified by phenol extraction and ethanol precipitation. cDNAs were resuspended in 20 μl TE buffer and 5 μl was used as the template for high fidelity *pfu* DNA polymerase (Stratagene) PCR amplification as described in section 2.2.15b. PCR amplified products were then purified by LMP agarose gel extraction and cloned into desired plasmid vectors using the appropriate methods described in section 2.2.

2.4 Molecular Biology - Protein techniques

2.4.1 Extraction of proteins from eukaryotic cells

Eukaryotic cells were grown in cell culture and washed in thoroughly 1x PBS prior to extraction. Cells were resuspended at approximately 1×10^7 cells/ml in cold 2x SDS lysis buffer (100 mM Tris-HCl pH 6.8, 200 mM DTT, 20 % glycerol, 4 % SDS) containing 10 mM PMSF protease inhibitor. Samples were boiled for 10 minutes and cell debris removed by centrifugation at 13,000 rpm for 5 minutes in a microfuge. Supernatants were transferred to fresh tubes and passed through a 21 ga needle several times until the viscosity was reduced to manageable levels. The protein supernatants were then stored at -20°C.

2.4.2 Quantification of total protein

Total protein concentrations were determined using a Protein assay kit (Bio-Rad) based on the standard Bradford dye binding assay (Bradford, 1976). Standard protein

solutions containing 2.5, 5, 10, 15 and 25 μg/ml BSA diluted in 0.008x SDS lysis buffer were made in a final volume of 0.8 ml. A concentration of SDS lysis buffer of 0.008x was necessary and required as no interference upon the assay was observed at this concentration (data not shown). 3.2 μl of extracted protein samples were diluted 250 fold in 796.8 μl H_2O (final concentration of 0.008x SDS lysis buffer). 200 μl Bio-Rad protein dye reagent was added, mixed and left to stand at room temperature for 10-20 minutes. The optical density of the standard and sample protein solutions were then measured at 595 nm in a Pharmacia LKB Ultrospec-III spectrophotometer. A standard linear curve was then plotted of the OD_{595} versus the concentration of BSA standard using the Cricket Graph software (Macintosh v1.3). The protein concentration of the extracted samples was then determined by comparison of OD_{595} readings against the standard curve and adjustment for any dilutions made. Protein concentrations were only determined if the OD_{595} fell within the range of the BSA standards.

2.4.3 SDS-PAGE of proteins

Proteins were resolved by electrophoresis on 10 % polyacrylamide gels containing 0.1 % SDS. 50 μl APS and 5 μl TEMED was mixed with 5 ml 10 % polyacrylamide resolving gel mix (375 mM Tris-HCl pH 8.8, 0.1 % SDS, 33 % Protogel (30 % polyacrylamide stock, National Diagnostics) and 3.5 ml poured between the gel plates of a Mini-Protean II (Bio-Rad) gel casting assembly. To ensure an even surface the top of the gel mix was overlaid with isopropanol and the gel allowed to set for at least 30 minutes. The isopropanol was removed and the top of the gel rinsed thoroughly with H_2O. 12 μl APS and 2 μl TEMED was mixed with 2 ml 5 % polyacrylamide stacking mix (125 mM Tris-HCl pH 6.8, 0.1 % SDS, 16.5 % Protogel) and 1 ml poured above the resolving gel to form the stacking gel. A 10 well comb was inserted and the gels were allowed to set for at least 30 minutes. 40 to 60 μg total protein was diluted to a final volume of 10 μl in 2x SDS lysis buffer and 5 μl SDS loading dye (100 mM Tris-HCl pH 6.8, 200 mM DTT, 20 % glycerol, 4 % SDS, 0.25 % bromophenol blue) added. Protein samples were boiled for 5 minutes and loaded into the stacking gel.

SDS-PAGE gels were electrophoresed in 1x running buffer (25 mM Tris-HCl, 0.2 M

Glycine, 0.1 % SDS) at a constant 200V. After electrophoresis gels were soaked in

H_2O for 5 minutes. For protein transfer to nitrocellulose gels were used immediately,

without staining. For total protein visualisation gels were stained in coomassie blue

solution (0.2 % coomassie blue, 10 % glacial acetic acid, 10 % IMS) for at least 1 hour

and then de-stained to the desired intensity in several changes of destain solution (30 %

methanol, 10 % glacial acetic acid). Stained gels were then dried down onto Whatman

3MM paper at 60°C for several hours in a vacuum slab gel dryer.

2.4.4 Semi-dry blotting of proteins onto nitrocellulose membranes

SDS-PAGE gels, nitrocellulose membrane (Amersham) and 12 pieces of Whatman

3MM filter paper were pre-equilibrated in transfer buffer (25 mM Tris-HCl, 0.19 M

glycine, 20 % methanol) for 10 minutes. A gel 'sandwich' was then assembled in the

base (cathode) of a semi-dry blotting apparatus consisting of, from bottom to top, 6

filter papers, SDS-PAGE gel, nitrocellulose membrane and another 6 filter papers. The

lid (anode) was placed on top and proteins transferred at a constant current of 80 mA for

1 hour. Nitrocellulose protein blots were then rinsed in H_2O and air dried for 15

minutes. Blots were stored at 4°C until use.

2.4.5 ECL Immunodetection of immobilised proteins

Anti-HTLV-I antibodies

Rat anti-HTLV-I envelope monoclonal antibodies 5a and 30g were a kind gift from T.

Schulz from the Chester Beatty laboratories, London. Monoclonal antibody 5a

recognises an epitope of the transmembrane HTLV-I envelope protein (TM or gp21)

and monoclonal 30g recognises the surface HTLV-I envelope protein (SU or gp46).

ECL detection

Nitrocellulose protein blots were blocked by incubating with 10 ml of TMT/SS buffer (1x TBS, 3 % skimmed milk powder, 0.5 % Tween-20, 10 % sheep serum) at room temperature for at least 1 hour. Blots were then probed with 1 µg/ml monoclonal antibody in a final volume of 5 ml in TMT/SS buffer at room temperature for 1 hour. Excess primary monoclonal antibodies were then removed by washing the blot three times at room temperature in 10 ml TBS-T (1x TBS, 0.05 % Tween-20). Blots were then incubated with 1:2000 diluted HRPO conjugated goat anti-rat IgG secondary detection antibody (Sera-Lab) in 5 ml TMS/SS at room temperature for 1 hour. Blots were then washed at room temperature, twice in 10 ml TBS-T and twice in 10 ml TBS.

HTLV-I env proteins were then detected using the ECL detection system from Amersham. Briefly, probed blots were thoroughly soaked in 5 ml Solution-2 and then 5 ml solution-1 added, mixed and incubated at room temperature for exactly 1 minute. Blots were then exposed to film (ECL, Amersham) for 1 minute, 2 minutes and 5 minutes exposures. Films were immediately developed in an Agfa-Gaevert automatic film developer.

2.5 Eukaryotic cells

2.5.1 Cell culture techniques

All cell culture work was performed in a class III containment facility and all appropriate safety practices employed. Eukaryotic cell lines and media used are described in section 2.9.

a) Maintenance of Cell lines

All cell lines were maintained in Nunclon cell culture flasks (T25 or T80) and grown in a humidified atmosphere at 37°C with 5 % CO_2. In order to maintain a consistent pure phenotype cells were only carried for a maximum of 30 passages before discarding and fresh cultures initiated from cryo-frozen stocks.

T-cells were grown in suspension in RPMI 1640 medium + 10 % FCS. Cells were pelleted by centrifugation at 1250 rpm for 5 minutes in a MSE3000i centrifuge. Supernatants were discarded and cells resuspended at 5×10^5 cells/ml in fresh pre-warmed (37°C) RPMI 1640 medium + 10 % FCS. Cells were split and grown at 3 to 4 day intervals to a maximum density of $1\text{-}2 \times 10^6$ cells/ml.

Adherent cells (COS and MCF7) were grown as monolayers in DMEM medium + 10 % NCS. Cells were washed in 1x PBS and detached from the flasks by incubation at 37°C with trypsin-EDTA solution (0.5 g/l trypsin, 0.2 g/l EDTA, Gibco) for 2 to 3 minutes. Trypsin was inactivated by addition of an equal volume of pre-warm (37°C) DMEM media + 10 % NCS and cells pelleted by centrifugation at 1250 rpm for 5 minutes. Cells were resuspended in an appropriate volume of fresh pre-warmed (37°C) DMEM media + 10 % NCS and seeded at 1×10^4 cells per cm^2 flask. Cells were split and grown at 3 to 4 day intervals or until confluent.

Viable cell counts were routinely made by mixing 100 µl cell suspension with 100 µl 0.2 % trypan blue solution (Gibco) and counting the unstained cells in all four corner quadrants (0.4 µl volume) in a haemocyometer. Viable cell counts were estimated using the following formula,

$$\text{Viable cell concentration (cells/ml)} = \text{cell count x dilution (2) x per ml (2500)}$$

Eukaryotic cells were stored as long term stocks under liquid nitrogen in 1x RPMI 1640 medium supplemented with 10 % FCS, 100 U/ml penicillin, 100 U/ml streptomycin, 200 mM glutamine and 10 % DMSO.

b) Isolation of PBMCs from whole blood

Preservative-free heparinised fresh whole blood was kindly obtained by venipuncture of HTLV-I infected individuals by S. Nightingale, Royal Shrewsbury hospitals. Blood

from non-HTLV-I infected heathly volunteer donors was obtained by venipuncture by Dr. P. Sheldon, University of Leicester.

10 ml DSM mix (3 % dextran, 3 % D-glucose, 0.15 M NaCl) was mixed with 50 ml whole blood and incubated at room temperature for 40 minutes. The upper plasma layer was removed to fresh tubes and cells pelleted by centrifugation at 1000 rpm for 10 minutes in a MSE3000i centrifuge. Cells were resuspended in 15 ml serum free 1x RPMI 1640 and gently layered onto 10 ml Ficoll-Paque (Pharmacia) in 50 ml Falcon tubes. Gradients were then centrifuged at 2250 rpm, room temperature for 20 minutes. Total PBMCs were then harvested from the Ficoll interface and transferred to fresh tubes. PBMCs were then washed by resuspending in 15 ml serum free 1x RPMI 1640 and pelleting at 1000 rpm for 10 minutes, three times. Cells were then counted and either used directly for PGP assays or mitogenically stimulated by resuspension at $2x10^6$ cells/ml in stimulation medium (1x RPMI 1640, 20 % FCS, 100 U/ml penicillin, 100U/ml streptomycin, 200 mM glutamine, 5 U/ml IL-2, 10 µg/ml PHA-P) and grown at 37°C, 5 % CO_2 for 72 hours. Typically, $1\text{-}2x10^6$ PBMCs per ml of whole blood were isolated. Stimulated cells were then pelleted by centrifugation at 1250 rpm for 5 minutes and maintained at $2x10^6$ cells/ml in growth medium (1x RPMI 1640, 20 % FCS, 100 U/ml penicillin, 100U/ml streptomycin, 200 mM glutamine, 5 U/ml IL-2).

c) Electroporation of Eukaryotic cells

Eukaryotic cells were electrotransformed (electroporated) with expression plasmids using a method described by Cann *et al.*, 1988. $5x10^6$ T-cells or $2x10^6$ COS-1 cells were resuspended in 250 µl cold electroporation medium (1x RPMI 1640, 20 % FCS, 100 U/ml penicillin, 100U/ml streptomycin, 200 mM glutamine). 25 µg plasmid DNA in a maximum volume of 25 µl was added to the cell suspensions and incubated on ice for 10 minutes. T-cells were electroporated at 250 V, 960 µF and COS-1 cells at 150 V, 960 µF in a Bio-Rad gene pulser with capacitance extender. Cells were incubated on ice for 10 minutes and then transferred to fresh normal room temperature media. Cells

were grown at $37^{\circ}C$, 5 % CO_2 for 24-72 hours before harvesting for the appropriate assay.

d) HTLV-I tax trans-activation CAT assay

HTLV-I tax expression was assayed using a HTLV-I LTR-CAT reporter gene plasmid and *trans*-activation assay previously described by Cann *at al.*, 1988. 12.5 µg plasmid DNA was co-electroporated with 12.5 µg LTR-I-CAT plasmid which contains the CAT gene downstream and under control of the HTLV-I LTR region (Chen *et al.*, 1985). CAT expression was assayed 48 hours after electroporation. Cells were washed in 1x PBS and resuspended in 140 µl 0.25M Tris-HCl, pH 7.5. Cells were lysed by freeze-thawing three times between dry-ice/ethanol and a $37^{\circ}C$ water bath. Cell lysates were then heated at $65^{\circ}C$ for 10 minutes and cell debris pelleted by centrifugation at 13,000 rpm for 10 minutes in a microfuge. Cell extracts were stored at $-20^{\circ}C$ until use.

Cell extracts were quantified for total protein and a constant amount of total protein of between 50 to 100 µg in a final volume of 70 µl (in 0.25M Tris-HCl, pH 7.5) was used for all CAT assays. 10 µl 4 mM AcCoA (Sigma) and 0.5 µl [14]-C chloramphenicol (0.05 µCi, ICN chemicals) were incubated with 70 µl of diluted cell extract at $37^{\circ}C$ for between 2 to 6 hours. 100 µl H_2O and 1 ml cold ethyl acetate was added, mixed and phases separated by centrifugation at 13,000 rpm for 5 minutes in a microfuge. The upper organic phase was transferred into fresh tubes and dried-off under vacuum (SpeedVac, Savant) for 30 minutes. Pellets were resuspended in 10 µl ethyl acetate and spotted onto TLC plates. Chromatography was then performed in a sealed tank containing 95:5 $CHCl_3$:methanol. TLC plates were air dried for 10 minutes then exposed to film for 24 to 48 hours at $-70^{\circ}C$ with an intensifying screen. Films were developed in an Agfa-Gaevert automatic film developer.

2.5.2 FACS Analysis

a) Fluorescence activated cell scanning (FACscan)

Fluorescently labelled cells were analysed using a Becton-Dickinson FACscan flow cytometer and LYSIS-II analysis software. The FACscan flow cytometer used a 15 mW argon-ion laser with the excitation wavelength at 488 nm. Rhodamine-123 (R123) and FITC fluorescence was collected after passing through a 515-545 nm (Fl-1) band-pass filter. PI and PE fluorescence was collected after passing through a 563-607 nm (FL-2) band-pass filter. Data for forward angle scatter, side angle scatter, Fl-1 fluorescence and Fl-2 fluorescence was routinely collected for 10,000 events on a 4 decade log scale. For two phytochrome work (R123/PI, FITC/PI and R123/PE) appropriate electronic compensation was applied to minimise spectral overlap. Fluorescence data was analysed on Lysis-II software where only viable cells (PI excluding cells) were counted.

b) R123 dye efflux assay for PGP activity

3×10^6 T-cells were resuspended in 3 ml 1x complete RPMI 1640 media supplemented with 2.5 % FCS. 1×10^6 cells (1 ml) was removed to fresh tubes and stored on ice (0 minute cells). Rhodamine-123 (R123) was added to a final concentration of 0.4 μM to the remaining 2×10^6 cells (2 ml) and labelled by incubation at 37°C, 5 % CO_2 for 20 minutes. Cells were washed by pelleting at 1250 rpm for 5 minutes in an MSE3000i centrifuge and resuspension in 1x PBS. Cells were pelleted again and resuspended in 2 ml 1x RPMI 1640 + 2.5 % FCS. 1×10^6 cell (1 ml) was removed to fresh tubes and store on ice (20 minute accumulation cells). The remaining 1×10^6 cells (1 ml) was allowed to time to efflux the R123 dye by incubation at 37°C, 5 % CO_2 for 60-90 minutes. These cells were then removed to fresh tubes (90 minute efflux cells). All 1×10^6 cell aliquots (0 minute, 20 minute accumulation and 90 minute efflux cells) were pelleted and washed in 1x PBS. Cells were resuspended at 1 ml PBS + 5 μg/ml PI solution and incubated on ice for 10 minutes. Cells were then pelleted and washed in 1x PBS. Cells were fixed by resuspension in 1 ml 1 % paraformaldehyde

(approximately 1×10^6 cells/ml) and incubation on ice for at least 20 minutes. R123 (FL-1) and PI (FL-2) cell fluorescence was then directly counted on the FACscan for 10,000 events and viable cells analysed for relative R123 accumulation and efflux. An overview of the R123 dye efflux assay is shown in figure 2.1.

c) Fluorescence activated cell sorting (FACSvantage)

High efficiency physical separation of high and low effluxing R123 cell populations was performed using a Becton-Dickinson FACSvantage cell sorter by R. Snowden at the MRC Toxicology unit, University of Leicester. Excitation wavelengths and band-pass filter sets were identical to those of the FACscan unit described in section 2.5.2a.

Fresh PBMC cells were isolated from HTLV-I infected individuals as described in section 2.5.1b. 2×10^7 unstimulated PBMCs were then tested for PGP activity using a slightly modified R123 efflux assay procedure described in section 2.5.2b. Briefly, 2×10^7 cells was incubated in 20 ml 1x RPMI 1640 + 2.5 % FCS containing 0.4 µM R123 for 20 minutes at 37°C, 5 % CO_2 in T80 flasks. The cells were then washed twice in 10 ml warm 1x PBS and incubated in 20 ml 1x RPMI 1640 + 2.5 % FCS at 37°C, 5 % CO2 for a further 90 minutes in T80 flasks. Cells were washed twice in 10 ml warm 1x PBS and fixed by incubation in 10 ml 1 % paraformaldehyde for 20 minutes on ice. Cells were then resuspended in 4 ml 1x PBS (5×10^6 cells/ml) and physically sorted into high and low effluxing cell populations (low and high cellular R123 fluorescence (FL-1) respectively) on the FACS Vantage using dual positive gating. Sorted cells were collected in tubes coated with 4 % BSA in order to reduce absorption of cells onto the tube walls. Cells were counted then pelleted at 1500 rpm, 20°C for 10 minutes in an MSE3000i centrifuge. Typically around 10 % of the original cells were effectively sorted and recovered. Sorted cell populations were DNA extracted for PCR as described in section 2.2.16. Quantitative HTLV-I PCRs were performed on both high and low R123 effluxing cell populations by G. Taylor, St. Mary's Hospital Medical School, London.

Figure 2.1. A schematic representation of the rhodamine 123 (R123) dye efflux assay for MDR cells. The diagram shows MDR P-glycoprotein (PGP) expressing cells (left) and normal non-MDR cells (right). Cells are sampled at the start of the experiment, after 20 minutes R123 accumulation and then after a 90 minutes efflux period. Cells are analysed for cellular R123 fluorescence by FACscan. Unlabelled zero time cells show negligible R123 fluorescence but 20 minute R123 accumulation cells show high uniform intracellular R123 fluorescence. The MDR cells are capable of active R123 export or efflux and the cells show a low intracellular R123 fluorescence. Normal non-MDR cells cannot remove the R123 dye and retain a high intracellular R123 fluorescence. Cells with a low R123 fluorescence after the 90 minute efflux period display the MDR efflux phenotype.
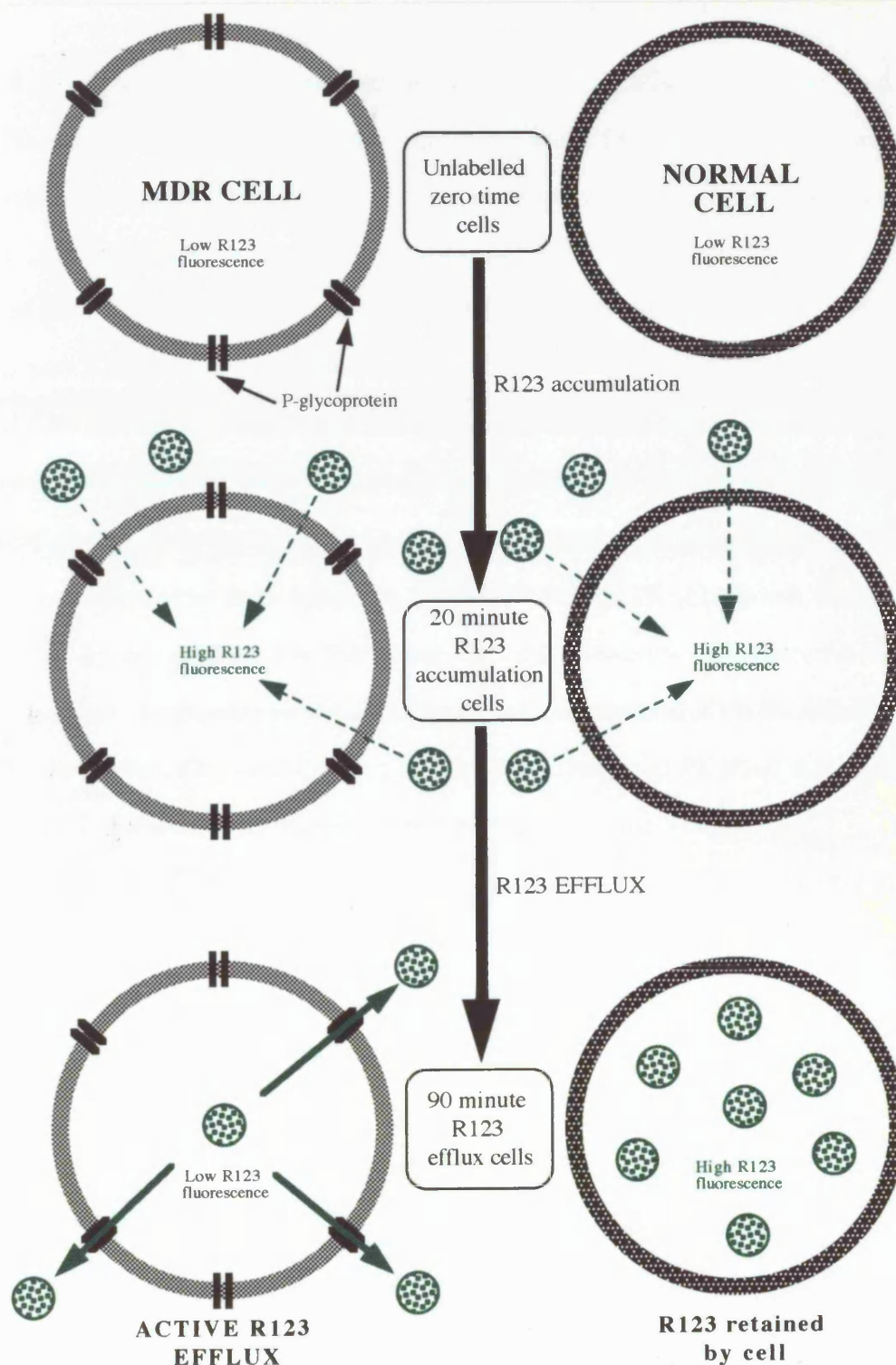
d) PBMC lymphocyte cell subset analysis

PBMC cell subset analysis of R123 effluxing cells was performed using PE conjugated lymphocyte cell typing antibodies from Sera-lab. T-cells, monocytes/macrophages and B-cells were typed using anti-CD3, anti-CD14 and anti-CD22 monoclonal antibodies respectively.

The R123 PGP efflux assay was performed on $3x10^6$ cells as described in section 2.5.2b except the cells were not labelled with PI, but just fixed in 1 % paraformaldehyde for 20 minutes. Cells were then pelleted and washed in 1x PBS. These cells were resuspended in 1 ml PBSH (1x PBS + 2 % human AB serum). Three 200 μl ($2x10^5$ cells) from the 90 minute efflux cell aliquot were transferred to new tubes and 2 μl PE-conjugated mouse anti-CD3, CD14 or CD22 (Sera-Lab) added. Cells were directly labelled for 30 minutes on ice then pelleted by centrifugation and washed in 1 ml cold 1x PBS. These cells were resuspended and fixed in 500 μl cold 1 % paraformaldehyde (in 1x PBS). Both the R123 assay and lymphocyte typing cells were then analysed by flow cytometry. R123 (FL-1) and PE (FL-2) cell fluorescence was directly counted on the FACscan for 10,000 events after spectral overlap compensation. High and low R123 effluxing cell populations of the 90 minute efflux cells were separated by virtual gating in Lysis II software and PE fluorescence of anti-CD3/14/22 monoclonals within these populations analysed. The PE (FL-2) fluorescence of cells was proportional to the amount of CD3, CD14 or CD22 antigen expressed on the cell surface.

e) Indirect immunofluorescent detection of PGP

Indirect immunofluorescent detection of cell surface associated PGP was performed using the anti-PGP monoclonal antibody MRK-16 and FACscan analysis. The MRK-16 monoclonal antibody recognises an extracellular epitope of membrane bound PGP (Kamiya Biomedical company, Thousand Oaks, CA, USA). MRK-16 is a murine IgG2a isotype monoclonal antibody and an IgG2a isotype non-specific murine control

antibody was used to gauge non-specific antibody binding. Antibodies were detected by the use of a FITC conjugated goat anti-mouse IgG secondary antibody (Dako). All antibodies were a kind gifts from T. Gant, MRC Toxicology unit, University of Leicester.

Cells were washed once in chilled 1x PBS then 2×10^5 cells resuspended in 200 μl chilled PBSG (1x PBS + 2 % goat serum). The cells were split into two 100 μl fractions and to each 100 μl fraction 2 μg (10 μg/ml final concentration) of either MRK-16 or IgG2a control primary antibody was added. The final volume was made up to 200 μl in PBSG (5×10^5 cells/ml). The cells were labelled by primary antibody at 4°C overnight. Cells were diluted to 1 ml in cold PBSGT (PBSG + 10 % Tween-20) and excess antibody washed out by pelleting the cells by centrifugation at 1250 rpm for 5 minutes in a MSE3000i centrifuge and resuspension in 1 ml cold PBSGT two times. Cells were then pelleted by centrifugation and resuspended in 200 μl cold PBSG containing 10 μl (1:10 dilution) of the FITC conjugated goat anti-mouse IgG secondary detection antibody (Dako). Cells were labelled at 4°C for 1 hour then diluted to 1 ml in cold PBST (1x PBS + 10 % tween 20). Excess antibodies were washed out by pelleting the cells by centrifugation and resuspension in 1 ml cold PBST two times. Cells were resuspended in 1 ml PBS containing 5 μg/ml PI and incubated on ice for 10 minutes. Cells were pelleted by centrifugation and fixed in 500 μl 1 % paraformaldehyde (in 1x PBS). Cells were analysed by FACscan with FITC cell fluorescence (FL-1) and PI cell fluorescence (FL-2) being counted for 10,000 events after spectral overlap compensation. Only viable cells were counted for FITC (FL-1) fluorescence which proportionally corresponds to the amount of PGP expressed on the cell surface.

2.6   Virus Assays

<u>2.6.1 HIV p24 antigen capture assay (ELISA)</u>

The presence of HIV particles in cell supernatants were assayed using a HIV p24 antigen capture ELISA system. The AMPAK alkaline phosphatase immunodetection system from DAKO Ltd was used. D7320 anti-p24 primary antigen capture antibody and EH12E1-AP alkaline phosphatase conjugated secondary detection antibody was supplied by the MRC Aids Directed Programme (ADP).

Cells were grown as normal and the medium removed to fresh tubes at appropriate time points. These cell free supernatants were then assayed for HIV particles by the presence of HIV p24 gag. Samples were prepared by the addition of 1 % Empigen detergent to cell free supernatants and viruses inactivated by heating at 56°C for 30 minutes. Inactivated supernatants were then stored at -20°C until use. Just prior to use samples were defrosted and diluted as appropriate in 0.1 % Empigen/10 % sheep serum in TBS. An appropriate number of wells on a 96 well ELISA microtitre plate (Dynatech Laboratories) were coated with 100 µl D7320 primary antibody (5 µg/ml in 100 mM NaHCO3) at room temperature overnight. The wells were washed three times with 200 µl TBS and excess sites blocked by incubation with 200 µl 2 % (w/v) skimmed milk powder in TBS at 30°C for 30 minutes. Wells were then washed three times with 200 µl TBS. 100 µl diluted samples and p24 standards (0, 0.03, 0.1, 0.31, 1, 3.1 ng/ml) were then added to the wells and p24 captured at 30°C for 3 hours. Wells were washed three times in 1x PBS and 100 µl EH12E1-AP alkaline phosphatase conjugated detection antibody (1:1000 diluted in TMT/SS) added. Plates were incubated at 30°C for 1 hour and then the wells washed five times in 200 µl 1x AMPAK wash buffer (AMPAK kit, Dako). 50 µl substrate solution (AMPAK kit, Dako) was added to each well and incubated at 30°C for 1 hour. 50 µl amplifier solution (AMPAK kit, Dako) was then added to each well and incubated at 30°C for 10-20 minutes for colour to develop. Reactions were stopped by the addition of 25 µl Stopping solution to each well (AMPAK kit, Dako). Plates were read at 495 nm wavelength on a Dynatech

MR600 microplate reader. A standard linear curve was then plotted of the OD495

verses the concentration of HIV p24 standards using the Cricket Graph software

(Macintosh v1.3). The HIV p24 concentration of the samples were then determined by

comparison of OD495 readings against the standard curve and adjustment for sample

dilution. Sample concentrations were only valid if the OD495 readings fell within the

range of the p24 standards.

2.6.2 HIV/HTLV reverse transcriptase virus particle assay

HTLV and HIV virus particles were also assayed by the presence of virus packaged

reverse transcriptase in cell culture media. Cells were grown using standard methods

and the culture medium removed to fresh tubes at appropriate time points. These cell

free supernatants were then assayed for reverse transcriptase activity by the

incorporation of tritiated thymidine into DNA from poly rA/poly dT templates. Suitable

controls consisting of cell supernatants from virus free (negative) and HTLV infected

(positive) cells were always included.

0.5 ml PEG solution (30 % (w/v) PEG 8000, 0.4 M NaCl) was added to 1 ml cell free

culture supernatant. Viral particles were then allowed to precipitate at $4^{o}C$ overnight.

Particles were then pelleted by centrifugation at 13,000 rpm for 10 minutes in a

microfuge. Virus particle pellets were lysed by resuspension in 25 μl solubilising

reagent (50 mM Tris-HCl pH 8.2, 80 mM NaCl, 10 mM PMSF, 2 mM DTT, 5 %

glycerol, 0.5 % Triton X-100). Reverse transcriptase activity of solubilised pellets was

assayed by addition of 100 μl RT template mix (50 mM Tris-HCl pH 8.2, 10 mM

$MgCl_2$, 2 mM DTT, 5 μCi ^{3}H-dTTP (Amersham), 0.05 ODu poly rA/poly dT

(Pharmacia). Reactions were incubated at $37^{o}C$ for 1 hour then stopped by the addition

of 5 μl 0.5M EDTA pH 8. Reactions were spotted onto DE81 DEAE ion exchange

filter disks (Whatman) and air dried for 15 minutes. Unincorporated radiolabel was

removed by washing the disks five times for 5 minutes in 5 % Na_2HPO_4 solution with

gentle agitation. Disks were soaked in 100 % ethanol for 5 minutes and then dried

under a heat lamp for 10 minutes. Individual dried disks were placed in vials and 5 ml scintillation fluid added (OptiSafe fluid, LKB). ^{3}H was then counted in a United Technologies Minaxi Tri-carb 4000 scintillation counter. Significant levels of virus particles were only assumed when the reverse transcriptase activity of the sample supernatants were at least three times the negative control counts.

2.7 Common buffers and solutions

All commonly used buffer solutions and their compositions are shown in table 2.2.

Table 2.2. Common buffer and stock solutions

Name	Buffer/solution	Composition (1x)
TAE	Tris-acetate-EDTA	40 mM Tris-HCl 0.57 % (v/v) glacial acetic acid 1 mM EDTA
TBE	Tris-borate-EDTA	89 mM Tris-HCl 89 mM boric acid 2.5 mM EDTA
TBS	Tris buffered saline	20 mM Tris-HCl pH 7.5 0.15 M NaCl
TE	Tris-EDTA	10 mM Tris-HCl pH 7.5 1 mM EDTA
TE.1	Tris-EDTA	10 mM Tris-HCl pH 8.0 0.1 mM EDTA
TEN	Tris-EDTA-NaCl	10 mM Tris-HCl pH 7.5 1 mM EDTA 0.1 M NaCl
PBS	Phosphate buffered Saline	0.14 M NaCl 2 mM KCl 5 mM Na$_2$H$_2$PO$_4$ 2 mM NaH$_2$PO$_4$
SSC	NaCl-Sodium citrate	0.15 M NaCl 15 mM Sodium citrate pH 7.0

2.8   Bacterial strains and growth media

All bacterial strains used were stored as 15 % glycerol stocks at -70°C and grown up by streaking out to single colonies on appropriate media agar plates. All bacterial strains used and genotypes are shown in table 2.3.

Table 2.3. Bacterial strains and genotypes

Strain	Genotype
AG1	*rec*A1, *end*A1, *gyr*A96, *thi*-1, *hsd*R17, (r_k-, m_k+), *sup*E44, *rel*A1, (uncharacterised mutation improves transformation efficiency)
DH5α	*sup*E44, Δ*lac*U169 (φ80 *lac*ZΔM15), *hsd*R17, *rec*A1, *end*A1, *gyr*A96, *thi*-1, *rel*A1
JM103	*end*A1, *hsd*R, *sup*E, *sbc*BC, *thi*-1, *str*A, Δ(*lac*-*pro*), [F' *tra*D36, lacI^{q}ZΔM15, *pro*AB]

All HTLV containing plasmids were routinely maintained in AG1 cells (Stratagene) as these cells reportedly conferred enhanced stability of HTLV plasmids (Kimata *et al.*, 1994a). JM103 and cells were grown on minimal media agar plates at 37°C for 24-48 hours to maintain the F' pilus for M13 phage infection. DH5α cells were used as the standard host strain for growth of all other plasmids.

Bacterial growth media used was prepared as shown in table 2.4 and sterilised by autoclaving at 121°C, 15 psi, 20 minutes before use. Agar plates were made by the addition of 1.5 % agar and poured into petri dishes whilst still molten. Plates were stored at 4°C for up to 1 month and dried for 10-20 minutes before use.

Table 2.4. Bacterial growth media

Media	Composition
2TY	1.6 % (w/v) Bacto-tryptone 1.0 % (w/v) Yeast extract 0.5 % (w/v) NaCl
SOB	2.0 % (w/v) Bacto-tryptone 0.5 % (w/v) Yeast extract 0.05 % (w/v) NaCl 2.5 mM KCl 10 mM MgCl$_2$
SOC	SOB media supplemented with additional 10 mM MgCl$_2$ 20 mM glucose
Minimal salts	73.5 mM K$_2$HPO$_4$ 19.7 mM g/l KH$_2$PO$_4$ 7.6 mM (NH4)$_2$SO$_4$ 3.4 mM Sodium citrate 0.8 mM MgSO$_4$
Minimal agar	50 % Minimal salts 50 % 3 % Agar 10 mM glucose 1 μg/ml thiamine

2.9 Eukaryotic cells and growth media

All cell culture work was performed in a class III containment facility and appropriate safety practices employed. All cells lines were carried for a maximum of 30 passages. Cell lines were obtained from the MRC Aids directed program (ADP) reagent repository, NIBSC, Potters Bar and are described in table 2.5.

Table 2.5. Eukaryotic cell lines and growth media

Cell line	Cell type	Media	Reference
C8166	Human T-cell	RPMI + 10 % FCS	Salahuddin et al., 1983.
CEM-4	Human T-cell	RPMI + 10 % FCS	Foley et al., 1965.
Hut-78	Human T-cell	RPMI + 10 % FCS	Gazdar et al., 1980.
Jurkat (E6-1)	Human T-cell	RPMI + 10 % FCS	Weiss et al., 1984.
Molt-4	Human T-cell	RPMI + 10 % FCS	Kikukawa et al., 1986.
SupT1	Human T-cell	RPMI + 10 % FCS	Smith et al., 1984.
COS-1	African green monkey kidney cells	DMEM + 10 % NCS	Gluzman, 1981.
C91/PL	HTLV-I transformed human T-cell	RPMI + 10 % FCS	Popovic et al., 1983a.
MT-2	HTLV-I transformed human T-cell	RPMI + 10 % FCS	Miyoshi et al., 1981a.
MT-4	HTLV-I transformed human T-cell	RPMI + 10 % FCS	Miyoshi et al., 1982.
MCF-7/Dox	Human breast carcinoma multidrug-resistant cells	RPMI + 10 % FCS	Batist et al., 1986.

RPMI =   1x RPMI 1640 medium supplemented with 100 U/ml penicillin, 100 U/ml streptomycin, 200 mM glutamine.

DMEM =   1x DMEM medium supplemented with 100 U/ml penicillin, 100 U/ml streptomycin, 200 mM glutamine.

All culture media and reagents were cell culture certified and purchased as "ready-to-use" 1x stocks from Gibco-BRL.

2.10   Oligonucleotide primers

All oligonucleotide primers were synthesised at a 40 nM scale by the Protein and nucleic acid chemistry (PNAC) laboratory at Leicester University and were obtained stored under ammonia. Oligonucleotides were recovered by ethanol precipitation with 0.1 volumes 3 M NaOAc pH 5.2 and 2 volumes ethanol on dry ice for 20 minutes. Oligonucleotides were pelleted by centrifugation at 13,000 rpm for 15 minutes. Pellets were washed in 70 % ethanol and dried under a vacuum source for 10 minutes. Oligonucleotide pellets were then resuspended in 250 μl H$_2$O. The concentration of oligonucleotide primers was determined spectrophotometrically by the optical density at

260 nm using the standard formulas shown below. All oligonucleotides used and their sequences are shown in table 2.6.

The molar concentration of oligonucleotides was calculated using the formula,

$$\text{Conc}^n \ (\mu M) = \frac{OD260 \times \text{dilution} \times 1000}{\Sigma \ [\{(^\#A \times 15.4) + (^\#C \times 7.3) + (^\#G \times 11.7) + (^\#T \times 8.8)\}]}$$

The molecular weight (mw) of oligonucleotides was calculated using the formula,

$$mw = \Sigma \ [(^\#A \times 312.2) + (^\#C \times 288.2) + (^\#G \times 328.2) + (^\#T \times 303.2)]$$

The melting temperature (T_m) of oligonucleotides was calculated using the formula,

$$T_m \ (^oC) = \Sigma \ [\{2 \times (^\#A + ^\#T)\} + \{4 \times (^\#C + ^\#G)\}]$$

Table 2.6. Oligonucleotide primers

Name	Sequence (length)	T_m	Comments
ATK-3	GCGAGCTGCATGCCCAAGACC CG (23)	78°C	HTLVatk primer. (position 5115 - 5137)
ATK-5	CGCTGTCTCAACATATTTCTAG ACTCC (27)	78°C	HTLVatk primer. (position 4063 - 4089)
ATK-6	GGAGTCTAGAAATATGTTGAGA CAGCG (27)	78°C	HTLVatk anti-sense primer. (position 4089 - 4063)
ATK-13	GCGTGGAGACAGTTCAGGAGG GG (23)	76°C	HTLVatk primer. (position 332 - 354)
ATK-14	GTAGAGTTGAGCAAGCAGGGT CAGG (25)	78°C	HTLVatk anti-sense primer. (position 8609 - 8631)
ATK-15	TTAAGCTTGCGAGCTGCATGCC CAAGAC (28)	68°C (88°C)	tax/rex cDNA cloning primer. Synthetic HindIII site.
ATK-16	AACTCGAGTCAGACTTCTGTTT CTCGGAAATG (32)	68°C (82°C)	tax/rex cDNA anti-sense cloning primer. Synthetic XhoI site.
hmdr1-2416s	AAAAAGATCAACTCGTAGGAG TG (23)	64°C	Human mdr-1 RNA RT-PCR detection primer. (Zhang et al., 1996)
hmdr1-2559as	GCACAAAATACACCAACAA (19)	52°C	Human mdr-1 RNA RT-PCR anti-sense detection primer. (Zhang et al., 1996)

Underlined sequences are synthetic restriction enzyme sites introduced to facilitate cloning. Melting temperatures (T_m) for primers with synthetic restriction enzyme sites are shown as; T_m minus restriction site sequence (T_m including restriction site sequence).

2.11 Plasmids

A list of names and a brief description of all the plasmids used and constructed are shown in the tables 2.7, 2.8, 2.9 and 2.10. Table 2.7 shows original plasmid vectors. Tables 2.8, 2.9 and 2.10 shows recombinant plasmids containing HTLV, HIV and mdr-1 gene promoter inserts respectively.

Table 2.7. Plasmid vectors

Plasmid vector	Reference	Comments
M13mp-18/19	Messing *et al.*, 1977. (Genbank[#]X02513)	M13 filamentous bacteriophage cloning vector.
pBR322	Bolivar *et al.*, 1977. (Genbank[#]J01749)	Standard cloning vector.
pBCCX	—	Eukaryotic expression vector (CMV IE promoter) based upon pBC12-IL2/CMV (Cullen *et al.*, 1986) with the IL-2 gene replaced by a *ClaI/XhoI* linker region.
pBUG-CAT	—	CAT gene containing plasmid based on pBR322. Also has SV40 origin of replication and termination signals. (AJ. Cann, personal communication)
pUC-18/19	Vieria *et al.*, 1982. Yanish-Perrun *et al.*, 1985. (Genbank[#]X02514)	Standard high copy number cloning vector.

Table 2.8. HTLV containing plasmids

Name	Plasmid vector	Comments
pBC-λHTLV	pBCCX	Eukaryotic HTLV-I proviral expression plasmid (R_xRE^-). HTLV$_{atk}$ SstI fragment (486-8763) from pUC19-λHTLV.
pBC-λHTLV-env	pBCCX	Eukaryotic HTLV-I envelope protein expression plasmid. HTLV$_{atk}$ env sequence derived from a HinD111-PstI fragment (4990-6729) of pUC19-λHTLV.
pBC-HTLVp	pBCCX	Eukaryotic HTLV-I proviral expression plasmid (R_xRE^+). HTLV-I provirus derived from the long PCR clone in pUC18-HTLV.
pBC-tax/rex	pBCCX	Eukaryotic HTLV tax and rex protein expression construct. Derived by RT-PCR cloning of tax/rex RNA using primers ATK-15 and 16.
pCLC	pBR322	CMV IE and HTLV-I LTR promoters linked to the CAT reporter gene. Used as a positive control for CAT expression in tax trans-activation assays (Cann et al., 1988).
pLTR-CAT	pBR322	HTLV-I LTR promoter upstream of the CAT reporter gene (Chen et al., 1985). A control CAT reporter gene construct for tax trans-activation assays.
pUC18-HTLVp	pUC18	HTLV-I partially LTR deleted (R_xRE^+) proviral clone, reconstructed from the long PCR 5' and 3' HTLV clones pUC18-HTLV136 and pUC19-HTLV145.
pUC18-ATK136	pUC18	5' HTLV-I proviral clone (332-4063) derived from long PCR of C91 genomic DNA using primers ATK-13 and 6.
pUC19-ATK145	pUC19	3' HTLV-I proviral clone (4063-8859) derived from long PCR of C91 genomic DNA using primers ATK-14 and 5.
pUC19-λHTLV	pUC19	HTLV-I LTR deleted proviral clone (R_xRE^-). HTLV$_{atk}$ SstI fragment (486-8763) from λHTLV-1c (Mori et al., 1987).

Table 2.9. HIV containing plasmids

Name	Plasmid vector	Comments
pBCCX-CSF	pBCCX	HIV$_{jr-csf}$ VLP proviral expression construct (Haddrick *et al.*, 1996).
pBCCX-CSFΔHS	pBCCX-CSF	HIV$_{jr-csf}$ VLP proviral expression construct, env deleted *Hind*III (6574) to *Sal*I (8483). RRE⁻ and rev⁻.
pBCCX-CSFΔS	pBCCX-CSF	HIV$_{jr-csf}$ VLP proviral expression construct env deleted *Sal*I (5797) to *Sal*I (8483). RRE⁻ and rev⁻.
pBCCX-CSFΔSB	pBCCX-CSF	HIV$_{jr-csf}$ VLP proviral expression construct env deleted *Sal*I (5797) to *Bam*HI (7342). RRE⁺ and rev⁻.
pBCCX-CSFΔHB	pBCCX-CSF	HIV$_{jr-csf}$ VLP proviral expression construct env deleted *Hind*III (4959) to *Bam*HI (7342). RRE⁺ and rev⁻.
pBCCX-CSF-DB31	pBCCX-CSF	HIV$_{jr-csf}$ VLP proviral expression construct env nonsense frameshift at *Dra*III (6603) by Bal31 nuclease digestion. RRE⁺ and rev⁺.

Table 2.10. mdr-1 promoter Plasmids

Name	Plasmid vector	Comments
pMDR-P3	pGEM3	1 kb 5' mdr-1 promoter *Pst*I (-426) to *Pst*I (+536) region (Ueda *et al.*, 1987b). A kind gift from Marilyn Cornwell, Fred Huchinson Cancer research center, Washington, USA.
pMDR5'-CAT(+)	pBUG-CAT	1 kb 5' *mdr*-1 promoter -426 to +536 derived from pMDR-P3 cloned into pBUG-CAT plasmid as a replacement for the SV40 ori in the correct orientation to drive CAT expression.
pMDR5'-CAT(-)	pBUG-CAT	1 kb 5' *mdr*-1 promoter -426 to +536 derived from pMDR-P3 cloned into pBUG-CAT plasmid as a replacement for the SV40 ori in a reverse or antisense orientation for expression.

The molecular cloning of HTLV-I and expression of recombinant HTLV-I proteins

---

3.1 Introduction

HTLV-I demonstrates a very tight cellular association in which transmission occurs predominantly via cell to cell contact and replicates through expanding the number of infected cells. Such a replicative strategy is in contrast to other retroviruses such as HIV in which transmission and replication occurs through the expression of extracellular virus particles. The inherent cellular nature of HTLV-I has hampered the *in vitro* study of the molecular mechanisms of replication and transformation. To circumvent the problems associated with HTLV-I propagation and to facilitate its molecular genetic analysis a recombinant viral expression system was employed in which viral protein expression is uncoupled from the inefficient process of infection. This system would facilitate structural and functional studies of HTLV-I proteins and may provide insights into the complex molecular mechanisms of HTLV-I replication, transformation and disease induction.

It was the initial intention of this part of the project to obtain and express a non-defective molecular HTLV-I proviral clone with a view to investigate any HTLV-I protein by mutational analysis. It was decided that the HTLV-I envelope proteins would be the specific focus of attention. At the time HTLV-I envelope proteins were believed to confer the mitogenic activity associated with HTLV-I but the regions of the proteins which were involved were unknown. In addition the regions of HTLV-I envelope involved in virus neutralisation, receptor binding, cell fusion and entry were ill-defined.

It was the intention to map the regions of the HTLV-I envelope proteins with respect to their function. The HTLV-I envelope proteins were investigated in a virus pseudotyping system in which an existing HIV-I virus particle expression system would be used to generate phenotypically mixed particles. The HTLV-I envelope proteins would be expressed on the surface of HIV-I particles and domains on the protein tested for specific functional activities by mutational analysis.

This chapter describes the initial part of the project which focused on the molecular cloning and expression of recombinant HTLV-I proteins. The production and characterisation of an infectious molecular clone of HTLV-I for use in a viral expression system was the primary aim and is described in section 3.3. The cloning and expression of HTLV-I envelope was attempted in order to produce a system for its structural and functional analysis. The molecular cloning and development of a pseudotype particle expression system for HTLV-I envelope is section 3.4 of this chapter. The development of the techniques used in the these experiments were then extended to the molecular cloning and expression of the HTLV-I tax protein for use in the investigation of mdr-1 gene trans-activation.

3.2 Cloning and expression plasmids

For the molecular cloning and routine propagation in bacterial host cells the HTLV-I genes were inserted into the standard bacterial cloning plasmids pUC18 or 19 (Vieria *et al.*, 1982; Yanish-Perrun *et al.*, 1985).

The mammalian expression vector used throughout these studies was based upon the plasmid pBC12/CMV/IL2 which was originally used to overexpress the cytokine IL-2 in mammalian cells (Cullen, 1986). This plasmid was subsequently modified for use as a general expression vector by replacing the IL-2 gene cassette with a short *ClaI-Xho*I restriction enzyme multiple cloning site (figure 3.1). The re-engineered expression plasmid was designated pBCCX (AJ. Cann, personal communication) and has been

used for HIV provirus expression by Haddrick *et al.*, 1996. The essential feature of these plasmids was that expression was driven by the powerful cytomegalovirus immediate early (CMV IE) promoter which is constitutively active at high levels in a large variety of mammalian cells (Boshart *et al.*, 1985; Schmidt *et al.*, 1990). Insertion of a gene immediately downstream of this promoter would drive its transcription when the recombinant construct is introduced into mammalian cells. Efficient transcription termination and polyadenylation of expressed RNA transcripts is provided by an SV40 termination/polyadenylation signal and the plasmid is capable of replication in COS-1 cells due to the SV40 origin of replication. In addition the expression vectors are based around a pBR322 plasmid backbone for propagation in bacterial cells.

Figure 3.1. The mammalian expression vector pBCCX.
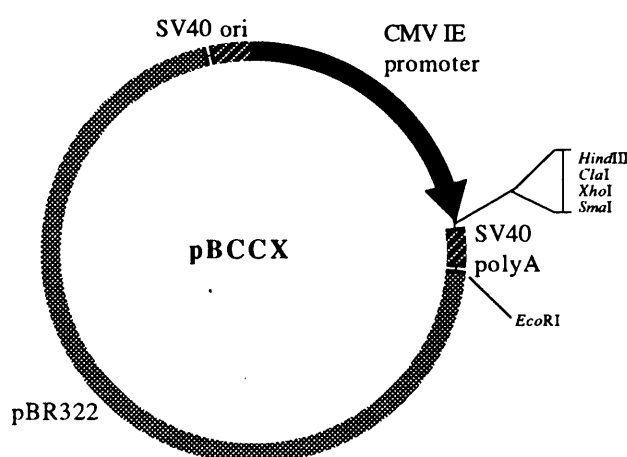
3.3 Molecular cloning and expression of the HTLV-I genome

3.3.1 Virus-like particle (VLP) expression system

The strategy for expressing the HTLV-I proviral genome was based on an analogous system used for the expression of HIV-I virus-like particles (VLP) described by Haddrick *et al.*, 1996. In this system an LTR deleted HIV-I proviral clone (strain JR-CSF) was placed downstream of the CMV IE promoter in pBCCX and electroporated into COS-1 cells. The recombinant construct, pBCCX-CSF, was found to direct high levels of HIV protein expression and produce VLPs which were structurally and

morphogenically similar to wild type virions. Hence a similar expression system was proposed for HTLV-I in which a HTLV-I proviral genomic clone would be inserted downstream of the CMV IE promoter and used to express HTLV-I proteins/VLPs (figure 3.2).

Figure 3.2. Recombinant retrovirus proviral expression plasmids. a) pBCCX-CSF; HIV-I proviral expression construct described by Haddrick *et al.*, 1996. b) pBC-HTLVI; proposed HTLV-I proviral expression construct. All constructs were based around the pBCCX expression plasmid.
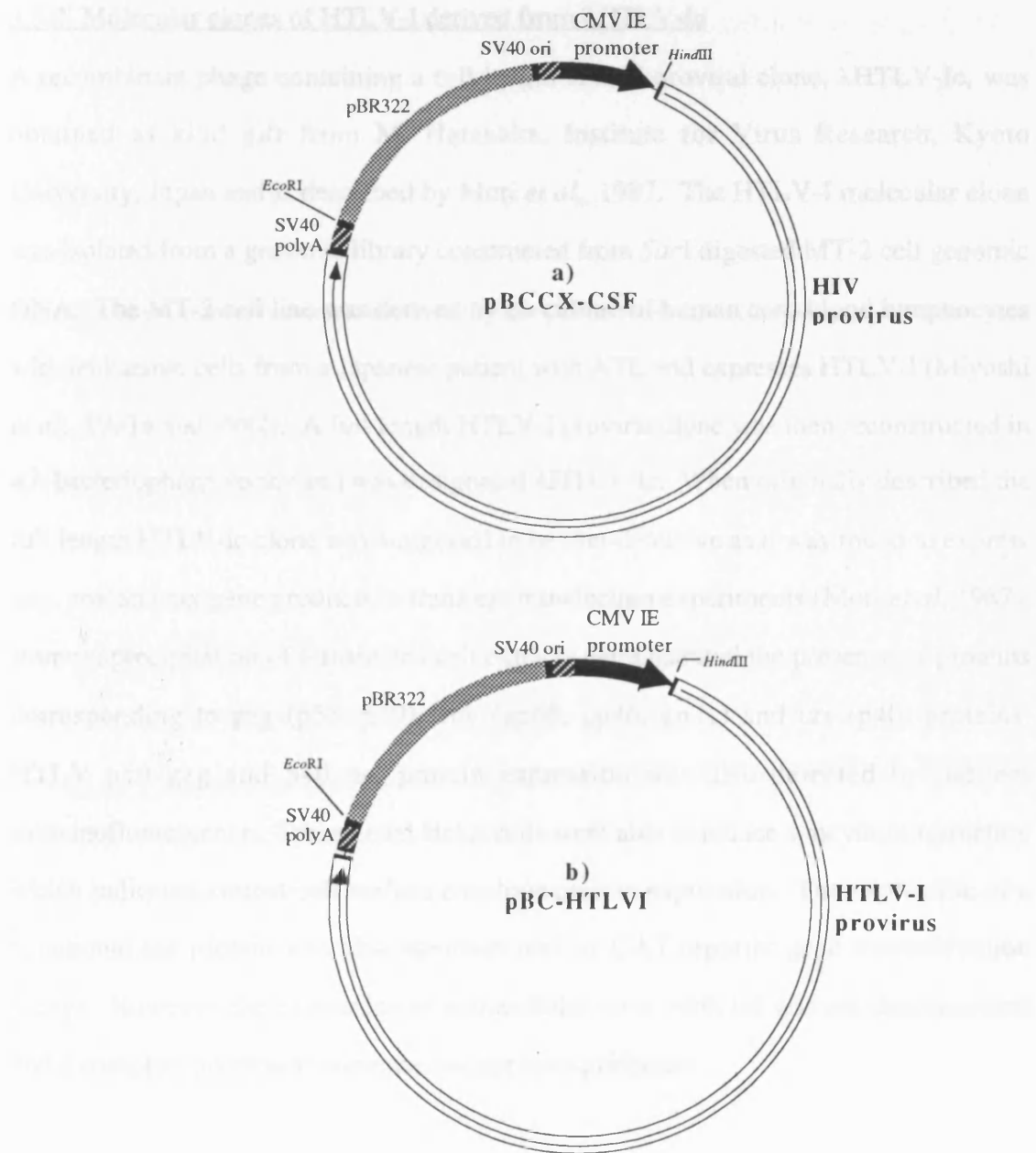
Such a molecular VLP expression system effectively uncouples viral gene expression from the inefficient processes of infection and transformation normally required for HTLV-I. Viral gene expression would be efficiently induced at high levels in days rather than weeks. The HTLV-I proviral clone could then be subject to deletion and mutation analysis and used in the functional study of any HTLV gene of interest. A schematic representation of the VLP expression system is shown in figure 3.3.

3.3.2 Molecular clones of HTLV-I derived from λHTLV-Ic

A recombinant phage containing a full length HTLV proviral clone, λHTLV-Ic, was obtained as kind gift from M. Hatanaka, Institute for Virus Research, Kyoto University, Japan and is described by Mori et al., 1987. The HTLV-I molecular clone was isolated from a genomic library constructed from SacI digested MT-2 cell genomic DNA. The MT-2 cell line was derived by co-culture of human cord blood lymphocytes with leukaemic cells from a Japanese patient with ATL and expresses HTLV-I (Miyoshi et al., 1981a and 1982). A full length HTLV-I proviral clone was then reconstructed in a λ bacteriophage vector and was designated λHTLV-Ic. When originally described the full length HTLV-Ic clone was suggested to be non-defective as it was found to express gag, env and tax gene products in transient transfection experiments (Mori et al, 1987). Immunoprecipitation of transfected cell extracts demonstrated the presence of proteins corresponding to gag (p53, p19), env (gp68, gp46, gp21) and tax (p40) proteins. HTLV p19 gag and p40 tax protein expression was also detected by indirect immunofluorescence. Transfected HeLa cells were able to induce syncytium formation which indicated correct cell surface envelope protein expression. The expression of a functional tax protein was also demonstrated by CAT reporter gene transactivation assays. However, the expression of extracellular virus particles was not demonstrated and a complete nucleotide sequence has not been published.

A SacI fragment of the HTLV-I proviral clone was sub-cloned from the recombinant phage λHTLV-Ic into the standard bacterial cloning vectors pUC18 and pUC19 by E.

124

Cancio, Department Microbiology and Immunology, University of Leicester. These plasmids were designated pUC18- or pUC19-λHTLV. The *Sac*I λHTLV-Ic fragment spanned bases 486 to 8758 of the full length HTLV-I$_{ATK-1}$ proviral genome. This clone encoded all the HTLV-I genes but was partially LTR deleted and did not contain any 5' LTR U3 promoter sequences (bases 1 to 352). In addition the 5' splice donor (base 471), 3' R$_X$RE (bases 8589 to 8844) and 3' RNA polyadenylation site (base 8856) were also missing from these genomic clones. Both pUC18- and pUC19-λHTLV clones were checked by detailed restriction mapping. These clones were found to differ from the predicted restriction site map of a published HTLV-I nucleotide proviral sequence known as ATK-1 (HTLV$_{ATK-1}$), which was also derived from ATL cells (Seiki *et al*, 1983). A *Hind*III site at 2330 and a *Cla*I site at 5864 was found to be missing from both pUC18- and pUC19-λHTLV recombinant clones. These discrepancies occur in the protease and envelope genes respectively. However, the *Hind*III site at base 2330 predicted from the HTLV$_{ATK-1}$ sequence (Seiki *et al.*, 1983) is not present in the nucleotide sequence of the HTLV-I provirus HS-35 (HTLV$_{HS-35}$), isolated from a patient of Caribbean origin with ATL (Malik *et al.*, 1988).

The pUC19-λHTLV clone was chosen for sub-cloning as it had convenient restriction sites (5'-HindIII-EcoRI-3') for forced orientation cloning into the expression vector pBCCX. An *Eco*RI/partial *Hind*III HTLV-I proviral fragment (486 to 8763) was sub-cloned from pUC19-λHTLV into the *Eco*RI/*Hind*III sites of pBCCX using standard protocols. Two recombinant clones, [#]10 and [#]15, were obtained and were used throughout these studies. These plasmids containing the λHTLV-Ic clone were known as pBC-λHTLV [#]10 and [#]15.

Figure 3.3. A schematic representation of the virus-like particle (VLP) proviral expression system. Expression plasmids are constructed from proviral genomic clones and viral proteins expressed in mammalian cells to produce VLPs.

126
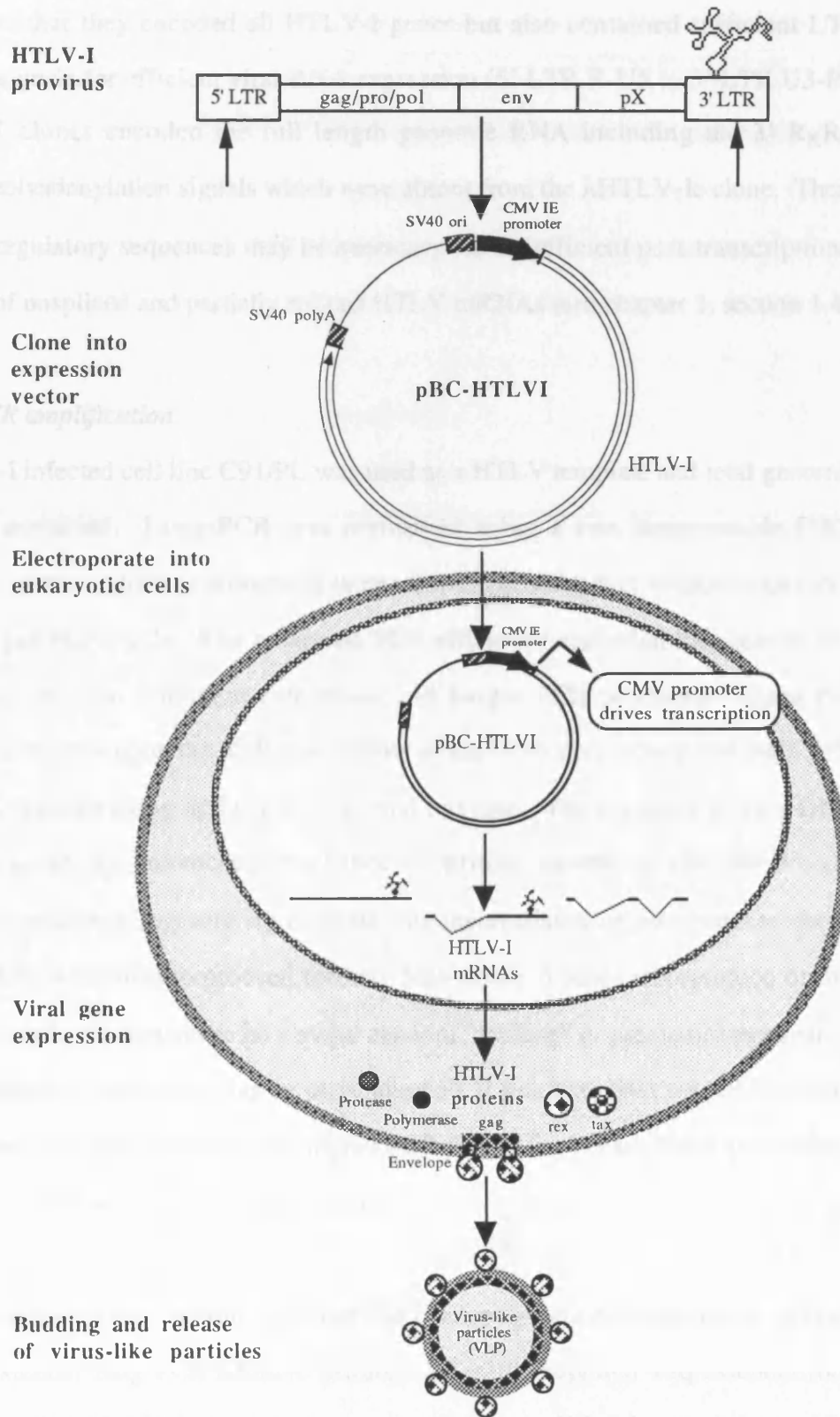
3.3.3 Molecular clones of HTLV-I derived by long PCR amplification

Alternative HTLV-I proviral clones were isolated from the HTLV-I infected cell line C91/PL (Popovic *et al.*, 1983a) by long PCR amplification. These PCR clones were amplified so that they encoded all HTLV-I genes but also contained sufficient LTR regulatory signals for efficient viral RNA expression (5' LTR R-U5 to 3' LTR U3-R). These PCR clones encoded the full length genomic RNA including the 3' R_XRE sequence, polyadenylation signals which were absent from the λHTLV-Ic clone. These additional regulatory sequences may be necessary for the efficient post-transcriptional regulation of unspliced and partially spliced HTLV mRNAs (see chapter 1, section 1.4).

a) Long PCR amplification

The HTLV-I infected cell line C91/PL was used as a HTLV template and total genomic DNA was extracted. Long-PCR was performed using a two thermostable DNA polymerase system which is thought to increase the efficiency and reliability of DNA elongation per PCR cycle. The enhanced PCR efficiency and reliability results in a greater proportion of complete extensions and longer PCR products. These two enzyme systems rely upon the high processivity of taq DNA polymerase and the 3'→5' exonuclease proofreading activity of a second enzyme. The presence of two DNA polymerases greatly enhances the chance of primer extension and the 3'→5' exonuclease proofreading activity corrects mis-incorporated or mis-matched bases allowing PCR extensions to proceed further. Mis-matched bases incorporated during primer extensions are thought to be a major cause of "stalling" or premature termination of PCR extensions leading to shorter incomplete PCR products (Barnes, 1994). Such amplifications may also demonstrate higher PCR fidelities over taq DNA polymerase alone due to the fewer mis-incorporated bases.

Long-PCR reactions were performed using Taq DNA polymerase (Promega) in addition with Taq extender long PCR additive (Stratagene) in the supplied Taq extender long PCR buffer. The HTLV-I provirus was successfully amplified in two halves using

fully complimentary primers to a reference $HTLV_{ATK-1}$ nucleotide sequence (Seiki *et al.*, 1983). The 5' half (332 to 4089) was amplified with primer pairs ATK-13 and ATK-6, and the 3' half (4063 to 8859) with primer pairs ATK-5 and ATK-14. These PCR generated HTLV-I proviral DNA halves were designated ATK136 and ATK145 respectively. It was not possible to amplify the full length HTLV proviral genome with a single primer set (e.g. ATK-13 and ATK-14) in a single long PCR reaction due to overlapping LTR sequences. The HTLV-I clone generated by PCR fragments ATK136 and ATK145 encompasses base 332 to 8859 of the HTLV-I provirus and encodes the entire full length genomic RNA. Long PCR amplification was successful for both primer sets using the recommended reaction conditions outlined in chapter 2 (section 2.2.15) and with the following cycling parameters,

94°C, 0.5 minutes denaturation time

62°C, 0.5 minutes annealing time

72°C, 45 seconds per kb to be amplified extension time

(2.8 minutes extension for primer pairs ATK-13 and ATK-6)

(3.5 minutes extension for primers pairs ATK-14 and ATK-5)

for a maximum of 30 PCR cycles

Long PCR amplifications were found to be more efficient with fewer short PCR artefacts using a "hot start" procedure to initiate PCRs and using highly purified genomic DNA preparations (OD_{260}/OD_{280} ratio >1.8). The use of gel purified primers and optimisation of magnesium concentrations were found to be unnecessary for this PCR amplification system. Both primer sets efficiently amplified PCR products of correct size under these conditions (figure 3.4). PCRs with primer set ATK-14 and 5 also generated unwanted smaller fragments, but these were removed by gel purification prior to cloning.

Long PCR amplification was also attempted using alternative single thermostable DNA polymerases with 3'→5' exonuclease or proofreading activity in order to enhance PCR

fidelity. *Vent* (NEB) and recombinant *Pfu* (Stratagene) DNA polymerases were also used individually to PCR amplify the HTLV proviral genome using the strategy outlined above. Extensive modifications to PCR reaction conditions including annealing temperatures, extension times, enzyme concentration, magnesium concentration, dNTP concentration, the use of gel purified primers, addition of PCR additives (DMSO and formamide) and multiple rounds of amplification yielded no desired HTLV PCR products.

Figure 3.4. EtBr stained agarose gel of HTLV-I provirus long PCR amplification on C91/PL genomic DNA using Taq extender PCR additive. M = λ DNA (HindIII cut) marker. Lane 1 = negative control PCR (H2O). Lane 2 = long PCR using PCR primers ATK-13 and ATK-6 which amplifies a 3757 bp 5' fragment of the HTLV-I provirus. Lane 3 = long PCR using primers ATK-14 and ATK-5 which amplifies a 4796 bp 3' fragment of the HTLV-I provirus.
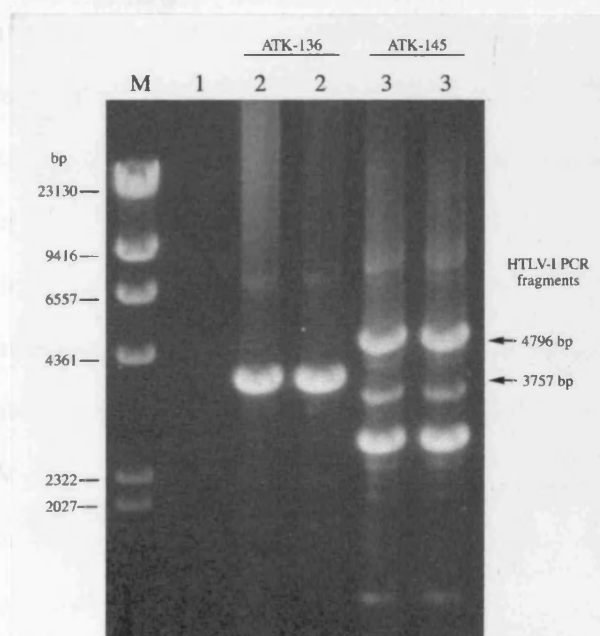
b) Molecular cloning of long PCR products

Long-PCR fragments yielded 5' and 3' halves of the HTLV-I provirus which overlapped between positions 4063 and 4083. This region contained a unique *Xba*I restriction enzyme site (base 4080) and this site was used to reconstruct the full length clones. Both long-PCR fragments ATK136 and ATK145 were gel purified, blunt-

ended and cloned individually into the *Sma*I site of the standard cloning vectors pUC18

and pUC19 respectively using standard protocols (chapter 2). These plasmids were

designated pUC18-ATK136 and pUC19-ATK145. In addition two independent

recombinant plasmids (a and b) were obtained for each ATK136 and ATK145 fragment

which were cloned from PCR products derived from two separate PCR reactions

(figure 3.4). A HTLV-I proviral genomic clone was then reassembled by double

restriction enzyme digestion of pUC18-ATK136 and pUC19-ATK145 plasmids with

*Eco*RI and *Xba*I restriction enzymes. The digested ATK136 and ATK145 HTLV-I

DNA fragments were purified by agarose gel extraction and both HTLV-I fragments

ligated together at a 1:1 molar ratio (90 fmols each) using standard protocols. HTLV-I

DNA fragment concatemers were then restriction enzyme digested with *Eco*RI to re-

generate a genomic HTLV proviral DNA. The re-assembled HTLV-I DNAs were then

directly cloned into the *Eco*RI site of pUC18. Only two recombinant clones were

isolated and these plasmids were designated pUC18-HTLVp [#]18, and [#]26. Clone [#]18

was generated by recombination of fragments ATK136a with ATK145a and clone [#]26

by recombination of ATK136a with ATK145b. No clones were obtained containing

ATK136b fragments despite repeated attempts. These full length pUC18-HTLVp

clones were then checked by restriction enzyme site mapping. All three PCR clones

contained the same restriction enzyme site profile and the sites tested were identical to a

reference HTLV$_{ATK-1}$ strain sequence (Seiki *et al*, 1983). The *Hind*III and *Cla*I

restriction enzyme sites found to be missing from the λHTLV-Ic clones were present in

these long PCR generated clones.

Expression plasmids were constructed by sub-cloning of the HTLV-I genomic clones

contained in pUC18-HTLVp into pBCCX. The overall cloning strategy used to

generate these constructs is shown schematically in figure 3.5. The pUC18-HTLVp

plasmids were restriction enzyme digested with *Eco*RI and 5'-DNA overhangs blunt-

ended by fill-in using Klenow polymerase. The blunt ended genomic HTLV-I fragment

was purified by agarose gel extraction and blunt-end ligated into the *Sma*I site of

pBCCX. Recombinant plasmid clones were checked for correct orientation insertion of HTLV by restriction digestion. Only three recombinant plasmids were isolated and were designated as pBC-HTLVp [#]14, [#]15a and [#]26b. pBC-HTLVp [#]14 and [#]15a was derived from the HTLV-I molecular clone in pUC18-HTLVp[#]18. pBC-HTLVp [#]26b from pUC18-HTLVp [#]26.

3.3.4 DNA nucleotide sequences of recombinant HTLV-I genomic clones

Due to the typically low yields of HTLV proviral DNA containing plasmids and the lack of financial resources, DNA sequencing of the entire 8.5 kb HTLV proviral clones was not possible. Instead all HTLV containing plasmids were routinely sequenced across the cloning sites to verify the insertion and orientation of HTLV in these constructs. In addition all genomic HTLV proviral clones were DNA sequenced using primers ATK-3 and ATK-5 which anneal to regions of the env and pol genes respectively. Limited DNA sequence information was thus generated for all the recombinant HTLV proviral clones isolated.

All clones generated from either the λHTLV-Ic or PCR templates were found to be identical in nucleotide sequence using the primers tested. Several nucleotide base changes were observed for both λHTLV-Ic and PCR generated clones compared to the published $HTLV_{ATK-1}$ (Seiki *et al.*, 1983) and $HTLV_{HS-35}$ (Malik *et al.*, 1988) sequences. However, all observed nucleotide changes were found to be conservative and did not disrupt the amino acid coding sequence of the HTLV-I proteins compared to $HTLV_{ATK-1}$ or $HTLV_{HS-35}$ in the regions sequenced (data not shown).

Figure 3.5. Schematic representation of the steps used to molecularly clone a HTLV-I provirus by long PCR amplification. Two halves of the HTLV-I provirus were PCR amplified, individually cloned and reassembled to give a full length HTLV-I genomic clone.

HTLV-I provirus

Splice donor | *Xba*I | PolyA site

| U3 | R | U5 | gag/pro/pol | env | pX | U3 | R | U5 |

ATK-13 →
ATK-6 ← *Xba*I
ATK-5 *Xba*I →
ATK-14 ←

Long PCR amplification

5' 3.8 kb ATK-13/6 HTLV-I fragment 3' — *Xba*I
5' 4.9 kb ATK-14/5 HTLV-I fragment 3' — *Xba*I

Blunt-end cloning | Blunt-end cloning

Clone into pUC cloning vectors

pUC18
pUC18 HTLV136
*Sma*I *Xba*I
*Eco*RI
*Sma*I 5'
HTLV ATK13-6

pUC19
pUC19 HTLV145
*Eco*RI *Sma*I 3'
*Sma*I
*Xba*I
HTLV ATK14-5

*Eco*RI & *Xba*I restriction digest | *Eco*RI & *Xba*I restriction digest

Excise partial 5' and 3' HTLV-I fragments

*Eco*RI — 3.8 kb — *Xba*I
*Xba*I — 4.9 kb — *Eco*RI

Ligate fragments

HTLV-I fragment concatermers

*Xba*I — *Eco*RI — *Xba*I — *Eco*RI — *Xba*I — *Eco*RI — *Xba*I

*Eco*RI restriction digestion

Reconstructed HTLV-I genomic clone

*Eco*RI — *Xba*I — *Eco*RI
5' 3'

Clone *Eco*RI digested fragments

CMV IE promoter
5'

pBC-HTLVI expression vector

3'
pBC-HTLVI
*Xba*I

132

3.3.5 Expression of recombinant HTLV-I genomic clones

All pBC-λHTLV and pBC-HTLVp expression constructs were electroporated into COS-1 cells and assayed for viral gene expression. COS-1 cells constitutively express SV40 large T antigen and are permissive for replication of SV40 ori containing plasmids such as pBCCX. The transcription of HTLV-I genes was tested by RNA northern blot analysis. HTLV-I regulatory protein expression was tested by a trans-activation CAT assay for expression of the tax protein. Finally structural gene expression and extracellular virus particle production was tested by western blotting, syncytia formation and reverse transcriptase activity assays. The following series of results were generated as part of the same experiment in which all plasmids, COS-1 cells and reagents were of the same batch and electroporations performed identically in parallel. These experiments were performed twice and data from a typical representative experiment are shown.

a) Northern blot analysis for HTLV-I RNA expression

Analysis of transcription of viral RNAs from the pBC-λHTLV and pBC-HTLVp expression constructs was assessed by northern blotting and probing with a full length HTLV ^{32}P random primed DNA probe (see chapter 2, section 2.3). COS cells were electroporated with the expression plasmids and 48 hours post electroporation total cellular RNA was extracted. Negative controls included RNA from non-electroporated COS cells and COS electroporated with the pBCCX expression vector (no insert) only. The positive control was total RNA extracted from HTLV-I transformed C91/PL cell line.

Northern blot autoradiograms of expressed HTLV RNAs from the long-PCR derived HTLV clones pBC-HTLVp $^{#}14$, $^{#}15a$ and $^{#}26b$ in COS cells are shown in figure 3.6. Figure 3.6a shows the formaldehyde gels prior to northern blotting and demonstrates that similar amounts of non-degraded total RNA were loaded per well. Figure 3.6b shows the northern blot autoradiogram and is from a 2 hour blot exposure. All negative

controls showed no bands and the positive control C91/PL RNA shows all three major HTLV viral RNA species with strong bands at 8, 4.2 and 2.1 kb. All three long PCR generated clones gave significant amounts of HTLV RNA expression as evidenced by the presence of the three major HTLV RNA species with bands at 8, 4.2 and 2.1 kb. Bands were clearly visible at similar intensities for all three PCR clones but were less intense (approximately 2-3 fold) than the bands from C91/PL cells. The most abundant species was the env 4.2 kb RNA and the least amount of transcript was of the tax/rex 2.1 kb RNA, which was barely detectable in the 2 hour exposure. It should be noted that at longer film exposures the 2.1 kb tax/rex RNA was readily detectable (data not shown).

Northern blot analysis of cells electroporated with pBC-λHTLV did not show the expression of any HTLV-I RNAs from similarly timed a 2 hour blot exposure (data not shown). Prolonged blot exposures (>48 hours) did show the presence of several faint bands but none corresponded exactly in size with the RNAs from C91/PL cells (data not shown), indicating incorrect RNA initiation and splicing events.

These results suggest the proper transcription of several HTLV RNA species from the long PCR derived molecular clones as demonstrated by the presence of bands corresponding to the three major viral RNAs of 8, 4.2 and 2.1 kb in length suggests. In contrast HTLV RNAs were found not to be expressed from the λHTLV derived molecular clones, indicating the lack of proper initiation of transcription and/or too low a level of expression to be detected.

Figure 3.6. Northern RNA blot of total RNA extracted from COS cells electroporated with pBC-HTLVp long PCR derived expression constructs. a) Ethidium bromide stained agarose gel of RNAs prior to blotting. All extracts show rRNA bands of equal intensity. b) Northern blot autoradiogram of RNAs (2 hour exposure). Lane 1 = negative control with RNA extracted from non-electroporated COS cells. Lane 2 = negative control with RNA extracted from cells electroporated with pBCCX. Lane 3 = RNA from cells electroporated with pBC-HTLVp #14. Lane 4 = RNA from cells electroporated with pBC-HTLVp #15a. Lane 5 = RNA from cells electroporated with pBC-HTLVp #26b. Lane 6 = Positive control with RNA extracted from C91/PL cells. All major HTLV-I RNA species can be seen in cells electroporated with pBC-λHTLV constructs.

a) Ethidium bromide stained agarose gel

b) Northern blot autoradiogram
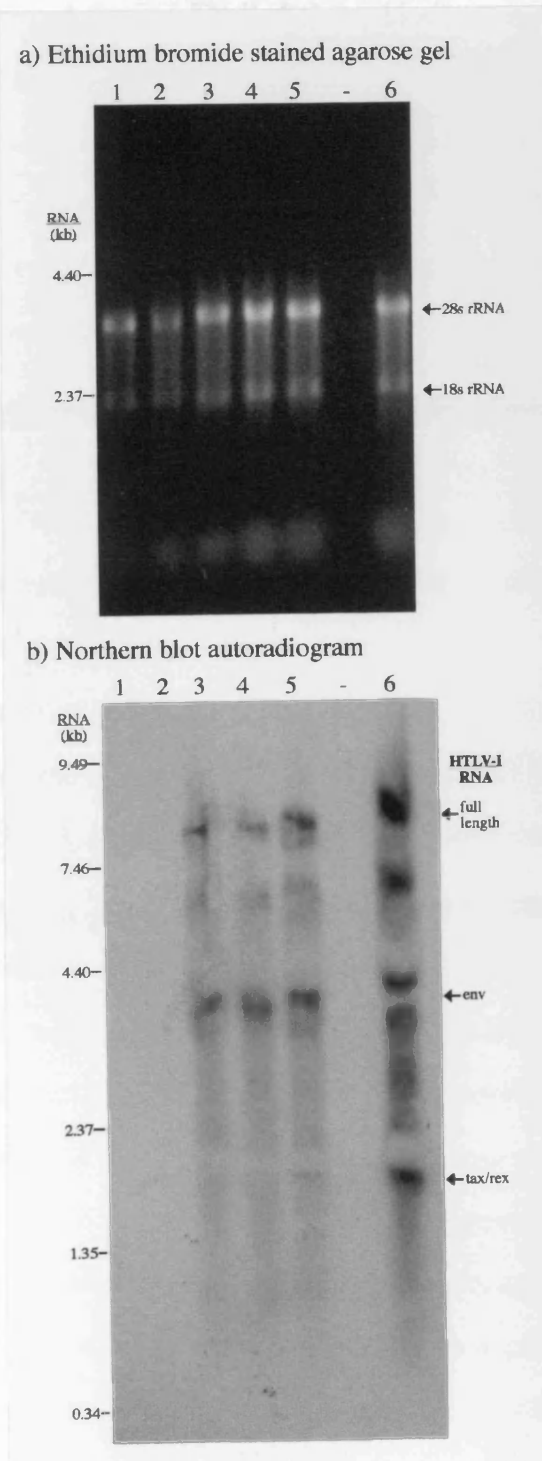
The reasons for the differences in RNA expression from the λHTLV and the PCR derived clones is likely to be due to the differences in the regulatory LTR regions contained by them. The PCR clones were constructed such that they retained all of the R region of the 5' and 3' LTR which included all the sequences required for efficient RNA processing. These sequences included the 5' LTR RNA splice donor, RNA polyadenylation site and the 3' LTR R_XRE rex binding regulatory sequence. These DNA sequence elements were absent from the λHTLV-Ic derived HTLV-I molecular clone and may explain the low levels of RNA expression observed. A greater efficiency of viral gene transcription can be predicted for the long PCR derived clones as they contain native HTLV-I 5' splice donor and RNA polyadenylation signals whereas the λHTLV-Ic clones utilise hetrologous SV40 derived regulatory sequences in the plasmid. The more efficient post-transcriptional processing of RNAs derived from the long PCR clones may explain its greater level of viral RNA expression compared to the λHTLV-Ic clones. The absence of the HTLV 5' splice donor in the λHTLV-Ic clones may also prohibit correct splicing events and generation of proper HTLV transcripts.

The molecular interaction between the rex regulatory protein and the R_XRE RNA stem loop motif may also play a significant role in efficient viral RNA expression from this system. The R_XRE RNA stem loop motif on HTLV-I viral mRNAs is thought to enable full length and single spliced env structural gene RNA transcripts to be efficiently expressed in the presence of the rex protein. The net effect of rex protein and R_XRE RNA stem loop interactions is to post-transcriptionally alter viral gene expression by enhancing the accumulation of nuclear and cytoplasmic unspliced gag and singly spliced env RNAs but decreasing the expression of tax/rex RNAs (Inoue *et al.*, 1991). Hence the absence of the R_XRE stem loop motif on RNAs generated from the λHTLV-Ic clones may not allow the efficient expression of the structural genes and may further explain the lack of viral RNA expression. This is in contrast to the long PCR derived clones where the RxRE would be present on viral RNAs allowing a steady state accumulation of structural gag and env RNAs but a concomitant decrease in tax/rex

RNAs. This predicted RNA expression profile was observed in the northern blot (figure 3.6) where gag and env structural gene RNAs were clearly observable and at a higher abundance than the tax/rex RNAs. However the influence of the suggested rex/R_XRE RNA interactions on viral gene expression also assumes the efficient expression of a functional rex protein in this system. Unfortunately the northern blot experiments could not determine the influence of rex upon HTLV RNA processing and expression as total cellular RNA (nuclear and cytoplasmic) was used. Hence, it is unclear whether full length or env mRNAs were efficiently exported from the nucleus for expression.

b) HTLV-I LTR trans-activation CAT assay for tax protein expression

HTLV-I regulatory protein expression from both λHTLV and PCR derived clones was examined using a HTLV-I LTR-CAT trans-activation assay for the tax protein. Expression of the tax protein from these clones would be used to trans-activate the expression of the CAT gene when co-electroporated with a HTLV-I promoter-CAT gene reporter construct pLTR-I-CAT (Chen *et al.*, 1985). Expression of active tax protein activates the HTLV-I LTR promoter in *trans* and drives the expression of the downstream CAT reporter gene. Cell extracts of co-electroporated cells were collected 48 hours post electroporation and assayed for CAT activity by the acetylation of chloramphenicol. The level of CAT activity in cellular extracts correlates positively with tax protein expression. Negative controls were cell extracts from cells electroporated with the pLTR-I-CAT reporter plasmid only. A positive control for CAT expression was of extracts of cells electroporated with a CAT gene expression plasmid pCLC (see chapter 2).

Tax trans-activation assays for the HTLV molecular clones are shown in figure 3.7. Negative controls showed minimal CAT activity with only 4 % conversion of chloramphenicol to acetylated forms. Cell extracts from cells electroporated with the positive control pCLC plasmid showed significant CAT activity as seen by the presence

of acetylated forms of chloramphenicol with conversion at 62 %. Extracts of cells co-electroporated with pBC-λHTLV #10 and #15 showed no difference in CAT activity (5 %) over the negative control (4 %). These results suggest an undetectable level or inactive tax protein expression from the λHTLV-Ic clones. Extracts of cells electroporated with the expression constructs pBC-HTLVp #14, 15a or 26b all showed enhanced CAT activity with 26 %, 23 % and 9 % conversion of chloramphenicol to acetylated forms. This represented a 6.5, 5.8 and 2.3 fold increase in CAT activity respectively, compared to the negative control samples (4 %). These results indicate the expression of an active tax protein from the long PCR derived HTLV-I molecular clones.

Figure 3.7. CAT tax trans-activation assays of extracts from COS cells electroporated with pBC-HTLV expression constructs. Lane 1 = negative control of cells electroporated with pLTR-I-CAT. Lane 2 = cells electroporated with pBC-λHTLV #10. Lane 3 = cells electroporated with pBC-λHTLV #15. Lane 4 = cells electroporated with pBC-HTLVp #14. Lane 5 = cells electroporated with pBC-HTLVp #15a. Lane 6 = cells electroporated with pBC-HTLVp #26b. Lane 7 = positive control of cells electroporated with pCLC CAT expression plasmid. All negative controls and pBC-λHTLV constructs (lanes 2 and 3) shows minimal CAT activity. Significant CAT activity is shown from cells electroporated with pBC-HTLVp constructs (lanes 4 to 6) and demonstrates the expression of an active tax protein. The positive control (lane 7) shows strong CAT activity. The percentage conversion of chloramphenicol to acetylated forms is shown.
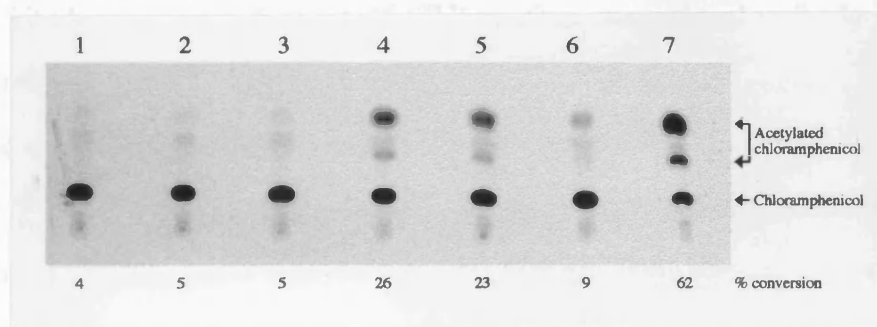
Long PCR clones #14 and #15a demonstrated a similar levels of tax protein expression but clone #26b showed a 2.6 fold lower level of expression as determined by the CAT trans-activation assays. However, northern blot analysis did not readily differentiate tax/rex RNA expression between these three long PCR derived clones and showed corresponding RNA bands of similar intensities (figure 3.6b). This suggests that long PCR clone #26b may encode a less active or defective tax protein compared to that

encoded by clones #14 and #15a. Such a reduction in tax activity may be due to defects

in the nucleotide DNA sequence in the tax gene of clone #26b in which amino acid

mutations may have caused a reduction in tax trans-activation activity.

These results show detectable levels of tax protein expression from the long PCR

derived HTLV clones but not the λHTLV-Ic clones. This indicates that the long PCR

clones are able to efficiently translate a functional tax protein from the expressed fully

spliced tax/rex RNA transcripts. Although a direct assay for rex protein expression was

unavailable the demonstration of functional tax protein expression indicates proper

translation from the tax/rex RNA and suggests rex may also be produced from these

clones.

c) Western blot and syncytia formation assays for envelope protein expression

HTLV-I envelope protein expression from the pBC-λHTLV and pBC-HTLVp

expression constructs was assessed by western blot analysis of total cell protein extracts

of COS-1 cells 48 hours post-electroporation. Protein blots were probed using an ECL

detection kit (Amersham) and anti-gp46 (SU) envelope monoclonal antibody 30g which

was a kind gift from T. Schulz, Chester Beatty laboratories, London. Figure 3.8

shows the results of a western blot using the anti-gp46 HTLV-I envelope monoclonal

antibody 30g. The negative control was total cellular protein extracts from non-

electroporated COS-1 cells and specific HTLV-I envelope protein bands were not

resolved. However, two faint bands corresponding to proteins of less than 34 kDa in

size were detected in these control lanes and in all other lanes. This suggests that these

bands are non-specific background artefacts and not HTLV-I envelope proteins. The

positive control was total cellular protein extracts from the HTLV-I transformed cell line

C91/PL and a major band corresponding to the gp68 envelope precursor and a band

corresponding to the gp46 (SU) envelope proteins can clearly be identified. The

detection of the gp68 envelope precursor protein was expected as monoclonal antibody

30g recognises the gp46 protein epitope in the precursor protein. Total cellular protein

extracts of COS-1 cells electroporated with both pBC-λHTLV clones showed the lack of detectable envelope protein expression with no bands being observed. Similarly, cellular protein extracts of cells electroporated with the pBC-HTLVp expression constructs did not show detectable HTLV-I envelope protein expression.

Figure 3.8. ECL western blot for HTLV-I envelope proteins expressed in cells electroporated with pBC-HTLV expression constructs. HTLV-I envelope proteins were detected using anti-gp46 antibody 30g. Lane 1 = negative control proteins from non-electroporated COS cells. Lane 2 = protein extracts from cells electroporated with pBC-λHTLV #10. Lane 3 = protein extracts from cells electroporated with pBC-λHTLV #15. Lane 4 = protein extracts from cells electroporated with pBC-HTLVp #14. Lane 5 = protein extracts from cells electroporated with pBC-HTLVp #15a. Lane 6 = protein extracts from cells electroporated with pBC-HTLVp #26b. Lane 7 = positive control proteins from C91/PL cells. All controls and extracts from all pBC-HTLV constructs (lanes 2 to 6) showed no bands. Positive control protein extracts shows the presence of gp68 and gp46 HTLV-I envelope proteins.
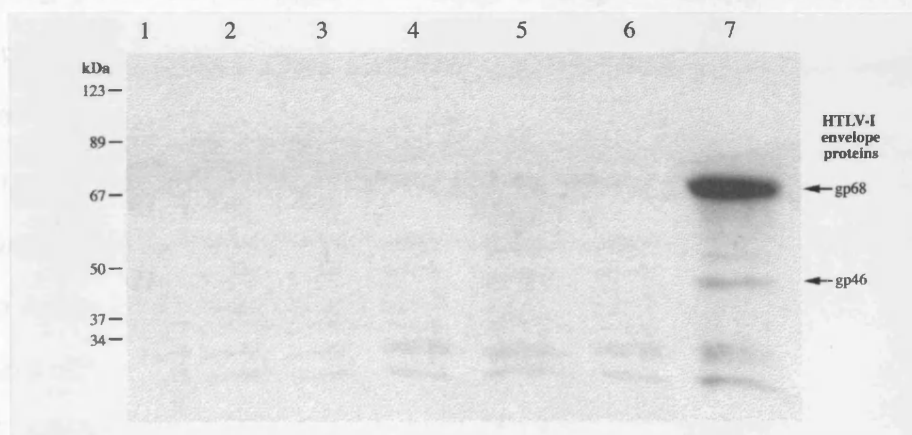
These results indicate the lack of detectable envelope protein expression from all recombinant HTLV-I clones. Western blot analysis using an anti-gp21 (TM) monoclonal antibody 5a (a kind gift from T. Schulz, Chester Beatty laboratories, London) also failed to detect HTLV-I envelope protein expression from these constructs (data not shown). For the λHTLV-Ic derived clones this result is in agreement to the northern blot data in which envelope RNA expression was not efficiently detected. However, HTLV-I envelope protein expression was not detected in cell extracts from the long PCR derived clones despite significant envelope RNA expression. This

140

indicates a post-transcriptional block in HTLV-I envelope protein expression or protein expression at too low a level to be detected in this assay. The lack of detectable HTLV-I envelope protein expression may be explained by the inefficient translation of the envelope proteins from their RNA transcripts or possibly rapid degradation of the expressed protein. This result could also be explained by a deficiency in the HTLV rex/R_XRE post-transcriptional regulatory mechanism, whereby full length and envelope RNAs may not be efficiently exported to the cytoplasm for translation.

Cell surface expression of a functional HTLV-I envelope proteins was assessed by the use of a syncytia formation co-culture assay. When HTLV-I envelope cell surface expressing cells are co-cultured with HTLV-I receptor bearing indicator cells large multinucleate cell aggregates or syncytia are formed. The formation of syncytia is a result of cell fusion between cells mediated by the interaction of the HTLV-I envelope proteins and its cellular receptor. The ability to form syncytia is characteristic of functional surface expressed HTLV-I envelope proteins and such assays are commonly used to assess its presence and functionality (e.g. Hoshino *et al.*, 1983b; Pique *et al.*, 1990 and 1992).

Cells were co-cultured with HTLV-I receptor bearing C8166 indicator cells at 2×10^5 each cell type in 1 ml media on a 24 well tissue culture plate (Nuncolon). Co-cultures were examined every 24 hours for 5 days post transfection for the presence of syncytia containing more than 20 nuclei. Negative controls for syncytium formation were co-culture of non-electroporated COS cells with C8166 cells and significant numbers of syncytia was not observed. The positive controls for syncytia formation was co-culture of HTLV-I transformed C91/PL cells with C8166 cells and large numbers of syncytia were observed as early as 24 hours after co-culture. However co-cultures of COS-1 cells electroporated with either pBC-λHTLV or pBC-HTLVp expression constructs with C8166 cells did not demonstrate significant syncytium formation at any time up to 5 days (data not shown). This results is consistent with the lack of intracellular

envelope protein expression from both pBC-λHTLV or pBC-HTLVp constructs where detectable envelope protein expression could not be observed. The lack of syncytium formation confirms the absence of significant levels of HTLV-I envelope protein expression from these molecular clones. It is known that HTLV-I envelope proteins are not tolerant to random mutations leading to non-functional protein (Pique *et al.*, 1990) and such changes may affect intracellular transport and expression (Pique *et al.*, 1992). Such gene mutations may have impaired protein translation and possibly cause rapid degradation of expressed protein products. It should also be noted that Pique *et al.*, 1990 and 1992 used COS-1 cells to express HTLV-I envelopes in their studies and demonstrates that COS-1 cells are competent for efficient processing and cell surface expression of HTLV-I envelopes.

d) Reverse transcriptase virus particle assay for VLP expression

Expression of the HTLV-I gag, pro and pol structural gene products was tested by the production of extracellular virus-like particles (VLPs). However the direct testing for HTLV-I gag protein expression from these clones could not be tested due to the unavailability of gag protein antibodies or patient sera. COS cells were electroporated with the recombinant expression plasmid constructs pBC-λHTLV and pBC-HTLVp and assayed for the expression of the envelope proteins and extracellular retrovirus particles in the cell culture supernatants by reverse transcriptase assays. Retrovirus particles contain viral reverse transcriptase and the presence of elevated RT activity in cell free culture supernatants are indicative of extracellular virus particles. A functional molecular clone of HTLV should produce gag, protease and polymerase proteins which if expressed correctly should produce VLPs which contain the reverse transcriptase (polymerase) protein. The amount of RT activity correlates positively with structural protein expression and VLP production (Rho *et al.*, 1981).

COS-1 cells were electroporated with the recombinant expression plasmid constructs pBC-λHTLV and pBC-HTLVp and culture supernatants were collected and tested for

reverse transcriptase activity at daily intervals for up to 5 days post electroporation. The results of the five day extracellular VLP RT-activity assays are shown in figure 3.9. Negative controls were of culture supernatants from non-electroporated COS cells and a constant low background level of RT activity was observed at around 2000 cpm/ml. Positive controls were of culture supernatants from cells electroporated with the HIV-1 VLP expression construct pBCCX-CSF (Haddrick *et al.*, 1996) and supernatants from the HTLV-I transformed cell line C91/PL. The pBCCX-CSF construct demonstrated high levels of extracellular RT-activity at 2 days post-electroporation with VLP production peaking at day three with over 10,000 cpm/ml. Extracellular culture supernatants from the HTLV-I transformed C91/PL cell line demonstrated a more modest level virus particle expression with RT-activity at a relatively constant 5000 cpm/ml. However, five day RT activity assay results for both pBC-λHTLV and pBC-HTLVp expression constructs did not show a significant increase in cell free RT activity over the negative controls.

These results indicate the absence or too low a level of VLP expression to be detected by RT assays from all the HTLV-I molecular clones tested. Northern blot RNA analysis demonstrated the expression of the three major HTLV viral RNA species from all long PCR derived clones but not from any of the λHTLV-Ic clones. The lack of detectable VLP expression from the λHTLV-Ic clones is consistent with their RNA expression pattern, whereby no gene products are produced. However, VLP expression was also not detectable from the long PCR derived HTLV-I molecular clones, despite viral RNA expression.

Figure 3.9. Reverse transcriptase assay for retrovirus-like particle (VLP) production. The reverse transcriptase (RT) activity in the extracellular culture medium from COS cells electroporated with HTLV-I expression plasmids is shown. a) RT assay data for λHTLV-Ic derived expression constructs pBC-λHTLV #8 and #10. b) RT-assay data for long PCR derived expression constructs pBC-HTLVp #14, #15a and #26b. Negative controls were culture medium from non-electroporated COS cells. Positive controls were culture supernatants electroporated with the HIV-I VLP expression plasmid pBCCX-CSF (Haddrick et al., 1996). All HTLV-I expression constructs failed to show significant extracellular RT-activity.

a) RT-activity of culture medium from cells electroporated with pBC-λHTLV plasmids
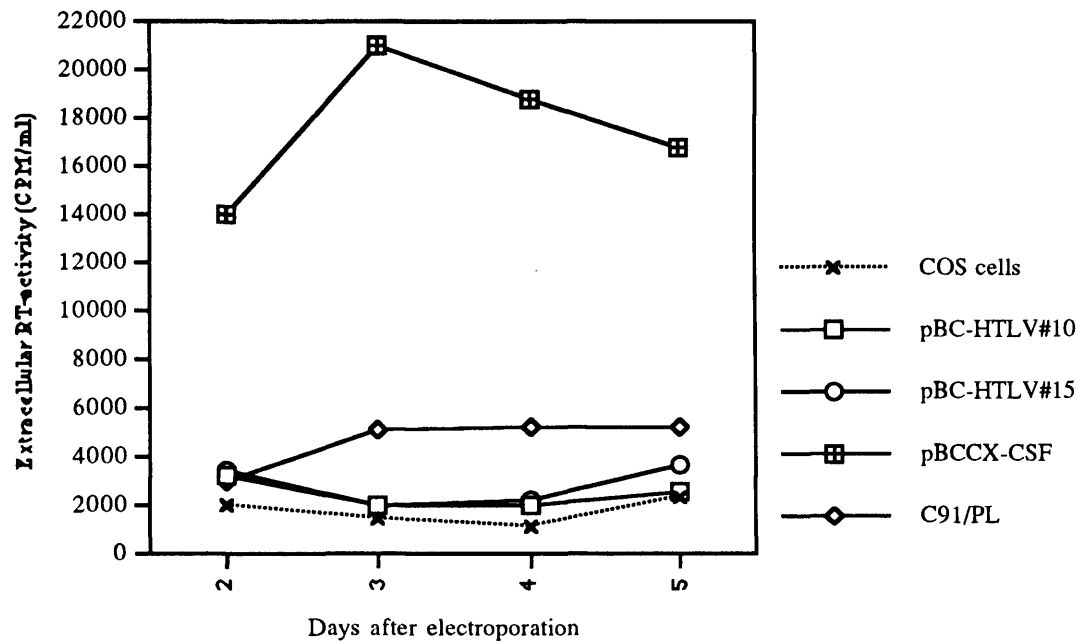
b) RT-activity of culture medium from cells electroporated with pBC-HTLVp plasmids
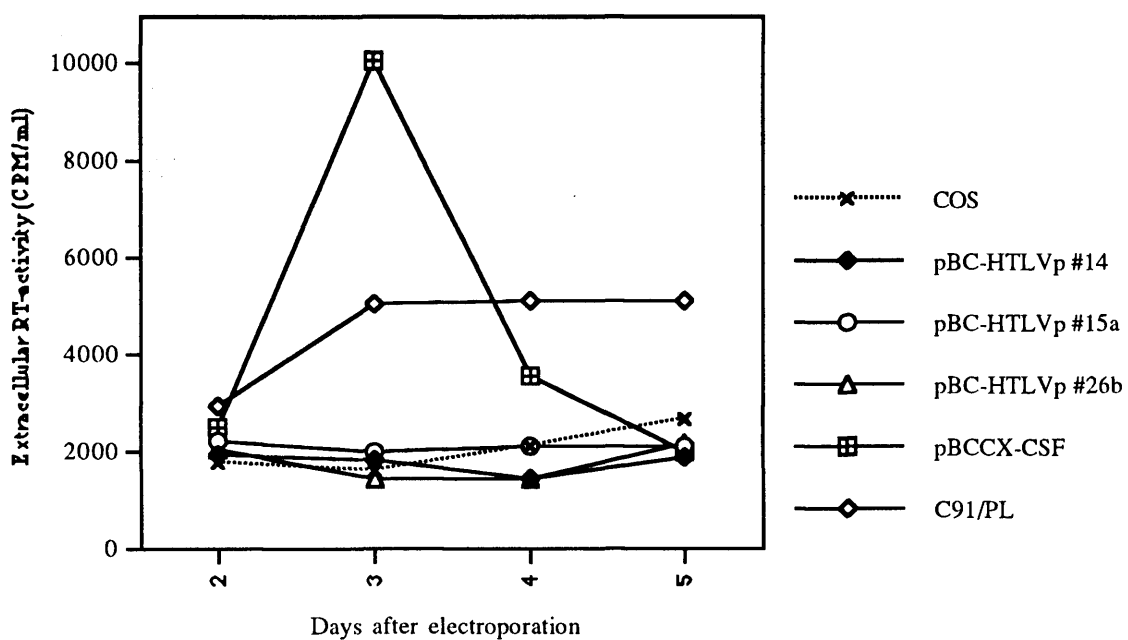
The absence of detectable VLP associated RT-activity from these PCR clones indicates a post-transcriptional block in VLP expression. These results could be explained by several factors. First, It may be possible that the long PCR derived clones are defective, containing nucleotide sequence errors in several critical genes. Errors in the pol gene may result in the expression of a defective, non-functional RT protein and thus demonstrate poor RT-activity in the VLP assays. Similarly, errors in the gag genes could produce defective proteins which may not allow efficient processing, assembly or release of VLPs from cells into the supernatants. Second, the rex/RxRE post-transcriptional regulatory mechanism for cytoplasmic RNA transport and expression may be defective, despite the PCR clones containing all the necessary regulatory elements. Although full length and partially spliced envelope RNAs were found to be expressed from all the PCR clones, the northern blot data could not distinguish nuclear from cytoplasmic RNAs. Hence, it may be that full length and envelope RNAs are transcribed correctly in the nucleus but inefficient rex/RxRE mediated post-transcriptional nuclear export does not allow significant cytoplasmic RNA accumulation for detectable protein expression.

In order to further examine the defects HTLV expression from the long PCR derived clones it would be necessary to increase the sensitivity of the VLP and envelope protein expression assays. Pelleting of viral particles by ultracentrifugation of the cell culture supernatants would concentrate the samples and may increase the sensitivity of the assays such that very low levels of virus expression may be detected. In this way it may be possible to demonstrate HTLV expression, abeit at a low level, from these molecular clones. The possible block in HTLV expression due to a defect in RNA transport could also be examined by physically separating nuclear and cytoplasmic fractions by preparative ultracentrifugation. RNAs could then be isolated from each fraction and the effects of rex/RxRE interactions examined by the relative distribution of HTLV RNAs in the nucleus and cytoplasm. However, in the absence of a suitable ultracentrifuge these experiments were not possible.

Overall the production of a functional HTLV-I proviral genomic clone and expression system was unsuccessful. The λHTLV-Ic derived molecular clones were found not to be able to direct detectable expression of any HTLV-I proteins. In contrast the HTLV-I molecular clones generated by long PCR amplification of C91/PL HTLV-I transformed cells' genomic DNA expressed all major classes of HTLV-I mRNAs and directed the expression of significant amounts tax proteins. The tax protein was also found to be functional being able to trans-activate expression from a HTLV-LTR promoter. However the expression of the HTLV-I envelope proteins and VLP production was not detected using standard assays. At this stage the further development of a functional molecular clone of HTLV-I was not pursued. Although a fully functional HTLV-I clone may have eventually been derived by further expression analysis and re-engineering of any defects found in the long PCR derived clones, several other investigators reported the isolation and characterisation of infectious molecular HTLV-I clones (Kimata *et al.*, 1994b; Derse *et al.*, 1995; Zhao *et al.*, 1995). Hence, the validity of producing a HTLV-I molecular clone and expression system was greatly reduced and these studies were not continued.

3.4 Structure and function of the HTLV-I envelope proteins

The focus of this part of the project was to specifically examine the role of the HTLV envelope proteins in relation to biological function and to identify regions and structural motifs involved in the processes of cell fusion, entry and mitogenicity. This was initially to be done using the VLP expression system described in section 3.3. Such a molecular system would then allow gene deletions and site specific mutations to be made in the HTLV envelope gene and its effects on envelope protein functionality assessed. However in the absence of a functional molecular HTLV-I proviral clone and VLP expression system an alternative method was employed using HTLV-I and HIV-I pseudotyped particles to study the HTLV envelope proteins. The development of a molecular pseudotyping system is described in the following sections.

146

3.4.1 Pseudotyping of HTLV-I envelope onto HIV-I VLPs

The phenotypic mixing of the viral envelope proteins of one virus to the heterologous viral core particle of another virus is known as pseudotyping and has been well characterised for a number of enveloped viruses (Boettiger *et al.*, 1979) including HTLV. These pseudotype particles are found to have expanded cell tropisms and possess the functional characteristics of the pseudotyped envelope glycoproteins. A number of reports have shown HTLV envelope glycoproteins can be successfully pseudotyped onto both M-MLV (Vile *et al.*, 1991; Denesvre *et al.*, 1996) and HIV retroviral core particles (Lusso *et al.*, 1990; Landau *et al.*, 1991).

It was the intention of this part of the project to develop a molecular HTLV-I envelope protein and HIV-I "core" particle pseudotyping system based on the pBCCX expression system. The use of pBCCX expression vector constructs provides a rapid system for HIV particle production and facilitates the molecular genetic manipulation of HTLV-I envelope genes. Modification of the existing HIV VLP expression construct pBCCX-CSF (Haddrick *et al.*, 1996) by deleting or disabling the HIV envelope gene would generate VLPs without the HIV envelope proteins. By co-expressing an envelope deficient pBCCX-CSF HIV VLP construct with a HTLV-I envelope protein expression construct it would be possible to form pseudotyped HIV particles which express HTLV-I envelope proteins on their surface but without any interference from the HIV-I envelope proteins. A schematic representation of this molecular VLP pseudotyping system is shown in figure 3.10. Phenotypic or functional activities elicited by these pseudotyped VLPs would be due solely to the heterologous pseudotyped HTLV-I envelope proteins. These pseudotyped VLPs should then confer functional envelope protein activities characteristic of HTLV-I. Molecular HTLV-I envelope clones would be amenable to deletion and site-directed mutagenesis analysis in this systems allowing the proposed functional mapping of envelope protein activities.

Figure 3.10. A schematic representation of the proposed pseudotype virus-like particle (VLP) expression system. The co-expression of envelope deleted HIV VLPs (pBCCX-CSF Δenv) with HTLV-I envelope proteins (pBC-HTLV-env) would produce HIV virus particles with HTLV-I envelope proteins on its surface.
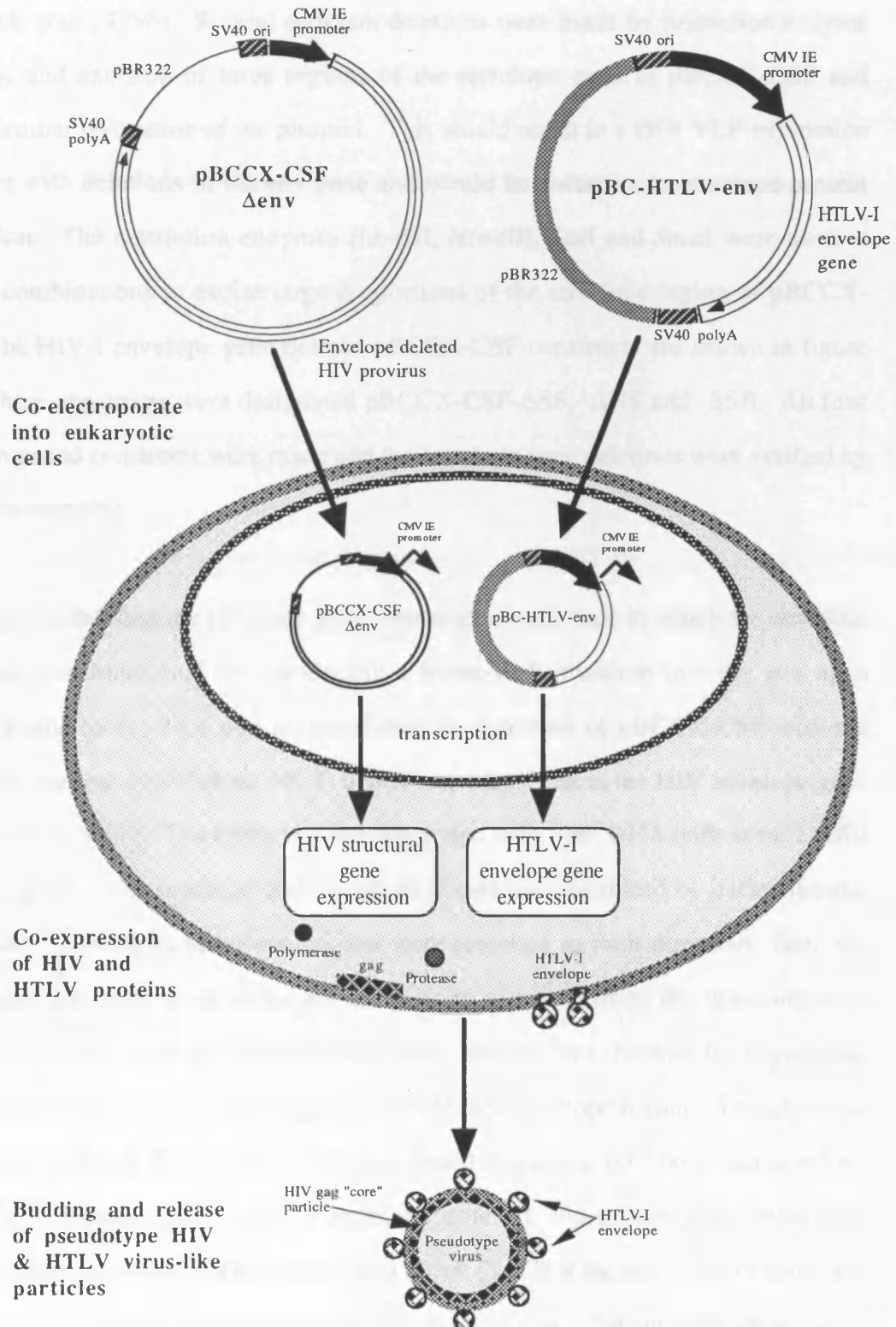
3.4.2 Construction of envelope deficient HIV VLP expression plasmids

Construction of envelope deficient HIV VLP expression constructs was done by deleting regions of the envelope gene in the VLP expression construct pBCCX-CSF (Haddrick *et al.*, 1996). Several different deletions were made by restriction enzyme digestion and excision of large regions of the envelope gene in pBCCX-CSF and intramolecular re-ligation of the plasmid. This would result in a HIV VLP expression construct with deletions in the env gene and would be defective in envelope protein expression. The restriction enzymes *Bam*HI, *Hind*III, *Sal*I and *Sma*I were used in various combinations to excise large proportions of the envelope region of pBCCX-CSF. The HIV-I envelope gene deleted pBCCX-CSF constructs are shown in figure 3.11. These constructs were designated pBCCX-CSF-ΔSS, -ΔHS and -ΔSB. All four of the proposed constructs were made and the envelope gene deletions were verified by restriction mapping.

In addition to deleting the envelope gene, constructs were made in which the env gene was made non-functional by introducing a frame-shift mutation into the env open reading frame (orf). This was accomplished by digestion of pBCCX-CSF with the restriction enzyme *Dra*III (base 6725) which is a unique site in the HIV envelope gene (bases 6358 to 8904). The DNA was then degraded from both DNA ends at the *Dra*III site using BAL-31 exonuclease and the whole plasmid reconstructed by intramolecular re-ligation. Several hundred nucleotides were removed in both directions from the *Dra*III site and may result in an orf frame-shift mutation when the plasmids were resealed. Several envelope deleted clones were isolated and checked for appropriate frame shift deletions by sequencing across the deleted envelope region. A single clone designated pBCCX-CSF-DB31 [#]22 was found contain a 607 bp deletion which introduced a frame-shift in the HIV envelope gene orf. Fortuitously the frame-shift mutation also introduced a translational stop codon (TAG) at the site of the deletion and thus clone [#]22 would express a truncated envelope protein. The envelope gene frame-shift deletion in pBCCX-CSF-DB31 [#]22 is shown in figure 3.12. This construct only

encodes the first 26 amino acids of the HIV gp120 envelope protein before the *Dra*III frame shift deletion. This small gp120 region only encodes the N-terminal leader peptide which is responsible for trafficking of the protein to the endoplasmic reticulum but does not contain any other known functional domains (Luciw, 1996).

Figure 3.11. Envelope protein deficient HIV-I VLP expression constructs. All constructs were based on the HIV-I VLP expression construct pBCCX-CSF (top). Regions of env gene deleted in the HIV-I provirus contained in pBCCX-CSF are shown by the dashed line. The presence or absence of the rev protein and RRE RNA stem loop post-transcriptional regulators are also shown.
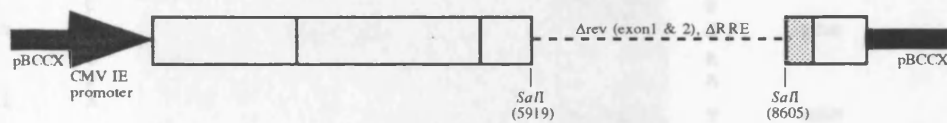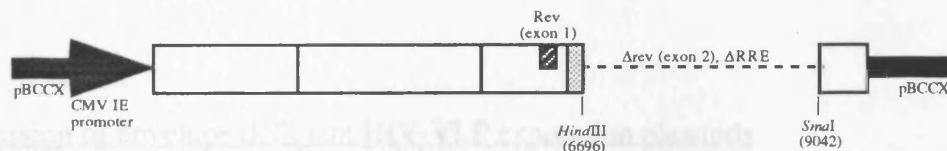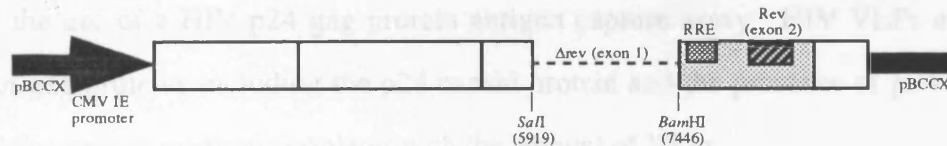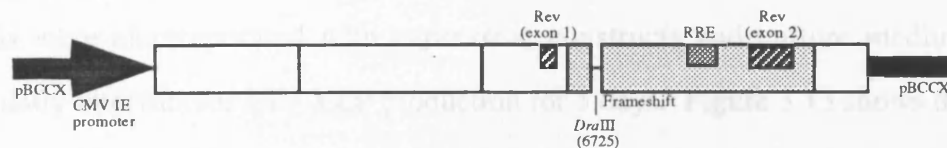
Figure 3.12. The DNA nucleotide sequence autoradiogram of the HIV-I env gene frameshift deletion in pBCCX-CSF-DB31 #22. The original wild type env gene nucleotide and amino acid sequence of pBCCX-CSF is shown on the left. The DNA nucleotide and amino acid sequence of the env gene in pBCCX-CSF-DB31 #22 is shown on the right. The arrow indicates the site of deletion between bases 79 and 686 of the HIV-I env gene. The deletion introduces a codon frameshift in the env gene resulting in a translational stop codon (TAG) and pBCCX-CSF-DB31 cannot express an intact envelope protein.
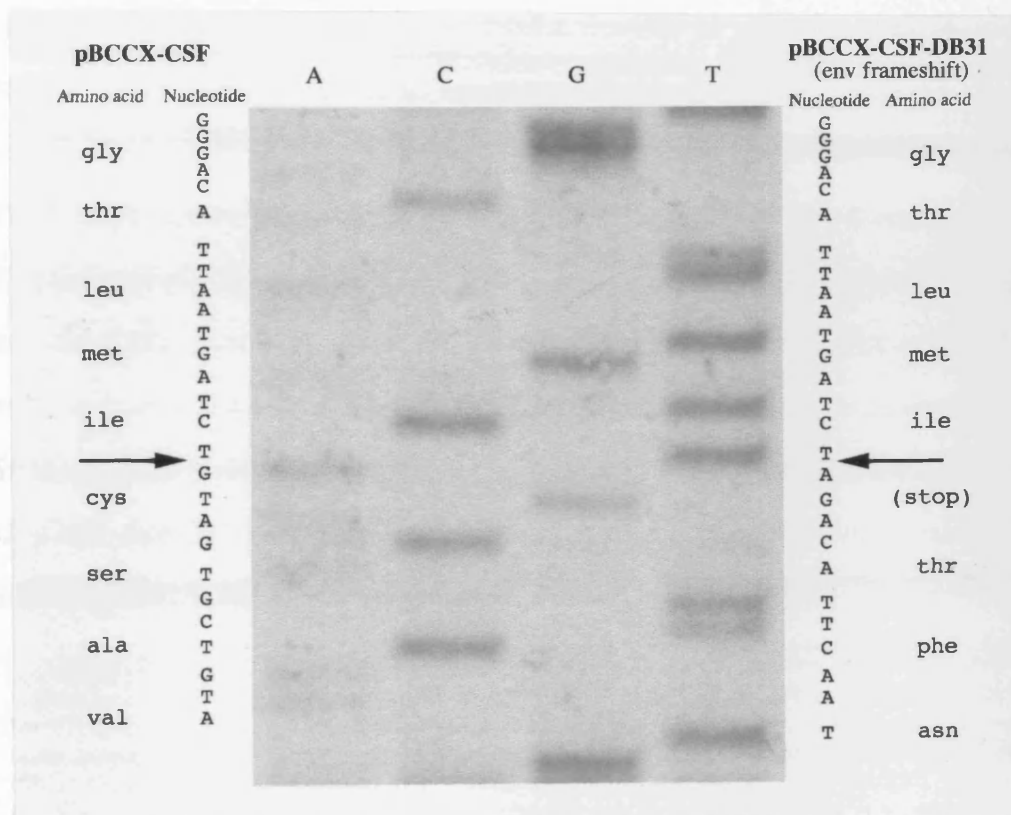
3.4.3 Expression of envelope deficient HIV-VLP expression plasmids

The production of VLPs from the envelope deleted pBCCX-CSF constructs was checked by the use of a HIV p24 gag protein antigen capture assay. HIV VLPs are composed of gag proteins including the p24 capsid protein and the presence of p24 in the extracellular culture medium correlates with the amount of VLPs.

COS-1 cells were electroporated with expression constructs and culture medium sampled at daily intervals for HIV VLP production for 5 days. Figure 3.13 shows the extracellular particulate p24 present in the culture medium from cells over a four day period. Negative controls for the experiment were culture media collected from non-

electroporated cells and showed a negligible level of extracellular p24 over the 4 day

sampling period. Positive controls for VLP expression were culture media collected

from cells electroporated with the parental pBCCX-CSF HIV expression plasmid.

Extracellular culture medium showed the presence of high levels of p24 and VLP

expression from this plasmid. VLP expression from the envelope deleted pBCCX-CSF

ΔSS, -ΔHS and -ΔSB constructs all showed negligible amounts of extracellular p24 at

levels comparable to the negative control. This indicates that these envelope deleted

HIV clones are deficient for VLP production. In contrast the env frame-shift mutant

HIV construct pBCCX-CSF-DB31 #22 did show significant VLP production with the

presence of high levels of p24 in the culture medium. However, the amount of p24

produced from this construct was only half that produced from the parental pBCCX-

CSF clone. This indicates that the env frameshifted HIV construct pBCCX-CSF-DB31

#22 is still capable of significant VLP production. This envelope defective construct

was subsequently used for the remaining pseudotyping studies.

Figure 3.13. HIV-I p24 antigen capture assay for HIV virus-like particle (VLP) production for the envelope deleted HIV-I VLP expression plasmids. Negative controls were culture medium from non-electroporated COS cells. Positive controls were culture medium from cells electroporated with the parental HIV-I VLP expression plasmids pBCCX-CSF. Only the pBCCX-CSF-DB31 env frameshift construct showed significant extracellular VLP expression.
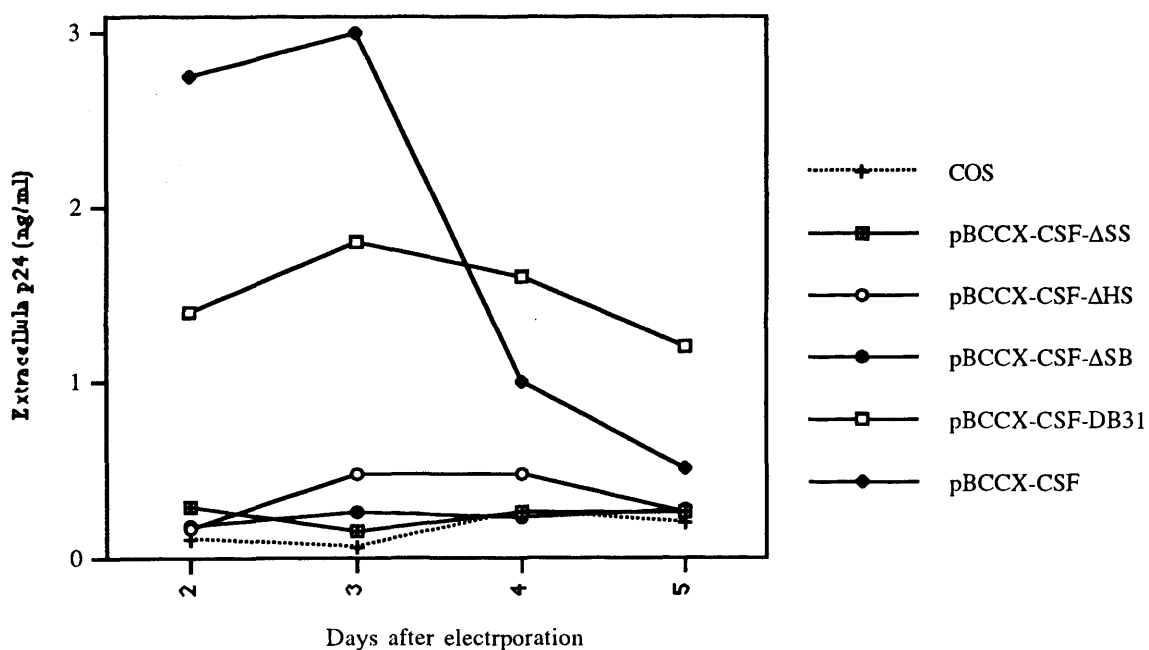
The lack of HIV-I VLP production from the envelope gene deleted pBCCX-CSF-ΔSS, -ΔHS and -ΔSB constructs can be explained by the deletion of other sequences within the env gene responsible for the efficient post-transcriptional regulation of HIV expression. HIV-I is a complex retrovirus like HTLV-I and also encodes several regulatory proteins which mediate the expression of the structural genes (see chapter 1, section 1.4.3 and figure 1.4). HIV-I encodes the regulatory protein rev which is analogous in function of the HTLV-I rex protein and similarly mediates the cytoplasmic accumulation of unspliced and singly spliced viral RNAs for efficient gag and env gene expression (Felber *et al.*, 1989; Malim *et al.*, 1989). The action of HIV-I rev, like HTLV-I rex, occurs through the interaction with a cis-acting RNA stem loop structure known as the rev responsive element or RRE present on unspliced and singly spliced viral RNAs (Rosen *et al.*, 1988; Malim *et al.*, 1989). The HIV-I rev regulatory protein, like HTLV-I rex, is encoded on a fully spliced mRNA transcript derived from two exons. The first 75 bp exon is present in a region between pol and env genes and the second 274 bp exon within the 3' end of the gp41 orf. The 240 bp RRE sequence is also found within the env gene orf and the RRE stem loop is only present in unspliced and singly spliced RNAs. Hence, the env gene deletions present in clones pBCCX-CSF-ΔSS, -ΔHS and -ΔSB disrupt either rev or RRE sequences or both in addition to the env gene. These constructs and their respective env, rev, RRE deletions are shown in figure 3.11. All these clones would therefore be defective in efficient gag gene expression due to the disruption of rev/RRE post-transcriptional regulation. The lack of gag gene expression would result in the absence of VLP production observed for these clones. In contrast the pBCCX-CSF-DB31 [#]22 envelope deficient HIV expression construct was found to be able to direct high levels of VLP expression. This envelope defective HIV clone was constructed by frame-shift deletion mutation of the env gene. The frame shift deletion occurred at the start of the env gene but did not disrupt any rev or RRE sequences and the clone was permissive for rev/RRE HIV RNA post-transcriptional regulation.

3.4.4 Molecular cloning of the HTLV-I envelope gene

A HTLV-I envelope protein expression plasmid was constructed by sub-cloning of the env gene from the λHTLV-Ic proviral clone described in section 3.3.2. The λHTLV-Ic proviral clone containing plasmid pBC-λHTLV was used as the template for sub-cloning and was shown in figure 3.2. The HTLV-I envelope gene is present as a single exon between bases 5498 to 6964 in this clone. pBC-λHTLV was partially restriction enzyme digested with *Pst*I (base 7047) and the 3' overhang generated was blunt ended by Mung bean nuclease treatment. The plasmid was then restriction enzyme digested with *Hind*III (base 5259) and the env containing fragment was purified by extraction from an agarose gel. The fragment was then cloned into the *Hind*III and *Sma*I restriction enzyme sites of the expression vector pBCCX. Recombinant env constructs were verified by restriction enzyme digestion and sequencing across the cloning sites. A single construct was isolated and designated pBC-HTLV-env [#]1.

3.4.5 Nucleotide sequence analysis of the HTLV-I envelope gene

The HTLV-I envelope gene of the λHTLV-Ic proviral clone was fully sequenced in order to verify its competence for functional protein expression. Sequencing of the HTLV-I env gene was performed with the aid of E. Bryan, Department Microbiology and Immunology, University of Leicester. A *Sph*I (base 5391) to *Pst*I (base 7047) fragment containing the entire env gene (bases 5498 to 6964) was excised from pBC-λHTLV and purified by extraction from an agarose gel. The 1656 bp env gene containing fragment was then restriction enzyme digested with Sau3AI to produce five smaller fragments. These fragments were then all individually cloned into the *Sph*I to *Bam*HI, *Bam*HI and *Bam*HI to *Pst*I restriction enzyme sites of M13mp18 and M13mp19 bacteriophage plasmids. Single stranded M13 templates of all these env fragments were then generated and multiple clones of each fragment sequenced.

The env gene from pBC-λHTLV was completely sequenced by this method and the complete nucleotide sequence is shown in figure 3.14. The HTLV-I env gene sequence

from pBC-λHTLV was compared to the env gene sequences from MT-2 HTLV-I transformed cells (Gray *et al.*, 1990) in which λHTLV-Ic was isolated (Mori *et al.*, 1987). All amino acid numbering starts at amino acid 1 (met) of the gp68 precursor envelope protein. The gp46 protein spans amino acids 1 through 312 and gp21 spans amino acids 313 to 488. The nucleotide sequence data showed a total of seven nucleotide base changes occurs within the env gene from pBC-λHTLV when compared to MT-2 cell env gene sequences. Four of these base changes where found to be conservative with respect to codon usage and did not alter the encoded amino acid (ser-155, asp-230, leu-234 and ala-261). Three nucleotide bases changes where found which altered the amino acid coding sequence of two amino acids. In addition these changes were not present in either HTLV$_{ATK-1}$ or HTLV$_{HS-35}$ envelope amino acid sequences (Seiki *et al.*, 1983; Malik *et al,*. 1988; data not shown). A leucine to valine change was found at amino acid 262 which occurs near the C-terminal end of gp46. This region of gp46 has not been shown to confer any specific envelope protein activity and the significance of this change is unknown. An alanine to glycine mutation was found at amino acid 313 which is the N-terminal amino acid of gp21. The mutation occurs immediately after the envelope cleavage site (arg-312) and in the putative gp21 fusion peptide domain (amino acids 313 to 342). Such a mutation may affect the efficient cleavage of the gp68 precursor protein and the fusogenic properties of the expressed HTLV-I envelope. If a negative effect on protein activity was found the mutations in the env gene could be easily changed back to a functional wild type nucleotide sequence by site directed mutagenesis.

It should be noted that the missing *Cla*I site found in the env gene of the pBC-λHTLV clones (see section 3.3) was also seen in the pBC-env clones. Both clones were derived from λHTLV-Ic and nucleotide sequence analysis of the envelope gene identified a base change which disrupts this *Cla*I site. However, this nucleotide base change did not alter the encoded amino acid (Asp-230) and indicates this change not significant with respect to the envelope protein function in both clones.

Figure 3.14. The complete 1467 bp nucleotide and predicted 488 amino acid (AA) coding sequence of the env gene in pBC-HTLV-env (λenv) in comparison to the env gene of MT-2 cells (Gray *et al.*, 1990). Only the nucleotide and amino acid changes in λenv are shown and all other nucleotides were found to be identical to the sequences MT-2 cells. A total of seven nucleotide base changes and two amino acid changes were found. Amino acid coding changes are shown in **bold**. The gp46 and gp21 cleavage site sequence is shown underlined.

```
λenv
MT-2     ATG GGT AAG TTT CTC GCC ACT TTG ATT TTA TTC TTC CAG TTC TGC CCC CTC ATC TTC GGT GAT TAC AGC CCC AGC TGC TGT ACT CTC ACA -  90
MT-2(AA)  M   G   K   F   L   A   T   L   I   L   F   F   Q   F   C   P   L   I   L   G   D   Y   S   P   S   C   C   T   L   T  -  30
λenv(AA)


λenv
MT-2     ATT GGA GTC TCC TCA TAC CAC TCT AAA CCC TGC AAT CCT GCC CAG CCA GTT TGT TCG TGG ACC CTC GAC CTG CTG GCC CTT TCA GCG GAT - 180
MT-2(AA)  I   G   V   S   S   Y   H   S   K   P   C   N   P   A   Q   P   V   C   S   W   T   L   D   L   L   A   L   S   A   D  -  60
λenv(AA)


λenv
MT-2     CAG GCC CTA CAG CCC CCC TGC CCT AAT CTA GTA AGT TAC TCC AGC TAC CAT GCC ACC TAT TCC CTA TAT CTA TTC CCT CAT TGG ATT AAA - 270
MT-2(AA)  Q   A   L   Q   P   P   C   P   N   L   V   S   Y   S   S   Y   H   A   T   Y   S   L   Y   L   F   P   H   W   I   K  -  90
λenv(AA)


λenv
MT-2     AAG CCA AAC CGA AAT GGC GGA GGC TAT TAT TCA GCC TCT TAT TCA GAC CCT TGT TCC TTA AAG TGC CCA TAC CTG GGG TGC CAA TCA TGG - 360
MT-2(AA)  K   P   N   R   N   G   G   G   Y   Y   S   A   S   Y   S   D   P   C   S   L   K   C   P   Y   L   G   C   Q   S   W  - 120
λenv(AA)


λenv
MT-2     ACC TGC CCC TAT ACA GGA GCC GTC TCC AGC CCC TAC TGG AAG TTT CAG CAA GAT GTC AAT TTT ACT CAA GAA GTT TCA CGC CTC AAT ATT - 450
MT-2(AA)  T   C   P   Y   T   G   A   V   S   S   P   Y   W   K   F   Q   Q   D   V   N   F   T   Q   E   V   S   R   L   N   I  - 150
λenv(AA)


λenv                      G
MT-2     AAT CTC CAT TTT TCA AAA TGC GGT TTT CCC TTC TCC CTT CTA GTC GAC GCT CCA GGA TAT GAC CCC ATC TGG TTC CTT AAT ACC GAA CCC - 540
MT-2(AA)  N   L   H   F   S   K   C   G   F   P   F   S   L   L   V   D   A   P   G   Y   D   P   I   W   F   L   N   T   E   P  - 180
λenv(AA)              S


λenv
MT-2     AGC CAA CTG CCT CCC ACC GCC CCT CCT CTA CTC CCC CAC TCT AAC CTA GAC CAC ATC CTC GAG CCC TCT ATA CCA TGG AAA TCA AAA CTC - 630
MT-2(AA)  S   Q   L   P   P   T   A   P   P   L   L   P   H   S   N   L   D   H   I   L   E   P   S   I   P   W   K   S   K   L  - 210
λenv(AA)


λenv                                                                                         C               C
MT-2     CTG ACC CTT GTC CAG TTA ACC CTA CAA AGC ACT AAT TAT ACT TGC ATT GTC TGT ATC GAT CGT GCC AGC CTA TCC ACT TGG CAC GTC CTA - 720
MT-2(AA)  L   T   L   V   Q   L   T   L   Q   S   T   N   Y   T   C   I   V   C   I   D   R   A   S   L   S   T   W   H   V   L  - 240
λenv(AA)                                                                                     D               L
```

```
λenv                                                                      C  G
MT-2      TAC TCT CCC AAC GTC TCT GTT CCA TCC TCT TCT TCT ACC CCC CTC CTT TAC CCA TCG TTA GCG CTT CCA GCC CCC CAC CTG ACG TTA CCA -  810
MT-2(AA)   Y   S   P   N   V   S   V   P   S   S   S   S   T   P   L   L   Y   P   S   L   A   L   P   A   P   H   L   T   L   P -  270
λenv(AA)                                                                            A   V


λenv
MT-2      TTT AAC TGG ACC CAC TGC TTT GAC CCC CAG ATT CAA GCT ATA GTC TCC TCC CCC TGT CAT AAC TCC CTC ATC CTG CCC CCC TTT TCC TTG -  900
MT-2(AA)   F   N   W   T   H   C   F   D   P   Q   I   Q   A   I   V   S   S   P   C   H   N   S   L   I   L   P   P   F   S   L -  300
λenv(AA)


λenv                                              GC
MT-2      TCA CCT GTT CCC ACC CTA GGA TCC CGC TCC CGC CGA GCG GTA CCG GTG GCG GTC TGG CTT GTC TCC GCC CTG GCC ATG GGA GCC GGG GTG -  990
MT-2(AA)   S   P   V   P   T   L   G   S   R   S   R   R   A   V   P   V   A   V   W   L   V   S   A   L   A   M   G   A   G   V -  330
λenv(AA)                                                   G


λenv
MT-2      GCT GGC GGG ATT ACC GGC TCC ATG TCC CTC GCC TCA GGA AAG AGC CTC TTA CAT GAG GTG GAC AAA GAT ATT TCC CAA TTA ACT CAA GCA - 1080
MT-2(AA)   A   G   G   I   T   G   S   M   S   L   A   S   G   K   S   L   L   H   E   V   D   K   D   I   S   Q   L   T   Q   A -  360
λenv(AA)


λenv
MT-2      ATA GTC AAA AAC CAC AAA AAT CTA CTC AAA ATT GCG CAG TAT GCT GCC CAG AAC AGA CGA GGC CTT GAT CTC CTG TTC TGG GAG CAA GGA - 1170
MT-2(AA)   I   V   K   N   H   K   N   L   L   K   I   A   Q   Y   A   A   Q   H   R   R   G   L   D   L   L   F   W   E   Q   G -  390
λenv(AA)


λenv
MT-2      GGA TTA TGC AAA GCA TTA CAA GAA CAG TGC TGT TTT CTA AAT ATC ACT AAT TCC CAT GTC TCA ATA CTA CAA GAA AGA CCC CCC CTT GAG - 1260
MT-2(AA)   G   L   C   K   A   L   Q   E   Q   C   C   F   L   N   I   T   N   S   H   V   S   I   L   Q   E   R   P   P   L   E -  420
λenv(AA)


λenv
MT-2      AAT CGA GTC CTG ACT GGC TGG GGC CTT AAC TGG GAC CTT GGC CTC TCA CAG TGG GCT CGA GAG GCC TTA CAA ACT GGA ATC ACC CTT GTC - 1350
MT-2(AA)   N   R   V   L   T   G   W   G   L   N   W   D   L   G   L   S   Q   W   A   R   E   A   L   Q   T   G   I   T   L   V -  450
λenv(AA)


λenv
MT-2      GCG CTA CTC CTT CTT GTT ATC CTT GCA GGA CCA TGC ATC CTC CGT CAG CTA CGA CAC CTC CCC TCG CGC GTC AGA TAC CCC CAT TAC TCT - 1440
MT-2(AA)   A   L   L   L   L   V   I   L   A   G   P   C   I   L   R   Q   L   R   H   L   P   S   R   V   R   Y   P   H   Y   S -  480
λenv(AA)


λenv
MT-2      CTT ATA AAA CCT GAG TCA TCC CTG TAA       -1467
MT-2(AA)   L   I   N   P   E   S   S   L  (STOP) -  488
λenv(AA)
```

3.4.6 Expression of the HTLV-I envelope proteins

The expression of HTLV-I envelope proteins from the pBC-HTLV-env [#]1 expression construct was checked by western blot and syncytium formation assays. Intracellular envelope expression was checked by western blot analysis of total cell protein extracts using the ECL detection kit (Amersham) in conjunction with monoclonal antibodies 5a and 30g which recognise epitopes on the gp21 and gp46 HTLV-I envelope proteins respectively. The monoclonal antibodies 5a and 30g were kind gifts from T. Schulz, Chester Beatty Laboratories, London. COS-1 cells were electroporated with pBC-HTLV-env [#]1 and after 48 hours total cell proteins were extracted and checked for HTLV-I envelope protein expression. Figure 3.15 shows representative blots using anti-gp21 monoclonal antibody 5a.

Figure 3.15. ECL western blot for HTLV-I envelope proteins expressed in COS cells electroporated with pBC-HTLV-env #1 expression construct. HTLV-I envelope proteins were detected using anti-gp21 antibody 5a. Lane 1 = negative control proteins from non-electroporated COS cells. Lane 2 = negative control proteins from cells electroporated with pBCCX-CSF-DB31. Lane 3 = protein extracts from cells electroporated with pBC-HTLV env #1. Lane 4 = empty lane. Lane 5 = positive control proteins from C91/PL cells. All controls and extracts from pBCCX-CSF-DB31 HIV expression constructs (lanes 1 and 2) showed no bands. Protein extracts from cells electroporated with pBC-HTLV-env shows strong expression of gp68 envelope precursor. Positive control protein extracts shows the presence of gp68 HTLV-I envelope proteins.
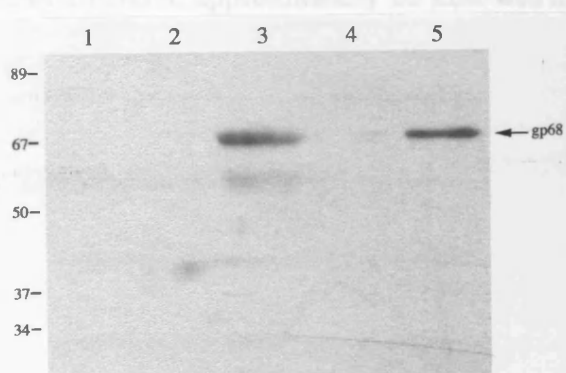
Negative controls were total protein extracts from non-electroporated cells and cells electroporated with the expression vector pBCCX only. No bands can be observed in the negative control lanes. Positive controls were total protein extracts from the HTLV-I transformed C91/PL cell line and a strong band at approximately 68 kDa corresponding to the envelope precursor gp68 protein was observed. Total protein extracts from cells electroporated with pBC-HTLV-env [#]1 clearly shows expression of the gp68 precursor protein. A band at 68 kDa is seen which corresponds exactly in size and of comparable intensity to gp68 protein found in the positive control C91/PL extracts. However, the presence of cleaved gp21 envelope protein product was not readily detected in any of the cell extracts using monoclonal 5a. A faint band at approximately 55 kDa is also detected in extracts from cells electroporated with pBC-HTLV-env [#]1 which was not present in C91/PL cells.

Figure 3.16 shows representative blots using anti-gp46 monoclonal antibody 30g. Negative controls were total protein extracts from non-electroporated cells and no bands can be observed. Positive controls were total protein extracts from the HTLV-I transformed C91/PL cell line and strong bands at approximately 68 and 46 kDa corresponding to the gp68 envelope precursor and gp46 SU proteins respectively were observed. The presence of a band at approximately 20 kDa was also observed, which may correspond to gp21. However, monoclonal antibody 30g is known not to cross-react with gp21 (T. Schulz, personal communication) and this band is likely to be a non-specific artefact or possibly the result of gp68, gp46 protein degradation. Total protein extracts from cells electroporated with pBC-HTLV-env [#]1 clearly shows expression of the gp68 precursor protein. A band at 68 kDa is seen which corresponds exactly in size and of comparable intensity with the gp68 band of positive control C91/PL cell extracts. Faint bands corresponding to gp46 and gp21 proteins can also be observed in protein extracts from pBC-HTLV-env [#]1 electroporated cells. These protein bands were far weaker in intensity to those observed in extracts from C91/PL cells and indicates a far lower level of gp68 cleavage. A weak band similar to that

detected by monoclonal antibody 5a (figure 3.15) at approximately 55 kDa is also

detected in extracts from pBC-HTLV-env #1.

Figure 3.16. ECL western blot for HTLV-I envelope proteins expressed in cells electroporated with pBC-HTLV-env #1 expression construct. HTLV-I envelope proteins were detected using anti-gp46 antibody 30g. Lane 1 = negative control proteins from non-electroporated COS cells. Lane 2 = negative control proteins from cells electroporated with pBCCX-CSF-DB31. Lane 3 = protein extracts from cells electroporated with pBC-HTLV env #1. Lane 4 = positive control proteins from C91/PL cells. All controls and extracts from pBCCX-CSF-DB31 HIV expression constructs (lanes 1 and 2) showed no bands. Protein extracts from cells electroporated with pBC-HTLV-env shows strong expression of gp68 envelope precursor but minimal levels of gp46. Positive control protein extracts shows the presence of gp68 and gp46 HTLV-I envelope proteins.
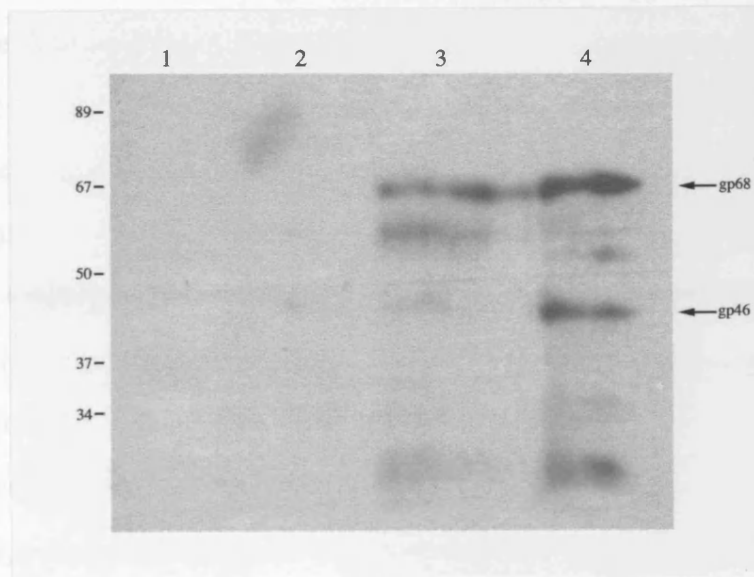
These results indicate that significant HTLV-I envelope protein expression can be driven

from the pBC-HTLV-env expression construct. The construct is able to express the

gp68 envelope precursor protein efficiently and at similar levels to that found in C91/PL

cells. In addition the expressed gp68 precursor protein migrates to exactly the same

position as gp68 from C91/PL cells in SDS-PAGE gels which indicates correct

glycosylation of the protein. However, the maturation of the envelope precursor was

found to be far less efficient than in C91/PL cells with a much lower level of gp46 and

gp21 proteins being observed. The presence of a 55 kDa protein product was also

detected by both anti-envelope antibodies 5a and 30g. This product was not detected in

extracts from C91/PL cells and may indicate the presence of incompletely glycosylated or partially degraded gp68. It is unlikely to be a completely non-glycosylated gp68 protein as this protein is reported to migrate at approximately 42 kDa in SDS-PAGE gels (Pique *et al.*, 1992). However, the 55 kDa band was found to be weak in intensity compared to the gp68 precursor protein and indicates it to be a minor protein species.

The expression of a functional envelope protein from pBC-HTLV-env [#]1 was checked by syncytium formation assays. Cells were co-cultured with C8166 indicator cells at 2×10^5 of each cell type in 1 ml media in a 24 well tissue culture plate (Nunclon). Co-cultures were examined every 24 hours for 5 days after electroporation for the presence of giant syncytia containing more than 20 nuclei. Negative controls were co-culture of non-electroporated COS cells with C8166 cells and significant syncytium formation was not observed. The positive controls for syncytia formation was co-culture of HTLV-I transformed C91/PL cells with C8166 cells and large numbers of giant syncytia was observed as early as 24 hours after co-culture. COS-1 cells when electroporated with pBC-HTLV-env [#]1 and co-cultured with C8166 cells did not form significant numbers of syncytia compared to the negative controls (data not shown). This result indicates that either the expressed envelope proteins were not functional with respect to cell fusion and syncytia formation ability or the level of protein expression may not be sufficient or at a high enough cell density to elicit a significant fusogenic response.

The expression of the gp68 envelope precursor protein which shows poor cleavage and no syncytium formation ability from pBC-HTLV-env [#]1 suggests that the env gene amino acid mutation described in section 3.4.5 may be responsible. The envelope protein alanine to glycine mutation (amino acid 313) in this clone occurred in the region of gp68 thought to be involved in protein cleavage and possibly syncytium formation. The mutation may have impaired both these functions and would account for the inefficient cleavage and lack of syncytia formation observed. Insertional mutagenesis studies around amino acid 313 has previously been shown to abolish gp68 cleavage and

syncytia formation (Pique *et al.*, 1990) and suggests a critical role in protein maturation. The lack of efficient cleavage of gp68 expressed from pBC-HTLV-env [#]1 would also account for its lack of syncytium formation as cleavage is thought to be required to expose the active fusion domain of gp21 (Pique *et al.*, 1990) and for cell surface expression (Pique *et al.*, 1992). The lack of cell surface expression makes this pBC-HTLV-env [#]1 clone unsuitable for use in a pseudotyping system. However the single alanine to glycine mutation thought to be responsible for the deficiencies in the expressed envelope protein could be simply reversed by site directed mutagenesis.

3.4.7 Co-expression of HIV-I VLPs and HTLV-I envelope proteins

Despite the functional deficiencies of the envelope proteins expressed from the pBC-HTLV-env [#]1 construct it was decided to test the co-expression system for when a functional env expressing clone was available. pBCCX-CSF-DB31 [#]22 and pBC-HTLV-env [#]1 plasmids were co-electroprated into COS-1 cells and co-expression of VLPs and HTLV-I envelope was tested by HIV-I p24 and HTLV-I envelope western blot assays. COS-1 cells were electroporated with a total of 25 μg of plasmid at a 1:1, 1:10 and 1:100 molar ratio of pBC-HTLV-env [#]1 to pBCCX-CSF-DB31 [#]22. Extracellular culture medium was sampled at daily intervals for 4 days post-electroporation for VLP expression and total cellular proteins extracted for HTLV envelope expression. Figure 3.17 shows the results from HIV p24 assays for VLP production. Negative controls were culture medium from non-electroporated cells and cells electroporated with pBC-HTLV-env [#]1. The levels of extracellular p24 were found to be negligible from these controls. Positive controls for VLP production was culture medium from cells electroporated with 25 μg pBCCX-CSF-DB31 [#]22 plasmid only. High levels of extracellular p24 was observed with over 20 times greater than the negative controls and indicates the expression of high levels of VLPs. Culture medium collected from cells co-electroporated with pBC-HTLV-env [#]1 and pBCCX-CSF-DB31 [#]22 at a 1:1 molar ratio showed negligible amounts of p24 comparable to the negative controls. Culture medium collected from cells co-electroporated at a 1:10 molar ratio

showed a slightly increased level of p24 production but with only a 2 to 3 fold enhancement over the negative controls. Culture medium collected from cells electroporated at a 1:100 molar ratio showed high levels of p24 comparable to that observed from the positive control. These results indicate the production of VLPs from co-electroprated cells in a manner dependent on the amount of pBCCX-HIV-DB31 [#]22 used. High molar ratios of pBCCX-CSF-DB31 [#]22 to pBC-HTLV-env [#]1 was required for efficient VLP production.

Figure 3.17. HIV-I p24 antigen capture assay for HIV virus-like particle (VLP) production from cells co-electroporated with pBC-HTLV-env #1 and pBCCX-CSF-DB31 #22 at 1:1, 1:10 and 1:100 molar ratios. Negative controls were culture medium from non-electroporated COS cells. Positive controls were culture medium from cells electroporated with the HIV-I VLP expression plasmids pBCCX-CSF.
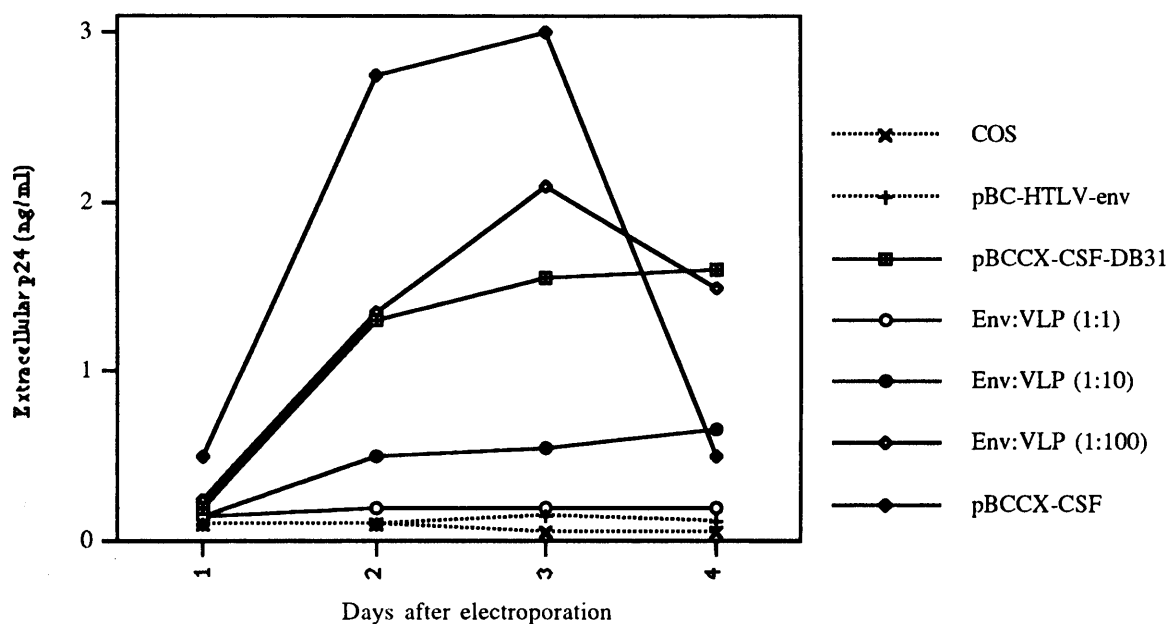
The intracellular expression of HTLV envelope proteins by pBC-HTLV-env [#]1 in co-elctropration with pBCCX-CSF-BD31 [#]22 was assessed by western blot analysis. Total cell extracts were isolated 2,3 and 4 days post co-electroporation and HTLV envelope protein detected by an ECL kit (Amersham) and the anti-gp46 monoclonal antibody 30g. Table 3.1 shows the results of western blot analysis of cell protein extracts probed for HTLV-I envelope expression. Negative controls were extracts from

non-electroporated cells and cells electroporated with pBCCX-CSF-DB31 [#]22 alone. No HTLV envelope expression was observed in these cells at any time period. Positive controls were cell extracts from cells electroporated with pBC-HTLV-env [#]1 alone and HTLV-I transformed C91/PL cells. Total protein extracts from cells electroporated with pBC-HTLV-env [#]1 demonstrated the expression of the gp68 HTLV envelope precursor protein at similar levels on days 2 and 3 but expression was markedly reduced by day 4. Cell extracts from C91/PL cells also demonstrated expression of gp68 as well as gp46 and gp21 cleaved products. Total protein extracts from cells co-electroporated with pBC-HTLV-env [#]1 and pBCCX-CSF-DB31 [#]22 at a 1:1 molar ratio showed a low level of gp68 expression at days 2 and 3 when compared to the positive controls. Total protein extracts from cells co-electroporated at 1:10 and 1:100 molar ratio did not show detectable levels of gp68 protein expression at any time period. These results indicate the poor expression of HTLV-I envelope proteins from pBC-HTLV-env [#]1 when co-electroporated with pBCCX-CSF-DB31 [#]22. Low level envelope expression could only be detected at a 1:1 molar ratio and not at lower pBC-HTLV-env [#]1 molar ratios which suggests a dose dependant level of expression.

Table 3.1. HTLV-I envelope protein expression in COS cells co-electroporated with pBC-HTLV-env #1 and pBCCX-CSF-DB31 #22 expression constructs. Western blot analysis was performed on total cell proteins using anti-gp46 monoclonal antibody 30g. Negative controls were extracts from non-electroporated COS-1 cells or cells electroporated with the HIV-I VLP expression construct pBCCX-CSF-DB31 #22 and no bands were observed at any time point. Positive controls were extracts from C91/PL cells and COS cells electroporated with pBC-HTLV-env #1 and HTLV-I envelope protein bands corresponding to gp68 and gp46 were observed. Co-electroporation of pBCCX-CSF-DB31 #22 with pBC-HTLV-env #1 yielded detectable envelope protein expression at a 1:1 molar ratio only. (- = no detectable protein expression; + = faint envelope protein bands and low expression; ++ = weak envelope protein bands and moderate expression; +++ strong envelope protein bands and high expression).

Days after electroporation	COS-1 cells only	pBCCX-CSF-DB31 #22 (a)	pBCCX-HTLV-env #1 (b)	1:1 molar ratio (b:a)	1:10 molar ratio (b:a)	1:100 molar ratio (b:a)	C91/PL cells only
2	-	-	+++	+	-	-	+++
3	-	-	+++	+	-	-	+++
4	-	-	+	-	-	-	+++

Overall these results do not favour an efficient particle pseudotyping system based on an expression vector co-expression system. Proteins produced from these expression constructs demonstrated a dose dependant level of expression in which a higher molecular ratio of one plasmid would favour its expression over the other. However, a ratio of plasmids which would allow significant expression from both constructs was not found. At a 1:1 molar ratio VLP production was negligible but detectable levels of envelope protein expression was found in these cells. Increasing the ratio of pBCCX-CSF-DB31 #22 to 1:10 in the co-electroporation increased VLP production significantly but the expression of HTLV-I envelope was not detected. A similar pattern was observed at a 1:100 molar ratio. At no molecular ratio of plasmids did the significant expression of HIV VLPs or HTLV-I envelope proteins coincide. Indeed no ratio of plasmids can be predicted in which expression would coincide based on these results. Hence, the production of pseudotyped particles by the co-expression of HIV VLP and HTLV envelope expression constructs was not possible in this system. It should be noted however that the VLP detection system may not be sufficiently sensitive enough to detect low level virus expression. Concentration of cell supernatants by ultracentrifugation may have increased the sensitivity of the assays, allowing low levels of pseudotype virus expression to be effectively detected. However, in the absence of a suitable ultracentrifuge these experiments could not be performed.

The development of a particle pseudotyping system was not pursued further due to the publication of several studies examining the structural and functional features of the HTLV-I envelope proteins (Delamarre *et al.*, 1994; Paine *et al.*, 1994) and increasing evidence suggesting gp46 is not mitogenic (Kimata *et al.*, 1993 and 1994a). Hence the validity of producing a system for examining HTLV-I envelope protein structure and function was greatly reduced and these studies were not continued.

3.5 Molecular cloning and expression of the HTLV-I tax protein

In order to facilitate studies with the HTLV-I tax trans-activator protein a mammalian expression plasmid was constructed based on pBCCX and contains the tax orf. The tax protein is encoded from the 2.1 kb doubly spliced HTLV tax/rex mRNA transcript derived from two exons found at the start of the env gene and in the pX region of the DNA provirus. Thus the 1061 bp tax orf could be obtained from the tax/rex mRNA transcripts of HTLV-I transformed C91/PL cells. However the rex and p21^{rex} proteins are also encoded on the same doubly spliced tax/rex mRNA transcript and within the tax coding region but in alternative reading frames. Hence molecular clones of the tax gene would also contain rex and p21^{rex} orfs and also potentially express these proteins in addition to tax. The tax/rex cDNA clones were obtained by reverse transcription PCR (RT-PCR) of HTLV RNA transcripts extracted from the HTLV-I transformed C91/PL cells. Long and accurate PCR techniques developed during the isolation of molecular HTLV-I proviral clones (section 3.3.3) were employed to amplify the tax orf.

3.5.1 RT-PCR cloning of HTLV-I tax/rex cDNA

Total genomic RNA was isolated from the HTLV-I transformed C91/PL cells and polyadenylated mRNAs reverse transcribed into first strand cDNA products using M-MLV reverse transcriptase and oligo-dT primers. A 1144 bp DNA fragment containing the entire 1061 bp tax/rex cDNA was then PCR amplified using specific tax primers ATK-15 and -16 and cloned directly between the *Hind*III and *Xho*I restriction enzyme sites of the mammalian expression vector pBCCX. Primers ATK-15 and -16 were designed against the HTLV$_{ATK-1}$ stain predicted tax/rex cDNA sequence and contained synthetic restriction enzyme sites (*HindIII* and *Xho*I respectively) at their 5' ends to facilitate cloning. Tax/rex molecular clones were amplified with Taq extender long PCR additive, Vent and Pfu thermostable DNA polymerases using protocols developed in the amplification of the HTLV-I provirus (section 3.3.3).

Initially tax PCR cDNA amplifications were done using the Taq extender PCR additive (Stratagene) two enzyme system which was found to be highly effective and efficient in long PCR amplification of the HTLV proviral clones (section 3.3.3). RT-PCR of the 1144 bp tax/rex cDNA fragments was performed on first round cDNA products using identical reaction conditions and general cycle parameters used for amplification of HTLV proviral DNA (section 3.3.3).

The PCR parameters for primer pairs ATK-15 and ATK-16 were;

92°C, 0.5 minute denaturation time

62°C, 0.5 minute annealing time

72°C, 0.8 minutes extension time (45 seconds per kb to be amplified)

for a total of 30 PCR cycles

PCR products of correct size were efficiently amplified under these conditions and are shown figure 3.18. PCR products were purified by extraction from agarose gels and cloned into the *Hind*III and *Xho*I restriction enzyme sites of pBCCX using standard techniques. Two clones were isolated and were designated pBC-tax/rex [#]8 and [#]10.

Figure 3.18. EtBr stained agarose gel of tax/rex cDNA PCR amplification using Taq extender PCR additive (Stratagene). Lane 1 = negative control PCR (H₂O). Lane 2 = Taq extender PCR using primers ATK-15 and ATK-16. Tax/rex PCR product is seen as a band at 1142 bp.
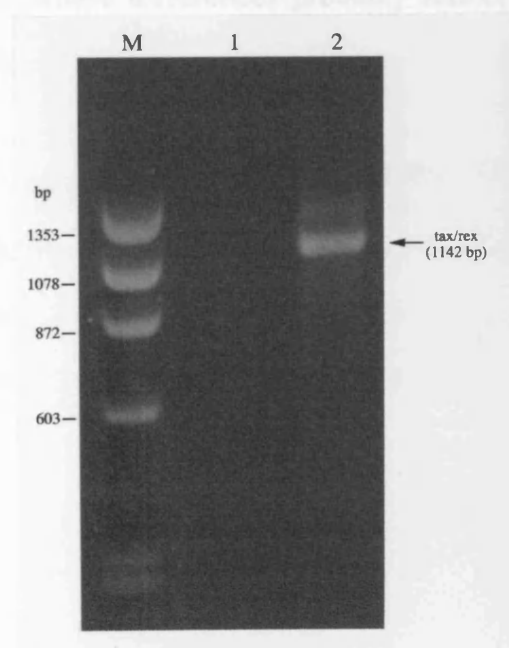
RT-PCR amplification of tax/rex cDNA using Vent DNA polymerase (NEB) required additional optimisation of PCR reaction conditions over the standard protocols. Using the suggested PCR parameters Vent polymerase PCR amplification only yielded smears or very high molecular weight products just migrating out of the wells when visualised on EtBr stained agarose gels. These are believed to be non-specific primer and template artefacts which are characteristic of failed or inefficient Vent polymerase PCRs (NEB protocol and data sheet). Standard PCR titrations of primer, magnesium and enzyme concentrations yielded no improvement in PCR amplification. However the addition of 0.1 µg/ml BSA to the standard PCR reactions seemed to effectively stabilise Vent polymerase and allowed tax/rex cDNA amplifications (figure 3.19) under the following conditions;

$92^{o}C$, 1.0 minute denaturation time

$50^{o}C$, 1.0 minute annealing time

$72^{o}C$, 1.5 minute extension time

for 30 cycles

Lower annealing temperatures of $50^{o}C$ and longer extension times of 1.5 minutes were needed for amplification of tax/rex cDNA products when compared to Taq extender PCR amplifications. These differences probably reflect the lower efficiency and processivity of the single Vent polymerase compared to the Taq extender two enzyme long PCR system.

Amplified PCR products were purified by extraction from agarose gels and cloned into the *Hin*DIII and *Xho*I sites of pBCCX using standard protocols. Only a single tax/rex cDNA clone was isolated despite repeated cloning attempts. This clone was designated pBC-tax/rex [#]11v.

Figure 3.19. EtBr stained agarose gel of tax/rex cDNA PCR amplification using Vent DNA polymerase (NEB) in the presence and absence of BSA. Lane 1 = negative control PCR (H_2O) with 0.1 µg/ml BSA. Lane 2 = Vent polymerase PCR using primers ATK-15 and ATK-16 in the presence of 0.1 µg/ml BSA. Lane 3 = negative control PCR (H2O) without BSA. Lane 4 = Vent polymerase PCR using primers ATK-15 and ATK-16 without BSA. Lane 5 = positive control tax/rex PCR product derived using Taq extender PCR additive (see figure 3.18). Tax/rex PCR product is seen as a band at 1142 bp. Vent DNA polymerase only amplifies tax/rex cDNA in the presence of 0.1 µg/ml BSA (lane 2).
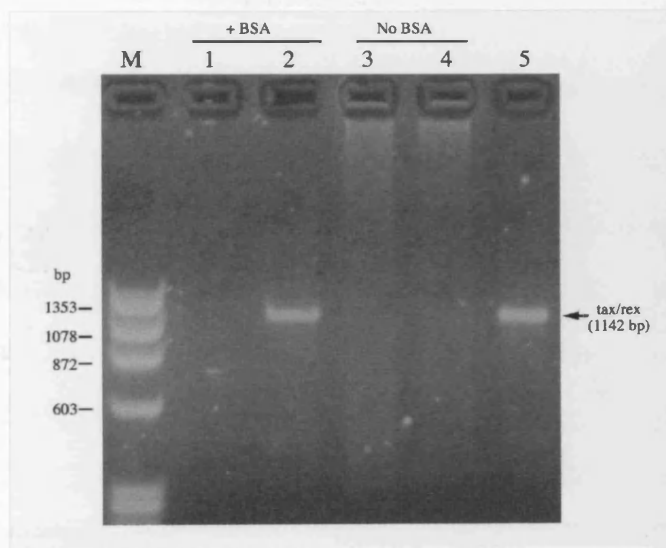
Tax/rex cDNA RT-PCR cloning using Pfu DNA polymerase alone was successful using the recommended standard reaction conditions but required two rounds of PCR amplification. Single round PCR amplifications only yielded smears when PCR products were visualised on EtBr stained agarose gels and indicated inefficient and non-specific amplification. The first round PCR was performed on first strand cDNA at a low annealing temperature for a small number of PCR cycles in order to promote primer annealing with a minimal loss in specificity. This initial round of PCR amplification would generate PCR amplicons with fully complimentary primer annealing sites allowing greater stringency in subsequent amplifications.

First round PCR amplification was performed on first strand cDNAs using standard

recommended reaction conditions using the following cycle parameters;

$92^{\circ}C$, 0.5 minute denaturation time

$50^{\circ}C$, 0.5 minute annealing time

$72^{\circ}C$, 2.0 minute extension time

for 5 cycles only

Second round PCR amplifications were performed on 10 % of the first round PCR

products using ATK-15 and ATK-16 primers but at a higher annealing temperature to

specifically amplify tax/rex cDNAs. PCRs were performed using standard

recommended reaction conditions and using the following reaction conditions;

$92^{\circ}C$, 1.0 minute denaturation time

$72^{\circ}C$, 2.5 minute combined annealing and extension time

for 30 cycles

PCR products of correct size were efficiently amplified under these conditions (data not

shown). PCR products were purified by extraction from agarose gels and cloned into

the expression vector pBCCX using standard techniques. Three tax/rex cDNA clones

were isolated and designated pBC-tax/rex [#]2p, [#]5p and [#]14p.

3.5.2 Nucleotide sequence analysis of recombinant HTLV-I tax/rex cDNA

All pBC-tax/rex clones were routinely sequenced across the _Hind_III and _Xho_I cloning

sites to check for correct insertion and thus nucleotide sequence data was generated for

all clones. Representative tax/rex nucleotide sequences for all clones from the 5' region

of the tax/rex cDNA was compared to a reference $HTLV_{ATK-1}$ nucleotide sequence

(Seiki _et al_, 1983) and is shown in figure 3.20. Nucleotide sequence analysis

demonstrated that all clones contained at least one nucleotide change compared to the

reference $HTLV_{ATK-1}$ strain sequence and that all clones derived from the same PCR

reaction were identical in sequence.

Figure 3.20. Representative nucleotide and predicted amino acid (AA) sequence of tax/rex open reading frames in the pBC-tax/rex expression constructs compared to the HTLV$_{ATK-1}$ tax/rex sequences (Seiki *et al.*, 1983). Only the first 120 nucleotides of are shown. a) Nucleotide DNA sequence starting from the rex initiation (ATG=1) codon. b) Predicted rex protein amino acid sequence. c) Predicted tax protein amino acid sequence (underlined ATG is the tax initiation codon). TE = Taq extender PCR derived clones. Vent = Vent DNA polymerase derived clones. Pfu = Pfu DNA polymerase derived clones. All clones derived using the same DNA polymerase were identical in sequence and data sequences is shown. Nucleotide base and amino acid changes are shown in **bold**.

a) Nucleotide DNA sequence

```
tax/rex   ATGCCCAAGACCCGTCGGAGGCCCCGCCGATCCCAAAGAAAAAGACCTCCAACACCATGGCCCACTTCCCAGGGTTTGGACAGAGTCTTCTTTTCGGATACCCAGTCTACGTGTTTGGAG   -120
TE                                                         A    G         C                            A
Vent                                                       A
Pfu                                                        A
```

b) rex protein amino acid sequence

```
rex (AA)   M  P  K  T  R  R  R  P  R  S  Q  R  K  R  P   P  T  P  W  P  T  S  Q  G  L  D  R  V  F  F  S  D  T  Q  S  T  C  L  E  T  - 40
TE                                                       P     A        S                       D
Vent                                                     P
Pfu                                                      P
```

c) tax protein amino acid sequence

```
tax (AA)                                                 M  A  H  F  P  G  F  G  Q  S  L  L  F  G  Y  P  V  Y  V  F  G  - 21
TE                                                                L                             R
Vent       (no changes)
Pfu        (no changes)
```

Cloning and expression of HTLV-1 proteins

For the Taq extender generated clones four nucleotide base changes at were observed out of 225 bases sequenced (1.78 % base change). Two of these nucleotide changes conferred two amino acid coding changes in the tax protein (amino acids 4 and 14). One of these nucleotide changes conferred a single amino acid coding change in the rex protein (amino acid 18). Both the vent polymerase and Pfu polymerase derived clones only showed single nucleotide base changes out of 241 nucleotide bases sequenced (0.41 % base change) and 286 bases sequenced (0.35 % base change) respectively. The single T to A base change at base 46 found for all the Vent and Pfu polymerase derived clones were identical and was also present in all Taq extender derived clone sequences suggesting that HTLV-I tax in C91/PL cells contains this change. This nucleotide base change was also degenerate and did not alter the amino acid coding sequence of the tax or rex protein. These observations indicate that this change is not significant with respect to the tax or rex protein amino acid sequence and is present in the template C91/PL wild type tax/rex nucleotide sequence. Thus the actual number of nucleotide base changes becomes 3 for Taq extender clones (1.33 %) and no changes for the Vent of Pfu polymerase derived tax/rex clones. Overall, these data demonstrate the higher fidelity of the proofreading vent and Pfu DNA polymerases over the Taq extender PCR additive two enzyme system.

3.5.3 Expression of the HTLV-I tax protein

The expression of a functional tax protein from all tax expression constructs were assessed using a HTLV-I LTR-CAT reporter gene trans-activation assay described in section 3.3.5b.

Figure 3.21 shows an autoradiogram of the CAT activity of cell extracts from Taq extender derived clones [#]8 and [#]10. Negative controls were extracts from cells electroporated with pLTR-I-CAT reporter plasmid only. This control extract demonstrated negligible CAT activity with only 4 % conversion of chloramphenicol to acetylated forms respectively. Positive control extracts from pCLC electroporated cells

demonstrated a high level of CAT expression with 48 % conversion to acetylated forms.

Cell extracts of cells electroporated with the Taq extender derived tax/rex clones [#]8 and

[#]10 did not show significant levels of CAT activity with both demonstrating only 5 %

conversion of chloramphenicol to acetylated forms. This result indicates that the Taq

extender derived tax expression constructs either to do not efficiently expresses the tax

protein or a non-functional tax protein is expressed which is unable to direct CAT

expression from pLTR-I-CAT plasmids.

Figure 3.21. CAT tax trans-activation assays of extracts from COS cells electroporated with pBC-tax/rex expression constructs derived from Taq extender PCR additive PCR amplification. Lane 1 = negative control of cells electroporated with pLTR-I-CAT. Lane 2 = cells electroporated with pBC-tax/rex #8. Lane 3 = cells electroporated with pBC-tax/rex #10. Lane 4 = positive control of cells electroporated with pCLC CAT expression plasmid. All negative controls and pBC-tax/rex constructs (lanes 2 and 3) shows minimal CAT activity and lack of functional tax protein expression. The positive control (lane 4) shows strong CAT activity. The % chloramphenicol conversion to acetylated forms is shown.
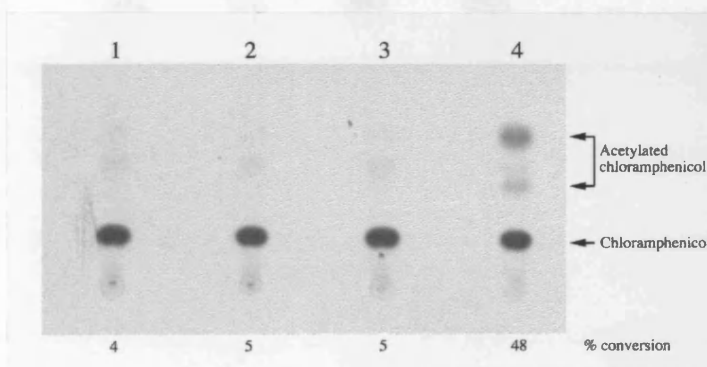
Figure 3.22 shows an autoradiogram of the CAT activity of cell extracts from the Vent

polymerase derived clone [#]11v. Negative controls were cell extracts from non-

electroporated cells and cells electroporated with pLTR-I-CAT reporter plasmid only.

These extracts demonstrated negligible CAT activity with only 6 % and 7 % conversion

of chloramphenicol to acetylated forms respectively. Positive control extracts from

pCLC electroporated cells demonstrated a high level of CAT expression with 59 %

conversion to acetylated forms. Cell extracts of cells electroporated with the Vent

polymerase derived tax/rex clone [#]11v demonstrated a high level of CAT activity with

73 % conversion of chloramphenicol to acetylated forms. This result indicates the expression of a functional tax protein from the vent polymerase derived tax/rex expression plasmids.

Figure 3.22. CAT tax trans-activation assays of extracts from COS cells electroporated with pBC-tax/rex expression constructs derived from Vent DNA polymerase PCR amplification. Lane 1 = negative control of cells electroporated with pLTR-I-CAT. Lane 2 = cells electroporated with pBC-tax/rex #11v. Lane 3 = positive control of cells electroporated with pCLC CAT expression plasmid (two fold diluted total extract). Lane 4 = negative control of non-electroporated cells. All negative controls show minimal CAT activity. Extracts from cells electroporated with pBC-tax/rex #11v (lane 2) show strong CAT activity and functional tax protein expression. The positive control (lane 3) shows strong CAT activity. The % chloramphenicol conversion to acetylated forms is shown.
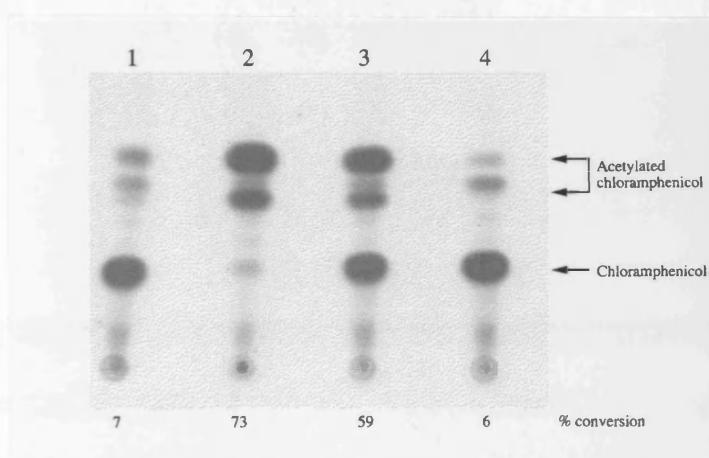
Figure 3.23 shows an autoradiogram of the CAT activity of cell extracts from Pfu polymerase derived clones #2, #5 and #14. Negative controls were cell extracts from non-electroporated cells and cells electroporated with pLTR-I-CAT reporter plasmid only. These extracts demonstrated negligible CAT activity with only 3 % and 4 % conversion of chloramphenicol to acetylated forms respectively. Positive control extracts from pCLC electroporated cells demonstrated a high level of CAT expression with 52 % conversion to acetylated forms. Cell extracts of cells electroporated with the Pfu polymerase derived tax/rex clones #2, #5 and #14 showed significant levels of CAT activity with 30 %, 44 % and 53 % conversion of chloramphenicol to acetylated forms respectively. This result indicates that the Pfu polymerase derived tax/rex expression constructs express a functional tax protein.

Figure 3.23. CAT tax trans-activation assays of extracts from COS cells electroporated with pBC-tax/rex expression constructs derived from Pfu DNA polymerase PCR amplification. Lane 1 = negative control of non-electroporated cells. Lane 2 = cells electroporated with pBC-tax/rex #2. Lane 3 = cells electroporated with pBC-tax/rex #5. Lane 4 = cells electroporated with pBC-tax/rex #14. Lane 5 = negative control of cells electroporated with pLTR-I-CAT . Lane 6 = positive control of cells electroporated with pCLC CAT expression plasmid. All negative controls shows minimal CAT activity. Cells electroporated with all three pBC-tax/rex constructs (lane 2 to 4) showed strong CAT activity and functional tax protein expression. The positive control (lane 6) shows strong CAT activity. The % chloramphenicol conversion to acetylated forms is shown.
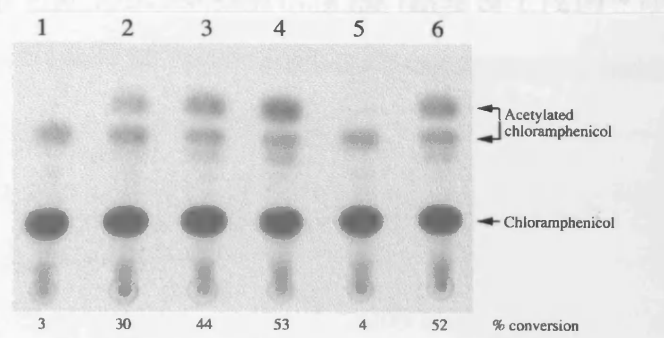
Overall these results highlight the effects of different PCR amplification strategies on the molecular cloning of functional proteins. All tax/rex cDNA clones generated by the Taq extender long PCR additive two enzyme system were found to contain several DNA nucleotide sequence errors and were deficient in tax trans-activation activity. However all tax/rex cDNA clones were obtained using single proofreading thermostable DNA polymerases Vent and Pfu did not contain any significant DNA nucleotide sequence errors over the regions sequenced and produced functional tax proteins able to efficiently trans-activate expression from the HTLV-I promoter. Both DNA sequencing results and functional tax trans-activation activity assays are consistent, suggesting that nucleotide sequence errors incorporated during Taq extender PCR amplification in turn caused significant amino acid sequence changes to the expressed tax protein resulting in loss of trans-activation activity. The difference between the expression of a functional or non-functional tax protein can be related to differences in PCR fidelity or error rates between Taq extender PCR additive, Vent and Pfu DNA polymerases.

Taq extender PCR amplifications use Taq DNA polymerase in combination with a small quantity of the proofreading Pfu DNA polymerase to enhance PCR efficiency. Taq DNA polymerase does not posses a 3'-5' proofreading exonuclease activity and thus demonstrates a relatively low fidelity during PCR amplifications resulting in a greater number of DNA sequence errors in its PCR products. The error rate of Taq DNA polymerase has been demonstrated to in the range of 1.1×10^{-4} (Barnes et al., 1989) to 2.0×10^{-5} (Lundberg et al., 1991) errors per bp, depending on the assay used. In the study by Lundberg et al., 1991 they also examined the fidelity of Pfu DNA polymerase and showed the error rate to be 12.5 fold lower than Taq polymerase at 1.6×10^{-6} errors per bp, reflecting its proofreading 3' -5' exonuclease activity. Hence the use of Taq DNA polymerase in Taq extender PCR amplification may yield significant numbers of DNA nucleotide sequence errors in the generated products. Sequence analysis of the tax/rex cDNA described in section 3.5.2 would support this idea and suggests the presence of a small quantity a proofreading DNA polymerase such as Pfu polymerase does not significantly enhance PCR fidelity over Taq polymerase alone. However, the use of Pfu DNA polymerase alone yielded PCR products with fewer DNA sequence errors. All tax/rex cDNA clones isolated did not contain any DNA sequence errors and expressed functional tax proteins. Similarly the use of Vent DNA polymerase, which also contains a 3'-5' exonuclease activity, produced tax/rex cDNA PCR products without any sequence errors and a expressed functional tax protein. The PCR fidelity of Vent DNA polymerase is quoted to be in the region of 4.5×10^{-5} (Ling et al., 1991) to 2.4×10^{-5} (Cariello et al., 1991) errors per bp and represented a 3.7 fold and 1.6 fold lower error rate compared to Taq DNA polymerase in their respective studies. Hence, the use of Pfu or Vent thermostable DNA polymerases possessing 3'-5' exonuclease proofreading activity significantly reduced the incorporation of nucleotide base errors during PCR amplification.

3.6 Discussion

The *in vitro* manipulation of retroviral proviral genomic DNA has proven difficult due mainly to their genetic instability leading to rearrangements, deletions, mutations and the general toxicity of envelope sequences to bacterial host cells (Sisk *et al.*, 1992; Cunningham *et al*, 1993; Yamada *et al.*, 1995). These factors have proven to be a major hindrance in the construction and maintenance of HTLV-I proviral clones as evidenced by the limited number of genomic HTLV-I clones available. The work presented in this study to generate a functional HTLV-I proviral clone is no exception. The technical difficulties in manipulating HTLV-I genomes *in vitro* played a major contributing factor in not obtaining a functional HTLV-I proviral clone. Throughout this project the inability of bacterial host cells to stably propagate HTLV-I genome containing plasmids led to the isolation of only a limited number clones and with very low yields. Ideally a relatively large number of HTLV-I clones would be tested for their ability to express viral proteins and VLPs in order to maximise the chance of isolating a fully functional clone. However, this was not the case and very few HTLV-I genomic clones were recovered despite repeated molecular cloning attempts. In addition the HTLV-I genomic clones that were eventually isolated were notoriously difficult to propagate in bacterial host cells with, on average, one out of three plasmid preparations containing HTLV-I deleted or no plasmid. The preparations which generated intact HTLV-I provirus containing plasmids produced very low yields when compared to other plasmids prepared by the same methods and restricted the number of experiments that were able to be performed at any one time. All these problems encountered reflect the toxicity and instability of HTLV-I genomes in bacterial host cells.

Throughout the course to these studies several techniques and strategies were progressively developed in order to enhance the yields and reliability of propagation of HTLV-I genome containing plasmids in bacterial host cells. A report by Kimata *et al.*, 1994b indicated that *E. coli* strain AG1 consistently supported the propagation of HTLV provirus containing plasmids. Subsequently all HTLV-I proviral plasmids were

transformed and propagated into AG1 *E. coli* cells. Consistent with the report by Kimata *et al.*, 1994b an increase in reliability of HTLV-I plasmid propagation was observed with two out of three plasmid preparations being successful compared to only one of three using a standard DH5α strain. The exact differences between AG1 and DH5α strains which result in the enhanced reliability of propagating HTLV-I genome containing plasmids is unclear, but presumably is related to the uncharacterised mutation in AG1 cells which improves transformation efficiency and possibly the lack of α-complementation of β-galactosidase activity. The reported genotypes of AG1 and DH5a cells are identical except for this uncharacterised mutation and an intact β-D-galactosidase gene in AG1 cells. In addition all HTLV-I containing plasmid preparations were performed on a small mini-preparation scale (see chapter 2, section 2.2.8) as it was found to increase HTLV-I genome stability over larger scale cultures.

Figures 3.24 and 3.25 demonstrates the stability of HTLV provirus containing plasmids when grown in small scale mini-preparation cultures (figure 3.24) compared to plasmids prepared in standard large scale single 500 ml maxi-preparation bacterial cultures (figure 3.25). HTLV-I genome containing plasmids when grown in large scale cultures routinely seemed to allow the deletion of HTLV-I inserts. However, when HTLV-I genome containing plasmids are grown in small scale cultures (< 10 ml) inoculated from single colonies the incidence of HTLV-I insert deletion was reduced. Again, the reason why the use of small scale cultures allows more stable propagation of HTLV-I genomes is unclear but may be related to a slower rate of cell growth in these cultures.

Figure 3.24. EtBr stained agarose gel of HTLV-I provirus containing plasmids prepared from small mini-preparation scale cultures. Three pBC-HTLVp plasmid clones #14, #15a and #26b are shown. Lane 1 = undigested plasmid DNA. Lane 2 = plasmid DNA restriction enzyme digested with *Hind*III. All pBC-HTLVp plasmids grown on this scale demonstrated an intact non--insert deleted plasmid with DNA fragment bands of 6809 bp, 1964 bp and 796 bp after *Hind*III digestion.
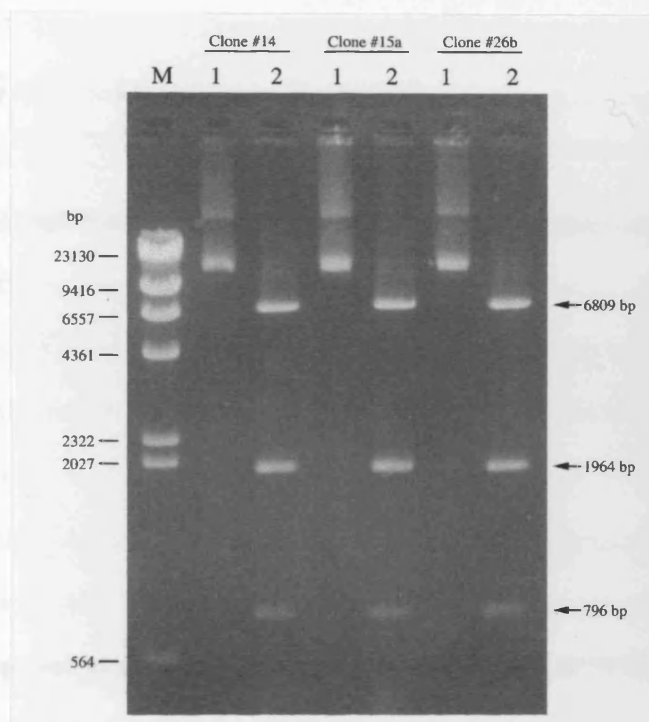
Figure 3.25. EtBr stained agarose gel of HTLV-I provirus containing plasmids prepared from large scale maxi-preparation cultures. Three pBC-HTLVp plasmid clones #14, #15a and #26b are shown. Lane 1 = undigested plasmid DNA. Lane 2 = plasmid DNA digested with *Bam*HI. Lane 3 = plasmid DNA digested with *Hind*III. Lane 4 = plasmid DNA digested with *Pst*I. All three plasmids grown on this scale showed deletion of the HTLV-I proviral inserts as demonstrated by the smaller than expected plasmid size and lack of *Bam*HI, *Hind*III and *Pst*I restriction enzyme sites. Clone #26b demonstrates partial HTLV-I proviral insert deletion with a small population of intact plasmid being observed. Faint bands of correct fragment size after *Bam*HI, *Hind*III and *Pst*I digestion can be seen for clone #26, e.g. after HindIII digestion expected bands 6809 bp and 1964 bp are observed.
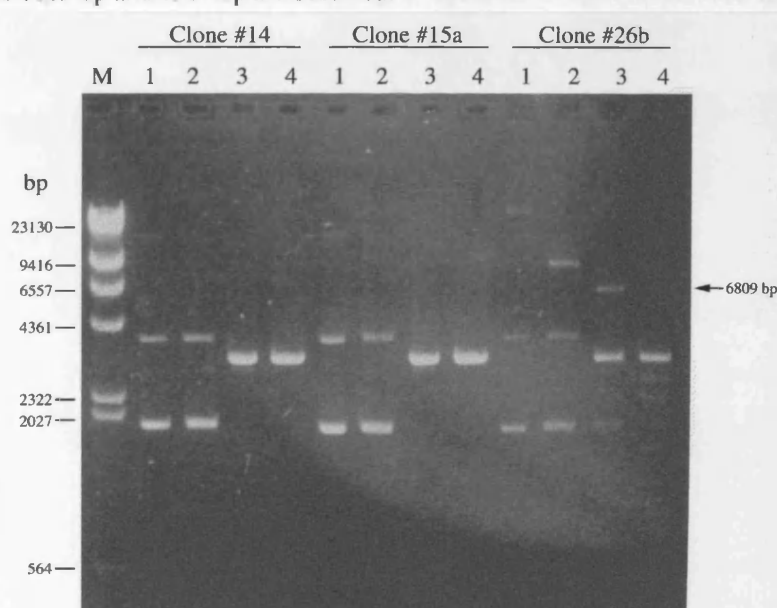
Despite the difficulties in manipulating HTLV-I genomes *in vitro* a total of five HTLV-I molecular clones were isolated which could be routinely propagated using the procedures described above. Two HTLV-I genomic clones were derived from sub-cloning of a HTLV-I provirus contained in the λHTLV-Ic vector (Mori *et al*, 1987) and designated pBC-λHTLV [#]8 and [#]10. Three HTLV-I genomic clones were generated by long PCR amplification of the HTLV-I provirus integrated into C91/PL cell genomic DNA and were designated pBC-HTLVp [#]14, [#]15a and [#]26b. Analysis of HTLV-I gene expression from these molecular clones demonstrated that the molecular clones derived from the λHTLV-Ic clone transcribed several classes of viral RNAs at low levels but did not to express any HTLV-I proteins at detectable levels. The λHTLV-Ic molecular clone is described by Mori *et al.*, 1987 and when the full length HTLV-I provirus alone was transfected into cells was found to express precursor and mature gag and envelope proteins and a functional tax protein. The formation of virus particles or functional envelope proteins was not tested. The lack of viral protein expression from pBC-λHTLV could however be attributed to the absence of sufficient post-transcriptional regulatory sequences present in the LTR regions required for efficient protein expression. Mori *et al.*, 1996 used the full length HTLV-I molecular clone in λHTLV-Ic which contained the entire 5' and 3' LTR sequences. The presence of regulatory sequences and RNA stem loop motifs contained in the HTLV-I LTRs facilitates the expression of full and singly spliced HTLV-I RNAs encoding the structural gag and envelope proteins (see chapter 1 and section 3.3). These LTR sequences were missing from the HTLV-I clone in pBC-λHTLV and would explain the poor levels of HTLV-I protein expression observed.

The HTLV-I molecular clones derived from long PCR amplification of the HTLV-I provirus contained in the C91/PL cell line produced all major viral RNAs and several proteins. These clones contained all the regulatory sequences required for efficient post-transcriptional processing and several classes of viral RNAs were found to be transcribed. These clones also expressed a functional tax protein. However expression

of the HTLV-I envelope proteins was not detected. Similarly the production of extracellular VLPs could not be demonstrated from these clones by RT-activity assays. These results may suggest a post-transcriptional block in HTLV-I protein expression where the RNA transcripts are inefficiently transported for translation and/or proteins are expressed but are non-functional, presumably due to nucleotide base mutations in these HTLV-I genes.

A deficiency in the rex/RxRE mediated post-transcriptional regulation of HTLV RNA transcripts may account for the observed lack of gag and env gene expression from the long PCR clones. It may be possible that rex/R_xRE mediated export of HTLV RNAs out of the nucleus for translation may not be occurring efficiently, despite the inclusion of all the regulatory sequences required for the processing of HTLV RNAs. The expression of a defective rex protein or a disruption of the 3' R_xRE RNA stem loop motif would not allow efficient export of full length and env RNA transcripts from the nucleus to the cytoplasm. This would result in poor gag and envelope protein expression. Due to the lack of a suitable rex protein assay it was impossible to directly test if rex was expressed from the long PCR derived HTLV clones. However, a functional tax protein was found to be expressed from the long PCR clones and as tax is encoded on the same mRNA transcript as rex it suggests correct processing and expression of genes from this tax/rex transcript. A deficiency in full length and env RNA export could be tested by performing northern blot RNA analysis of nuclear and cytoplasmic cell fractions. In this way it would be possible to determine whether HTLV RNAs were exported to the cytoplasm or not. However, in the absence of a preparative ultracentrifuge it was impossible to efficiently separate intracellular fractions for analysis.

Coding mutations in the gag gene products may have significantly altered HTLV-I capsid protein functionality leading to inefficient particle budding and release from cell surfaces. The HTLV-I gag proteins by analogy to other retroviruses such as HIV are

thought to play a critical role in virus particle budding and release from cells. The presence of a mutated pol gene in these clones may also explain the observed lack of extracellular RT-activity. The expression of a defective reverse transcriptase protein may abolish its RT-activity and any VLPs produced would be undetectable by assays for RT. However, in the absence of a suitable anti-gag protein antibody to detect VLPs the identification of which of these mechanisms is responsible for the lack of extracellular RT activity cannot be determined. The presence of nucleotide mutations within the env gene may similarly lead to defective proteins incapable of formation of syncytia. Many different random mutations in the env gene are known to impair envelope protein expression and produce syncytia formation defective proteins (Pique *et al.*, 1990 and 1992). Similarly the mutation of glycosylation sites which are found to be critically involved intracellular transport and efficient cell surface expression may also abolish syncytia formation ability (Pique *et al.*, 1992).

The introduction of nucleotide sequence mutations within the gag, pol or env genes may have occurred during the long PCR amplification of these HTLV-I molecular clones. These clones were all derived by long PCR using Taq extender PCR additive (Stratagene) and two enzyme PCR amplification system. Although this PCR amplification system was very efficient, generating specific long PCR products with high yield, it was found to demonstrate a relatively low PCR fidelity. Studies using this PCR amplification system for the cloning of tax/rex cDNA (section 3.5) found a number nucleotide base changes in the PCR products compared to the wild type template sequence which conferred a non-functional tax protein unable to trans-activate the HTLV-I LTR promoter. The low fidelity of Taq extender PCR amplifications was due to the use of the non-proofreading Taq DNA polymerase. Hence, PCR amplifications of the HTLV-I provirus using Taq extender may have been performed at a similarly low fidelity and resulted in the introduction of significant gene mutations resulting in non-functional proteins. However, limited sequence analysis of these PCR generated HTLV-I did not reveal any significant gene coding changes. High fidelity

thermostable DNA polymerases such as Vent or Pfu (section 3.5) were used in the amplification of the HTLV-I provirus but did not yield any PCR products. This observation demonstrates the lower efficiency in long PCR amplifications of single enzymes compared to the dual enzyme Taq extender system. Thus, the use of Taq extender PCR additive is ideal for generating long PCR products but not for use when high fidelity is required. To determine if nucleotide sequence errors are in fact responsible for the expression defects of the long PCR derived clones it would be necessary to sequence a large proportion of the clones. The identification of nucleotide sequence errors incorporated during PCR amplification would allow these errors to be reversed. The use of site directed mutagenesis techniques could be employed to alter the incorrect nucleotides back to a functional wild type sequence. However due to the lack of time and resources available the complete nucleotide sequencing of the HTLV-I molecular clones was not possible.

It should be noted that the HTLV-I proviral clones were amplified from genomic DNA extracted from C91/PL cells (Popovic *et al.*, 1983a). C91/PL cells were used as controls in all experiments for the analysis of HTLV-I protein expression and were found to be positive for all assays. Hence, the original HTLV-I proviral DNA template for long PCR amplification was competent for functional HTLV-I protein expression. C91/PL cells were used as it was initially thought that they only contain a complete non-defective integrated HTLV proviral genome (Orita *et al.*, 1993). However, recent evidence has contradicted this earlier finding and suggests that C91/PL cells may in fact contain several defective HTLV proviral copies (T. Schulz, personal communication). Hence, it may be possible that a defective HTLV proviral clone was PCR amplified from C91/PL cells and may account for the lack of expression observed.

Attempts at isolating a functional HTLV-I molecular clone for use in a VLP expression system has been unsuccessful due mostly to technical difficulties in working with HTLV-I. Studies on the HTLV-I proviral clones derived from long PCR were

encouraging and with continued investigation it would have been possible to re-engineer these clones to rectify their expression defects. However, the urgency in which an infectious HTLV-I molecular clone was required has been reduced due to the isolation of such clones by other groups. Kimata *et al.*, 1994b, Derse *et al.*, 1995 and Zhao *et al.*, 1995 all reported the isolation of infectious molecular clones of HTLV-I which were able express viral RNAs, proteins and produce extracellular virus particles similar to wild type virions. Hence, at this stage the further development of a functional molecular clone of HTLV-I was not pursued.

The development of a pseudotype VLP expression system by co-expression of HIV-I VLP and HTLV-I envelope expression constructs was unsuccessful. This was thought to be due to the incompatibility of both plasmids to efficiently express proteins within the same cell. VLPs and HTLV-I envelope proteins were efficiently expressed from their respective expression plasmids when electroporated into COS cells alone but when co-electroporated at a 1:1 molar ratio the expression from both plasmids was severely reduced. Expression was found to be dose dependant and when the amount of one plasmid was increased over the other expression of the increased plasmid predominated. This suggests the inability of COS-1 cells to efficiently express proteins from these two plasmids simultaneously. The amount of one plasmid required to generate significant protein expression does not allow a sufficient amount of the second plasmid for significant expression. Hence, the co-expression of these two plasmids in this system would not allow the production of pseudotype particles. However, the use of a plasmid co-expresion system analogous to the proposed pseudotyping described here has been demonstrated. Landau *et al.*, 1991 used a envelope deleted HIV provirus expression plasmid in conjunction with a HTLV-I envelope expression plasmid and demonstrated the expression of pseudotype particles by co-transfection of both these plasmids in COS cells. Their success in creating such a system suggests a significantly higher level of HIV particle or HTLV-I envelope expression in which both can be generated at sufficiently high levels to be detected. Landau et al., 1996 utilised expression plasmids

driven by the SV40 promoter and constructed a chimeric HTLV-envelope expression plasmid in which the HTLV-I env gene was placed immediately upstream of the HIV RRE sequence. The presence of HIV RRE RNA stem loop structures on viral RNAs in conjunction with HIV rev protein is thought to enhance the expression of these RNAs (Rosen et al., 1988; Malim et al., 1989). The rev protein was encoded on the HIV provirus expression construct and thus co-transfection of these plasmids may have supported or enhanced the co-expression of the HTLV-I envelope through the interaction with the RRE motif. The pBC-HTLV-env [#]1 plasmid did not contain the HIV RRE sequence and may not have been efficiently expressed when co-electroporated with the HIV VLP expression constructs. Hence, it would be possible to insert a HIV RRE sequence downstream of the env gene in pBC-HTLV-env to allow and efficient pseudotyping system. Alternatively an efficient pseudotyping system could be generated using pBCCX-CSF-DB31 and pBC-HTLV-env constructs in which one plasmid would be used to produce a stably expressing cell line. The production of an envelope deficient HIV VLP expressing packaging cell line cell line stably transfected with pBCCX-CSF-DB31 would allow the generation of pseudotype VLPs by simply transfecting these cell lines with the HTLV-I envelope expression construct. The problems with the transient expression from two separate expression plasmids would be eliminated. In addition the efficiency and level of pseudotype virus expression would be greatly enhanced. Such a system has been described for HTLV-I in which an M-MLV particle expressing cell line was transfected with a HTLV-I envelope expression plasmid and produced pseudotyped virus particles (Vile et al., 1991; Denesvre et al., 1996). However at this stage the validity of producing another HTLV-I envelope pseudotyping system to study the structure and function of the HTLV-I envelope proteins was in doubt. Reports by Delamarre et al., 1994 and Paine et al., 1994 both described the functional mapping of domains within the HTLV-I envelope proteins. Reports by Kimata et al., 1993 and 1994a also indicated that the HTLV-I envelope proteins may not elicit the mitogenic activities associated with HTLV-I infected cells and their significance in cellular transformation and pathogenesis is in question. Hence, at

this stage it was decided not to pursue the development of a HTLV-I envelope pseudotype expression system.

Studies on the HTLV-I provirus and HTLV-I envelope pseudotype expression systems did demonstrate the critical role of post-transcriptional regulators in the expression of viral proteins from retroviral genomes. The presence of HTLV-I rex or the analogous HIV rev protein in conjunction with their respective RNA stem loop motifs, RxRE and RRE, was found to be necessary for the efficient expression of viral structural proteins. The absence of the RxRE sequence in the pBC-λHTLV clone did not permit significant gag or env gene expression but when these sequence were present as in the long PCR derived pBC-HTLVp clones expression was observed (section 3.3). Similarly the HIV proviral expression construct used in HTLV-I envelope pseudotyping experiments (section 3.4) required the presence of both rev and RRE sequences for gag gene expression and VLP production. Hence, the efficient expression of full and partially spliced viral RNA from both HTLV-I and HIV-I retroviral genomes still requires their post-transcriptional regulatory mechanisms despite high levels of transcription being driven from a heterologous CMV IE promoter in pBCCX. However, it should be noted that expression of single viral genes seems not to require these post-transcriptional mechanisms as both pBC-HTLV-env (section 3.4) and pBC-tax/rex (section 3.5) efficiently express envelope and tax proteins respectively. This further suggests that rex-RxRE and rev-RRE interactions are only required for expression from whole retroviral genomes which transcribe intron containing unspliced and alternatively spliced mRNAs in this system.

Although the generation of an infectious HTLV-I molecular clone and envelope pseudotype expression system was initially unsuccessful the further investigation of both projects may have eventually yielded workable systems. The lack of scientific relevance, time and resources available for both projects meant that the continued development was not pursued. However, valuable techniques and insights into the

mechanism of transient viral transfections and proteins expression was gained during these investigations. These experiences were employed in the generation of tax/rex cDNA clones and rapidly led to the production of a functional tax expression plasmid. This tax expression plasmid was vital in the investigation of the mechanisms of HTLV-I induced multiple drug resistance. The role of HTLV-I in mediating multiple drug resistance cell phenotypes forms the final part of this project and is described in the following chapter.

CHAPTER 4

The role of HTLV-I infection in the development of multiple drug resistance phenotypes

4.1 Introduction

The failure of chemotherapy in patients suffering from systemic cancers such as leukaemia, lymphoma and multiple myeloma can often be attributed to a pleotropic drug resistant phenotype of these cells. This clinically defined multiple drug resistance (MDR) phenotype was found to be associated with several distinct cellular anomalies, overexpression of P-glycoprotein (classical MDR), alteration of topoisomerase II (atypical MDR) or overexpression of MDR-related protein (non-PGP MDR). The predominant and best characterised MDR phenotype is classical MDR which results from the overexpression the mdr-1 gene encoding the trans-membrane drug efflux pump P-glycoprotein (PGP). Observations that HTLV induced tumours are highly resistant to chemotherapy coupled with the inherent biological mitogenic and cellular trans-activation activities of HTLV-I led to the hypothesis that a MDR phenotype may be activated in these tumour cells by HTLV-I (See chapter 1, section 1.7). Using standard assays for the presence of MDR phenotypes we set out to test this hypothesis in both cultured cell lines and primary PBMCs from HTLV-I infected individuals.

4.2 Optimisation of MDR assays for lymphoid cells

In collaboration with T. Gant at the MRC toxicology unit, University of Leicester several assays for the classical MDR cell phenotype were devised. The primary assay was a fluorescent dye efflux activity assay in which the drug export or efflux capability of cells were tested (see chapter 2, section 2.5.2b). The other assay was a quantitative

RT-PCR for mdr-1 mRNA to examine the levels of PGP expression in cells (see chapter 2, section 2.3.9). Both MDR assays are routinely used by T. Gant at the University of Leicester and are described by Davies *et al.*, 1996. However, both assays needed to be optimised for use with lymphoid cell types and available laboratory equipment.

4.2.1 Initial screening of T-cell lines for MDR expression

As a starting point to optimise the MDR assays it was decided to test several T-cell lines with the R123 dye efflux and mdr-1 RT-PCR assays using the original experimental parameters and conditions described by Davies *et al.*, 1996. The non-HTLV infected T-cell line HUT78, HTLV-I infected T-cell lines C91/PL and MT4 and 48 hour PHA stimulated PBMCs from a non-HTLV infected donor were initially tested.

The R123 dye efflux assay was performed as described by Davies *et al.*, 1996. 3×10^6 cells were resuspended at 1×10^6 cells/ml in serum free RPMI medium containing 1.66 μM R123 dye and incubated for a 20 minute passive dye uptake period. The cells were washed of excess R123 dye and incubated for a further 90 minute efflux period in serum and R123 free RPMI medium. The cells were stained with PI for 10 minutes and then fixed in 1 % paraformaldehyde. After R123/PI spectral overlap compensation 10,000 cells were counted. Live cells, as determined by PI exclusion, were then examined for their R123 fluorescence profiles. The cell viability was between 85-90 % for all three cell types but was lower at 80 % for PBMCs. Figure 4.1 shows the R123 fluorescence FACScan profiles for HUT78, C91/PL, MT4 and PHA stimulated PBMCs. All the cells tested showed R123 dye efflux or PGP MDR activity after the 90 minute efflux period. MT4 cells (figure 4.1a) showed the greatest R123 dye efflux at 51.6 % R123 loss over a 90 minute efflux period. Both HUT78 (figure 4.1b) and C91/PL (figure 4.1c) cells showed similar R123 dye efflux capabilities at 41.2 % and 37.5 % R123 loss respectively. PHA stimulated PBMCs (figure 4.1d) showed a distinct pattern of R123 dye efflux with both a high R123 dye efflux (low overall mean

fluorescence at 52) and low R123 dye efflux (high overall mean fluorescence at 1170) cell populations being observed.

Figure 4.1. R123 FACscan profiles of lymphoid cells using 1.66 μM R123 in the assay. a) MT4 cells (51.6 % R123 loss). b) HUT78 cells (41.2 % R123 loss). c) C91/PL cells (37.5 % R123 loss). PBMCs stimulated with PHA for 48 hours (Two populations; high efflux = 94 % R123 loss; low efflux = 28.5 % R123 accumulation).
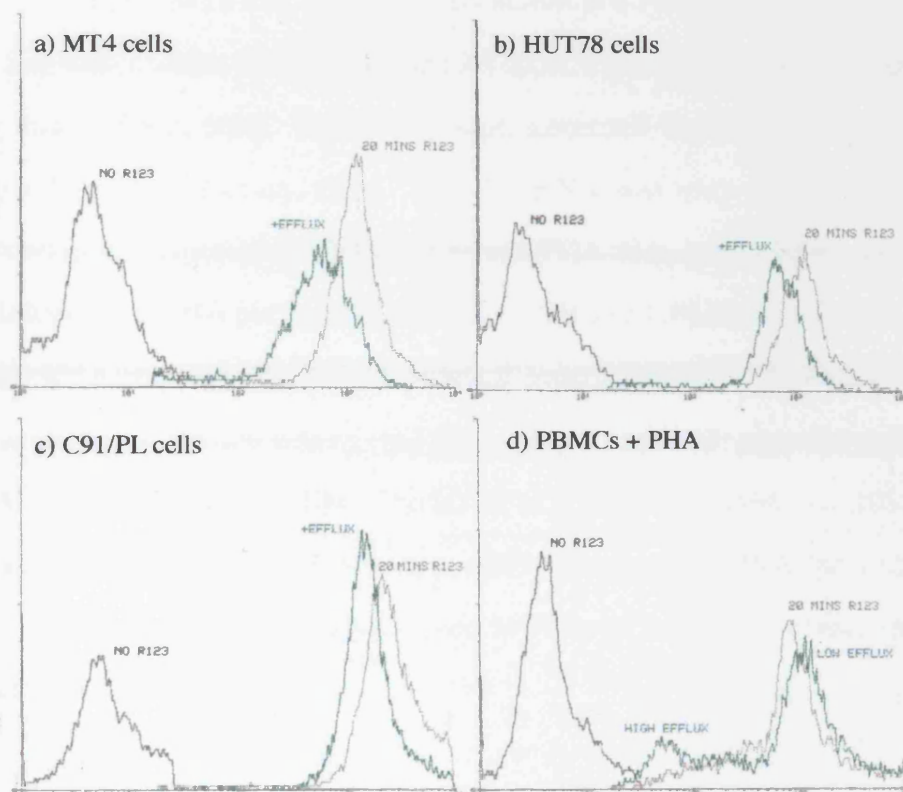
The high R123 efflux cell population comprised of 24 % of the total number of cells and showed 94 % R123 dye efflux over 90 minutes. The low efflux population however seems to have accumulated 28.5 % more intracellular R123 over 90 minutes (mean fluorescence from 806 to 1128). Such accumulations have previously been reported for R123 dye efflux assays (Lee *et al.*, 1994) and were attributed to intracellular concentration of the dye within mitochondria. R123 is a lipophilic cationic fluorescent dye which incorporates into mitochondria (Johnson *et al.*, 1980). Any

accumulation of R123 dye over the efflux period would be indicative of cells without any MDR activity and suggests the population observed is a low R123 dye effluxing cell population. These results indicate the presence of a subset of cells within PHA stimulated PBMCs which shows enhanced MDR or drug efflux activity.

Quantification of mdr-1 mRNA was performed on total cellular RNA extracted from HUT78, C91/PL, MT4 and 48 hour PHA stimulated PBMCs by RNAzol B reagent. Extracted total cellular RNAs were then RT-PCR'd and mdr-1 mRNA quantified by J. Riley and T. Gant, MRC Toxicology unit, Leicester University using the method described by Davies et al., 1996. Mdr-1 mRNA was only found for the HTLV-I transformed and expressing MT4 cell line and PHA stimulated PBMCs at 11 and 37.2 molecules mdr-1 RNA per pg total RNA (or 0.018 and 0.06 attomoles mdr-1 RNA per ng total RNA respectively; T.Gant personal communication). A positive control for mdr-1 mRNA expression was of total RNA from a high PGP expressing sub-clone of the MCF7/Dox MDR cell line (Davies et al., 1996) with 364 and 108 fold more expression at 4004 molecules of mdr-1 mRNA per pg total RNA (or 6.65 attomoles mdr-1 mRNA per ng total RNA) over MT4 cells and PHA stimulated PBMCs respectively.

The results from both R123 dye efflux assays and quantitative mdr-1 RT-PCRs were not entirely consistent. R123 dye efflux assays suggested the presence of PGP mediated dye efflux for all four cell types at various degrees. However, RT-PCRs showed that mdr-1 mRNA was only quantifiable in the PHA stimulated PBMC and MT4 cell types, suggesting significant expression of PGP in these cells only. The apparent presence of PGP mediated R123 dye efflux in the absence of molecular PGP expression in HUT78 and C91/PL cells can be explained by an unoptimised R123 dye efflux assay. The original assay described by Davies et al., 1996 was developed to examine PGP dye efflux from the MDR cell line MCF-7/Dox, which were a breast adenocarcinoma cell line made drug resistant by exposure to increasing concentrations

of doxorubicin (Batist *et al.*, 1986). MCF-7/Dox cells were 192-fold more resistant to the cytotoxic effects of doxorubicin compared to wild type cells and also cross-resistant to other drugs such as actinomycin D and vinblastine (Batist *et al.*, 1986). This artificially induced MDR cell line was found to have undergone amplification of the mdr-1 gene and greatly overexpress PGP (Cowan *et al.*, 1986; Fairchild *et al.*, 1987). Cellular drug efflux in MDR cells was found to be a combination of both reversible, non-saturable passive drug transport governed by substrate concentration gradients across the cell membrane and non-reversible, saturable ATP dependant PGP mediated drug efflux (Spoelstra *et al.*, 1992; Thimmaiah *et al.*, 1990). In these cells at relatively low intracellular substrate concentrations active PGP mediated efflux would predominate but at high substrate concentrations when PGP becomes saturated the effects of passive efflux would dominate (figure 4.2). Also any net substrate efflux is a compromise between both passive cellular transport (influx and efflux) and active PGP mediated efflux in MDR cells. Thus for effective R123 dye efflux to be observed cells must accumulate sufficiently high amounts of dye to allow good R123 loss over the efflux period but at an intracellular concentration which does not saturate PGP mediated efflux. During the labelling period in the efflux assay cells are required to accumulate R123 intracellularly and as such the rate of passive R123 dye influx must be greater than the rate of efflux. For cells with greater rates of efflux, i.e. more PGP, a greater concentration of R123 is required in the labelling period to allow intracellular R123 dye accumulation. Therefore, high PGP expressing cells such as MCF-7/Dox requires a much higher concentration of R123 during the labelling period to allow a sufficient intracellular level of R123 to accumulate for the assay. However the PBMC, HUT78, C91/PL and MT4 lymphocyte cells have a much lower level of PGP expression as seen by the relative amounts of mdr-1 mRNA. The incubation of these cells at a similar R123 concentration to MCF7/dox cells (1.66 µM) would lead to similar rates of dye influx but with a greatly reduced rate of dye efflux during the labelling period. The result would be greater dye accumulation and possible overloading of these cells with R123 dye.

Figure 4.2. Active MDR mediated efflux versus passive efflux at increasing intracellular substrate concentration. At low intracellular substrate concentrations active MDR mediated efflux predominates. At high intracellular substrate concentrations active MDR mediated efflux becomes saturated and passive efflux predominates. (Modified from Wigler et al., 1996).
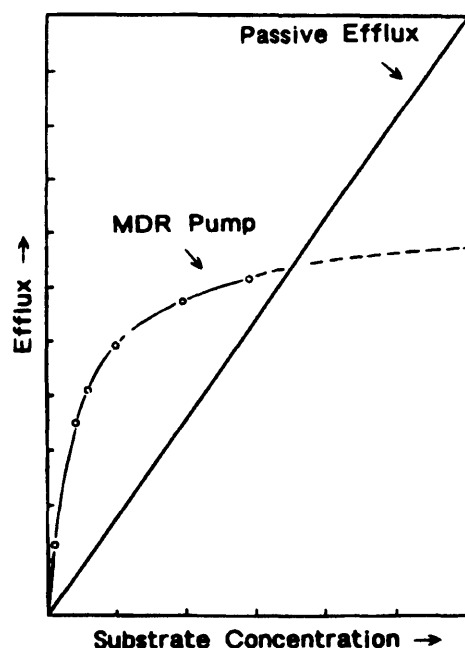
The assays performed on PBMC, HUT78, C91/PL and MT4 cells were in conditions optimised for high PGP expressing cells and would have accumulated much greater amounts of R123 dye. Hence, the apparent efflux observed for all of these cells could be explained by the effects of passive cellular diffusion rather than active PGP mediated efflux. The intracellular R123 concentrations would have been high and incubation at low extracellular R123 concentrations during in the efflux period would result in a large R123 concentration gradient. Active PGP mediated efflux may have been saturated and passive diffusion across the concentration gradient would have dominated (figure 4.2). The result being significant observable R123 dye efflux but without the involvement of PGP as demonstrated by HUT78 and C91/PL cellular efflux. An additional undesirable affect of excessive intracellular R123 concentrations would be the concentration of R123 dye within the mitochondria of cells leading to build up of intracellular R123 fluorescence. This was demonstrated in PHA stimulated PBMCs in which the low

R123 efflux cell population accumulated a significant amount of R123 dye over the efflux period. Such unwanted dye accumulations would make interpretation of R123 dye efflux assay data difficult as mitochondrial R123 accumulation may lead to significant underestimation of R123 dye efflux. Lowering intracellular R123 dye concentrations would minimise any such accumulation effects. Thus, it was necessary to optimise the R123 dye efflux assay to achieve a lower intracellular R123 dye concentration for use with lower PGP expressing lymphoid cells.

4.2.2 Rhodamine-123 (R123) FACScan assay optimisation

R123 dye efflux assays and FACs analysis are sensitive to various experimental parameters which have to be optimised and adjusted for. These parameters in the R123 dye efflux assays included the concentration of R123, time of R123 uptake and time of R123 efflux. The concentration of serum in the culture medium and 1 % paraformaldehyde cell fixation were also tested for any significant effects upon the R123 dye efflux assay.

A R123 titration was performed in a comparative study using the T-cell lines HUT78 and MT4 at a constant 20 minute labelling and 90 minute efflux incubation periods. These cell lines were found to be non-PGP expressing and PGP expressing respectively by quantitative mdr-1 RT-PCR analysis (section 4.2.1). Labelling of cells with doubling dilutions of R123 from 3.3 μM to 0.4 μM in the 20 minute uptake period were performed in serum free RPMI medium for both cell lines. Cells were washed, resuspended in R123 free medium and then incubated for a further 90 minute efflux period. Cells were then fixed in 1 % paraformaldehyde before FACs analysis. R123 dye efflux from HUT78 and MT4 cells at decreasing concentrations of R123 are shown in table 4.1 and diagramatically in figure 4.3.

Table 4.1. The effect of R123 concentration on dye efflux from mdr-1 RNA positive MT4 and mdr-1 RNA negative HUT78 T-cell lines. Cells were labelled by incubation with various concentrations of R123 for 20 minutes, washed and allowed to efflux for 90 minutes in R123 free medium. Cells were fixed in 1% paraformaldehyde and analysed by FACscan. R123 efflux was derived by comparing the R123 fluorescence of cells at the labelling step with R123 fluorescence of cells after efflux. R123 dye efflux is reduced in HUT78 cells by reducing the R123 concentration in the labelling step. R123 dye efflux is unaffected in MT4 cells at all R123 concentrations tested indicating an active mechanism of dye efflux.

Concentration of R123 in the labelling step of dye efflux assays (µM)	3.3	1.66	0.8	0.4
R123 dye efflux from HUT78 cells	54.8 %	41.7 %	19.2 %	8.6 %
R123 dye efflux from MT4 cells	56.7 %	56.6 %	54.4 %	53.5 %

Figure 4.3. R123 dye efflux from MDR positive MT4 and MDR negative HUT78 cells over various concentrations of R123. Increasing R123 concentration in the labelling step causes a corresponding proportional increase in R123 dye efflux in HUT78 cells and indicates a passive mechanism of R123 loss. In contrast MT4 cells show little variation in R123 dye efflux over the range of R123 concentrations tested and indicates an active mechanism of dye efflux.
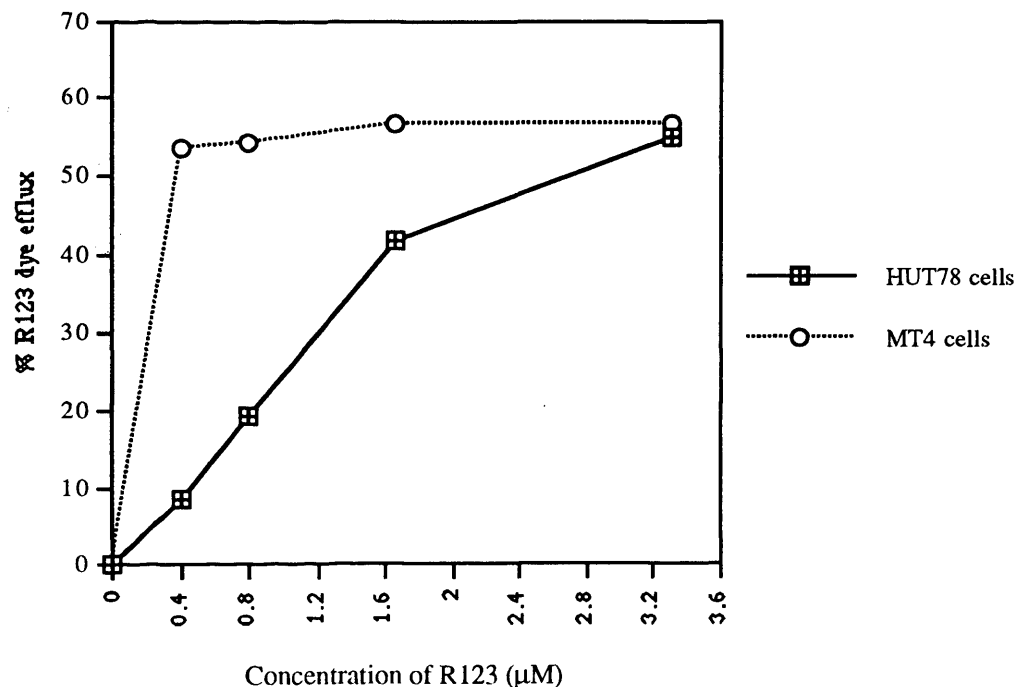
R123 dye efflux from HUT78 cells after 90 minutes when exposed to 3.3 μM, 1.66 μM, 0.8 μM and 0.4 μM R123 after the labelling step were found to be lower at reduced concentrations of R123. The pattern of R123 dye efflux over these R123 concentrations was almost linear as predicted for passive efflux in section 4.2.1 and figure 4.2. At 0.4 μM R123 concentration the apparent PGP-mediated dye efflux was found to be minimal (8.6 % R123 loss) and in line with that predicted by quantitative mdr-1 RT-PCR analysis (section 4.2.1). In contrast the PGP expression positive cell line MT4 showed little reduction in R123 dye efflux over the range of R123 concentrations tested. This is indicative of an active mechanism of dye efflux within MT4 cells and is consistent with the mdr-1 RNA results in section 4.2.1. Assuming a constant level of R123 dye influx, these results indicated that the optimal R123 concentration for lymphoid cells was 0.4 μM R123 in the 20 minute labelling step. At this concentration non-PGP mediated passive R123 efflux by HUT78 cells was minimised but the sensitivity of the assay for PGP mediated active efflux by MT4 cells was not significantly reduced. All subsequent R123 assays on lymphoid cell types were performed using 0.4 μM R123 concentration during the 20 minute labelling period.

R123 dye efflux assays were originally performed in serum free medium in order to minimise the sequestering of R123 dye by serum proteins. However using serum free medium with lymphocytes over the course of the assay the cell viability was only just found to be acceptable (>80 %) for FACScan analysis (section 4.2.1). In addition, stress responses such as serum starvation of cells have been found to promote mdr-1 expression (Tanimura et al., 1992). In order to increase cell viability and reduce the stress on cells it was decided to perform a serum titration from 0 to 10 % FCS in the R123 dye efflux assay of MT4 cells and assess its effects. Table 4.2 shows the effects of increasing FCS concentration in cell culture medium upon R123 dye efflux and percentage cell viability after the assay from MT4 cells. Cell viability was determined

by PI dye exclusion by FACs analysis and expressed as a percentage of the total cells (10,000) counted.

Table 4.2. The effects of FCS concentration on R123 fluorescence, dye efflux and cell viability in the R123 dye efflux assay. Standard R123 dye efflux assays were performed on the MDR positive cell line MT4 in the presence of various concentrations of FCS in the medium. The mean R123 fluorescence before and after dye efflux and % R123 dye efflux was assessed by FACscan analysis. Cell viability was determined by PI dye exclusion.

Concentration of FCS in medium	(a) Mean R123 fluorescence before efflux	(b) Mean R123 fluorescence after efflux	(c) % R123 dye efflux	(d) % Viable cells after efflux
no FCS	78	36	53.9	83
2.5 % FCS	66	31	53.0	91
5.0 % FCS	63	30	52.4	94
10 % FCS	59	30	49.2	94

The increasing presence of FCS from 0 to 10 % in the culture medium correlated with decrease in absolute R123 fluorescence after 20 minute labelling from 78 to 59 units (table 4.2, column a) but only with a slight decrease in overall R123 dye efflux from 53.9 to 49.2 % R123 loss in MT4 cells (table 4.2, column c). Uptake of R123 by cells was reduced by the presence of FCS, possibly due to the reduction of free R123 concentration by its sequestration to serum proteins. However, the rate of R123 dye efflux from MT4 cells over the 90 minute efflux period remained relatively constant leading to only a small difference in R123 dye efflux. This suggests the presence of FCS results in reduced R123 uptake but that enough R123 still accumulates within cells to not significantly interfere with cellular R123 dye efflux. The cell viability after R123 dye efflux was also assessed and is shown in table 4.2, column d. Increasing FCS concentration resulted in the stabilisation of cells during the course of the assay and is seen by enhanced cell viability from 83 % in the absence of FCS to 94 % in the presence of 10 % FCS. Hence, the presence of even a small percentage of FCS significantly increased the cell viability over the course of the R123 dye efflux assay.

Although only a small variation in R123 dye efflux is observed over a 10 % FCS concentration range it was decided to use a low amount of FCS in order to maximise the sensitivity of the assay whilst still retaining good cell viability (>90 %). Hence, all subsequent R123 dye efflux assays were performed in cell culture medium containing 2.5 % FCS.

The fixation of cells with paraformaldehyde was assessed for its effects on R123 fluorescence and R123 dye efflux activity. The effect of 1 % paraformaldehyde fixation on absolute R123 fluorescence was assessed by measuring the R123 fluorescence of HUT78 cells with and without fixation (table 4.3). HUT78 cells showed a small (11.8 %) variation in R123 fluorescence with and without 1 % paraformaldehyde fixation (table 4.3) although a slight increase in the forward light scatter (FSC) of fixed cells was observed (figure 4.4). The increase in FSC may be attributed to an increase in the refractive index of cells as a result of protein cross-linking and membrane stabilisation characteristic of aldehyde fixation (Shapiro, 1988) and no alteration in fluorescence was observed. Similarly the fixation of cells with 1 % paraformaldehyde showed no significant fluorescence quenching effects upon FACs analysis after R123 dye efflux assays. Cells tested were still found to be fluorescent after 1 % paraformaldehyde fixation (figure 4.1) and it showed no significant effect upon PGP mediated R123 dye efflux from MT4 cells. These results indicated that the presence of 1 % paraformaldehyde has no significant effects upon R123 fluorescence or the R123 dye efflux assay. However, it must be noted that the effects of 1 % paraformaldehyde upon FACScan analysis in R123 dye efflux assays for MT4 cells could not be directly tested, by assaying MT4 cells with and without fixation, due to safety considerations. MT4 cells are HTLV-I infected (a class III pathogen) and cannot be removed from the class III containment facility without prior destruction or fixation.

Table 4.3. R123 fluorescence of HUT78 cells labelled with 0.4 µM R123 for 20 minutes with and without 1 % paraformaldehyde fixation. Only a slight reduction (11.8 %) in cellular R123 fluorescence is observed after fixation.

HUT78 cells	Mean R123 fluorescence
No fixation	127
+ 1% paraformaldehyde fixation	112

Figure 4.4. Forward light scatter (FSC) versus side light scatter (SSC) of HUT78 cells; a) without paraformaldehyde fixation; b) fixed with 1 % paraformaldehyde. An increase in FSC can be observed for paraformaldehyde fixed cells.

a) Unfixed cells   b) Fixed cells
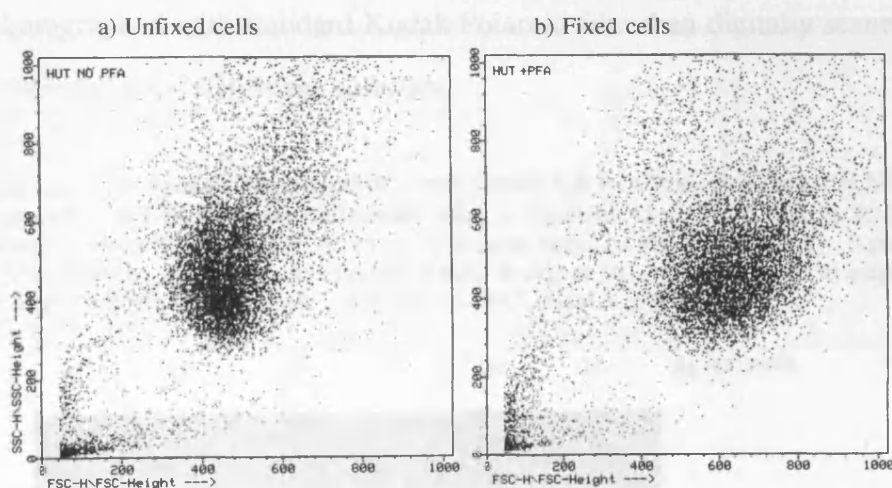
4.2.3 Quantitative mdr-1 mRNA RT-PCR modifications

Quantitative RT-PCR analysis of mdr-1 RNA was based on the method described by Davies *et al.*, 1996 but adapted for non-radioisotopic detection. The RT-PCR assay was modified for use with standard EtBr staining and UV light visualisation from high resolution agarose gels (NuSieve GTG). Densitometry was then performed using a standard desktop image scanner and a public domain image analysis software package, NIH image (see chapter 2, section 2.3.9). Total RNA extracted from the high PGP expressing sub-clone of the MCF7/Dox MDR cell line (MCF7/Dox HP-gp) was used as

the reference RNA throughout the quantitative RT-PCR optimisation. Davies *et al.*, 1996 RT-PCR quantified the mdr-1 RNA from this subclone at 6.65 + 2.29 attomoles mdr-1 RNA per ng total RNA (or 4004 $\pm$ 1379 molecules mdr-1 RNA per pg total RNA). Using the modified version of this quantitative RT-PCR protocol total RNA was extracted from MCF7/Dox HP-gp cells and was quantified for mdr-1 RNA. Quantitative RT-PCR of total RNA from MCF7/Dox HP-GP cells was performed twice to confirm the results and a representative quantification is described below. RT-PCR was performed on 40 ng total MCF7/Dox HP-gp cellular RNA mixed with either 0.5, 1, 5, 10 or 25 pg of ISC RNA. Figure 4.5 shows an EtBr stained and UV visualised agarose gel of 10 % of the mdr-1 quantitative RT-PCR reaction. Amplification of ISC RNA can be seen as bands of 212 bp and cellular mdr-1 mRNA as bands of 161. Gels were photographed with standard Kodak Polaroid film then digitally scanned and the image imported into NIH Image software.

Figure 4.5. EtBr stained agarose gel of a mdr-1 mRNA RT-PCR quantification of MCF7/Dox HP-gp cells. RT-PCRs were performed using a constant 40 ng total sample RNA in the presence of either 0.5, 1.0, 5, 10 or 25 pg of internal standard RNA (ISC RNA). Bands at 212 bp corresponds to amplification from ISC RNA. Bands at 161 bp corresponds to amplification from mdr-1 mRNA in the sample. M = Φx174 DNA (HaeIII cut) marker.
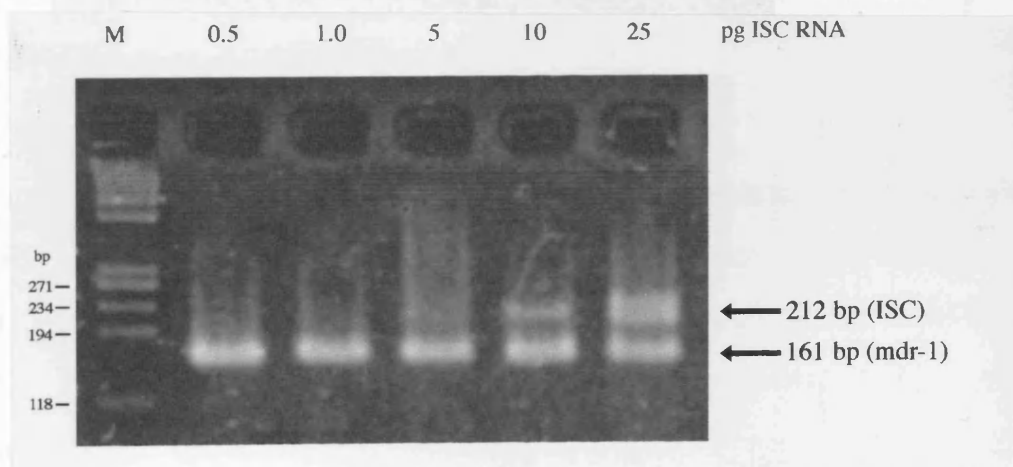
Figure 4.6 shows a screen shot of the determination of band intensities using NIH Image software. The ISC RNA (212 bp) and mdr-1 mRNA (161 bp) bands were selected using the box tool and marked as lanes 1 and 2 respectively. A band density plot of both lanes was then produced and the areas automatically calculated using the

wand tool. Regions 1 to 5 were the areas of ISC RNA bands and regions 6 to 10 the areas of mdr-1 mRNA bands. Regions 1, 6 corresponded to RT-PCR with 0.5 pg ISC RNA, regions 2, 7 to 1 pg ISC RNA, regions 3, 8 to 5 pg ISC RNA, regions 4, 9 to 10 pg ISC RNA and regions 5, 10 to 25 pg ISC RNA.

Figure 4.6. Screen shot of NIH Image software in MCF7/Dox HP-gp cell mdr-1 mRNA RT-PCR quantification.
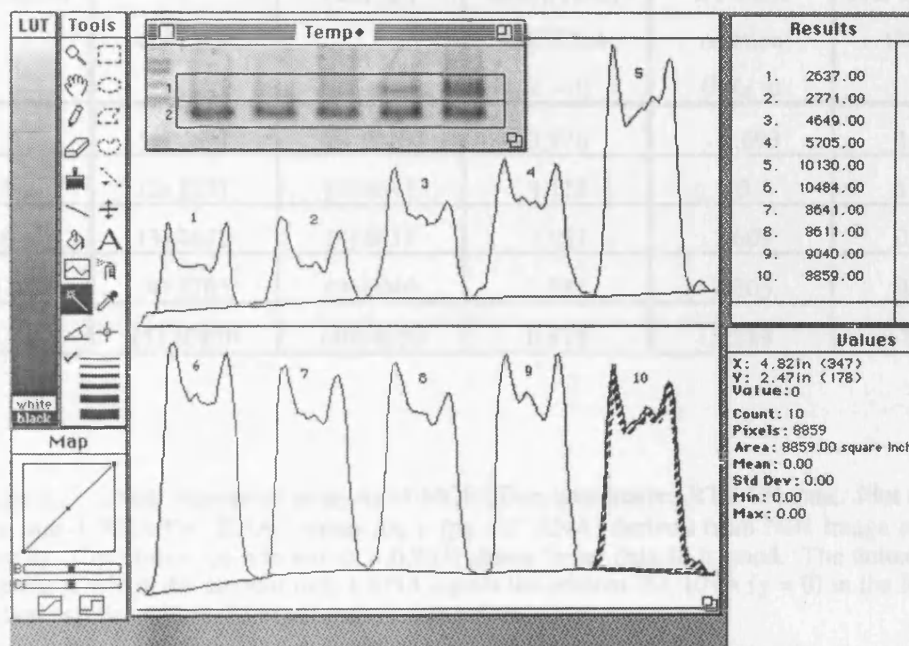
The area of mdr-1 mRNA divided by the area of ISC RNA was then calculated for each amount of ISC RNA in the RT-PCR reaction and is described in table 4.4. From this data a linear regression plot of $\log_e$ (area mdr-1 mRNA/area ISC RNA) verses $\log_e$ (pg ISC RNA) was produced using Cricket Graph software and is shown in figure 4.7. A linear line equation was produced in the form of,

$$y = mx + c$$

where   y = $\log_e$ (area mdr-1 RNA/area ISC RNA)

              x = $\log_e$ (pg ISC RNA)

              m = line gradient

              c = constant value

Table 4.4. Densitometry data of quantitative mdr-1 RT-PCRs from MCF7/Dox cells. Areas of RT-PCR bands were determined by NIH Image software. Bracketed numbers are the numbers of the bands assigned by NIH Images in figure 4.6. Bands 1 to 5 correspond to RT-PCR products of 212 bp or mdr-1 internal standard (ISC). Bands 6 to 10 correspond to RT-PCR products of 161 bp or mdr-1 mRNA. For mdr-1 RNA quantification the ratio of the area of mdr-1 RNA over area of ISC RNA was calculated. Log e values for pg ISC RNA and ratio areas mdr-1 RNA over ISC RNA was also calculated.

(a) pg of ISC RNA in RT- PCR reaction	(b) Area of ISC RNA bands (212 bp)	(c) Area of mdr-1 mRNA bands (161 bp)	(d) Ratio of areas of mdr-1 mRNA over ISC RNA (c ÷ d)	(e) Log_e of pg ISC RNA in RT-PCR reaction (log_e a)	(f) Log_e of areas mdr-1 mRNA over ISC RNA (log_e d)
0.5	(1) 2637	(6) 10484	3.976	- 0.693	1.380
1.0	(2) 2771	(7) 8641	3.118	0	1.137
5.0	(3) 4649	(8) 8611	1.852	1.609	0.616
10.0	(4) 5705	(9) 9040	1.585	2.303	0.460
25.0	(5) 10130	(10) 8859	0.875	3.219	- 0.134

Figure 4.7. Linear regression analysis of MCF7/Dox quantitative RT-PCR data. Plot of log e (area mdr-1 RNA/ISC RNA) versus log e (pg ISC RNA) derived from NIH Image software (table 4). Correlation co-efficient (r = 0.987) shows linear data fit is good. The dotted line is the point at which the amount mdr-1 RNA equals the amount ISC RNA (y = 0) in the RT-PCR reaction and lies within the experimental data points.

$$y = -0.363x + 1.159 \quad r = 0.987$$

Log e (pg ISC RNA)
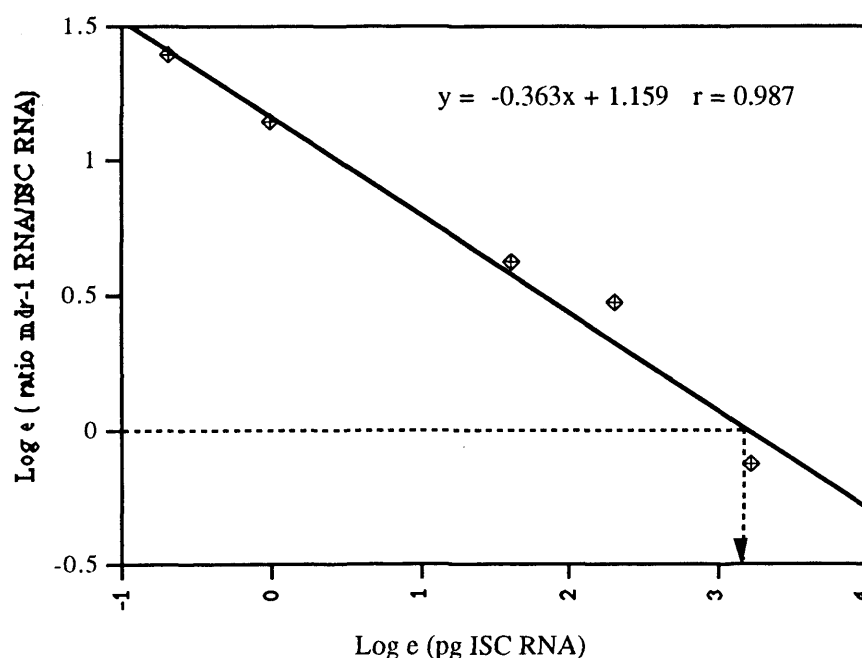
For MCF7/Dox HP-gp cells the linear regression equation for mdr-1 RNA quantification shown in figure was,

$$y = -0.363x + 1.159$$

At the point where the amount mdr-1 RNA equals the amount ISC RNA, the area of mdr-1 RNA divided by the of area ISC RNA = 1 or,

$$y = \log_e (\text{area mdr-1 RNA/area ISC RNA})$$

$$= \log_e (1)$$

$$= 0$$

The $\log_e$ (pg of ISC RNA) when area mdr-1 RNA = area ISC RNA (or y = 0) becomes,

$$x = \log_e (\text{pg ISC RNA}) = \frac{-1.159}{-0.363}$$

$$= 3.19$$

Hence, the amount of mdr-1 RNA per 40 ng total MCF7/Dox HP-gp RNA is equivalent to,

$$e^x = e^{3.19}$$

$$= 24.36 \text{ pg ISC RNA in the RT-PCR reaction}$$

This value fell within the range of experimental data (0.5 to 25 pg ISC RNA) and was considered a valid measurement. Linearity of the mdr-1:ISC RNA ratio was never assumed outside the range of experimental data and total RNA concentration in the quantitative RT-PCR was adjusted such that the experimental data points always spanned the ratio of mdr-1 RNA:ISC RNA equal to one.

The amount of mdr-1 RNA per ng total RNA becomes,

$$= \frac{24.36 \text{ pg mdr-1 RNA}}{40 \text{ ng total RNA in RT-PCR reaction}}$$

$$= 0.609 \text{ pg mdr-1 RNA per ng total RNA}$$

The number of moles of mdr-1 RNA per ng total RNA is,

$$= \frac{0.609 \text{ pg mdr-1 RNA per ng total RNA}}{\text{Mw mdr-1 RNA } (90851.4)}$$

$$= \frac{6.09 \times 10^{-13} \text{ g mdr-1 RNA per ng total RNA}}{90851.4}$$

$$= 6.70 \times 10^{-18} \text{ moles mdr-1 RNA per ng total RNA}$$

$$= \textbf{6.70 attomoles mdr-1 RNA per ng total RNA}$$

or alternatively the number of molecules mdr-1 RNA per pg total RNA is,

$$= 5.94 \times 10^{-18} \text{ moles mdr-1 RNA per ng total RNA}$$

$$= 5.94 \times 10^{-21} \text{ moles mdr-1 RNA per pg total RNA x Avagadro's number}$$

$$= \textbf{4036.3 molecules mdr-1 RNA per pg total RNA}$$

Quantitative RT-PCR of MCF7/Dox HP-gp cells was performed in two separate experiments and a combined value of 6.32 ± 0.38 attomoles mdr-1 RNA per ng total RNA or 3807.3 ± 229 molecules mdr-1 per pg total RNA was obtained. This result was in good agreement with the value obtained by Davies *et al.* 1996 of 6.65 ± 2.29 attomoles mdr-1 RNA per ng total RNA and was within the specified error limits of the procedure. Statistical testing of the difference between these two means shows no significant difference at the 5 % level ($z = 0.245$, as $|z| < 1.96$). The results demonstrated that the modifications to the original quantitative RT-PCR procedure (Davies *et al.*, 1996) did not significantly effect mdr-1 RNA quantification and the method was used for all subsequent mdr-1 quantifications.

4.3 Analysis of mdr-1 gene expression in cultured T-cell lines

Several HTLV and non-HTLV transformed T-cell lines were examined using optimised R123 dye efflux and quantitative mdr-1 RT-PCR assays for the presence of classical MDR. The non-HTLV transformed cell lines tested were CEM4, HUT78, Jurkat,

Molt4 and SupT1 cells. The HTLV transformed cell lines tested were C8166, C91/PL, MT2 and MT4 cells. C91/PL, MT2 and MT4 cells actively express HTLV-I proteins. C8166 cells were transformed by HTLV and are found to express HTLV-I tax but not other HTLV-I structural proteins (Salahuddin *et al.*, 1983). All nine of these cell lines were analysed in order to determine whether cells transformed with and expressing HTLV-I were significantly different to non-HTLV transformed/expressing cell lines with respect to development of classical MDR.

4.3.1 R123 dye efflux FACScan assays for MDR activity

All nine lymphoid cell lines were analysed for MDR activity by optimised R123 dye efflux assays. R123 dye efflux assays were performed at least twice for each cell line. Figure 4.8 shows the R123 dye efflux after 90 minutes from all nine cell lines. R123 dye efflux from MCF7/Dox HP-gp cells was also included as a reference cell line for high PGP expression and assays were performed exactly as described by Davies *et al.*, 1996. Low levels of R123 dye efflux can be seen by non-PGP mediated passive efflux (see section 4.2) and a small amount of R123 leakage is found to occur upon transfer to R123 free medium (Holló *et al.*, 1994). No detectable mdr-1 gene expression was detected in C91/PL, HUT78 or MT2 cells (see section 4.2.1) and the dye efflux observed in these cells cannot be due to PGP mediated MDR. Thus it was decided that cells with R123 dye efflux values of less than 20 % R123 dye loss after the 90 minutes efflux period were MDR negative (T. Gant personal communication). Using these criteria significant R123 efflux was only detected in MT4 and MCF7/Dox HP-gp control cells at 55.2 ± 3.9 and 84.3 ± 3.84 % R123 loss after 90 minutes efflux respectively.

Figure 4.8. R123 dye efflux assays of transformed cell lines. R123 dye efflux is expressed as a percentage of cellular R123 lost after a 90 minute efflux period. The dotted line marks the cut-off point for significant MDR mediated drug efflux (20% R123 loss). Only the MT4 HTLV-I transformed cells line showed significant R123 dye efflux at 55.2 %. As a reference R123 dye efflux from the MCF7/Dox PGP expressing cell line is also shown with 84.3 % R123 loss over 90 minutes.
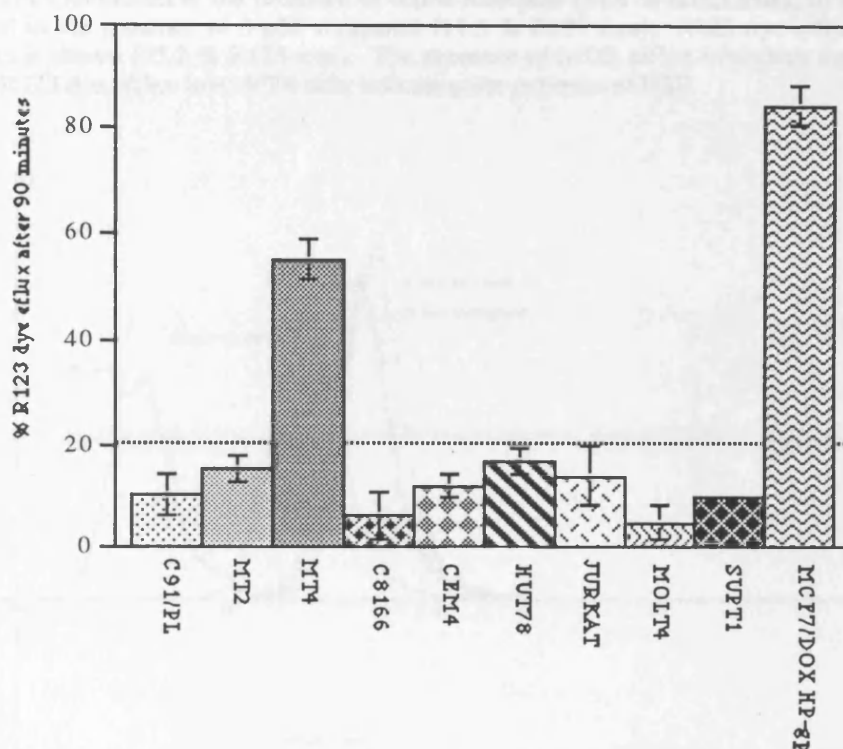
The specificity of PGP mediated R123 dye efflux in MT4 cells was also assessed by performing the dye efflux assay in presence of 5 μM reserpine or verapamil. Both reserpine and verapamil are known to be potent inhibitors of PGP mediated or classical MDR drug efflux (Tsuruo *et al.*, 1981) and act as high efficiency competitive substrates for PGP mediated drug efflux. Figure 4.9 is a R123 dye efflux assay FACScan profile of MT4 cells incubated in the presence of reserpine (figure 4.9a) and verapamil (figure 4.9b). The presence of both these PGP inhibitors on MT4 cells shows a significant reduction in R123 dye efflux from R123 55.2 % efflux to 11.8 % efflux with reserpine and 11.5 % efflux with verapamil. This corresponds to a 78.6 % and 79.2 % modulation of PGP activity by reserpine and verapamil respectively. These results

demonstrate that the R123 dye efflux from MT4 cells is mediated predominantly by PGP which can be blocked by the use of specific PGP inhibitors reserpine and verapamil.

Figure 4.9. R123 efflux assay FACscan profiles of MT4 cells incubated with PGP inhibitors. a) MT4 cells incubated in the presence of 5 µM reserpine (11.8 % R123 loss); b) MT4 cells incubated in the presence of 5 µM verapamil (11.5 % R123 loss). R123 dye efflux without inhibitors is shown (55.2 % R123 loss). The presence of MDR efflux inhibitors significantly reduced R123 dye efflux from MT4 cells indicating the presence of PGP.
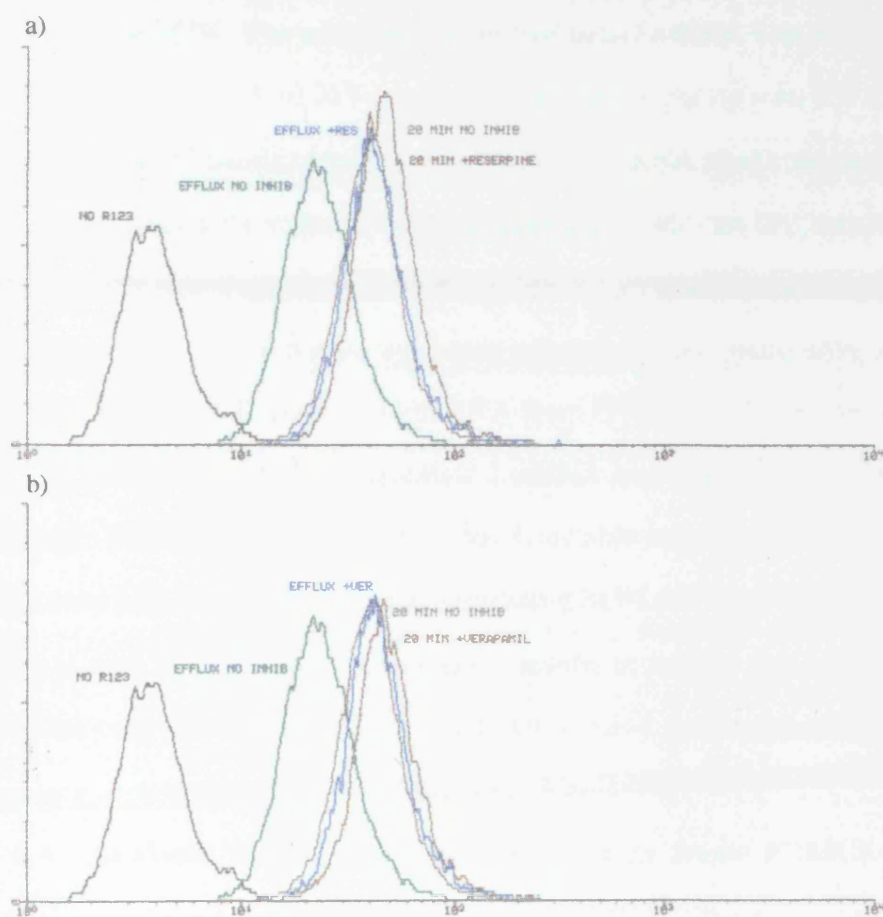
All other cell lines tested lost less than 20 % R123 during the 90 minute efflux period which was considered to be too low to be mediated by active PGP efflux (T. Gant personal communication). Hence, the only cell line to demonstrate significant PGP mediated R123 dye efflux or MDR phenotype was the HTLV transformed and

expressing cell line MT4. The lack of PGP mediated R123 dye efflux in all the other T-cell lines tested demonstrated the absence of a MDR phenotype these cells.

4.3.2 Quantitative RT-PCR assays for mdr-1 gene expression

Total RNA was extracted from all nine cell lines and between 200 and 500 ng analysed for mdr-1 mRNA expression by quantitative RT-PCR. Consistent with the R123 dye efflux assay results mdr-1 mRNA could only be detected and quantified in the HTLV transformed cell line MT4. The estimated amount of mdr-1 mRNA was 10.4 molecules mdr-1 RNA per pg total RNA (0.017 attomoles mdr-1 RNA per ng total RNA). For all other cell lines RT-PCR bands corresponding to mdr-1 mRNA could not be visualised in EtBr stained agarose gels under UV illumination and could not be quantified. The level of mdr-1 mRNA in these cells were at too low a concentration to be detected by this RT-PCR protocol. These results were also consistent with quantitative RT-PCRs performed by J. Riley and T. Gant on total RNA from C91/PL, HUT78 and MT4 cells (section 4.2.1) who also found detectable mdr-1 mRNA expression at a similar level in MT4 cells only. These results demonstrate that detectable mdr-1 mRNA expression is found only in the HTLV transformed and expressing MT4 cell line. These results are also consistant with the R123 dye efflux assay results in section 4.3.1 as significant R123 dye efflux only occurred in cells with detectable mdr-1 gene expression.

4.4 Analysis of mdr-1 gene expression in fresh PBMCs

In addition to established T-cell lines, fresh primary PBMCs were also analysed for classical MDR phenotypes. PBMCs from both HTLV-I infected and non-HTLV-I control individuals were tested for MDR activity by R123 dye efflux assays and quantitative mdr-1 RT-PCRs. Preservative-free heparinised fresh whole blood from HTLV-I infected individuals was obtained by venipuncture kindly performed by S. Nightingale, Royal Shrewsbury hospitals, Shrewsbury and G. Taylor, St. Mary's Hospital Medical School, London. Altogether the PBMCs from ten HTLV-I infected individuals were tested for classical MDR activity. Of these ten individuals six were

asymptomatic carriers, two were diagnosed with TSP/HAM, one was diagnosed with lymphoma type ATL and one with acute ATL. As controls non-HTLV-I infected fresh blood was obtained by venipuncture of six healthy volunteer subjects kindly performed by P. Sheldon, University of Leicester, Leicester.

4.4.1 R123 dye efflux FACScan assays for MDR activity

Fresh PBMCs were isolated from whole blood by Ficoll-Paque (Pharmacia) density centrifugation and classical MDR activity assayed by optimised R123 dye efflux assays. The basal level of MDR activity in the PBMCs from non-HTLV-I infected individuals was assessed by R123 dye efflux assays and the results for all 6 subjects are shown in table 4.5. The R123 FACScan profiles of PBMCs from non-HTLV-I infected individuals all showed a single discrete population of cells after 90 minute efflux with an average R123 dye loss of only 11.8 ± 7.2 %. Cells with less than 20 % R123 loss during the assay period was considered to be MDR negative (T. Gant, personal communication). A representative R123 FACScan profile is shown in figure 4.10a. This demonstrates a negligible level of drug/dye pumping MDR activity within circulating cells of the PBMC population of non-HTLV-I infected "normal" individuals.

Table 4.5: R123 dye efflux from the PBMCs of non-HTLV-I injected individuals. For all subjects only a single low effluxing cell population was observed.

Non HTLV-I infected subject	% R123 dye efflux after 90 minutes
#1	22
#2	12
#3	2
#4	3
#5	15
#6	17
mean % R123 dye efflux	11.8 ± 7.2

MDR activity in the PBMCs from HTLV-I infected individuals was assessed by R123

dye efflux assays and the results from all 10 subjects are shown in table 4.6. For 9 out

of the 10 HTLV-I infected individuals the R123 dye efflux FACScan profiles clearly

showed the presence of two discrete cell populations and a representative R123 dye

efflux FACScan profile is shown in figure 4.10b.

Table 4.6. R123 dye efflux from the PBMCs of HTLV-I infected subjects. Nine out of 10 HTLV-I infected subjects showed significant MDR efflux with both a high and low effluxing cell population being observed. The proportion of cells within each cell population is also shown in parenthesis. Confirmation of HTLV-I infection was also performed on subjects whenever possible by PCR and is shown in the last column.

HTLV-I infected subject	% R123 dye efflux from the high effluxing cell population after 90 minutes	% R123 dye efflux from the low effluxing cell population after 90 minutes	HTLV-I PCR results + = PCR positive n/t = not tested
Asymptomatics			
#1 (MDR⁻)	0 (0)	11 (100%)	+
#2	88 (31.8%)	6 (68.2%)	n/t
#3	90 (44.6%)	3 (55.4%)	n/t
#4	85 (28.8%)	1 (71.2%)	+
#5	83 (30.8%)	1 (69.2%)	+
#6	92 (33.2%)	10 (66.8%)	+
mean efflux (asymptomatic)	73 (32.6%)	5 (67.4%)	
TSP/HAM			
#7	92 (50.5%)	7 (49.5%)	+
#8	86 (40.5%)	15 (59.5%)	+
ATL			
#9	90 (55.3%)	11 (44.7%)	+
lymphoma type			
#10	87 (39%)	2 (61%)	n/t
mean efflux (disease)	88.8 (46.8%)	8.8 (53.2%)	

Figure 4.10. Representative R123 dye efflux assay FACscan profiles of freshly isolated PBMCs from a) non-HTLV infected subject; b) HTLV-I infected subject; c) HTLV-I infected subject in the presence of 5 µM verapamil. No R123 dye efflux was observed from PBMCs from the non-HTLV infected subject. Two distinct populations of cells can be observed from the PBMCs of the HTLV-I infected subject. High R123 dye effluxing (88.1 % R123 loss) and low R123 dye effluxing (6.6 % R123 loss) cell populations were observed. The inhibition of R123 dye efflux in the presence of verapamil indicates active PGP mediated dye efflux.
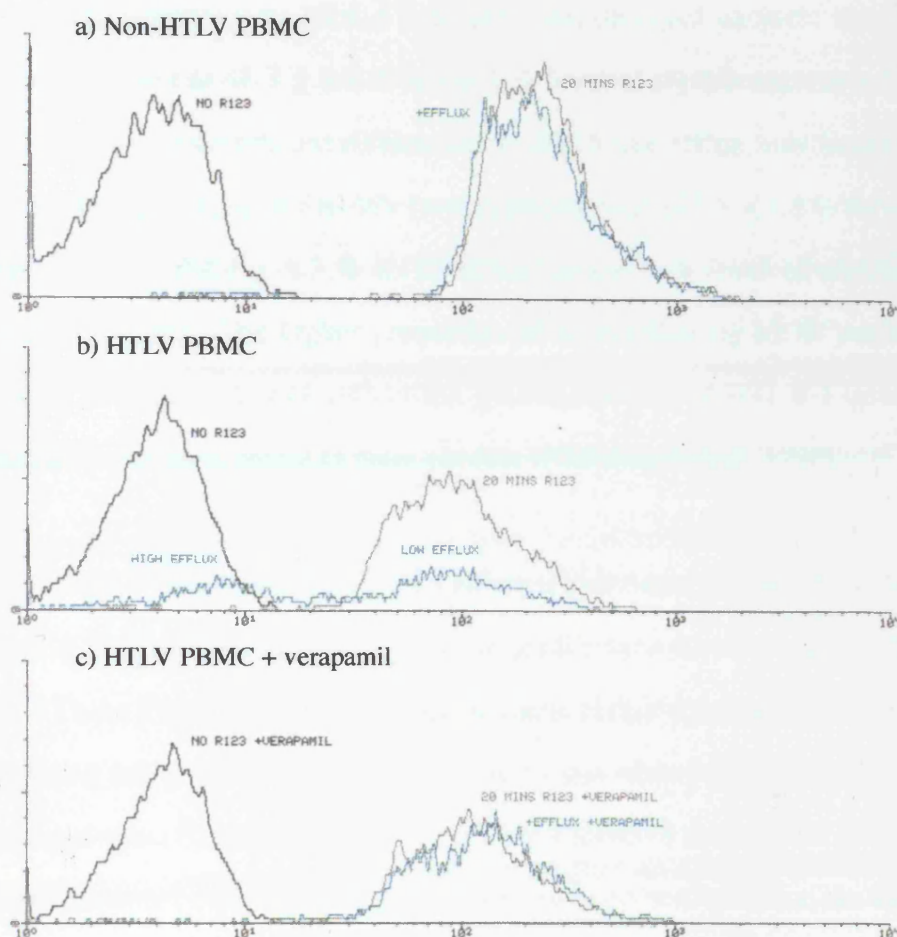
A cell population which effluxed greater than 80 % R123 and a cell population which effluxed less than 20 % R123 during the course of assay was observed in the PBMCs of 8 out of 9 HTLV-I infected subjects tested. These cell populations were designated the high R123 effluxing (> 80 % R123 loss) and low R123 effluxing (< 20 % R123 loss) cell populations respectively. The low effluxing population was considered to be MDR negative and the high effluxing population to be MDR positive. The mean R123 dye efflux from the high R123 effluxing cell population was 88.1 ± 3.0 % and the low

211

effluxing cell population was 6.6 ± 4.7 %. The population of high R123 effluxing cells was also found to be in range of 28.8 to 55.3 % of the total number of PBMCs assayed. With the exception of asymptomatic [#3] the proportion of high effluxing cells was between 18 to 48 % lower in the PBMCs from asymptomatic individuals compared to TSP/HAM or ATL subjects. The mean proportion of high R123 effluxing cells from asymptomatic subjects was 32.6 ± 7 % and from diseased subjects was found to be significantly higher at 46.3 ± 6.8 % at the 5 % level of significance (z = 2.96, as |z| > 1.96). However no significant differences in R123 dye efflux was found in the high effluxing cell populations of PBMCs from asymptomatic (87.6 ± 3.3 % R123 efflux) or diseased subjects (88.8 ± 5.7 % R123 efflux) at the 5 % level of significance (z = 0.374, as |z| < 1.96). The higher proportion of high effluxing MDR positive cells in individuals with disease may reflect the greater number of HTLV-I infected and/or activated cells normally found in these patients (Nishimura *et al.*, 1990).

Only the PBMCs from a single HTLV-I infected individual did not show the dual high and low R123 dye effluxing cell population profile seen for the other HTLV infected subjects. These PBMCs were from asymptomatic HTLV-I carrier [#1] and only a single low effluxing cell population (11 % R123 loss) was observed. It is presently unclear how asymptomatic [#1] differs from other HTLV-I infected subjects (S. Nightingale and S. Daenke, personal communication). These results demonstrate that the PBMCs from the majority of HTLV-I infected individuals contain a distinct sub-population of cells which are significantly MDR positive. Moreover, it can be seen that a greater proportion of cells within HTLV-I infected individuals with disease demonstrate an MDR phenotype as determined by R123 dye efflux assays.

The involvement of PGP in mediating R123 dye efflux in PBMCs from HTLV-I infected patients was assessed by performing the R123 dye efflux assays in the presence of 5 μM of the specific MDR inhibitors reserpine and verapamil. It was not possible to perform the inhibitor assay on PBMCs from all the HTLV-I infected patients

due to the limited number of cells isolated from whole blood and was only performed when enough cells remained after removal for R123 dye efflux assays, DNA and RNA extraction. Enough cells remained for inhibitor studies only with PBMCs isolated from HTLV-I infected asymptomatic #6. The results of R123 dye efflux from PBMCs incubated in the presence of 5 μM reserpine or verapamil PGP inhibitors are shown in table 4.6. A representative R123 FACScan profile of HTLV-I infected PBMCs incubated in the presence of verapamil is shown in figure 4.10c. The presence of 5 μM reserpine or verapamil significantly reduced the R123 dye efflux from the high effluxing population such that only a single low cell effluxing population was observed. HTLV-I infected asymptomatic #6 without any PGP inhibitors gave the characteristic dual high and low effluxing cell populations with 92 % and 10 % R123 loss respectively (see table 4.6). In the presence of 5 μM reserpine the high efflux population was not seen and a single low R123 dye effluxing cell population with 27 % R123 efflux was observed. The presence of reserpine inhibited PGP mediated R123 dye efflux and resulted in a 71 % reduction in R123 dye efflux from the original high efflux population. Similarly the presence of 5 μM verapamil resulted in a single low effluxing population with 25 % R123 dye efflux and represented a 73 % reduction in R123 dye efflux from the original high efflux population (data not shown). This result demonstrates that the R123 dye efflux from these cells was mediated by specifically by PGP as its activity could be modulated by the specific PGP MDR inhibitors reserpine and verapamil.

To confirm that the HTLV-I infected subjects were still HTLV-I positive, HTLV-I proviral DNA PCR was performed on total genomic DNA extracted from PBMCs using specific HTLV-I primers ATK-2 and ATK-5 (see chapter 2, section 2.10). Figure 4.11 shows a representative HTLV-I proviral DNA PCR on total genomic DNA isolated from HTLV-I infected subject [#]1. Negative controls were PCR with water instead of DNA templates and total genomic DNA from the non-HTLV-I infected Jurkat T-cell line. Positive control reactions were PCR using total genomic DNA from the HTLV-I

transformed cell line MT4 and with the HTLV-I provirus containing plasmid pUC18-HTLVp (see chapter 3, section 3.3.3). A HTLV-I specific band of 1077 bp was observed for all positive control PCRs and for HTLV-I infected subject [#]1. All negative control reactions contained no PCR bands. Table 4.6 shows the results of HTLV-I specific proviral DNA PCR on total genomic DNA extracted from PBMCs. Total genomic DNA extracted from HTLV-I infected subjects PBMCs were all found to be HTLV-I PCR positive. This result confirms that all the HTLV-I infected individuals tested by PCR were indeed still HTLV-I infected.

Figure 4.11. HTLV-I PCR confirmation of PBMCs from HTLV-I infected subjects. PCR was performed using HTLV-I primers ATK-2 and ATK-5 which amplifies a 1077 bp region of the pol gene. M = l DNA (HindIII cut) marker. Lane 1 = negative control PCR with H2O. Lane 2 = negative control PCR with Jurkat cellular genomic DNA. Lane 3 = PCR of genomic DNA isolated from PBMCs of a HTLV-I infected patient. Lane 4 = positive control PCR with C91/PL genomic DNA. Lane 5 = blank. Lane 6 = positive control PCR with pBC-HTLVp plasmids (see chapter 3, section 3.3). The presence of HTLV-I proviral DNA is demonstrated by a band at 1077 bp.
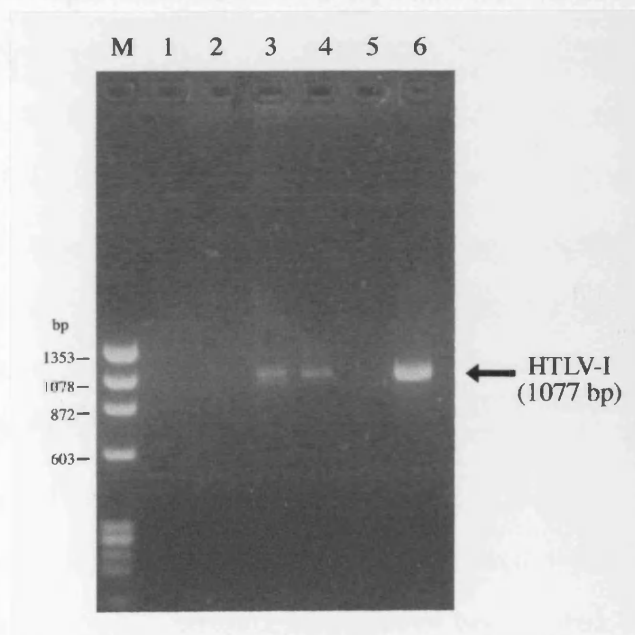
4.4.2 Identification of cell types in high R123 efflux PBMCs

In order to further characterise the high R123 effluxing MDR cell population identified in the PBMCs of HTLV-I infected individuals the lymphocyte cell types within this population were identified by direct immunofluorescence and FACs. By dual colour

fluorescent labelling of cells using R123 (green) and PE (red) it was possible to select cells on the basis of R123 fluorescence after efflux and stain for specific cell markers using PE conjugated antibodies. Lymphocyte cell marker typing was performed using PE-conjugated monoclonal antibodies (Sera-Lab) against CD3, CD14 and CD22 cell surface molecules which are markers for T-cell, monocyte/macrophage and B-cell lymphocytes respectively. Standard R123 dye efflux assays were performed on HTLV-I infected PBMCs and then labelled using the PE-conjugated monoclonal antibodies as recommended by the enclosed protocols (see chapter 2, section 2.5.2d). Cells were passed through a FACScan and both R123 fluorescence (FL-1) and PE fluorescence (FL-2) collected. High and low R123 dye efflux cell populations were identified and analysed for their respective PE fluorescence.

Figure 4.12 shows representative FACScan profiles for the dual R123 dye efflux and cell typing experiment of PBMCs from HTLV-I infected TSP/HAM [#]7. Figures 4.12a to 4.12c shows the R123 dye efflux profile (FL-1 fluorescence) of total PBMCs incubated with PE conjugated anti- CD3, CD14 and CD22 monoclonal antibodies respectively. As expected the efflux patterns are similar for all three monoclonals and the characteristic high and low R123 dye effluxing cell populations are observed. The horizontal bars labelled R2 and R3 designate the selected regions identifying the high efflux and low R123 dye effluxing cell populations respectively. Figures 4.12d to 4.12f shows the PE fluorescence cell profile (FL-2 fluorescence) of total PBMCs incubated with anti- CD3, CD14 and CD22 monoclonal antibodies respectively. All three monoclonal antibodies produce two distinct populations, a high PE fluorescing and low PE fluorescing population. The low FL-2 or PE fluorescing population are unlabelled cells and the high FL-2/PE fluorescing cells are labelled and identified as marker positive. Figure 4.12d shows the total number of cells labelled with the PE-conjugated anti-CD3 monoclonal antibody or T-cells. The number of $CD3^+$ or T-cells was found to be 58 % of the total number of cells counted with a mean fluorescence of 44. Figure 4.12e shows the total number of cells labelled with the PE-conjugated anti-

CD14 monoclonal antibody. The proportion of CD14$^+$ or monocyte/macrophage cells was found to be 15 % of the total number of cells counted. Figure 4.12f shows the total number of cells labelled with the PE-conjugated anti CD22 monoclonal antibody or B-cells. The number of CD22$^+$ or B-cells was found to be 12 % of the total number of cells counted. 15 % of the total number of cells did not label with either anti-CD3, CD14 or CD22 monoclonal antibody.

Figures 4.12g to 4.12i show the PE (FL-2) fluorescence of the high R123 dye effluxing cells only as selected for using region 2 (R2) gating shown figures 4.12a to 4.12c. Figure 4.12g shows the number of CD3$^+$ T-cells in the high effluxing cell population (R2) and both a high and low PE fluorescing cell populations are observed. The high PE fluorescing population are CD3$^+$ or T-cells and comprise 47 % of the number of the high efflux (R2) cell population or 27 % of the total number of cells. This indicates that the high dye efflux population is composed of 47 % CD3$^+$ T-cells and 53 % CD3$^-$. The high PE fluorescing or CD3$^+$ cells in the high R123 dye effluxing population (R2) was found have a mean FL-1 fluorescence of 31. Figure 4.12h shows the number of CD14$^+$ monocyte/macrophage cells in the high R123 dye effluxing cell population (R2). Here only a single low PE fluorescing cell population is observed indicating that none of the cells in the high effluxing population are CD14$^+$ or monocytes/macrophages. Figure 4.12i shows the number of CD22+ B-cells in the high R123 dye effluxing cell population (R2). Both a high and low PE fluorescing cell population is observed with the high PE fluorescing cells comprising only 8 % of the high efflux population or 1 % of the total number of cells. This indicates that only 8 % of the high efflux population comprises of CD22$^+$ B-cells. Figures 4.12j to 4.12l show the PE or FL-2 fluorescence of the low R123 dye effluxing cell population as selected for using the region 3 (R3) shown in figures 4.12a to 4.12c. Figures 4.12j to 4.12l identify that the low efflux cell population consists of a mixture of the remaining T-cells, monocyte/macrophages and B-cells not present in the high efflux population.

Figure 4.12. Identification of cell types in the high and low efflux cell populations of HTLV-I infected individuals. FACScans a to c are R123 dye efflux FACScan profiles for HTLV-I infected PBMCs. Region R2 corresponds to cells with high MDR R123 dye efflux and region R3 corresponds to cells with low R23 dye efflux. FACScans d to f are the PE fluorescence of PBMCs dual labelled with PE-conjugated anti-CD3, CD14 and CD22 monoclonal antibodies respectively. FACScans g to i are the PE fluorescence of the high R123 efflux cell population (R2) labelled with anti-CD3, CD14 and CD22 respectively. FACScans j to l are the PE fluorescence of the low R123 dye efflux cell population (R3) labelled with anti-CD3, CD14 and CD22 respectively.
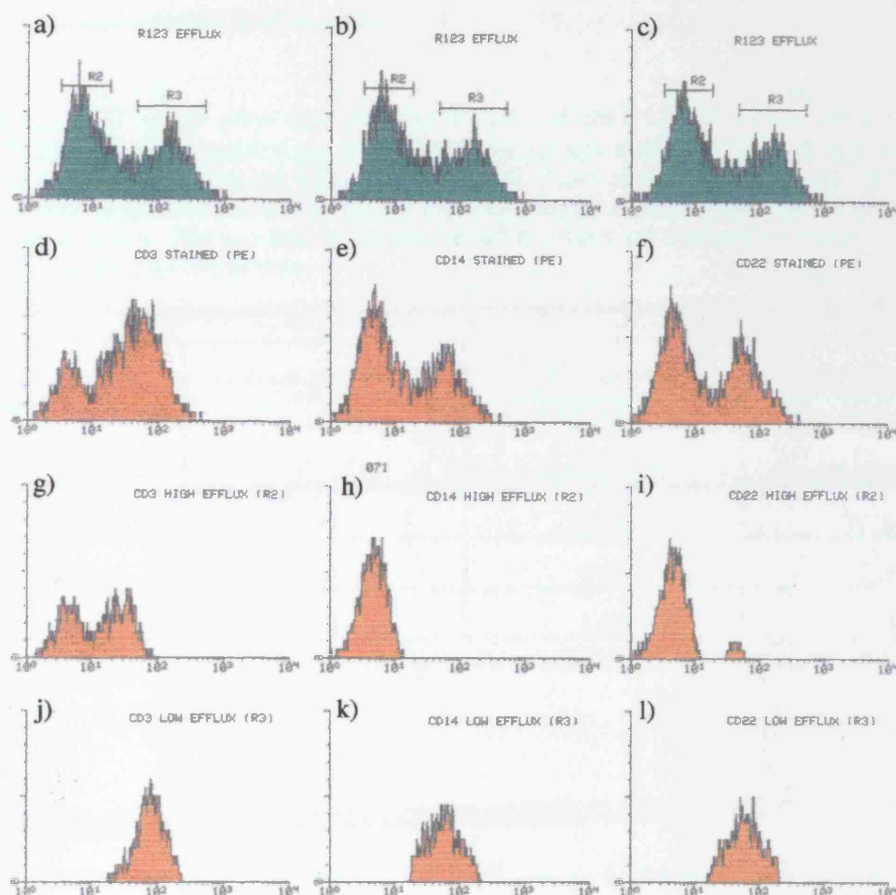
Lymphocyte cell typing experiments were performed on the PBMCs isolated from three HTLV-I infected subjects, two asymptomatic [#4], [#5] and one TSP/HAM [#7]. The relative lymphocyte cell distribution within the high and low effluxing cell populations was similar for all three PBMCs tested and the results are shown in table 4.7. The mean number of CD3+, CD14+ and CD22+ cells in total PBMCs were 59 ± 1.3 %, 13 ± 1.3 % and 13 ± 1.7 % respectively. The mean number of CD3^{+}, CD14^{+} and CD22^{+}

cells in the high R123 dye efflux MDR positive population (R2) only were 48 ± 0.8 %,

0 % and 8 ± 0.8 % respectively. This corresponds to a value of 28 % CD3+ T-cells

and 1 % CD22+ B-cells of the total number of PBMCs. These results indicate that the

majority of labelled cells within the high R123 effluxing MDR cell population expressed

the CD3 cell surface marker and were of T-cell origin. In contrast the low R123

effluxing non-MDR cell population contained a mixture of all the remaining T-cell,

monocytes/macrophages and B-cells.

Table 4.7. Cell surface phenotype labelling of high and low R123 dye efflux cell populations. The R123 dye efflux populations from PBMCs of asymptomatics #4, and #5 and TSP/HAM subject #7 were examined for CD3, CD14 and CD22 cell surface markers. All three results were similar and the mean cell frequency from all subjects expressed as a % of the total cells analysed is shown. The numbers in parenthesis are the mean cell frequency expressed as a % of the cells in that population only.

Cell surface marker	% Total cells stained	% cells stained in the HIGH EFFLUX cell populations	% cells stained in the LOW EFFLUX cell populations
CD3	59	28 (48)	26 (44)
CD14	15	0 (0)	11 (82)
CD22	12	1 (8)	11 (81)

4.4.3 Indirect immunofluorescent detection of PGP

Indirect immunofluorescent detection of PGP was performed on cells using the murine

anti-PGP monoclonal antibody MRK-16 (Kamiya Biomedical company, Thousand

Oaks, CA, USA) in conjunction with FITC conjugated goat anti-mouse IgG (Dako

Ltd.) and FACScan analysis. The MRK-16 monoclonal antibody recognises an

extracellular cell surface epitope of human PGP (Thiebaut et al., 1989) and both

MRK16 and IgG2a control antibodies were kind gifts from T. Gant, MRC Toxicology

unit, University of Leicester. Due to the limited amount of antibody and restricted

availability of HTLV-I infected blood it was only possible to perform indirect

immunofluorescence using MRK-16 on PBMCs from the HTLV-I infected subject with

ATL #9. Figure 4.13 shows the MRK16 and IgG2a control FACScan profiles of both

PBMCs from ATL subject #9 and HP-gp MCF7/Dox cells. The negative control for non-specific antibody binding for all labelling was the use of murine IgG2a (Dako Ltd.) which is the same isotype as MRK-16. The IgG2a antibody was used instead of MRK-16 as the primary antibody. A positive control for these experiments was MRK-16 labelling of the high PGP expressing subclone of MCF7/Dox cells (Davies *et al.*, 1996).

Figure 4.13a is the FACScan profile for HP-gp MCF7/Dox cells and shows a high FITC fluorescing and PGP expressing population using the MRK-16 antibody. Using the IgG2a control antibody the cells did not significantly label with FITC (low fluorescence) and demonstrates the specificity of the experiment. Figure 4.13b shows the FACScan profiles of PBMCs from ATL subject #9. Using the IgG2a control antibody a single low fluorescing population is observed indicating the absence of non-specific binding. However using the anti-PGP MRK16 antibody two cell populations can be observed. Both high and low FITC fluorescing cell populations are derived from MRK-16 staining of fresh PBMCs. The high fluorescing cell population expresses a significant amount of membrane bound PGP molecules whereas the low fluorescing population does not. The proportion of high FITC fluorescing PGP expressing cells was found to be 59.3 % of the total number of PBMCs. This indicates that the PBMCs from HTLV-I infected ATL subject #9 contains two distinct populations of cells differentiated by the level of membrane bound PGP. Both high and low PGP cell surface expressing cell populations can be found in this subject and is in good agreement with the MDR activity found by R123 dye efflux assays in section 4.4.1. In addition the relative proportion of cells found in the high PGP expressing and high R123 dye effluxing populations were found to similar at 59.3 % and 55.3 % respectively. This would suggest that the high PGP expressing and high R123 dye effluxing populations are the same cells. However double labelling of the R123 high efflux populations with MRK-16 would be required to definitively confirm this.

Figure 4.13. Indirect immunofluorescence MRK-16 anti-PGP staining of cells. a) Positive control high PGP expressing MCF7/Dox HP-gp cells. b) Freshly isolated PBMCs from ATL HTLV-I infected subject #9. Non-specific antibody binding was assessed using a matched isotype IgG2a antibody instead of MRK-16. Both cell types label with MRK-16 antibody and demonstrates the presence of PGP on the surface of these cells.
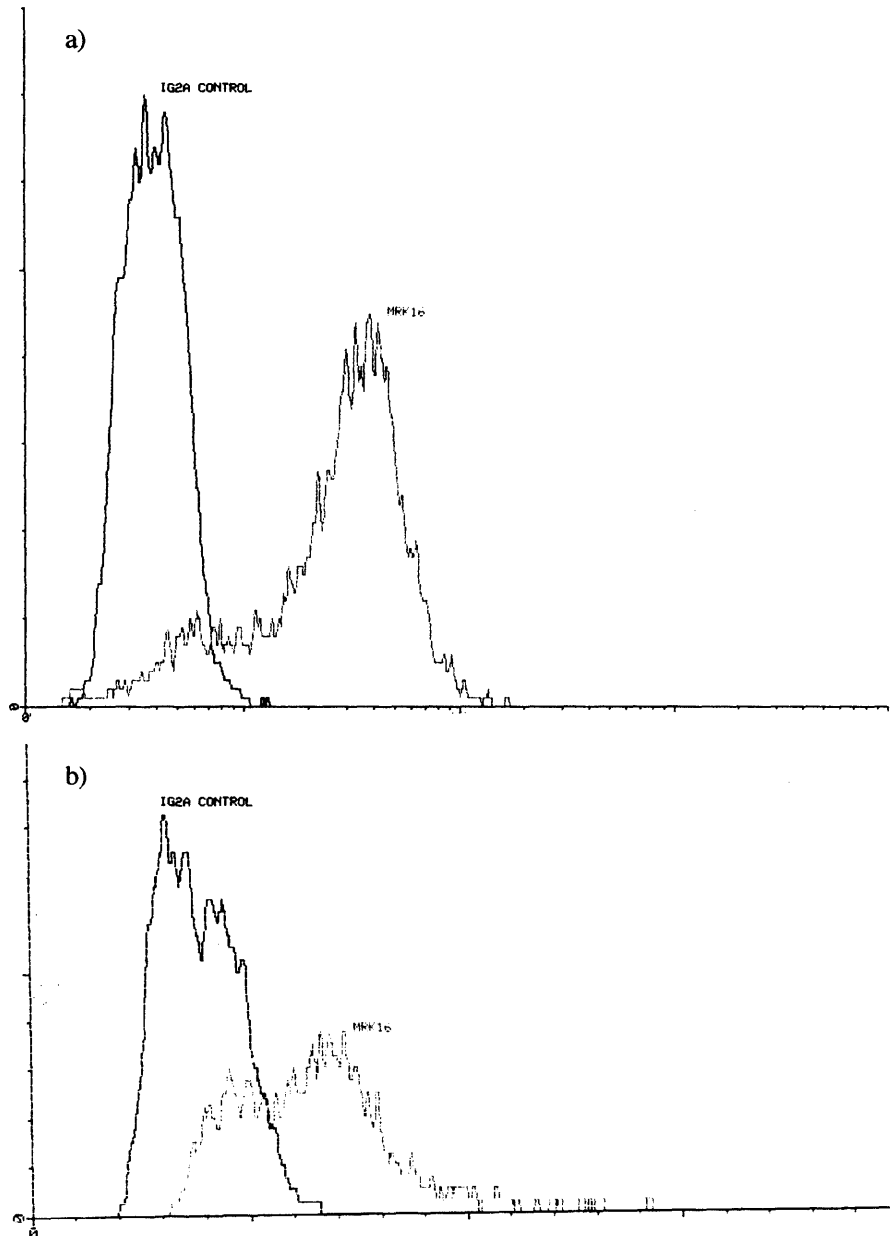
4.4.4 Quantitative RT-PCR assays for mdr-1 gene expression

Total cellular RNA was extracted from 1×10^7 PBMCs of all six non-HTLV-I infected individuals and nine HTLV-I infected individuals by RNAzol B reagent. The steady state amount of mdr-1 mRNA was then quantified by RT-PCR as described in section 4.2.3. Quantification of mdr-1 mRNA in PBMCs from the HTLV-I infected lymphoma type individual [#]10 was not possible due to the limited quantity of blood available. Table 4.8 shows the quantitative RT-PCR results for all non-HTLV-I and HTLV-I infected individuals. The results show that for all six non-HTLV-I infected individuals the steady state levels of mdr-1 RNA were consistently low with a mean of 7.36 ± 2.84 molecules mdr-1 RNA per pg total RNA. In contrast the average steady state level of mdr-1 RNA expression in the PBMCs from the eight HTLV-I infected and R123 dye efflux MDR positive cells was 4 fold higher at 29.40 ± 10.68 molecules mdr-1 RNA per pg total RNA. The average amount of mdr-1 RNA in the PBMCs from the five HTLV-I infected and MDR efflux positive asymptomatic individuals was 23.61 ± 6.36 molecules mdr-1 RNA per pg total RNA. The average amount mdr-1 RNA from the two HTLV-I infected individuals with TSP/HAM ([#]7 and [#]8) was 33.55 ± 9.91 molecules mdr-1 RNA per pg total RNA, over 4.5 times the amount in non-HTLV-I infected controls and 30 % more than in asymptomatics. The greatest single mdr-1 quantification was for the HTLV-I infected individual with ATL ([#]9) at 49.11 molecules mdr-1 per pg total RNA which is over 6.5 times the amount in non-HTLV-I infected controls, 2 times more than in asymptomatics and 32 % more than in TSP/HAM. However the amount of mdr-1 mRNA in the ATL individual could not be verified as quantitative mdr-1 RT-PCR was only performed once. Overall the amount of mdr-1 mRNA in HTLV-I infected individuals with disease ([#]7, [#]8 and [#]9) was 36.15 ± 10.74 molecules mdr-1 per pg total RNA. This value is almost 5 times greater than in non-HTLV-I infected PBMCs and 35 % greater than in PBMCs from HTLV-I infected MDR efflux positive asymptomatic individuals. In addition statistical testing of the significance of two means between the diseased and asymptomatic subjects indicated that the amount of mdr-1 RNA in HTLV-I infected and diseased individuals is

significantly greater than the amount in asymptomatics at the 5 % level of significance.

The amount of mdr-1 RNA in PBMCs from the one HTLV-I infected asymptomatic

individual without any R123 dye efflux (asymptomatic [#]1) was low at 5.96 ± 3.87

molecules mdr-1 RNA per pg total RNA and in line with mdr-1 expression in the

PBMCs from non-HTLV-I infected subjects.

Table 4.8. Quantitative RT-PCR of mdr-1 mRNA in PBMCs from all subjects tested. Mean values are given for all subjects more than once. Quantitative RT-PCR analysis shows greater levels of mdr-1 mRNA from HTLV-I infected subjects when compared to the non-HTLV-I infected controls.

Subjects	Molecules mdr-1 RNA per pg total RNA
Non-HTLV-I infected	
[#]1	6.4
[#]2	7.3
[#]3	3.8
[#]4	5.6
[#]5	8.3
[#]6	12.9
Mean mdr-1 RNA (non HTLV infected)	7.36 ± 2.84
HTLV-I infected - Asymptomatic	
[#]1 (R123 efflux negative)	6 ± 3.9
[#]2	21.9 ± 1.34
[#]3	26.8 ± 11.1
[#]4	21.1
[#]5	22.4
[#]6	24.3
Mean mdr-1 mRNA (asymptomatic)	23.6 ± 6.4
Mean mdr-1 mRNA (MDR[+], [#]2 to [#]6)	29.4 ± 10.68
HTLV-I infected - TSP/HAM	
[#]7	37.8 ± 7.1
[#]8	27.3 ± 10.2
Mean mdr-1 mRNA (TSP/HAM)	33.55 ± 9.91
HTLV-I infected -ATL	
[#]9	49.11
Mean mdr-1 mRNA (all disease, [#]7 to [#]9)	36.15 ± 10.74

PBMCs from all eight HTLV-I infected and high MDR R123 dye effluxing individuals [#]2 to [#]9 demonstrated a corresponding 3 to 5 fold increase in mdr-1 mRNA over the non-HTLV-I infected R123 dye efflux MDR negative PBMCs. The quantitative mdr-1 RT-PCR results are consistent with the R123 dye efflux MDR assay results shown in section 4.4.2. These results indicate that the enhanced R123 dye efflux activity of PBMCs from HTLV-I infected individuals corresponds with an increased level of mdr-1 gene expression.

4.4.5   Sorting and characterisation of R123 dye efflux cell populations

Further characterisation of both the high and low R123 dye efflux cell populations was done in relation to HTLV-I proviral load. This was done by dual positive cell sorting and quantitative HTLV-I PCR and is described in chapter 2. PBMCs were isolated from fresh blood of TSP/HAM HTLV-I infected subjects [#]8 and [#]9 which consistently had the largest proportion of high R123 dye effluxing cells in the region of 40 to 50 %. A scaled up version of the R123 dye efflux assay was performed on 1×10^7 PBMCs. These cells were then physically sorted in a Becton Dickson FACSvantage cell sorter by R. Snowden, MRC Toxicology unit, University of Leicester. Cells were sorted into two populations based upon cellular R123 dye fluorescence after the R123 dye efflux assays. High R123 fluorescing cells (low R123 dye efflux population) and low R123 fluorescing (high R123 dye efflux population) were separated and total genomic DNA extracted from each cell population.

HTLV-I proviral DNA was quantified from both high and low R123 dye efflux sorted cell populations by G. Taylor, St Mary's Hospital medical school, Imperial College, London. For both TSP/HAM subjects [#]8 and [#]9 a similar pattern of HTLV-I provirus DNA distribution was observed in which both the high and low R123 dye efflux cell populations contained an equal number of proviral copies per 100 cells. TSP/HAM subject [#]8 contained 14 copies of HTLV-I proviral DNA per 100 cells and TSP/HAM subject [#]9 contained 35 copies per 100 cells in both high low R123 efflux cell

populations. These results indicate that between the high and low R123 dye effluxing cell populations no detectable difference in HTLV-I proviral DNA content can be observed. It should be noted that the efficiency of cell sorting was undetermined and these results may not be truly representative of the high and low efflux populations. Despite the use of dual positive cell sorting it may be possible that a number of cells from one population may have contaminated the other. Although this was unlikely to have a significant impact of the PCR data it cannot be ruled out.

The finding that no differences in HTLV-I proviral DNA content can be observed between the high and low drug efflux cell populations seems surprising. It was hypothesised that the high drug efflux cells were the HTLV-I infected cells and as such should have a greater proviral load than the low efflux cell population. However this was not the case and suggested that HTLV-I infection *per se* may not be sufficient for significant mdr-1 gene activation and induction of an MDR phenotype. Although it has been demonstrated that an active MDR phenotype is present in a significant population of T-cells from HTLV-I infected individuals the role of HTLV in mediating this effect is unclear. It may be possible that the enhancement of MDR observed is not a direct result of HTLV infection but due indirectly to host immune system activation or dysfunction in response to HTLV. Indeed, the experiments on several *in vitro* transformed HTLV expressing cells (C91/PL, MT2) have shown the lack of detectable mdr-1 RNA expression and insignificant R123 efflux activity (see section 4.3), further suggesting that HTLV expression is not sufficient to direct mdr-1 gene/PGP expression.

4.5 Mechanisms of activation of mdr-1 gene expression

It has already been noted in the previous sections that an increase in drug efflux activity (section 4.4.1) and mdr-1 gene expression (section 4.4.4) is consistently found in the PBMCs from HTLV-I infected individuals. However it was also found that cellular HTLV-I proviral DNA content did not correlate with drug efflux activity (section 4.4.5) and suggests that HTLV-I infection alone is not sufficient to mediate the induction of the

cellular MDR phenotypes observed. It was therefore necessary to further investigate the mechanisms of MDR enhancement by HTLV-I. Several possible mechanisms for the enhancement of mdr-1 gene expression and drug efflux activity in the PBMCs of HTLV-I infected individuals were described in chapter 1, section 1.7. It was hypothesised that mdr-1 gene expression may be stimulated by the mitogenic and cytokine-like effects characteristic of HTLV-I infected cells and by the cellular gene trans-activation activity of HTLV-I tax protein. Both mechanisms were assessed *in vitro* for their ability to stimulate mdr-1 gene expression and MDR activity.

4.5.1 PHA mitogenic activation of mdr-1 gene expression in T-cells

The ability of mitogenic stimulation to enhance mdr-1 gene expression and MDR efflux activity was assessed by culturing fresh PBMCs in the presence of the mitogenic plant lectin phytohaemagglutinin (PHA). PHA is a polymeric protein which binds non-specifically to carbohydrate residues of cell surface glycoproteins including the CD3/TCR receptor complex which stimulates the proliferation of T-cells.

PBMCs from a non-HTLV-I infected donor were isolated from whole blood and cultured at 2×10^6 cells/ml in growth medium (1x RPMI 1640, 20 % FCS, 5 U/ml Il-2) supplemented with or without 10 µg/ml PHA for up to 72 hours. Samples of cells were then removed for R123 dye efflux and mdr-1 RNA RT-PCR assays after 24, 48 and 72 hour intervals. Figure 4.14 shows the R123 dye efflux activity FACScan profiles of PBMCs before and after PHA stimulation for 24, 48 and 72 hours. Figure 4.14a shows the R123 dye efflux FACScan profile of freshly isolated un-stimulated PBMCs and demonstrates that very low R123 dye efflux activity (single population, 19 % R213 dye efflux) can be observed (consistent with the findings in section 4.4.1). However after mitogenic stimulation with PHA R123 dye efflux can clearly be observed in a significant proportion (28 %) of the cultured PBMCs after only 24 hours (figure 4.14b).

Figure 4.14. R123 dye efflux FACScan profiles of non-HTLV-I infected PBMCs cultured and stimulated with 10 µg/ml PHA. a) Freshly isolated uncultured PBMCs. b) PBMCs cultured with PHA after 24 hours. c) PBMCs cultured with PHA after 48 hours. d) PBMCs cultured with PHA after 72 hours culture. Negligible R123 dye efflux was observed from freshly isolated uncultured PBMCs. Significant R123 dye efflux can be observed in a distinct sub-population of PBMCs at all time periods after 24 hours PHA stimulation and display relatively uniform R123 fluorescence profiles.
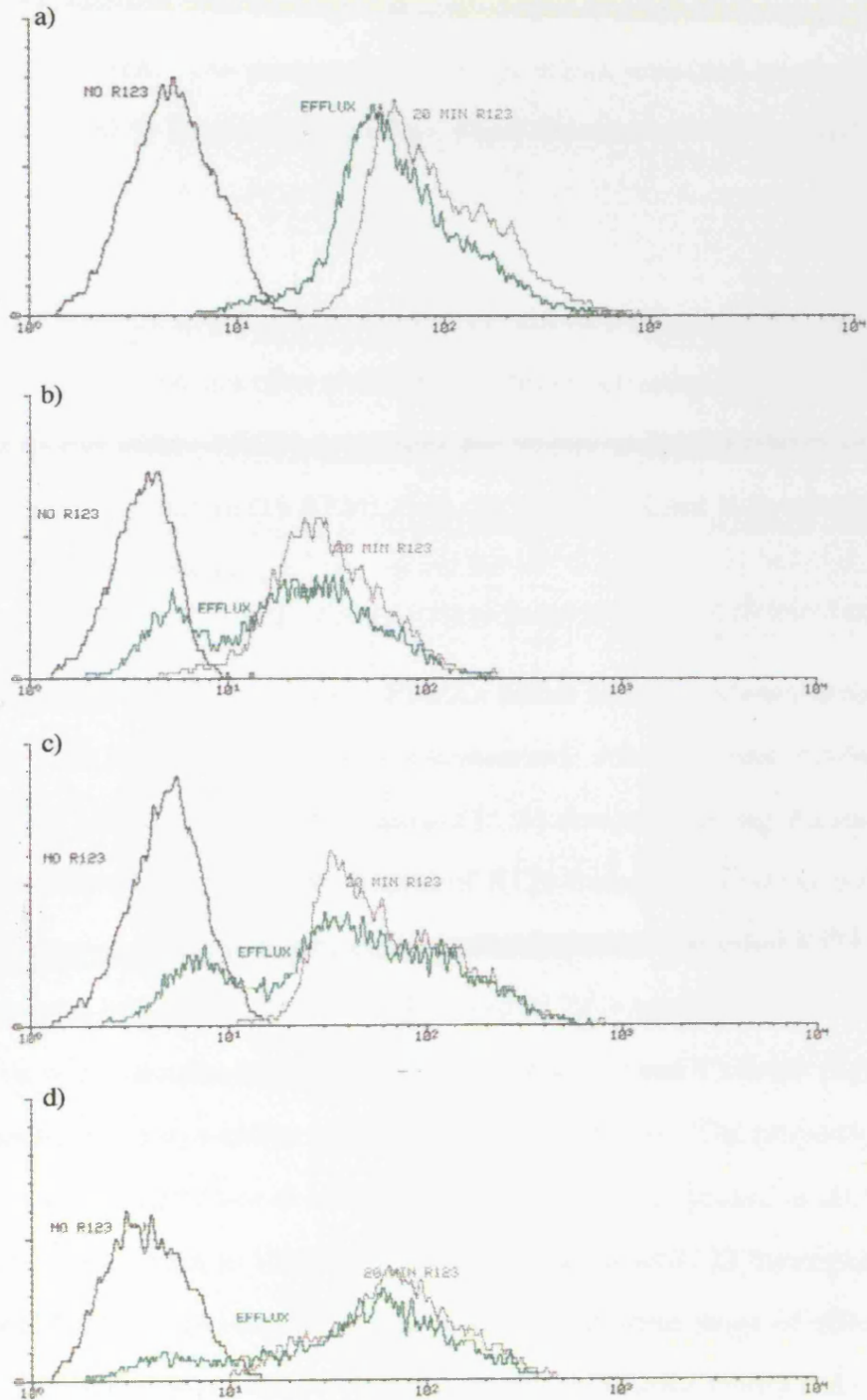
The largest proportion of high R123 effluxing cells is observed at 48 hours post stimulation (figure 4.14c) with 33 % of the total number of cells effluxing R123. After 72 hours of PHA stimulation (figure 4.14d) the proportion of high R123 effluxing cells decreased to only 20 % of the total number of cells and showed a more diffuse pattern of R123 fluorescence. The reduction in cell number may be attributed to the general cytotoxicity of PHA. The percentage R123 dye efflux remained relatively constant between 84 to 93 % from the high efflux populations over the 72 stimulation hour period.

Culturing of PBMCs in growth medium in the absence of mitogenic stimulation by PHA was also assessed as a control for specific MDR activation by PHA. Figure 4.15 shows R123 dye efflux FACScan profiles for freshly isolated PBMCs and PBMCs cultured in growth medium (1x RPMI 1640, 20 % FCS, 5 U/ml Il-2) without PHA for 24, 48 and 72 hour periods.

FACScan profiles for freshly isolated PBMCs before culture is shown in figure 4.15a where a minimal level of R123 dye efflux is observed. After 24 hours of culture (figure 4.15b) a small proportion of PBMCs (around 15 %) demonstrated significant R123 dye efflux but showed a much broader pattern of R123 fluorescence which is difficult to distinguish from the main population of low effluxing cells. The mean R123 dye efflux was moderate at approximately 47 %. The broad R123 fluorescence pattern of the high efflux cells was maintained after 48 hours (figure 4.15c) and 72 hours (figure 4.15d) and the mean R123 dye efflux was constant around 80 %. The proportion of high efflux cells was initially low at around 15 % after 24 hours, peaked at 20 % after 48 hours then declined back to 15 % after 72 hours. The broad R123 fluorescent patterns of high R123 effluxing cells after efflux indicates a diverse range of efflux activity within different cells with some having a relatively large efflux ability and others with small efflux activities. This is in contrast with PHA stimulated PBMCs in which the high R123 dye effluxing cells display a relatively uniform efflux activity and R123

fluorescence after efflux. The diffuse nature of R123 fluorescence after efflux from these unstimulated cells indicates a heterogeneous mixture of MDR activities and suggests a non-specific upregulation of efflux activity. In addition the number of high efflux cells in the absence of PHA stimulation was 25 to 40 % less than the number from PHA stimulated PBMCs and with a slower time course of activation.

Semi-quantitative RT-PCR analysis of mdr-1 mRNA from both PHA stimulated and unstimulated PBMCs was performed using 250 ng of total RNA extracted with RNAzol B. RT-PCR reactions were performed at a lower level of sensitivity by using only 25 PCR cycles in order to better differentiate band intensities. 10 µl of the RT-PCR reaction was loaded on 3 % GTG NuSieve agarose gels containing EtBr and visualised under UV illumination.

Figure 4.16 shows a gel photo of mdr-1 RT-PCRs from unstimulated and PHA stimulated PBMCs after 24, 48 and 72 hours of culture. Negative control reactions included RT-PCR without RNA (lane 1) and with total RNA from the mdr-1 negative cell line C91/PL (lanes 3, 7 to 9; also see section 4.2.1 and 4.3.2). All control reactions were negative with no bands corresponding to mdr-1 RNA. Total RNA from freshly isolated uncultured PBMCs is shown in lane 2 and was found not to show a band corresponding to mdr-1 RNA at this level of detection. Mdr-1 RNA from PBMCs cultured for 24, 48 and 72 hours in the absence of PHA is shown in lanes 4, 5 and 6 respectively. Mdr-1 RNA was also undetectable in these cells at this level of detection. This result indicates that the level of mdr-1 gene expression in the absence of PHA is too low to be detectable by RT-PCR. Mdr-1 RNA from PBMCs cultured in the presence of PHA for 24, 48 and 72 hours is shown in lanes 10, 11 and 12 respectively. Mdr-1 RNA can be clearly detected in these cells by the presence of band at 161 bp. Relative band intensities show that mdr-1 RNA expression is detectable as early as 24 hours post stimulation and that maximal expression occurs after 48 hours.

Figure 4.15. R123 dye efflux FACScan profiles of non-HTLV-I infected PBMCs cultured in growth medium without exogenous mitogenic stimulation. a) Freshly isolated uncultured PBMCs. b) PBMCs after 24 hours culture. c) PBMCs after 48 hours culture. d) PBMCs after 72 hours culture. Negligible R123 dye efflux was observed from freshly isolated uncultured PBMCs. Minimal R123 dye efflux was observed in a small population of PBMCs after 24 hours culture and display diffuse R123 fluorescence profiles.
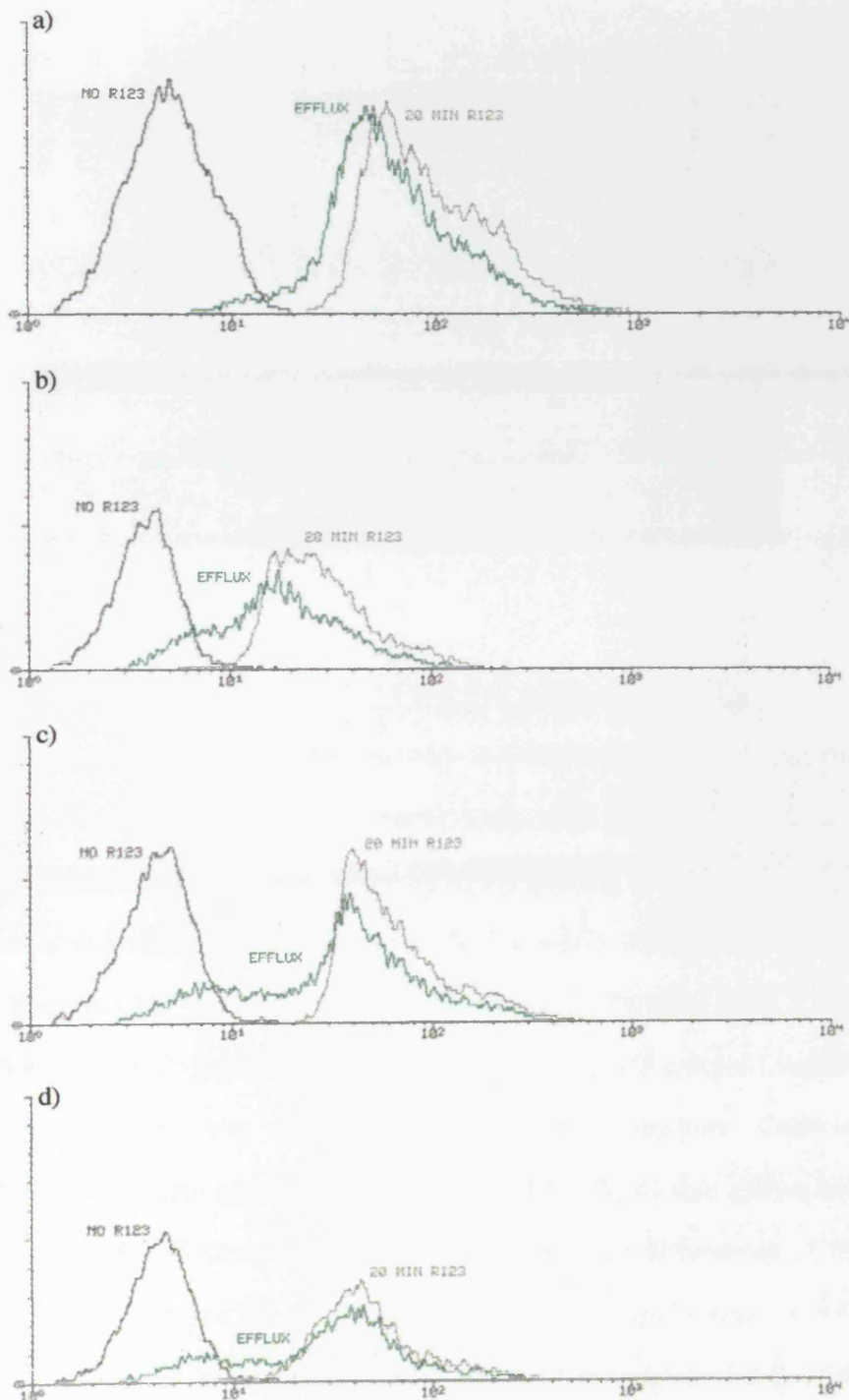
Figure 4.16. EtBr stained agarose gel of semi-quantitative RT-PCR for mdr-1 mRNA in unstimulated and stimulated PBMCs. M = Φx174 DNA (HaeIII cut) marker. Lane 1 = Negative control RT-PCR (H$_2$O). Lane 2 = RT-PCR of total RNA from freshly isolated uncultured PBMCs. Lanes 3, 7 to 9, are negative controls RT-PCRs using PGP negative C91/PL total RNA. Lanes 4 to 6 are RT-PCRs of total RNA from PBMCs cultured in the absence of PHA stimulation for 24, 48 and 72 hours respectively. Lanes 10 to 12 are RT-PCRs of total RNA from PBMCs cultured with 10 μg/ml PHA for 24, 48 and 72 hours respectively. The presence of mdr-1 mRNA expression is demonstrated by a band at 161 bp. Detectable mdr-1 mRNA expression was only observed for PBMCs cultured in the presence of PHA (lanes 10 to 12).
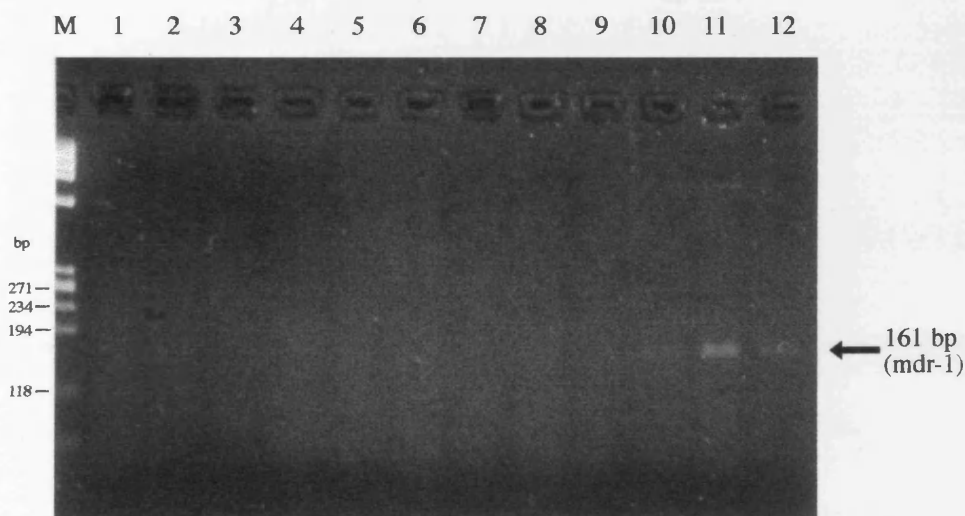
4.5.2 Short term co-culture of a HTLV-I cell line with fresh PBMCs

The mitogenic stimulation of MDR activity in PBMC by HTLV-I was then directly assessed by co-culture of HTLV-I infected cells with freshly isolated unstimulated PBMCs. HTLV-I induced stimulation of MDR activity was tested using R123 dye efflux assays and semi-quantitative RT-PCR for mdr-1 RNA every 24 hours over a short 72 hour period. Freshly isolated unstimulated PBMCs from a non-HTLV-I infected donor were incubated with C91/PL HTLV-I infected cells at 1.4x10^6 cells each per T25 tissue culture flask (Nunclon) in 5 mls growth medium. Cells were gently agitated to disperse cell aggregates then removed for R123 dye efflux and RT-PCR assays after 24, 48 and 72 hours. Due to the relative size differences of PBMCs and C91/PL cells it was possible to distinguish both cell populations by FACScan by plotting the side light scatter (SSC) against forward light scatter (FSC) of the cells. A representative SSC against FSC FACscan plot is shown in figure 4.17. At all time

points over the 72 hour co-culture PBMCs were found as a distinct cell population of smaller size (lower SSC and FSC) compared to C91/PL cells. Both cell populations were electronically gated in software and individually assessed for R123 dye efflux activity.

Figure 4.17. Side light scatter (SSC) versus forward light scatter (FSC) FACscan plot of PBMC and C91/PL co-cultured cells on day 0. PBMCs were much smaller in size than C91/PL cells and were seen as the cell population with low FSC and SSC.
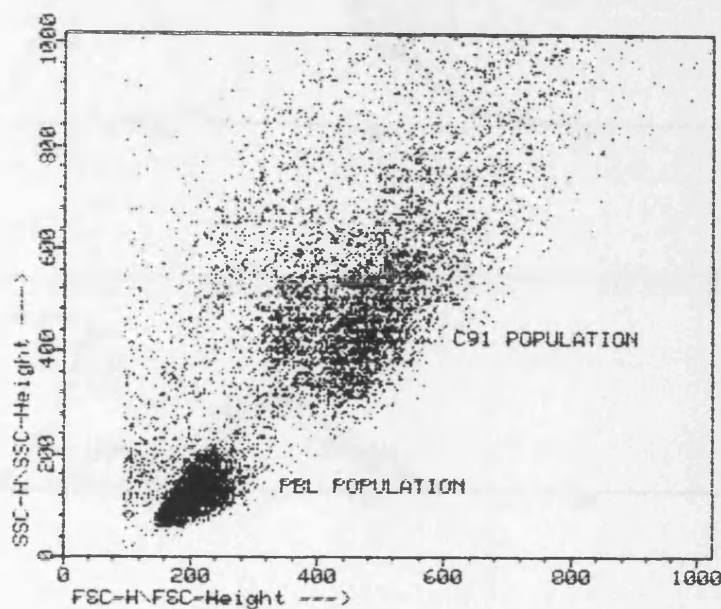
Figure 4.18 shows the R123 efflux assay FACScan profiles of the PBMC population in the C91/PL co-culture. Figure 4.18a shows the R123 dye efflux FACScan profiles of freshly isolated un-cultured PBMCs which show minimal efflux activity. After 24 hours co-cultivation (figure 4.18b) PBMCs show the characteristic pattern of high R123 dye efflux (82 % R123 loss) from a distinct sub-population of cells (20 %). After 48 hours (figure 4.18c) R123 dye efflux increases to 84 % R123 loss and the proportion of effluxing cells also rises to 29 %. After 72 hours (figure 4.18d) the number of PBMCs in the co-culture is significantly reduced in number with a diffuse pattern of R123 fluorescence and made assessment of R123 efflux in-accurate.

Figure 4.18. R123 dye efflux FACScan profiles of the PBMC cell population in C91/PL co-cultures. a) Freshly isolated uncultured PBMCs. b) PBMCs co-cultured after 24 hours. c) PBMCs co-cultured after 48 hours. d) PBMCs co-cultured after 72 hours. Negligible R123 dye efflux is observed from freshly isolated uncultured PBMCs. After co-culture with C91/PL cells R123 dye efflux is observed from a distinct sub-population of PBMCs after 24 and 48 hours with a relatively uniform R123 fluorescence profile. After 72 hours the number of PBMCs in culture was too low to be accurately assessed.
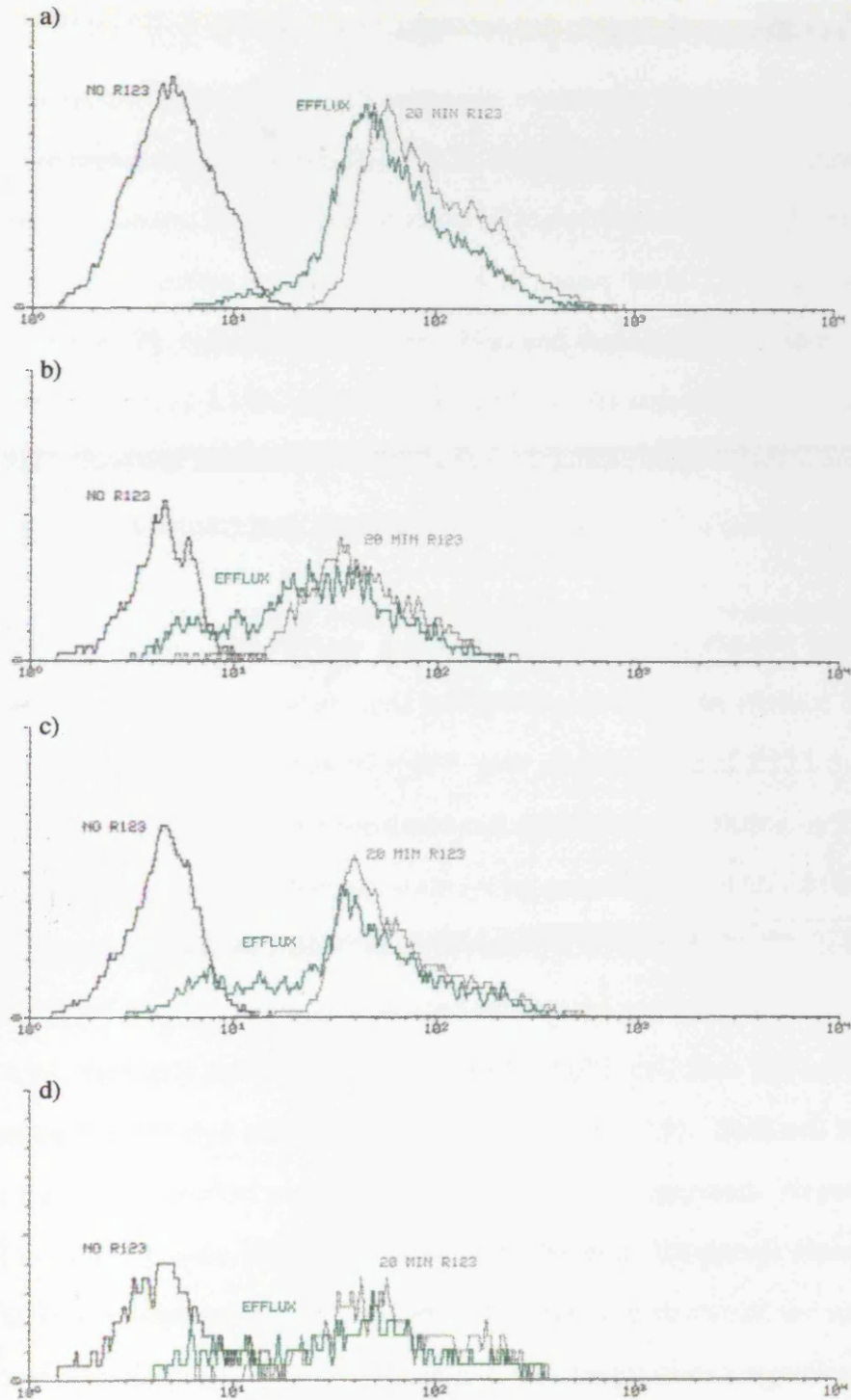
The results demonstrate the possible mitogenic stimulation of MDR efflux at an early stage in infection in a distinct sub-population of PBMCs (20 to 29 %) by co-culture with HTLV-I expressing C91/PL. Upregulation of R123 dye efflux activity was found to be immediate (24 hours) and a uniform high level of R123 dye efflux (>80%) was observed in the majority of these cells. This pattern of MDR R123 dye efflux stimulation paralleled that from PHA mitogenic stimulation (fig. 4.14) and is in contrast to that from unstimulated PBMCs (fig. 4.15) which show a slower time course of MDR stimulation (48 hours) and a smaller number of high efflux cells (<20%) with a diffuse range of R123 dye efflux activities. Figure 4.19 shows the R123 dye efflux FACScan profiles for C91/PL cells before (figure 4.19a) and during the co-culture after 24, 28 and 72 hours (figures 4.19b, c and d respectively). At any time period no R123 dye efflux was observed from these cells during co-culture with PBMCs and shows no alteration in MDR activity over the course of the assay.

The PBMC controls (culture with and without PHA) have already been described previously in section 4.5.1 and showed low MDR activity in the absence of mitogenic stimulation but direct activation of mdr-1 gene expression and R123 dye efflux by stimulation with PHA. HTLV-I mediated cell attachment and fusion by C91/PL cells was confirmed by syncytium formation assays by co-cultivation with C8166 cells at the cell densities described for PBMC co-cultivation. C8166 and C91/PL cells incubated alone over a 72 hour period in growth medium showed no significant R123 dye efflux (table 4.9). Similarly co-culture of C8166 and C91/PL cell lines did not result in the stimulation of R123 dye efflux in either cell type (table 4.9). Both cell lines were of similar size and individual populations could not be distinguished. Negative controls for MDR activity were PBMCs, C8166 and C91 cells incubated alone in growth medium and demonstrated no R123 dye efflux over the course of the assay. These results indicate that C8166 and C91/PL cells do not demonstrate a significant R123 dye efflux activity when cultured in growth medium over a 72 hour period and any increase in MDR activity in co-culture experiments cannot be attributed to these cells.

Figure 4.19. R123 dye efflux FACscan profiles of the C91/PL cell population co-cultured with PBMCs. a) Non-co-culture C91/PL cells. b) C91/PL cells co-cultured after 24 hours. c) C91/PL cells co-cultured after 48 hours. d) C91/PL cells co-cultured after 72 hours. No R123 dye efflux was observed for C91/PL cells co-cultured with PBMCs at any time point.
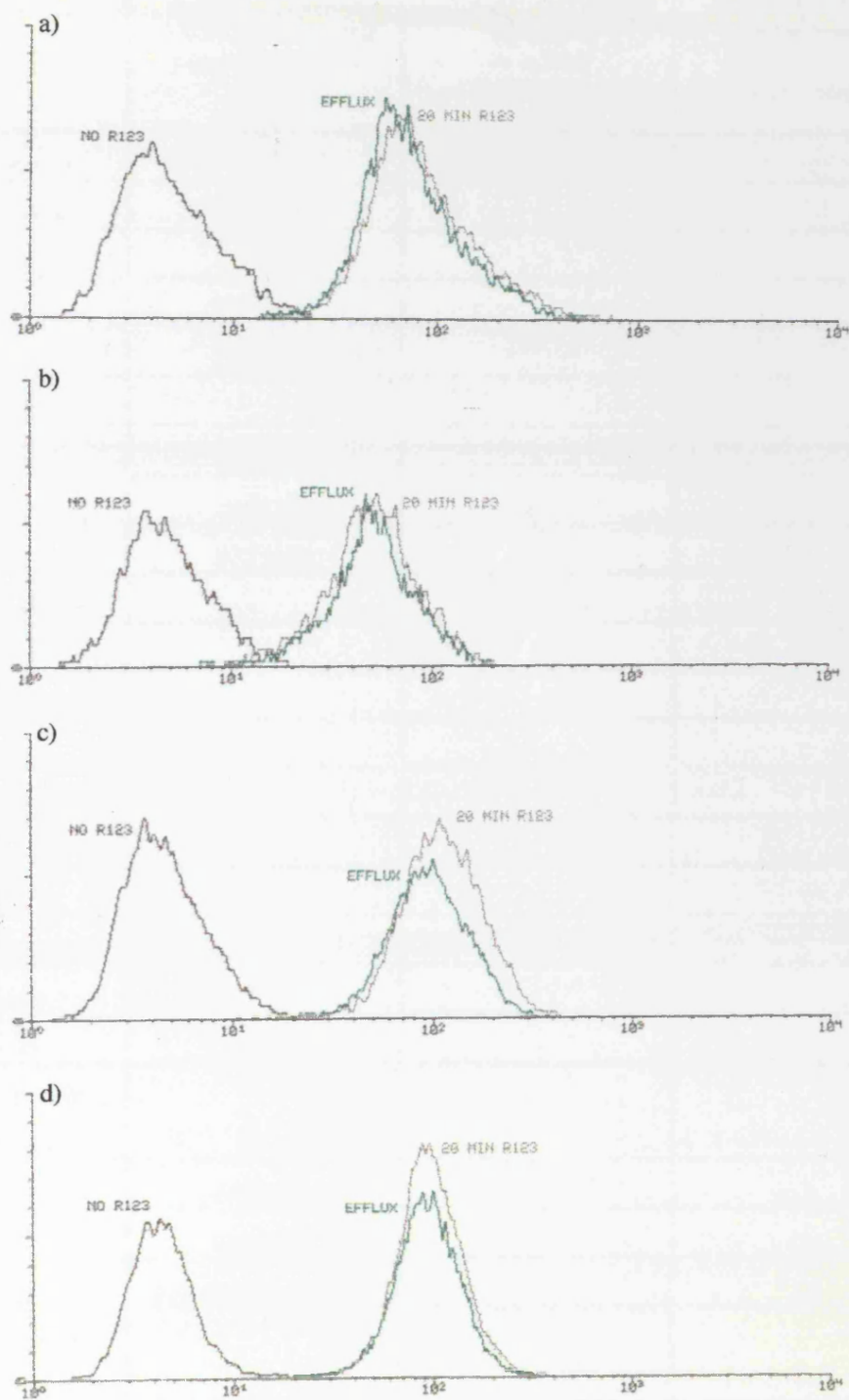
Table 4.9. Summary of PBMC and C91/PL co-culture experiments for MDR activation. R123 dye efflux and semi-quantitative RT-PCR analysis were performed on co-cultures after 24, 48 and 72 hours to assess MDR activation. The R123 dye efflux assay data only shows the % efflux from any high efflux cell populations found. The numbers in parenthesis are % of cells in the population. Mitogenic stimulation of PBMCs with PHA and co-culture with C91/PL cells showed significant R123 dye efflux activity and enhanced mdr-1 mRNA expression.

Culture	% R123 dye efflux (HIGH effluxing cell populations only)	Relative mdr-1 mRNA expression (+ = low) (++ = moderate)	Syncytia formation (+ = low) (++ = moderate) (+++ = high)
PBMC day 0	-	-	-
PBMC only			
+ 24 hours	47 (?15%)	-	-
+ 48 hours	80 (20%)	-	-
+ 72 hours	80 (15%)	-	-
PBMC + PHA			
+ 24 hours	84 (28%)	+	-
+ 48 hours	84 (33%)	++	-
+ 72 hours	93 (20%)	+	-
C91/PL cells			
Day 0	-	-	-
+ 24 hours	-	-	-
+ 48 hours	-	-	-
+ 72 hours	-	-	-
C8166 cells			
Day 0	-	-	-
+ 24 hours	-	-	-
+ 48 hours	-	-	-
+ 72 hours	-	-	-
PBMC & C91/PL co-culture			
+ 24 hours	82 (20%)	+	-
+ 48 hours	84 (29%)	++	+
+ 72 hours	cell number too low	-	++
C8166 & C91/PL co-culture			
+ 24 hours	-	-	+++
+ 48 hours	-	-	+++
+ 72 hours	-	-	+++

Semi-quantitative RT-PCR analysis for mdr-1 RNA was performed on total cellular RNA extracted as described in section 4.5.1 and chapter 2. Figure 4.20 shows a gel photograph of mdr-1 RT-PCR reactions from PBMC, C8166 and C91/PL cells cultured alone, PBMCs cultured with PHA and from C91/PL cells co-cultured with either PBMCs or C8166 cells. Lanes 1 to 3 are RT-PCR of C8166, C91/PL and fresh unstimulated PBMCs respectively before culture. Bands corresponding to mdr-1 RNA were not observed and indicated that mdr-1 RNA expression was not detectable in any of these cells at this time point. Lanes 4 to 6 are mdr-1 RT-PCRs of unstimulated PBMCs cultured in growth medium for 24, 28 and 72 hours respectively and shows no detectable mdr-1 RNA expression at any time point (see section 4.5.1). Lanes 7 to 9 are mdr-1 RT-PCRs of C91/PL cells cultured in growth medium for 24, 48 and 72 hours respectively and shows no detectable mdr-1 RNA expression at any time point. Lanes 10 to 12 are mdr-1 RT-PCRs of PBMCs cultured in growth medium supplemented with PHA over 24, 48 and 72 hours. Mdr-1 RNA can be detected after 24 hours with maximal expression at 48 hours post PHA stimulation and indicates mitogenic stimulation of mdr-1 gene expression by PHA (see section 4.5.1). Lanes 13 to 15 are mdr-1 RT-PCRs of C8166 cells cultured in growth medium for 24, 48 and 72 hours respectively. No detectable mdr-1 RNA can be observed. Lanes 16 to 18 are mdr-1 RT-PCRs of C8166 cells co-cultured with C91/PL cells for 24, 48 and 72 hours respectively. No detectable mdr-1 RNA expression can be observed in the mixed population of both cell types. Lanes 19 to 21 are mdr-1 RT-PCRs of unstimulated PBMCs co-cultured with C91/PL cells. Faint mdr-1 RNA expression can be observed after 24 hours co-culture. The strongest mdr-1 expression can be observed after 48 hours co-culture but after 48 hours mdr-1 RNA becomes undetectable. The mdr-1 RT-PCR results are in good agreement with the R123 dye efflux assays as detectable mdr-1 expression only coincided with observable R123 dye efflux.

Figure 4.20. EtBr stained agarose gel of semi-quantitative RT-PCRs for mdr-1 mRNA of
PBMC and C91/PL cell co-cultures. M = Φx174 DNA (HaeIII cut) marker. Lane 1 = Negative
control RT-PCR (H$_2$O). Lane 2 = RT-PCR of total RNA from freshly isolated uncultured
PBMCs. Lanes 4 to 6 are PBMCs cultured in the absence of PHA stimulation for 24, 28 and
72 hours respectively. Lanes 7 to 9 are C91/PL cells cultured in growth medium for 24, 48 and
72 hours respectively. Lanes 10 to 12 are PBMCs cultured with 10 µg/ml PHA for 24, 48 and
72 hours respectively. Lanes 13 to 15 are C8166 and C91/PL cells co-cultured for 24, 48 and
72 hours respectively. Lanes 16 to 18 are C8166 and C91/PL cells co-cultured for 24, 48 and
72 hours respectively. Lanes 19 to 21 are PBMC and C91/PL cells co-cultued for 24, 28 and
72 hours respectively. The presence of mdr-1 mRNA expression is demonstrated by a band at
161 bp. Detectable mdr-1 mRNA expression was observed for PBMCs cultured in the presence
of PHA for 14, 28 and 72 hours and PBMCs co-cultured with C91/PL cells for 24 or 48 hours.
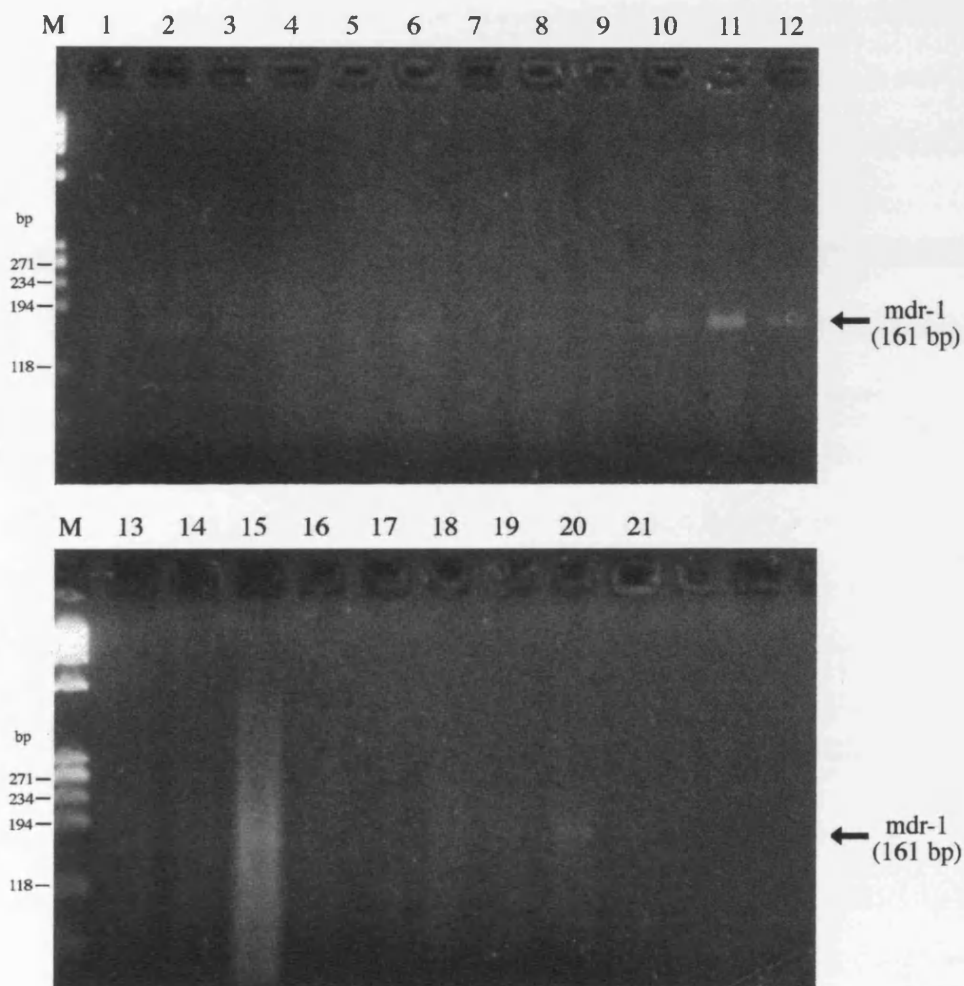
Table 4.9 summarises all the results from the co-culture experiments. Syncytia were
clearly observed for C8166 and C91/PL co-culture and demonstrates the attachment and
cell fusion ability of HTLV-I envelope glycoprotein on C91/PL cells. C8166 cells and
C91/PL cells were unaffected with respect to R123 dye efflux or mdr-1 gene expression
when cultured in growth medium showing undetectable MDR activities. PBMCs

cultured in the absence of mitogenic stimulation (PHA) showed low levels of R123 dye efflux but no detectable increase in mdr-1 RNA expression. PBMCs stimulated with the mitogen PHA showed significantly higher levels of R123 dye efflux from a sub-population of cells and increased mdr-1 RNA expression. Similarly PBMCs stimulated by co-culture with HTLV-I expression cells C91/PL showed a marked increase in R123 dye efflux and mdr-1 gene expression over a 48 hour period. However after 72 hours of co-culture the number of viable PBMCs was greatly reduced and R123 dye efflux assays and mdr-1 RT-PCRs could not accurately be assessed. The reduction of PBMCs is thought to be due to cell death as a result of prolonged cell culture and overgrowth of the C91/PL cells.

Mechanism of activation of mdr-1 gene expression

Both R123 dye efflux assays and semi-quantitative RT-PCR for mdr-1 gene expression are in good agreement with R123 dye efflux corresponding to mdr-1 gene expression. The mitogenic stimulation of PBMCs with PHA causes a significant increase in both mdr-1 gene expression and R123 dye efflux activity within a sub-population (20 to 33 %) of PBMCs. These observations are in good agreement with a study by Gupta *et al.*, 1992a in which PHA stimulation of PBMCs augmented the expression mdr-1 RNA and activity effluxing membrane PGP in 24 to 43 % of the total number of PBMCs. They found mdr-1 RNA expression was detected as early as 12 hours post PHA stimulation and the MDR positive cells were predominantly CD8$^+$. PHA augmentation of MDR phenotypes were also found to be modulated by the protein kinase C (PKC) signalling pathway (Gupta *et al.* 1992b) probably through PHA interaction with CD3/TCR and associated cell receptors. Similarly the observed mitogenic activity of HTLV infected cells was found to be mediated by cell surface receptor complexes CD2/LFA-3 (Kimata *et al.*, 1993) with co-stimulation through CD3/TCR (Kimata *et al.*, 1994a). These observations may suggest that mitogenic activation of T-cells via direct cell-cell contact with HTLV producer cells may lead to a concomitant increase in mdr-1 gene and PGP expression through these signalling pathways.

Interestingly in the absence of PHA mitogenic stimulation cultured PBMCs still demonstrated a small population of cells (<20 %) which efflux a significant percentage of R123 but was not associated with a detectable increase in mdr-1 gene expression. The upregulation of efflux activity in these cells may have been due to slight antigenic activation with components of the culture medium such as FCS or the plastic of the tissue culture flasks. Such activation may have led to increased mdr-1 gene expression by the pathways described earlier which shows detectable PGP mediated R123 dye efflux but expresses mdr-1 mRNA at too low a level to be detected by the RT-PCR reactions. Alternatively it may be speculated that membrane bound PGP activity may be modulated by these antigenic activations or via the intracellular signalling pathways associated with IL-2R stimulation as the culture medium also contained the T-cell growth factor IL-2. Such pathways may not necessarily lead to upregulation of mdr-1 gene expression but act by modifying existing membrane bound PGP into active forms which could also explain the lack of detectable mdr-1 RNA in these cells. Indeed it has long been suggested that PGP efflux activity may be modulated by direct phosphorylation of serine residues in the linker region of PGP although this theory still remains controversial (see chapter 1, section 1.6.3). In addition the involvement of IL-2/IL-2R autocrine stimulation in MDR is purely speculation. However such stimulation mechanisms could be extended to HTLV-I infection whereby enhanced IL-2/IL-2R expression is often observed (see chapter 1). A third equally speculative alternative reason for R123 dye efflux from cultured unstimulated PBMCs in the absence of mdr-1 gene expression could be the upregulation of efflux mechanisms apart from PGP such as the multidrug resistance related protein or MRP (see chapter 1, section 1.6.4). However it can be shown that stimulation of PBMCs with the mitogen PHA leads to a greater increase in MDR activity, both in R123 dye efflux and mdr-1 gene expression in a sub-population of cells over unstimulated PBMC controls.

Stimulation by HTLV-I cells or PHA both lead to the generation of a distinct sub-population of PBMCs which display uniform high R123 dye efflux activity in as little as 24 hours. Increased mdr-1 gene expression is observed for both HTLV-I cell and PHA stimulated PBMCs with maximal expression occurring at 48 hours. This is in contrast to unstimulated PBMCs which display highly variable R123 dye efflux from only a low proportion of cells and shows no detectable increases in mdr-1 gene expression. However these experiments could not determine the specificity of HTLV-I stimulation of MDR activity in PBMCs. It was undetermined whether MDR stimulation resulted from the activities of a specific HTLV-I protein on PBMCs or from independent cell surface expressed antigens on C91/PL cells. It may be also be possible that normal cell surface antigens not restricted to HTLV infected cells may be eliciting the activation of MDR observed. In hindsight a parallel PBMC co-culture with a non-HTLV-I infected cell line may have helped to resolve this issue. However the unique mitogenic activity of HTLV infected cells is well documented and although it may not be mediated directly by a HTLV protein it is thought to occur through co-stimulation through the CD2/LFA3 and CD3/TCR receptors (Gazzolo *et al.*, 1987; Wucherpfennig *et al.*, 1992; Kimata *et al.*, 1993 and 1994a).

4.5.3 Trans-activation of the mdr-1 gene by the HTLV protein tax

The transcriptional activation from the mdr-1 gene promoter by the HTLV-I trans-activating protein tax was assessed by co-electroporation of the p5'MDR-CAT(+) reporter gene construct with the tax protein expression plasmid pBC-tax/rex. p5'MDR-CAT(+) is a reporter gene construct containing a 1 kb 5' upstream fragment of the mdr-1 gene promoter from bases -426 to +536 relative to the transcriptional start point (Ueda *et al.*, 1987b) linked upstream to a CAT reporter gene in the correct orientation to direct transcription. pBC-tax/rex is a tax/rex cDNA expression construct known to express a functional tax protein and is described in chapter 3, section 3.5. Trans-activation of the mdr-1 gene promoter by tax was tested by co-electroporation of both plasmids (12.5 μg each) into cells and assaying cell extracts for CAT activity as described in chapter 2,

section 2.5.1d. The experiment was performed three times with identical results and a representative autoradiogram of the CAT assays is shown in figure 4.21.

Figure 4.21. CAT activity assays of total protein extracts from COS cells electroporated with mdr-1 gene promoter-CAT-reporter construct (p5'MDR-CAT) and a tax/rex expression construct (pBC-tax/rex; see chapter 3, section 3.5). Lane 1 = Negative control electroporation with no DNA. Lane 2 = Negative control electroporation with pLTR-I-CAT. Lane 3 = Cells electroporated with p5'MDR-CAT(+) only. Lane 4 = Cells electroporated with p5'MDR-CAT(-) only. Lane 5 = Cells electroporated with pBC-tax/rex only. Lane 6 = Cells co-electroporated with p5'MDR-CAT(+) and pBC-tax/rex. Lane 7 = Cells co-electroporated with p5'MDR-CAT(-) and pBC-tax/rex. Lane 8 = Positive control co-electroporation of pLTR-I-CAT and pBC-tax/rex. Significant CAT activity is shown by the presence of acetylated forms of chloramphenicol. All negative controls (lanes 1 to 5, 7) showed minimal CAT activity. The positive control (lane 8) showed strong CAT activity. Trans-activation of the mdr-1 gene promoter can be demonstrated by the presence of significant CAT activity in lane 6. The percentage chloramphenicol conversion to acetylated forms is also shown.
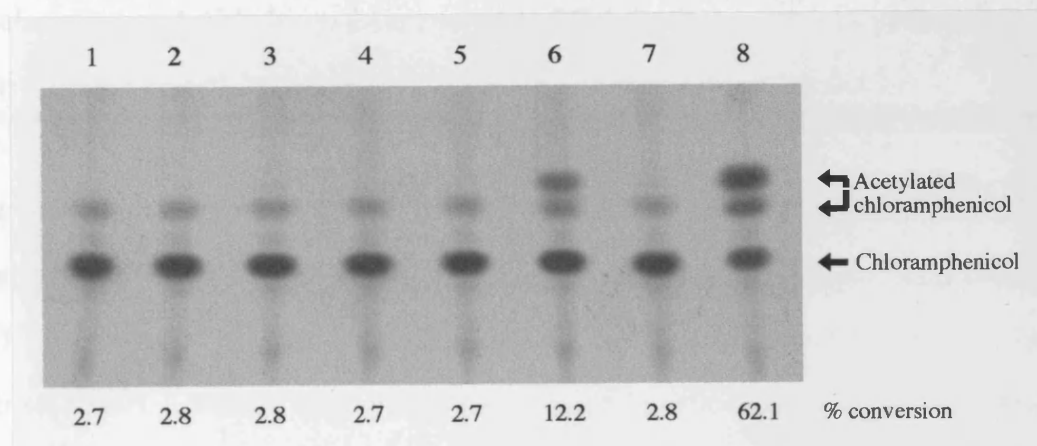
Standard controls for CAT trans-activation assays were electroporation of cells with single plasmids (12.5 µg plasmid + 12.5 µg "carrier" pUC18 DNA) only and mock transfected cells without DNA. Positive controls for tax trans-activation was co-electroporation of cells with pBC-tax/rex and pLTR-CAT, which is the HTLV-I LTR promoter linked upstream of the CAT reporter gene and demonstrates strong trans-activation by tax (see chapter 3, section 3.5). The specificity of trans-activation of the mdr-1 promoter by tax was gauged by co-electroporation of pBC-tax/rex with p5'MDR-CAT(-) in which the 5' mdr-1 gene promoter linked upstream of the CAT reporter gene in a reverse orientation and should not be able to direct transcription. Lanes 1 to 5 were negative controls with single plasmids only and all showed minimal CAT activity at 2.7 to 2.8 % conversion to acetylated forms of chloramphenicol. Lane 6 was CAT assays

of cells co-transfected with p5'MDR-CAT(+) and pBC-tax/rex and clearly shows the presence of more acetylated forms of chloramphenicol with conversion at 12.2 % after 3 hours incubation. This demonstrates a moderate 4 fold transcriptional activation of the mdr-1 gene promoter by HTLV tax over the negative controls. The specificity of trans-activation can be demonstrated in lane 7 were minimal CAT activity (2.8 % conversion) is observed for co-electroporation of p5'MDR-CAT(-) with pBC-tax/rex. Here tax is unable to trans-activate transcription from the mdr-1 gene promoter sequence when placed in an anti-sense or reverse orientation showing the specific and orientation dependant nature of the promoter. Lane 8 shows strong CAT activity in extracts of cells co-electroporated with the positive control pLTR-I-CAT plasmid with pBC-tax/rex and demonstrated 62.1 % chloramphenicol conversion after 3 hours incubation.

The involvement of HTLV-I in the activation of transcription of the mdr-1 gene promoter was also checked by single electroporation of the p5'MDR-CAT(+) into the HTLV-I expressing cell lines C91/PL and MT4. Both C91/PL and MT4 cells actively express HTLV-I proteins including tax and should be able to activate the transcription from appropriate promoters. Figure 4.22 shows a representative autoradiogram of CAT assays of extracts from C91/PL and MT4 cells. Negative controls were mock electroporated cells without DNA and electroporation with p5'MDR-CAT(-) reverse orientation mdr-1 promoter plasmid. Positive controls were cells electroporated with pLTR-I-CAT and the CAT expression plasmid pCLC. Lanes 1 to 5 are extracts from p5'MDR-CAT(+) electroporated C91/PL cells and lanes 6 to 10 are extracts from MT4 cells. Lanes 1 and 6 are the negative controls of extracts from C91/PL and MT4 cells electroporated in the absence of DNA and shows minimal CAT activity with only 2.3 and 2.5 % conversion respectively. lanes 2 and 7 are extracts from C91/PL and MT4 cells electroporated with p5'MDR-CAT(+) plasmid and shows a high level of CAT activity signified by the presence of 2- and 3- acetylated and 2,3 di-acetylated forms of chloramphenicol. The chloramphenicol conversion was 93.2 % and 91 % for C91/PL and MT4 cells respectively after 3 hours incubation. This shows that HTLV-I infected

242

cell lines were able to significantly activate the transcription from the mdr-1 gene promoter. Lanes 3 and 8 are extracts from C91/PL and MT4 cells electroporated with p5'MDR-CAT(-) plasmid and shows a minimal level of CAT activity with only 2.8 and 2.1 % conversion respectively. This demonstrates the specificity of HTLV tax trans-activation of the mdr-1 gene promoter as when the mdr-1 gene promoter is placed in an anti-sense or reverse orientation upstream of the CAT reporter gene in p5'MDR-CAT(-) it is unable to direct the expression of CAT. Lanes 4, 5, 9 and 10 were positive controls and good CAT expression was observed from each extract with 49.5 %, 94.4 %, 85.5 % and 93.1 % conversion respectively.

Figure 4.22. CAT activity assays of total protein extracts from C91/PL and MT4 cells electroporated with mdr-1 gene promoter-CAT-reporter construct (p5'MDR-CAT). Lanes 1 and 6 = Negative control electroporation with no DNA. Lanes 2 and 7 = Cells electroporated with p5'MDR-CAT(+). Lanes 3 and 8 = p5'MDR-CAT(-). Lanes 4 and 9 = Positive control electroporation with pLTR-I-CAT. Lanes 5 and 10 = Positive control electroporation with pCLC CAT expression plasmids. Significant CAT activity is shown by the presence of acetylated forms of chloramphenicol. Lanes 4, 5, 9 and 10 were positive controls and demonstrate significant CAT activity. Lanes 2 and 7 shown significant CAT activity and demonstrates transcriptional upregulation of the mdr-1 gene promoter in both C91/PL and MT4 cells. The percentage chloramphenicol conversion to acetylated forms is also shown.
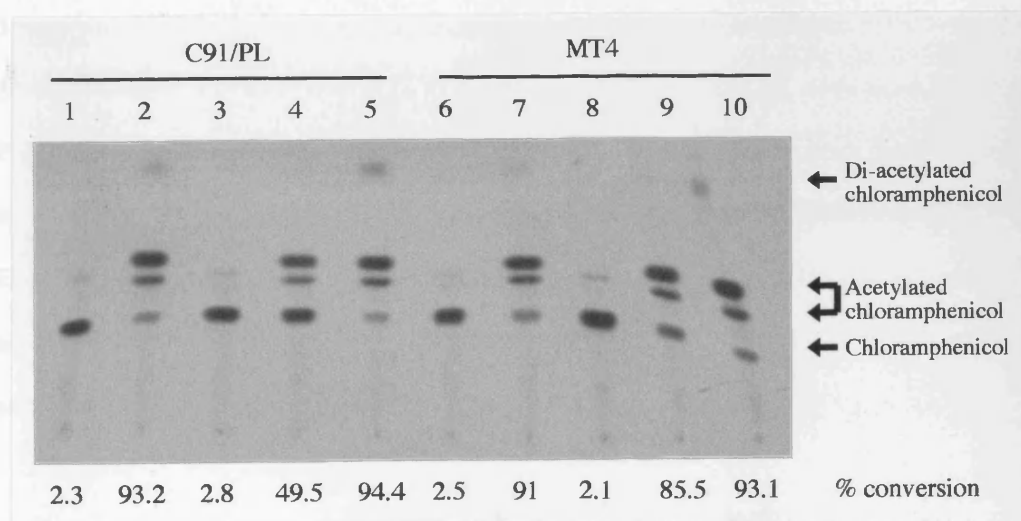
These experiments showed that the HTLV-I expressing cell lines C91/PL and MT4 were able to direct transcription of the CAT reporter gene via the mdr-1 gene promoter. Interestingly C91/PL cells were previously found not to display an MDR phenotype

(see section 4.3), suggesting that either the mdr-1 gene is defective or that a negative regulatory element is suppressing mdr-1 gene expression in these cells. It should be noted that these CAT assays were not done in parallel to the pBC-tax/rex and p5'MDR-CAT co-electroporation experiments described earlier. In addition electroporations were performed using double the amount of plasmid DNA (25 µg). Hence the relative transcriptional activation between both sets of experiments could not be accurately determined.

It is likely that the transcriptional upregulation of expression from the mdr-1 gene promoter occurs through the well documented pleotropic cellular trans-activation activities of the HTLV-I protein tax as described in chapter 1. However the involvement of other HTLV-I proteins in mediating the expression from the mdr-1 gene promoter cannot be excluded. The expression plasmid pBC-tax/rex was constructed by RT-PCR cloning of the doubly spliced tax/rex RNA (see chapter 3, section 3.5). In addition to encoding the p40 tax protein this transcript also encodes the p27 rex protein and another HTLV pX protein of ill-defined function p21. Other HTLV-I proteins p12^I, p13^{II} and p30^{II} derived from alternative splicing of the pX region of HTLV were not encoded by this tax/rex cDNA clone. The enhancement of gene transcription has been documented for p27 rex whereby IL-2Rα RNA transcripts can be stabilised (Kanamori et al., 1990) and may act indirectly in concert with tax to trans-activate IL-2 gene expression (McGuire et al., 1993). However it is not known if pBC-tax/rex expresses all (or any) of these HTLV-I non-structural proteins other than tax.

Overall these experiments demonstrated the ability of HTLV-I to enhance transcription from the basal 1 kb 5' mdr-1 gene promoter *in vitro*. Moreover it can be demonstrated that HTLV proteins expressed solely from the tax/rex cDNA expression plasmid pBC-tax/rex are sufficient to enhance expression from the mdr-1 gene promoter 4 to 5 fold. This indicates that the HTLV-I non-structural proteins can upregulate mdr-1 expression at the level of gene transcription *in vitro* and suggests the possibility of a mechanism of

MDR activation within HTLV-I infected and expressing cells. However, it is unclear from these experiments whether tax/rex can mediate such effects *in vivo*.

4.6 Discussion

Analysis of mdr-1 gene expression in cultured T-cell lines

R123 dye efflux and quantitative mdr-1 RT-PCR assays demonstrated the absence of significant MDR activity in 8 out of the 9 T-cell lines tested (section 4.3; figure 4.8). Only one T-cell line, the HTLV-I infected and expressing MT4 cell line, showed significant MDR activity and by both R123 dye efflux and mdr-1 RT-PCR analysis. The results indicated most transformed cells of T-cell lineage do not express significant levels of mdr-1 RNA or PGP to display a MDR phenotype. This is consistent with the findings of Lee *et al.*, 1994 who examined the R123 dye efflux patterns of several leukaemia/lymphoma cell lines and also found no significant R123 efflux in 5 of 6 cell lines tested including MOLT4 cells. One lymphoid cell line CCRF-CEM was found to be marginally R123 efflux positive according to their scoring system but many other groups consider this cell line to be MDR negative and use them as MDR negative control cells (e.g. Damiani *et al.*, 1993). In contrast MT4 cells were found to express detectable amounts of mdr-1 RNA (10.4 molecules mdr-1 per pg total RNA) and efflux significant R123 dye (55.2 % R123 loss) to be considered MDR positive. The involvement of PGP as the major determinant in mediating drug efflux in MT4 cells was confirmed by the use of reserpine and verapamil PGP efflux antagonists.

Both classical PGP-mediated MDR and atypical MRP-mediated MDR has been shown to be involved in cellular drug efflux (see chapter 1, section 1.6.4). R123 is a well characterised and efficient substrate for PGP (Tapiero *et al.*, 1984; Lampidis *et al.*, 1985; Neyfakh, 1988) but also found to be a substrate for MRP (Zaman *et al.*, 1994). However MRP effluxes R123 less efficiently than PGP and comparable R123 dye efflux was only found after extended periods (>60 minutes) of efflux (Twentyman *et al.*, 1994). Another group has suggested that R123 is not a substrate for MRP and

showed negligible R123 efflux from MRP cell lines but the efflux periods were not extended past 60 minutes (Feller *et al.*, 1995). As all R123 dye efflux assays were conducted with a 90 minute period of efflux it suggests that the assay may also be sensitive to MRP mediated dye efflux in addition to PGP. Hence any R123 dye efflux observed after 90 minutes may be due to PGP, MRP or a combination of both. The MDR chemosensitisers reserpine and verapamil are substrates for PGP and act as efflux inhibitors by competing with R123 or other drugs for efflux. They work as efficient efflux inhibitors as their rates of passive diffusion across membranes are much greater than for R123 with verapamil reaching equilibrium in minutes and R123 after 1 hour (Eytan *et al.*, 1996) leading to saturation of PGP. The rate of efflux of R123 becomes reduced and the net result is an increase in R123 or drug accumulation within cells. However verapamil has been shown to be a poor modulator of MRP mediated atypical MDR activity (Cole *et al.*, 1989; Barrand *et al.* 1993) compared to PGP and probably reflects their different substrate specificities (McGrath *et al.*, 1989). Hence the ability of verapamil to efficiently block (79.2 % inhibition) R123 dye efflux from MT4 cells (section 4.3.1) demonstrates the presence of active classical PGP mediated MDR efflux in favour of atypical MRP mediated efflux or non-specific passive R123 loss across the cell membrane.

The MT4 cell line was established from lymphocytes from a patient with ATL and found to express HTLV-I proteins (Myoshi *et al.*, 1982). This observation suggests a possible association between HTLV-I transformation/expression and development of MDR as no other transformed cell line tested showed a detectable MDR phenotype. Furthermore CAT reporter gene assays (section 4.5.3; figure 4.22) showed that MT4 cells were capable of directing expression from a 1 kb upstream mdr-1 gene promoter (Ueda *et al.*, 1987b) and suggests an active mechanism of transcriptional upregulation in MT4 cells, probably through the trans-activation activities of tax (see chapter 1). However the HTLV-I transformed cell line C8166 and the HTLV-I expressing cell lines C91/PL and MT2 did not show any significant R123 dye efflux or mdr-1 RNA

expression. In addition all these cell lines constitutively express HTLV-I tax, which has been shown to trans-activate the mdr-1 gene promoter *in vitro* (see section 4.5.3). This suggest two possible explanations; either that MT4 cells demonstrates enhanced mdr-1 expression independently of HTLV-I or that C8166, C91/PL and MT2 cells are defective for mdr-1 expression. It may be possible that MT4 cells uniquely overexpress mdr-1 mRNA as a result of the transformation process not specifically due to HTLV-I infection. Alternatively it may be possible that C8166, C91/PL and MT2 cells have developed a defective mdr-1 gene/promoter and have lost PGP mediated MDR activity as a consequence of cellular transformation or continuous cell culture. The latter explanation can be supported by the fact that CAT reporter gene assays (section 4.5.3) showed that C91/PL cell were still able to direct transcription from the 1 kb mdr-1 gene promoter. This suggests that HTLV-I expressing C91/PL cells are still capable of upregulation of an exogenous mdr-1 gene promoter by tax but the cells themselves are defective in its expression. This may also be true of C8166 and MT2 cells but without directly testing them in conjunction with HTLV-I negative control cells by mdr-1 promoter CAT reporter gene assays it remains undetermined. It should be noted that the p5'MDR-CAT(+) reporter gene construct is not active in HTLV-I negative cells (section 4.5.3; figure 4.21 lane 3) when electroporated alone and suggests trans-activation in MT4 and C91/PL cells is due to HTLV-I protein expression, probably tax. The CAT reporter gene assays also cannot exclude the possibility of negative acting regulatory factors influencing mdr-1 gene expression in these cells as the mdr-1 gene promoter used only contains sequences 1 kb immediately upstream of the start codon.

The discrepancies in mdr-1 gene expression between the HTLV-I infected cell lines could be resolved by a number of methods. An overactive mdr-1 gene in MT4 cells or a defective one in C8166, C91/PL and MT2 cells could be determined by cloning and/or sequencing the mdr-1 gene and its promoter from each cell line. Any errors and anomalies in the mdr-1 genes would then be known. The ability of tax to direct trans-activation of the cellular mdr-1 gene could be tested by expressing tax in an MDR

negative (but with an intact, viable mdr-1 gene), HTLV negative cell line (e.g. CCRF-CEM) and looking for mdr-1 mRNA expression by RT-PCR or PGP by FACs analysis. By comparing the relative level of expression to CAT reporter gene assays using the 1kb 5' mdr-1 promoter sequence it would be possible to determine if negative acting regulatory elements were involved. However, due to lack of time and resources these experiments were not conducted and the differences in mdr-1 gene expression between the HTLV-I infected cell lines remains unclear.

Overall the MDR assays for T-cell lines were inconclusive, not establishing a consistent relationship between HTLV-I transformation or expression and stimulation of classical MDR. The only significantly MDR positive cell line was the HTLV-I transformed and expressing cell line MT4. However the use of *in vitro* transformed stable cell lines may not accurately reflect the situation *in vivo* and it was decided to extend the studies to primary cells from HTLV-I infected subjects.

Analysis of mdr-1 gene expression in fresh PBMCs

R123 dye efflux assays (section 4.4.1) showed the presence of an active MDR efflux phenotype within a sub-population of cells freshly isolated from the periphery of 9 out of 10 HTLV-I infected individuals. This MDR efflux positive cell population comprised between 28.8 to 55.3 % of the total number of PBMCs isolated and was not found in the periphery of any of the six non-HTLV-I infected control subjects. Furthermore the specific involvement of classical PGP mediated MDR drug efflux from these cells was demonstrated by the use of the PGP specific MDR chemosensitisers reserpine and verapamil. The presence of reserpine or verapamil effectively abolished R123 dye efflux from the high R123 efflux populations in HTLV-I infected PBMCs (section 4.4.1; figure 4.10c) and implicates PGP as the major contributor to MDR efflux activity in these cells. The presence of PGP on the surface of cells in the PBMCs of HTLV-I infected subjects was confirmed by indirect immunofluorescence using the anti-PGP antibody MRK-16. MRK-16 labelling of PBMCs from a HTLV infected

ATL subject showed the presence of a sub-population of cells in which PGP was expressed on the cell surface (section 4.4.3; figure 4.13b). These experiments indicated that a significant number of circulating active MDR PGP positive cells are found in the periphery of the majority of HTLV-I infected subjects.

Further characterisation of the composition of cells within the high MDR efflux cell populations in HTLV-I infected subjects was assessed by dual colour FACScan analysis using R123 dye efflux assays and PE-conjugated monoclonal antibodies to specific cell type surface markers (section 4.4.5). These experiments demonstrated that the majority of labelled cells in the high efflux populations from HTLV-I infected individuals were $CD3^+$ T-cells. Less than 1 % were found to be CD22+ B-cells and no CD14+ monocyte/macrophage were found in this cell population. The low effluxing cell population consisted of a mixture of the remaining $CD3^+$ T-cells, $CD14^+$ monocyte/macrophage and CD22+ B-cells. The cellular tropism of HTLV-I *in vivo* was found to be toward T-cells (Richardson *et al.*, 1990; Koyanagi *et al.*, 1993) and identification of $CD3^+$ T-cells as the major cell type in the high R123 dye effluxing cell population suggests the possibility that these cells may be HTLV-I infected. However, without directly co-staining for HTLV infection this is still undetermined. Gessain *et al.*, 1990 and Mita *et al.*, 1993 estimated that the proportion of cells in PBMCs which harbour HTLV-I proviruses was up to 30 % and this is in good agreement with the proportion of $CD3^+$ T-cells (28 ± 1 %) found in the high R123 dye effluxing MDR cell populations of HTLV-I infected individuals. Also the high PE fluorescing or $CD3^+$ cells in the high R123 dye effluxing population (R2) was found to fluoresce at slightly lower intensities (figure 4.12g, mean fluorescence = 31) than that found for total $CD3^+$ cells (figure 4.12d, mean fluorescence = 44). This result can be explained by the observation that HTLV-I infected cells often show decreased CD3 cell surface expression (Matsuoka *et al.*, 1986; Tsuda *et al.*, 1984; Shirono *et al.*, 1989). Downregulation of CD3/TCR expression on the surface of HTLV-I infected cells would cause these cells to have less CD3 molecules and would label and fluoresce slightly less

249

strongly than normal CD3$^+$ T-cells. Quantitative mdr-1 RT-PCR analysis (section 4.4.4) was entirely consistent with the view of enhanced MDR activity in HTLV-I infected subjects as increased steady state levels of mdr-1 RNA coincided exactly with the presence of MDR efflux activity. Non-HTLV-I infected control subjects (all efflux negative) demonstrated a consistently low basal level of mdr-1 gene expression at 7.36 $\pm$ 2.84 molecules mdr-1 RNA per pg total RNA. All 8 HTLV-I infected and MDR efflux positive PBMCs tested for mdr-1 RNA showed enhanced mdr-1 gene expression with a four fold increase in the steady state level of mdr-1 mRNA at 29 $\pm$ 10.68 molecules mdr-1 RNA per pg total RNA.

These observations indicate that within the circulating PBMC of HTLV-I infected individuals a significant MDR cell population is present in which the majority of identified cells were T-cells. Such MDR cell phenotypes are not present in PBMCs from non-HTLV-I infected individuals and suggests that HTLV-I infection and/or transformation may induce classical MDR. The presence of classical MDR cell phenotypes was also found not to be related to disease status as similar levels of R123 dye efflux MDR activity was found in PBMCs from both asymptomatic and diseased individuals (section 4.4.1). However an increase in the overall number of high R123 effluxing MDR positive cells was observed in the PBMCs from HTLV-I infected individuals with disease (Table 4.6). Quantitative RT-PCR analysis of PBMCs from HTLV-I infected individuals with disease, TSP/HAM or ATL, demonstrated a significant 30 % greater enhancement of mdr-1 gene expression when compared to PBMCs from asymptomatic individuals (section 4.4.4). However the 30 %+ increases in mdr-1 gene expression in PBMCs from TSP/HAM and ATL subjects over asymptomatic individuals found by quantitative RT-PCR were not accurately reflected by R123 dye efflux (section 4.4.1). For both asymptomatic and diseased individuals no significant difference in R123 dye efflux was observed from the MDR positive cell populations during the course of the assay. Figure 4.23 is a regression plot of the mean mdr-1 mRNA expression against the mean percent R123 dye efflux from the PBMCs of

HTLV-I infected and MDR positive individuals ([#]2 to [#]9). This plot demonstrates only a moderate (r = 0.495) positive correlation between mdr-1 gene expression and R123 dye efflux.

The lower than expected level of R123 dye efflux was however offset by the relative sizes of the high R123 effluxing MDR cell population in each individual. Generally, it was noted that the TSP/HAM ([#]7, [#]8) and ATL ([#]9) subjects had a larger number of cells in the high R123 dye effluxing MDR positive cell population but no increase in actual R123 efflux by these cells. Figure 4.24 is a regression plot of the percentage of cells in the high efflux population versus mdr-1 gene expression. The plot demonstrates a much higher degree of positive correlation (r = 0.926) between mdr-1 gene expression and the number of MDR efflux positive cells. This can be further demonstrated in figure 4.25 which is a histogram showing the number mdr-1 mRNA molecules/pg per percentage R123 dye effluxing cells in PBMCs from HTLV-I infected and MDR positive individuals. The mean number of mdr-1 molecules/pg per percentage efflux cells from asymptomatic individuals was 0.5678 $\pm$ 0.0598 and from diseased individuals was slightly higher at 0.5865 $\pm$ 0.0375. Calculation of the difference between two means gives a value of z = 0.497 and suggests no significance between these means at the standard 5 % level of significance (| z | < 1.92). This suggests that the increased mdr-1 mRNA levels found are due mainly to the greater proportion of MDR positive mdr-1 expressing cells in the PBMCs from TSP/HAM or ATL subjects. However, It should be noted that these statistical analyses are based on comparisons of data obtained from only six asymptomatic subjects and three subjects with disease. Similarly few replicate experiments were possible due to the limited number and availability of HTLV-I infected subjects. Hence, the interpretation of the statistical analysis of the data must be taken with care as a minor change in any of the data points may alter the statistical significance of the analyses. Without further experimental replicates the reliability and accuracy of these analyses must be questioned.

Figure 4.23. Correlation between mdr-1 gene expression and R123 dye efflux activity of PBMCs from HTLV-I infected and MDR positive individuals. The regression co-efficient (r = 0.495) shows only a moderate positive correlation.

Mean % R123 dye efflux from the high efflux cell population
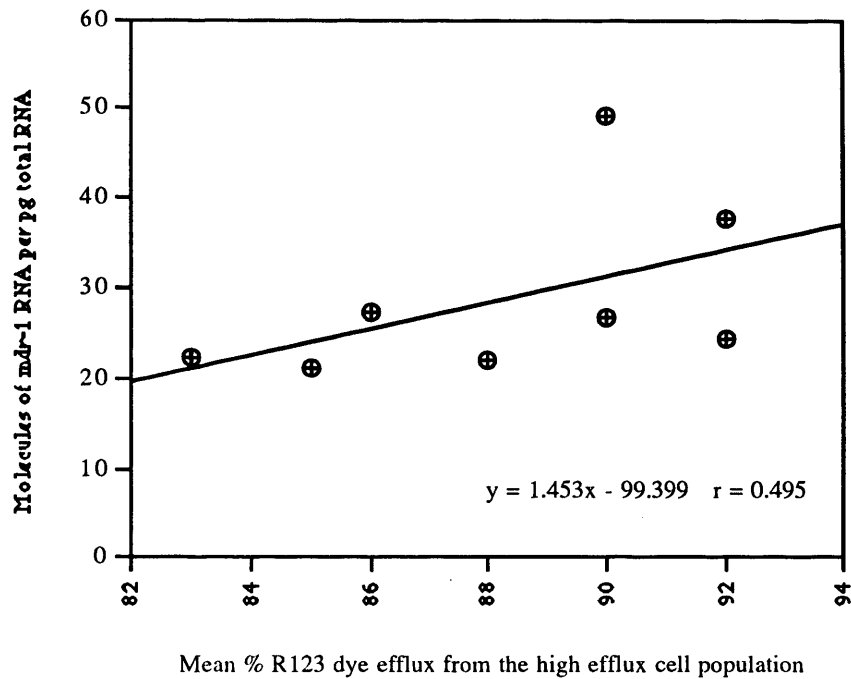
Figure 4.24. Correlation between mdr-1 gene expression and the number of cells in the high efflux cell population. The regression co-efficient (r = 0.926) shows a high degree of positive correlation.

% of cells in the high R123 dye efflux cell population
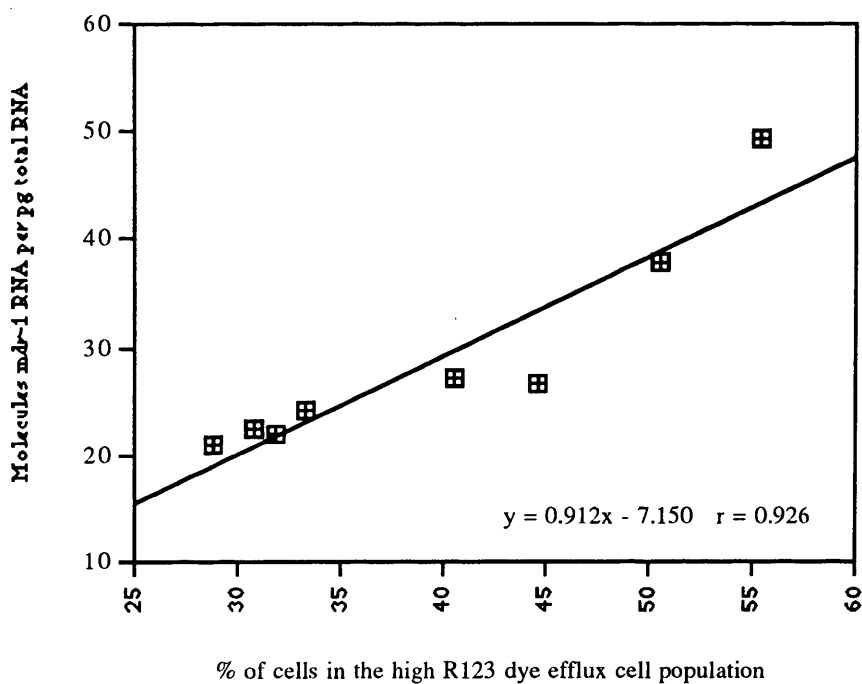
Figure 4.25. The number of molecules mdr-1 RNA per % cells in the high R123 dye efflux cell population of HTLV-I infected and MDR positive individuals. No significant differences can be observed in mdr-1 gene expression in the high effluxing cell populations between asymptomatics (#2 to #6) and TSP/HAM or ATL subjects (#7 to #9).
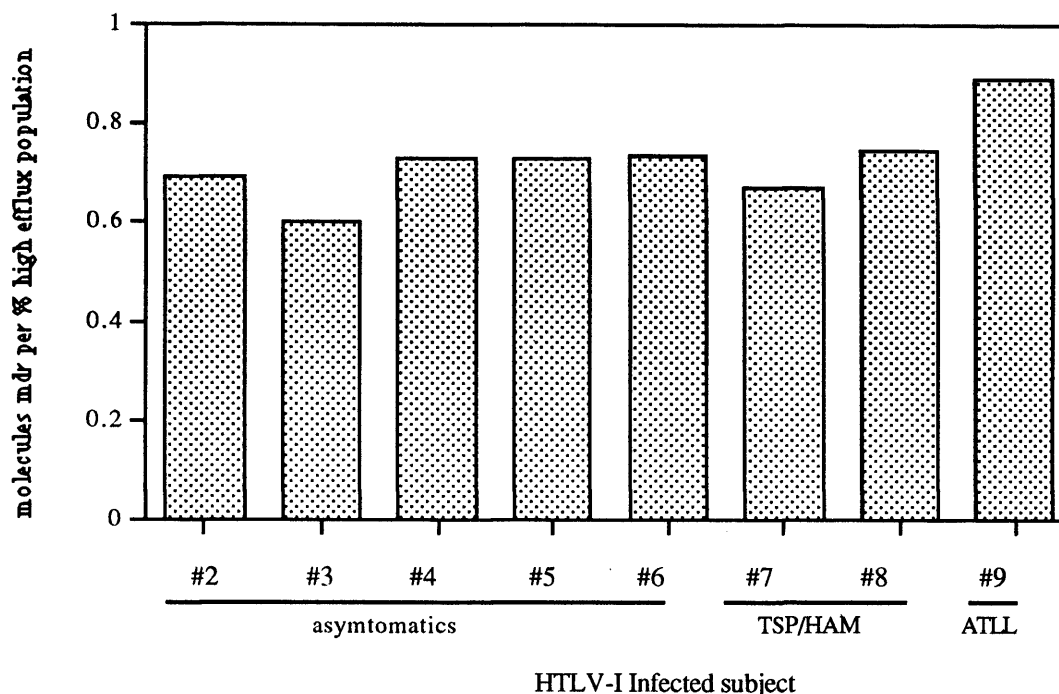
The observation that a greater proportion of MDR positive cells are present in the PBMCs from TSP/HAM or ATL subjects may correspond to the increased number of HTLV-I infected and/or activated cells in the peripheral blood of patients with disease. It has been demonstrated that TSP/HAM patients show a greater percentage of HTLV-I infected and activated lymphocytes (Nishimura *et al.*, 1990) with greater proviral loads (Yoshida *et al.*, 1989; Gessain *et al.*, 1990; Kira *et al.*, 1991; Kubota *et al.*, 1993) when compared to both asymptomatic carriers and non-HTLV infected control subjects. The data suggests that the proportion of PBMCs from both asymptomatic and diseased individuals overexpress the mdr-1 gene at a similar constitutive level and that the increase in mdr-1 mRNA found in diseased individuals is due to a greater number of MDR positive possibly HTLV-I expressing cells. This possibility would also argue in favour of a basal level of HTLV virus expression in the PBMC population from HTLV-I infected individuals regardless of disease status and suggests that HTLV-I is a chronic

infection. Such arguments can also be supported by the fact that chronically active CTL responses to tax (Parker *et al.*, 1992 and 1994) and low amounts of HTLV-I RNA (Kinoshita *et al.*, 1989; Gessain *et al.*, 1991b; Cho *et al.*, 1995) can be found within the PBMC of HTLV-I infected individuals regardless of disease status. It has been shown that HTLV-I tax is able to direct the transcription from the mdr-1 gene promoter *in vitro* (see section 4.5.3 and figure 4.21). Thus it may be argued that a constitutive level of tax expression in a population of HTLV-I infected T-cells may upregulate mdr-1 gene expression in these cells. However, despite several reports to the contrary it is still generally believed that HTLV-I genes, including tax, are not expressed at significant levels in ATL cells *in vivo* (e.g. Franchini *et al.*, 1984). Hence, the exact molecular mechanisms in which tax mediates the leukaemogenic process is still unclear (see chapter 1, section 1.5) and thus the role of HTLV in upregulating MDR activity in infected cells is similarly uncertain. Although it has been shown that their is a significant number of active MDR$^+$ cells in the periphery of HTLV-I infected individuals, the data presented in this thesis cannot definitively prove that they are HTLV infected or express tax. Indeed, cell sorting of the high and low efflux MDR cells and quantitative HTLV PCR analysis argues against this, with HTLV proviruses being found at the same level in both populations (see section 4.4.4). Similarly examination of several HTLV-I transformed and tax expressing cell lines have shown the absence of mdr-1 gene expression and MDR activity (see section 4.3). However, it should be noted that all these cell lines were artificially derived from normal PBMCs transformed by co-culture with HTLV-I infected donor cells *in vitro*, and may not accurately reflect the situation *in vivo*.

Previous studies have shown by *in situ* hybridisation and PCR analysis of PBMCs from HTLV infected subjects that the number of HTLV-I expressing cells is lower than the total number of HTLV proviral DNA containing cells (Cho *et al.*, 1995; Ohshima et al., 1996). Hence, one possible explanation of the quantitative PCR results could be that the high effluxing MDR cell population may consist of the HTLV-I provirus

positive and HTLV-I expressing (tax?) T-cells which are capable of inducing mdr-1 gene transcription, PGP expression and MDR efflux. The low effluxing cell population would then consist of the HTLV-I provirus positive but non-expressing T-cells which may not be able to induce mdr-1 transcription, PGP expression or an MDR efflux phenotype. The result would also show a HTLV-I proviral DNA content in both the high and low R123 efflux cell populations as observed. If this were the case then the implications for therapy would be that the non-HTLV expressing cells could be eliminated by conventional chemotherapy treatment but the HTLV expressing cells may become drug resistant. It may be that the use of HTLV proviral DNA content alone may not be an appropriate probe for co-labelling studies. The detection of HTLV-I expression (e.g. tax mRNA by RT-PCR analysis) in MDR cells may prove to be a more useful probe in such studies.

It may be postulated that upregulation of mdr-1 gene expression and/or PGP activities may occur by activation of cells in the absence of HTLV-I infection. The mitogenic stimulation of mdr-1 gene expression and R123 dye efflux of fresh PBMCs with both PHA and HTLV-I expressing C91/PL cells *in vitro* was demonstrated in section 4.5.1 and 4.5.2. The exogenous activation of cells in the periphery by other HTLV-I infected cells in the absence of infection by mitogenic stimulation and extracellular cytokine effects have been long suggested and implicated in disease status (see chapter 1). Such enhancements of mdr-1 gene expression in the absence of HTLV-I infection would also support the finding of no differences in HTLV-I proviral load between the high and low efflux cell populations. The high effluxing cell populations may contain a significant number of activated MDR positive but HTLV-I provirus negative cells. This mechanism of MDR activation seems likely as the number of HTLV-I expressing cells is suggested to be low, up to 30 % (Ohshima *et al.*, 1996), but the number of MDR efflux positive cells relatively high between 28.8 to 55.3 % of the PBMC population. Hence, the larger number of MDR positive cells cannot be fully accounted for by HTLV-I expressing cells alone and may comprise of a mixture with activated PBMCs.

Thus a model may be speculated upon whereby modulation of mdr-1 gene expression may occur through exogenous cell activation mechanisms in addition to tax trans-activation. Therefore the enhanced mdr-1 gene expression clearly observed in HTLV-I infected individuals may be related to both cellular HTLV-I protein expression and cellular activation.

Although a significant population MDR cells can be demonstrated within PBMCs from HTLV-I infected subjects the possible involvement of HTLV infection and expression in these cells was not resolved. Similarly, the observation that tax can trans-activate a 1kb 5' MDR promoter *in vitro* does not necessarily prove that tax may be mediating a similar effect *in vivo*. The results presented in this thesis may also be explained by factors other than that described for HTLV. It may be that the MDR cell populations are activated T-cells resulting from hyperimmune responses to HTLV. Indeed, the chronically activated CTLs against tax which was described earlier (Parker *et al.*, 1992 and 1994) may be the MDR$^+$ population. If this case were to be the case then the MDR cells would not necessarily be HTLV positive and the use to MDR inhibitors in chemotherapy would not be warranted. Hence, further investigation of the MDR cell populations within the PBMCs of HTLV-I infected subjects is required to determine the impact of HTLV in drug resistance. In order to test these hypothesises it would be necessary to assay the high MDR effluxing cells using association markers other than HTLV-I proviral load. By correlating MDR$^+$ cells with leukaemic cell surface markers it may be possible to determine a link, if any, between them. This could be done with dual colour FACScan analysis using cellular activation surface markers such as HLA-DR or IL-2R, which are commonly found on ATL cells (Hattori *et al.*, 1981), in conjunction with R123 efflux assays or MRK-16. Further typing of these cell populations into CD4 and CD8 T-cell subsets may also help determine a role of HTLV in MDR, as ATL cells are typically CD3$^+$CD4$^+$CD8$^-$ (Hattori *et al.*, 1981). Similarly, cell sorting of MDR cell populations in conjunction with quantitative RT-PCR analysis for HTLV-I mRNA (probably tax) may shed light upon the involvement of HTLV

expression in MDR *in vivo*. Finally, the use of *in-situ* hybridisation techniques may also prove useful in co-localising tax and mdr-1 mRNA expression.

The MDR assay results demonstrate the presence of a significant number of circulating MDR efflux positive cells in the periphery of HTLV-I infected subjects which is closely associated with the enhanced expression of the mdr-1 gene and PGP. Cell population analysis demonstrated the high efflux MDR population to consisted of $CD3^+$ T-cells. Analysis of mdr-1 gene expression *in vitro* also suggests a possible mechanism of mdr-1 upregulation by intracellular tax trans-activation and HTLV induced cellular activation via modulation of cell signalling pathways. The suggested mechanisms of enhancement of mdr-1 gene expression by HTLV-I is shown in figure 4.26. However, without direct evidence linking HTLV infection/expression with mdr-1 gene activation *in vivo*, the implications for the treatment of HTLV-I infected patients remains unclear. If a direct link were established, the presence of a significant number of cells with a MDR phenotype in HTLV-I infected subjects may imply a poor prognosis for conventional cancer chemotherapy to such individuals. These HTLV infected cells would be inherently drug resistant and upon the start of chemotherapy would be quickly selected for and would result in only a very short period before relapse. Previous investigations into other systemic haematological cancers such as acute myeloid leukaemia (AML) have shown P-glycoprotein associated MDR to be an unfavourable prognostic factor. Several studies have demonstrated the overexpression of PGP in AML at diagnosis to confer a poor prognosis in response to chemotherapy, resulting in lower remission rates, earlier times of death and shorter overall disease free survival times when compared to AML without PGP expression (Kuwazuru *et al.*, 1990b; Sato *et al.*, 1990; Zhou *et al.*, 1992). Hence, the discovery of MDR phenotypes in blood lymphocytes from HTLV-I infected individuals regardless of disease status or type may predict drug resistance disease and a poor response to chemotherapy. The use of traditional chemotherapy regimes such as COP, VEMP, VEPA, CHOP or MACOP-B

combinations in HTLV-I associated disease treatment becomes invalid as most of the drugs used in these combinations are substrates for PGP efflux.

The presence of PGP mediated MDR in HTLV-I infected cells suggest an alternative course of treatment for HTLV-I disease in which the MDR phenotype itself is a target. The circumvention of cellular MDR would allow the use and enhance the efficacy of chemotherapy resulting in higher complete remission rates and an improved prognosis. Studies using PGP efflux inhibitors on haematological cancers such as AML and multiple myeloma (MM), which are known to posses MDR phenotypes, have shown encouraging results. PGP inhibitors verapamil (Tsuro *et al.*, 1981) and cyclosporin A (CSA; Twentyman, 1992) have both been used in phase I or II clinical trials for the treatment of AML and MM in combination with cytotoxic drugs. High doses of verapamil was has been used to treat refractory MM (Durie *et al.*, 1988) and lymphoma (Miller *et al.*, 1991) resulting in enhanced complete remission rates. CSA has been effectively used to treat both AML (Sonnevled *et al.*, 1990) and MM (Sonneveld *et al.*, 1992) refractory patients which resulted in a significant reduction in the number of PGP positive cells and enhanced responses to chemotherapy. However, both verapamil and CSA were limited in their effectiveness due to their dose dependant toxicities and side effects. Verapamil was noted to be associated with heart dysfunction and CSA with musculoskeletal pain and hyperbilirubinaemia. The use of new, more powerful and less cytotoxic MDR inhibitors such as the CSA analogue SDZ PSC 833 (Twentyman, 1992) and VX-710 (Vertex pharmaceuticals) may provide a better effectiveness in the treatment of MDR cancers.

Figure 4.26. A schematic representation of the possible mechanisms involved in the overexpression of P-glycoprotein and the induction of multiple drug resistance phenotypes in the cells of HTLV-I infected individuals.

259
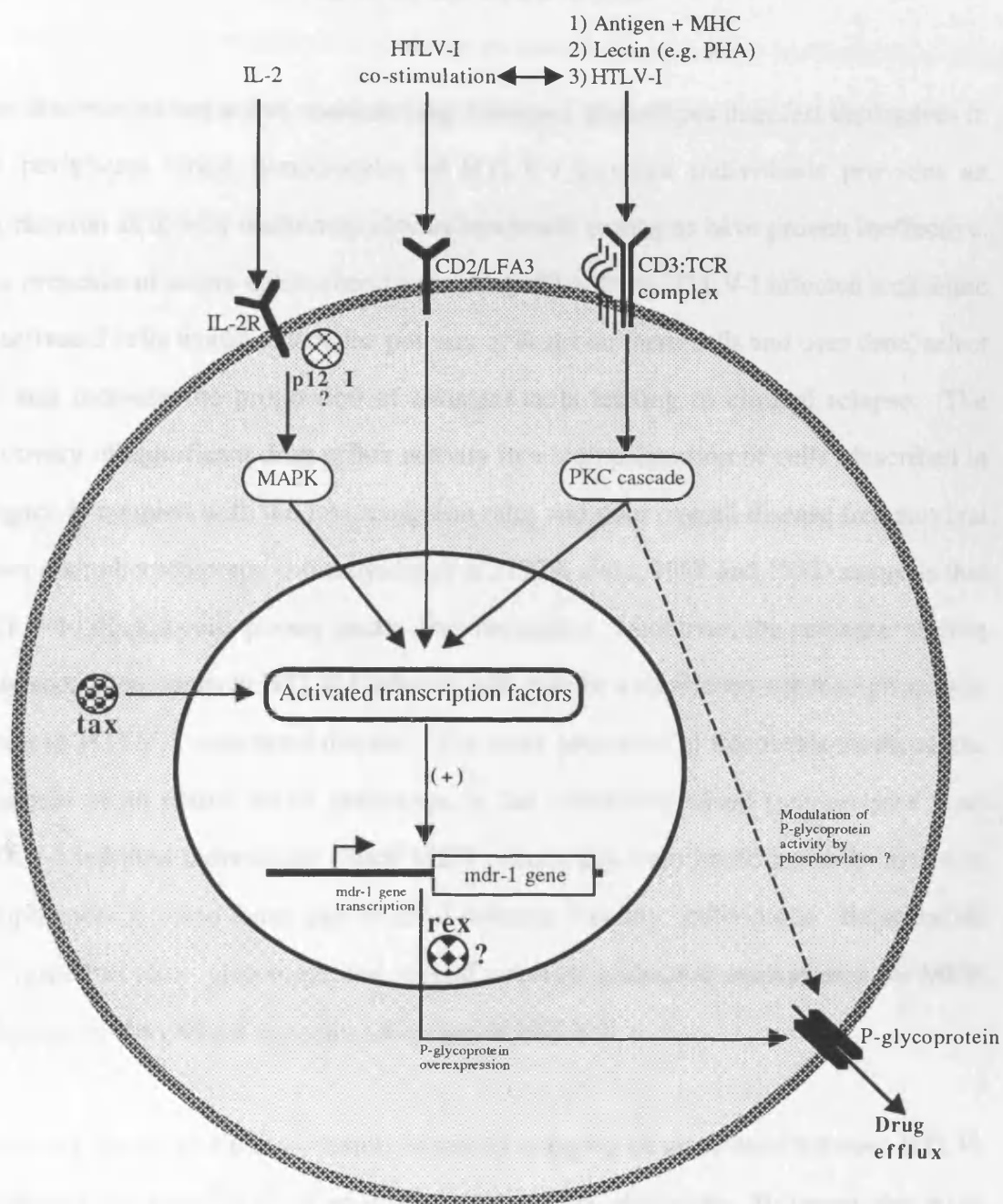
CHAPTER 5

Conclusions

The observation that active multiple drug resistance phenotypes manifest themselves in the peripheral blood lymphocytes of HTLV-I infected individuals provides an explanation as to why traditional chemotherapeutic strategies have proven ineffective. The presence of active chemotherapeutic drug efflux from HTLV-I infected leukaemic or activated cells would reduce the potency of drugs on these cells and over time, select for and increase the proportion of resistant cells leading to clinical relapse. The discovery of significant drug efflux activity in a high proportion of cells (described in chapter 4) coupled with the low remission rates and poor overall disease free survival times after chemotherapy (Shimoyama et al., 1979, 1982, 1988 and 1992) suggests that HTLV-I infected cells posses innate drug resistance. Moreover, the presence of drug resistance phenotypes in HTLV-I infected cells may be a significant negative prognostic factor in HTLV-I associated disease. The work presented in this thesis confirms the presence of an active MDR phenotype in the circulating blood lymphocytes from HTLV-I infected individuals. Such MDR phenotypes were found not to be active in lymphocytes isolated from non-HTLV-I infected "healthy" individuals. Experiments performed in vitro also suggested several potential molecular mechanisms for MDR induction by the cellular activation activities of HTLV-I.

This work shows preliminary results indirectly implying an association between HTLV-I infection and stimulation of an active cellular MDR phenotype. However, this work falls short of establishing a definite link between HTLV infection and the stimulation MDR activity within the same cells. Without this, the value of using MDR inhibitors in the treatment of HTLV-I induced disease remains uncertain. What is apparent is that further extension of this work is required to fully understand the mechanism of MDR induction within HTLV infected individuals. If a direct link could be established it may

have significant clinical implications for the way in which HTLV-I infections are treated. This may include the use of chemosensitizing drugs like those used in the treatment of other MDR associated cancers. This may provide a more effective chemotherapeutic regime to HTLV-I infected individuals than those currently available today. Such chemosensitizing compounds, although not toxic themselves, act as competitive inhibitors for drug binding or transport by PGP and when used in conjunction with conventional drugs may allow greater chemotherapeutic potentials to be achieved. Ultimately this may lead to a greatly improved prognosis for patients with HTLV-I induced disease.

References

Achong, BG., Mansell, PWA., Epstein, MA., Clifford, P. (1971). An unusual virus in cultures from human nasopharyngeal carcinoma. *J. Natl. Cancer. Inst.* **46.** 299.

Ahmad, S., Glazer, RI. (1993). Expression of the antisense cDNA for protein kinase C-alpha attenuates resistance in doxorubicin resistant MCF-7 breast carcinoma cells. *Mol. Pharmacol.* **48.** 858.

Ahmad, S., Safa, AR., Glazer, RI. (1994). Modulation of P-glycoprotein by protein kinase C in a baculovirus expression system. *Biochem.* **33.** 10313.

Ahmed, YF., Gilmartin, GM., Hanly, SM., Nevins, JR., Greene, WC. (1991). The HTLV-I rex responsive element mediates a novel form of mRNA polyadenylation. *Cell.* **64.** 727.

Akagi, Y., Shimotohno, K. (1993). Proliferative response of tax1-transduced primary T cells to anti-CD3 antibody stimulation by an interleukin-2-independent pathway. *J. Virol.* **67.** 1211.

Akizuki, S., Nakaato, O., Higuchi, Y. *et al.* (1987). Necropsy findings in HTLV-I associated myelopathy. *Lancet.* **1** 156.

Al-Shawi, MK., Senior, AE. (1993). Characterisation of the adenosine triphosphate activity of Chinese hamster P-glycoprotein. *J. Biol. Chem.* **270.** 22983.

Alexandre, C., Verrier, B. (1991). Four regulatory elements in the human c-fos promoter mediate transactivation by HTLV-I tax protein. *Oncogene.* **6.** 543.

Ames, GFL. (1986). Bacterial periplasmic transport systems: Structure, mechanism, and evolution. *Annual Review of Biochemistry.* **55.** 397.

Alexandropoulos, K., Cheng, G., Baltimore, D. (1995). Proline rich sequences that bind to Src homology domains with individual specificities. *Proc. Natl. Acad. Sci. USA.* **92.** 3110

Anderson, MG., Dynan, WS. (1994). Quantitative studies of the effect of HTLV-I tax protein on CREB proteins-DNA binding. *Nucleic Acids Res.* **22.** 3194.

Angel, P., Karin, M. (1991). The role of Jun, Fos and the AP-1 complex in cell-proliferation and transformation. *Biochem. Biophys. Acta.* **1072.** 129.

Araki, K. and the T- and B-cell malignancy study group. (1988). The third nation-wide study on adult T-cell leukemia/lymphoma (ATL) in Japan: characteristic patterns of HLA antigen and HTLV-I infection in ATL patients and their relatives. *Int. J. Cancer.* **41.** 505.

Arceci, RJ., Croop, JM., Horwitz, SB., Housman, DE. (1988). The gene encoding multidrug resistance is induced and expressed at high levels during pregnancy in the secretory epithelium of the uterus. *Proc. Natl. Acad. Sci. USA* **85.** 4350.

Arima, N., Daitoku, Y., Ohgaki, S. *et al.* (1986). Autocrine growth of interleukin 2 producing leukemic cells in a patient with adult T cell leukemia. *Blood.* **68.** 779.

Armstrong, AP., Franklin, AA., Uittenbogaard, MN., Giebler, HA., Nyborg, JK. (1993). Pleiotropic effect of the human T cell leukemia virus Tax protein on the DNA binding activity of eukaryotic transcription factors. *Proc. Natl. Acad. Sci. USA* **90.** 7303.

Asou, N., Sakai, K., Yamaguchi, K. *et al.* (1985). Autologous bone marrow transplantation in a patient with lymphoma type adult T-cell leukemia. *Rinsgou Ketsueki.* **26.** 229.

Azzaria, M., Schurr, E., Gros, P. (1989). Discrete mutations introduced in the predicted nucleotide-binding sites of the mdr1 gene abolish its ability to confer multidrug resistance. *Mol. Cell. Biol.* **9.** 5289.

Ballard, DW., Böhnlein, E., Hoffman, JA., Bogerd, HP., Dixon, EP., Franza, BR., Greene, WC. (1989). Activation of the interleukin 2 receptor a gene: regulatory role for DNA-protein interactions flanking the κB enhancer. *New Biol.* **1.** 83.

Bar-Shira, A., Panet, A., Honigman, A. (1991). An RNA secondary structure juxtaposes two remote genetic signals for human T-cell leukemia virus type I RNA 3' end processing. *J. virol.* **65.** 5165.

Baranger, AM., Palmer, CR., Hamm, MK. *et al.* (1995). Mechanism of DNA-binding enhancement by the human T-cell leukaemia virus transactivator Tax. *Nature.* **376.** 606.

Barnes, WM. (1994). PCR amplification of up to 35-kb DNA with high fidelity and high yield from l bacteriophage templates. *Proc. Natl. Acad. Sci. USA.* **91.** 2216.

Barrand, MA., Rhodes, T., Center, MS., Twentyman, PR. (1993). Chemosensitisation and drug accumulation effects of cycosporin A, PSC833 and verapamil in human MDR large cell lung cancer cells expressing a 190 k membrane protein distinct from P-glyocprotein. *Eur. J. Cancer.* **29A.** 408.

Barre-Sinoussi, F., Chermann, JC., Rey, F., *et al.* (1983). Isolation of a T-lymphotrophic retrovirus from a patient at risk of acquired immune deficiency syndrome (AIDS). *Science.* **220.** 868

Bastian, I., Gardner, J., Webb, D., Gardner, I. Isolation of a human T-lymphotropic virus type I strain from australian aboriginals. *J. Virol.* **67.** 843.

Bates, SE., Lee, JS., Dickstein, B *et al.* (1993). Differential modulation of P-glycoprotein transport by protein kinase inhibition. *Biochem.* **32.** 9156.

Batist, G., Tulpule, A., Sinha, BK. et al. (1986). Overexpression of a novel anionic glutathione transferase in multidrug-resistant human breast cancer cells. *J. Biol. Chem.* **261.** 15544.

Beck, WT., Mueller, TJ., Tanzer, LR. (1979). Altered surface membrane glycoprotein in vinca alkaloid-resistant human leukaemic lymphoblasts. *Cancer Res.* **39.** 2070.

Beck, WT., Cirtain, M. (1982). Continued expression of vinca alkaloid resistance by CCRF-CEM cells after treatment with tunicamycin or pronase. *Cancer Res.* **42.** 184.

Beck, WT., Qian, XD. (1992). Photoaffinity substrates for P-glycoprotein. *Biochem. Pharmacol.* **43.** 89.

Bell, DR., Gerlach, JH., Kartner, N., Buick, RN., Ling, V. (1985). Detection of P-glycoprotein in ovarian cancer: A molecular marker associated with multidrug resistance. *J. Clin. Oncol.* **3.** 311.

Béraud, C., Lombard-Pletet, G., Michal, Y., Jalinot, P. (1991). Binding of the HTLV-I tax transactivator to the inducable 21 bp enhancer is mediated by the cellular factor HEB1. *EMBO J.* **10.** 3795.

Berneman, ZN., Gartenhaus, RB., Reitz, MS jr. *et al.* (1992). Expression of alternatively spliced human T-lymphotrophic virus type-I pX mRNA in infected cell lines and in primary uncultured cells from patients with adult T-cell leukemia/lymphoma and healthy carriers. *Proc. Natl. Acad. Sci. USA.* **89.** 3005.

Bhat, NK., Thompson, CB., Lindsten, T. *et al.* (1990). Reciprocal expression of human ETS1 and ETS2 genes during T-cell activation: Regulatory role for the protooncogene ETS1. *Proc. Natl. Acad. Sci. USA.* **87.** 3723.

Bhushan, A., Abramson, R., Chiu, JF., Tritton, TR. (1992). Expression of c-fos in human and murine multidrug-resistant cells. *Molecular pharmacology.* **42.** 69.

Black, AC., Nimers, SD., Chen, ISY., Rosenblatt JD. (1990). The effects of tax and rex proteins of HTLV-I/-II on viral and cellular gene regulation. *UCLA Symposium on Human Retroviruses* **119.** 33.

Blattner, WA., Kalyanaraman, VS., Robert-Guroff, M. *et al.* (1982). The human type-C retrovirus HTLV in blacks from the Caribbean region and relationship to adult T-cell leukemia/lymphoma. Int. J. Cancer. **30.** 257.

Blattner, WA. (1989). Retroviruses in viral infection of human epidemiology and control. In *Retroviruses*. 545. New York: Plenum Press.

Blattner, WA., Gallo, RC. (1994). Epidemiology of HTLV-I and HTLV-II infection. In *Adult T-cell leukemia*. 45. Oxford: Oxford University Press.

Blobe, GC., Sachs, CW., Khan, WA., et al. (1993). Selective regulation of expression of Protein Kinase C (PKC) isoenzymes in multidrug resistant MCF-7 cells. *J. Biol. Chem.* **268**. 658.

Boettiger, D. (1979). Animal virus pseudotypes. *Prog. Med. Virol.* **25**. 37.

Bogerd, HP., Huckaby, GL., Ahmed, YF., Hanly, SM., Greene, WC. (1991). The type 1 human T-cell leukemia virus (HTLV-I) rex trans-activator binds directly to the HTLV-I rex and the human immunodeficiency virus type I response elements. *Proc. Natl. Acad. Sci. USA.* **88**. 5704.

Bogerd, HP., Fridell, RA., Madore, S., Cullen, BR. (1995). Identification of a novel cellular cofactor for the Rev/Rex class of retroviral regulatory proteins. *Cell.* **82**. 485.

Böhnlein, E., Lowenthal, JW., Siekevitz, M. et al. (1988). The same inducible nuclear proteins regulates mitogen activation of both interleukin-2 receptor alpha gene and type I HIV. *Cell.* **53**. 827.

Bolivar, F., Rodriguez, RL., Greene, PJ. et al. (1977). Construction and characterisation of new cloning vehicles. *Gene.* **2**. 95.

Boshrat, M., Weber, F., Jahn, G. et al. (1985). A very strong enhancer is located upstream of an immeadiate early gene of human cytomegalovirus. *Cell.* **41**. 521.

Bosselut, R., Duvall, JF., Gégonne, A., Bailly, M., Hemar, A., Brady, J., Ghysdael, J. (1990). The product of the c-ets-1 proto-oncogene and the related Ets2 protein act as transcriptional activators of the long terminal repeat of human T-cell leukemia virus HTLV-I. *EMBO. J.* **9**. 3137.

Bosselut, R., Lim, F., Romond, PC., Frampton, J., Brady, J., Ghysdael, J. (1992). Myb protein binds to multiple sites in the human T cell lymphotrophic virus type I long terminal repeat and transactivates LTR-mediated expression. *Virology.* **186**. 764.

Bourhis, J., Goldstein, LJ., Riou, G., Pastan, I., Gottesman, MM., Bernard, J. (1989). Expression of a human multidrug resistance gene in ovarian carcinomas. *Cancer Res.* **49**. 5062.

Brady, J., Jeang, KT., Duvall, J., Khoury, G. (1987). Identification of p40x-responsive regulatory sequences within the human T-cell leukemia virus type-I lon terminal repeat. *J. Virol.* **61**. 2175.

Brauweiler, A., P. Garl, et al. (1995). A molecular mechanism for human T-cell leukemia virus latency and tax transactivation. *Journal of Biological Chemistry.* **270**. 12814.

Brew, BJ., Price, RW. (1988). Another retroviral disease of the nervous system: chronic progressive myleopathy due to HTLV-I. *New Engl. J. Med.* **318**. 1195.

Brock, J., Hipfner, DR., Neilsen, BS et al. (1995). Sequential coexpression of the multidrug resistance genes MRP and mdr1 and their products in VP-16 (etoposide)-selected H69 small cell lung cancer cells. *Cancer Res.* **55**. 459.

Burger, H., Nooter, K., Sonneveld, P. et al. (1994). High expression of the multidrug resistance associated protein (MRP) in chronic and polymorphic leukemia. *Br. J. Haematol.* **88**. 348.

Campos, L., Guyotat, D., Archimbaud, E., Calmard-Oruiol, P., Tsuro, T., Troncy, J., Treille, D., Fiere, D. (1991). Clinical significance of multidrug resistance P-glycoprotein expression on acute nonlymphoblastic leukaemia cells at diagnosis. *Blood.* **79**. 473.

Cann, A., Koyanagi, Y., Chen, ISY. (1988). High efficiency transfection of primary human lymphocytes and studies of gene expression. *Oncogene.* **3**. 123.

Cariello, NF., Swenberg, JA., Skopek, TR. (1991). Fidelity of Thermococcus Litoralis DNA polymerase (Vent) in PCR determined by denaturing gradient gel electrophoresis. *Nucl. Acid. Res.* **19**. 4193.

Cassé, H., Girerd, Y., Gazzolo, L., Duc Dodon, M. (1994). Critical involvement of the human T-cell leukemia virus type I virions mediating the viral mitogenic effect. *J. Gen. Virol.* **75**. 1909.

Cassens, S., U. Ulrich, et al. (1994). Inhibition of human T cell leukaemia virus type I long terminal repeat expression by DNA methylation: Implications for latency. *J. Gen. Virol.* **75**. 3255.

Chambers, TC., Zheng, B., Kuo, JF. (1992). Regulation by phorbol ester and protein kinase C inhibitors, and by a protein phosphatase inhibitor (okadaic acid)m of P-glycoprotein phosphorylation and relationship to drug accumulation in multidrug resistant human-KB cells. *Mol. Pharmacol.* **41**. 1008.

Chambers, TC., Pohl, J., Raynor, RL., Kuo, JF. (1993). Identification of specific sites in human P-glycoprotein phosphorylated by protein kinase C. *J. Biol. Chem.* **268**. 4592.

Chambers, TC., Pohl, J., Glass, DB., Kuo, JF. (1994). Phosphorylation by protein kinase C and cyclic AMP-dependant protein kinase of synthetic peptides derived from the linker region of human P-glycoprotein. *Biochem. J.* **299**. 309.

Chambers, TC., Germann, UA., Gottesman, MM *et al.* (1995). Bacterial expression of the linker region of human MDR1 P-glycoprotein and mutational analysis of phosphorylation sites. *Biochem.* **34**. 14156.

Chan, HSL., Thorner, PS., Haddad, G., Ling, V. (1990). Immunohistochemical detection of P-glycoprotein: Prognostic correlation in soft tissue sarcoma of childhood. *J. Clin. Oncol.* **8**. 689.

Chaudhary, PM., Roninson, IB. (1991). Expression and activity of P-glycoprotein, a multidrug efflux pump, in human hematopoietic stem cells. *Cell.* **66**. 85.

Chaudhary, PM., Roninson, IB. (1992). Activation of MDR1 (P-glycoprotein) gene expression in human cells by protein kinase C agonists. *Oncol. Res.* **4**. 281.

Chen, ISY., Quan, SG., Golde, DW. (1983). HTLV-I transforms normal human lymphocytes. *Proc. Natl. Acad. Sci. USA.* **80**. 7006.

Chen, ISY., Slamon, DJ., Rosenblatt, JD., Shah, NP., Quan, SG., Wachsman, W. (1985). The x gene is essential for HTLV replication. *Science.* **229**. 54.

Chen, CJ., Chin., JE., Ueda, K., Clark, D., Pastan, I. *et al.* (1986). Internal duplication and homology with bacterial transport proteins in the mdr1 (P-glycoprotein) gene from multidrug-resistant human cells. *Cell.* **47**. 381.

Chen, CJ., Clark, D., Ueda, K., Pastan, I., Gottesman, MM., Ronninson, IB. (1990). Genomic organization of the human multidrug resistance (MDR1) gene and origin of P-glycoproteins. *J. Biol. Chem.* **265**. 506.

Cheng, S., Chang, SY., Gravitt, P., Respess, R. (1994). Long PCR. *Nature.* **369**. 684.

Chin, K., Tanaka, S., Darlington, G., Pastan, I., Gottesman, MM. (1990). Heat shock and arsenite increase expression of the multidrug resistance (MDR1) gene in human renal carcinoma cells. *J. Biol. Chem.* **265**. 221.

Cho, I., Sugimoto, M., Mita, S. *et al.* (1995). In vivo proviral burden and viral RNA expression in T-cell subsets of patients with human T-lymphotropic virus type-I associated myleopathy/tropical spastic paraparesis. *Am. J. Trop. Med. Hyg.* **53**. 412.

Choi, K., Frommel, TO., Stern, RK., Perez, CF., Kriegler, M., Tsuruo, T., Roninson, IB. (1991). Multidrug resistance after retroviral transfer of the human MDR1 gene correlates with P-glycoprotein density in the plasma membrane and is not affected by cytotoxic selection. *Proc. Natl. Acad. Sci. USA.* **88**. 7386.

Ciminale, V., Pavlakis, G., Derse, D., Cunningham, CP., Felber, BK. (1992). Complex splicing in the human T-cell leukemia virus (HTLV) family of retroviruses: novel mRNAs and proteins produced by HTLV type 1. *J. Virol.* **66**. 1737.

Clark, NM., Smith, MJ., Hilfinger, JM., Markowitz, DM. (1993). Activation of the human T cell leukemia virus type I enhancer is mediated by binding sites for Elf-1 and the Pets factor. *J. Virol.* **67**. 5522.

Coffin, JM. (1990). retroviridae and their replication. In: *Virology*, 2nd edition. pp1437. Raven Press Ltd.

Cole, SPC., Downes, HF, Slovak, ML. (1989). Effects of calcium antagonists on tyhe chemosensitivity of two multidrug resistant human tumor cell lines that do not overexpress P-glycoprotein. *Br. J. Cancer.* **59**. 42.

Cole, SPC., Bhardwaj, G., Gerlach, JH., Mackie, JE., Grant, CE., Almquist, KC., Stewart, AJ., Kurtz, EU., Duncan, AMV., Deelay, RG. (1992). Overexpression of a transporter gene in a multidrug-resistance human lung cancer cell line. *Science.* **258**. 1650.

Combates, NJ., Rzepka, RW., Chen, YNP., Cohen, D. (1994). NF-IL6, a member of the C/EBP family of transcription factors, Binds and trans-activates the Human MDR1 gene promoter. *J. Biol. Chem.* **269**. 29715.

Conner, LM., Oxman, MN., Brady, JN., Marriott, SJ. (1993). Twenty one base pair repeat elements influence the ability of a Gal4-Tax fusion protein to trans-activate the HTLV-I long terminal repeat. *Virology.* **195**. 569.

Coon, JS., Wang, Y., Bines, SD. et al. (1991). Multidrug resistance activity in human lymphocytes. *Hum. Immunol.* **32**. 134.

Cordon-Cardo, C., O'Brien, JP., Casal, D., Rittman-Grauer, L., Biedler, JL., Melamed, MR., Bertino, JR. (1989). Multidrug-resistance gene (P-glycoprotein) is expressed by endothelial cells at blood-brain barrier sites. *Proc. Natl. Acad. Sci. USA.* **86**. 695.

Cordon-Cardo, C., O'Brien, JP., Boccia, J. et al. (1990). Expression of a multidrug resistance gene product (P-glycoprotein) in human normal and tumor tissues. *J. Histochem. Cytochem.* **38**. 1277.

Cornwell, MM., Gottesman, MM., Pastan, I. (1986). Increased vinblastine binding to membrane vesicles from multidrug-resistant KB cells. *J. Biol. Chem.* **262**. 7921.

Cornwell, MM., Tsuruo, T., Gottesman, MM., Pastan, I. (1987). ATP-binding properties of P-glycoprotein from multidrug resistant KB cells. *FASEB J.* **1**. 51.

Cowan, KH., Batist, G., Tupule, A. et al. (1986). Similar biochemical changes associated with multidrug resistance in human breast cancer cells and carcinogen-induced resistance to xenobiotics in rats. *Proc. Natl. Acad. Sci. USA.* **83**. 9328.

Croop, JM., Raymond, M., Haber, D., Devault, A., Arceci, RJ. Gros, P., Housman, DE. (1989). The three mouse multidrug resistance (mdr) genes are expressed in a tissue-specific manner in normal mouse tissues. *Mol. Cell Biol.* **9**. 1346.

Courcoucé, AM., Pillonel, J., Lemaire, JM. et al. (1993). Seroepidemoilogy of HTLV-I/II in universal screening of blood donors in France. *AIDS.* **7**. 841.

Cullen, BR. (1986). Trans-activation of human immunodeficiency virus occurs via a bimodal mechanism. *Cell* **46**. 973.

Cullen, BR. (1991). Human immunodeficiency virus as a prototypic complex retrovirus. *J. virol.* **65**. 1053.

Cunningham, TP., Montelaro, RC., Rushlow, KE. (1993). Lentivirus envelope sequences and proviral genomes are stabilised in *Escherichia coli* when cloned in low copy-number plasmid vectors. *Gene*. **124**. 93.

Daenke, S., Nightingale, S., Cruickshank, J. K., Bangham, CRM. (1990). Sequence variants of human T-cell lymphotrophic virus type-I from patients with tropical spastic paraparesis and adult T-cell leukaemia do not distinguish neurological from leukaemic isolates. *J. Virol* **64**. 1278.

Damiani, D., Michieli, M., Michelutti, A. *et al.* (1993). Expression of multidrug resistance gene (MDR-1) in human normal leukocytes. *Haematologica*. **78**. 12.

Davies, R., Budworth, J., Riley, J., Snowden, R., Gesher, A., Gant, T. (1996). Regulation of P-glycoprotein 1 and 2 expression and protein activity in two MCF7/Dox cell line subclones. *British J. Cancer*. **73**. 307.

De Revel, T., A. Mabondzo, et al. (1993). In vitro infection of human macrophages with human T-cell leukemia virus type 1. *Blood*. **81**. 1598.

De Thé, G., Bomford, R. (1993). An HTLV-1 vaccine: Why, how and for whom?. *AIDS Res. Hum. Retroviruses*. **9**. 381.

Dearden, C., Matutes, E., Catovsky, D. (1991). Deoxycoformycin in the treatment of mature T-cell leukaemias. *Br. J. Cancer*. **64**. 903.

Delamarre, L., Pique, C., Pham, D. *et al.* (1994). Identification of functional regions in the human T-cell leukaemia virus type I SU glycoprotein. *J. Virol.* **68**. 3544.

Denesvre, C., Carrington, C., Corbin, A. *et al.* (1996). TM domain swapping of murine leukemia virus and human T-cell leukemia virus envelopes confers different infectious abilities despite similar incorporation into virions. *J. Virol.* **70**. 4380.

DeRossi, A., Aldovini, A., Franchini, G. *et al.* (1985). Clonal selectional of T lymphocytes infected by cell-free human T cell leukemi/lymphoma virus type 1: Parameters of virus integration and expression. *Virology*. **143**. 640.

Derse, D., Mikovits, J., Polianova, M. *et al.* (1995). Virions released from cells transfected with a molecular clone of human T- cell leukemia virus type I give rise to primary and secondary infections of T cells. *J. Virol.* **69**. 1907.

Deuchars, KL., Du, R., Naik, M., Evernden-Porelle, D., Karter, N. *et al.* (1987). Expression of hamster P-glycoprotein and multidrug resistance in DNA-mediated transformants of mouse LTA cells. *Mol. Cell Biol.* **7**. 718.

Duc Dodon, M., Gazzolo, L. (1987). Loss of interleukin 2 requirement for the generation of T colonies defines an early event of human T-lymphotrophic virus (HTLV-I) infection. *Blood*. **69**. 12.

Duc Dodon, M., Bernard, A., Gazzolo, L. (1989). Peripheral T-lymphocyte activation by human T-cell leukaemia virus type-1 interferes with the CD2 but not the CD3/TCR pathway. *J. virol.* **63**. 5413.

Durie, BGM., Dalton, WS. (1988). Reversal of drug-resistance in multiple myeloma with verapamil. *Br. J. Haematol.* **68**. 203.

Eastman, RD. (1984). In: Clinical Haematology. pp163. John Wright & Sons Ltd.

Endicott, JA., Ling, V. (1989). The biochemistry of P-glycoprotein-mediated multipledrug resistance. *Annu. Rev. Biochem.* **58**. 137.

Eytan, GD., Regev, R., Oren, G., Assaraf, TG. (1996). The role of transbilayer movement in multidrug resistance and its modulation. *J. Biol. Chem.* **271**. 12897.

Fairchild, CR., Kao-Shan, CS., Weng-Peng, J. *et al.* (1987). Isolation of amplified and overexpressed DNA sequences from adriamycin resistant human breast cancer cells. *Cancer Res.* **47**. 5141.

Fan, N., Gavalchin, J., Paul, B., Wells, KH., Lane, MJ., Poiesz, BJ. (1992). Infection of peripheral blood mononuclear cells and cell lines by cell-free human T-cell lymphoma/leukemia virus type I. *J. Clin. Microbiol.* **30**. 905.

Felber, BK., Hadzopoulou-Cladaras, M., Cladaras, C. *et al.* (1989). Rev protein of human immunodeficiency virus type 1 affects the stability and transport of the viral mRNA. *Proc. Natl. Acad. Sci. USA.* **86**. 1495.

Feller, N., Kuiper, CM., Lankelma, J. *et al.* (1995). Functional detection of MDR1/P170 and MRP/P190-mediated multidrug resistance in tumor cells by flow cytometry. *Br. J. Cancer.* **72**. 543.

Finbow, ME., Pitts, JD., Goldstein, DJ. *et al.* (1991). The E5 oncoprotein target: a 16 kDa channel forming protein with diverse functions. *Mol. Carcinogenesis.* **4**. 441.

Fojo, AT., Ueda, K., Slamon, DJ., Poplack, DG., Gottesman, MM., Pastan. I. (1987). Expression of a multidrug-resistance gene in human tumors and tissues. *Proc. Natl. Acad. Sci. USA.* **84**. 265.

Foley, GE., Prolet, BP., McCarthy, M. et al. (1965). Isolation and serial propagation of malignant and normal cells in semi-defined media: origins of CCRF cell lines. *Cancer Res.* **20**. 930.

Franchini, G., Wong-Staal, F., Gallo, RC. (1984). Human T-cell leukemia virus (HTLV-I) transcripts in fresh and cultured cells of proteins with adult T-cell leukemia. *Proc. Natl. Acad. Sci. USA.* **81**. 6207.

Franchini, G., Mulloy, JC., Koralnik, IL *et al.* (1993). The human T-cell leukaemia/lymphotrophic virus type I P12^{I} protein co-operates with the E5 oncoprotein and bind the 16-kilodalton subunit of the vacuolar H^{+} ATPase. *J. Virol.* **67**. 7701.

Franchini, G., Streicher, H.. (1995a). Human T-cell leukaemia virus. *Baillière's Clin. Haematol.* **8**. 131.

Franchini, G. (1995b). Molecular mechanisms of human T-cell leukemia/lymphotropic virus type I infection. *Blood.* **86**. 3619.

Franklin, AA., Kubik, MF., Uittenbogaard, MN., Brauweiler, A., Utiasincharoen, P., Matthews, MAH., Dynan, WS., Hoeffer, JP., Nyborg, JK. (1993). Transactivation by human T-cell leukemia virus tax protein is mediated through enhanced binding of activating transcription factor-2 (ATF-2) and cAMP element binding protein (CREB). *J. Biol. Chem.* **268**. 21225.

Fujii, M., Niki, T., Mori, T., Matsuda, M., Nomura, N., Seiki, M. (1991). HTLV-1 tax induces expression of various immediate early serum response genes. Oncogene. **6**. 1023.

Fujii, M., Tsuchiya, H., Chuhjo, T., Akizawa, T., Seiki, M. (1992). Interaction of HTLV-1 Tax1 with p67(SRF) causes the aberrant induction of cellular immediate early genes through CArG boxes. *Genes Dev.* **6**. 2066.

Fujii, M., Chuhjo, T., Minamino, T., Masaaki, N., Miyamoto, K., Seiki, M. (1995). Identification of the Tax interaction region of serum response factor that mediates the aberrant induction of immediate early genes through CArG boxes by HTLV-I Tax. *Oncogene.* **11**. 7.

Fujisawa, JI., Toita, M., Yoshimura, T., Yoshida, M. (1991). The indirect association of human T-cell leukemia virus tax protein with DNA results in transcriptional activation. *J. Virol.* **65**. 4525.

Fukasawa, M., Tsujimoto, H., Ishikawa, K. *et al.* (1987). Human T-cell leukemia virus type I isolates from Gabon and Ghana: Comparative analysis of proviral genomes. *Virology.* **161**. 315.

Fukuhara, S., Hinuma, Y., Gotoh, YI., Uchino, H. (1983). Chromosome aberrations in T-lymphocytes carrying adult T-cell leukemia associated antigens (ATLA) from healthy adults. *Blood.* **61**. 205.

Furukawa, K., Shiku, H. (1991). Alternatively spliced mRNA of the pX region of human T-lymphotrophic virus type I proviral genome. *FEBS letters*. **295**. 141.

Gallo, RC., Sliski, A., Wong-Staal, F. (1983). Origin of human T-cell leukemia-lymphoma virus. *Lancet*. **ii**. 962.

Gavalchin, J., Fan, N., Lane, MJ., Papsidero, L., Poiesz, B. (1993). Identification of a putative cellular receptor for HTLV-I by a monoclonal antibody, Mab 34-23. *Virology*. **194**. 1.

Gazdar, AF., Carney, DN., Bunn, PA. *et al.* (1980). Mitogen requirements for the *in vitro* propagation of cutaneous T-cell lymphomas. *Blood*. **55**. 409.

Gazzolo, L., Duc Dodon, M. (1987). Direct activation of resting T-lymphotrophic virus type-1. *Nature* **326**. 714.

Gerlach, JH., Endicott, JA., Juranka, PF., Henderson, G., Sarangi, F. *et al.* (1986). Homology between P-glycoprotein and a bacterial haemolysin transport protein suggests a model for multidrug resistance. *Nature*. **324**. 485.

Germann, UA., Chambers, TC., Ambudkar, SV. *et al.* (1996). Characterisation of phosphorylation defective mutants of human P-glycoprotein expressed in mammalian cells. *J. Biol. Chem.* **271**. 1708.

Gessain, A., Barin, F., Vernant, JC *et al.* (1985). Antibodies to human T-lymphotrophic virus type-I in patients with tropical spastic paraparesis. *Lancet*. **ii**. 407.

Gessian, A., Saal, F., Gout, O. *et al.* (1990). High human T-cell lymphotropic virus type-I proviral DNA load with polyclonal integration in peripheral blood mononuclear cells of French West Indian, Guianese and African patients with tropical spastic paraparesis. *Blood*. **75**. 428.

Gessain, A., Yanagihara, R., Franchini, G. *et al.* (1991). Highly diverent molecular variant of human T-lymphotrophic virus type I from isolated populations in Papua New Guinea and the Solomon islands. *Proc. Natl. Acad. Sci. USA*. **88**. 7694.

Gessain, A., Louie, A., Gout, O. *et al.* (1991b). Human T-cell leukemia-lymphoma virus type-I (HTLV-I) expression in fresh peripheral blood mononuclear cells from oatients with tropical spastic parapareis/HTLV-I-associated myelopathy. *J. Virol.* **65**. 1628.

Gessain, A., Gallo, RC., Franchini, G. (1992). Low degree of human T-cell leukemia/lymphoma virus type I genetic drift in vivo as a means of monitoring viral transmission and movement of ancient human populations. *J. Virol.* **66**. 2288.

Gessain, A., Boeri, E., Yanagihara, R. *et al.* (1993). Complete nucleotide sequence of a highly divergent human T-cell leukemia (lymphotropic) virus type I (HTLV-I) variant from Melanesia: genetic and phylogenetic relationship to HTLV-I strains from other geographical regions. *J. Virol.* **67**. 1015.

Gessain, A., Koralnik, IJ., Fullen, F. *et al.* (1994). Phylogenetic study of ten new HTLV-I strains from the Americas. *AIDS Res. Hum. Retro.* **10**. 103.

Giam, CZ., Xu, YL. (1989). HTLV-I Tax gene product activates transcription via pre-existing cellular factors and cAMP responsive element. *J. Biol. Chem.* **264**. 15236.

Gill, PS., Harrington, W., Kaplan, MH., Ribeiro, RC., Bennett, JM. *et al.* (1995). Treatment of adult T-cell leukemia-lymphoma with a combination of interferon alfa and zidovudine. *New England J. Med.* **332**. 1744.

Gitlin, SD., Lindholm, PF., Marriott, SJ., Brady, NJ. (1991a). Transdominant human T-cell lymphotrophic virus type-1 tax₁ mutant that fails to localise in the nucleus. *J. Virol.* **65**. 2612.

Gitlin, SD., Bosselut, R., Gégonne, A., Ghysdael, J., Brady, JN. (1991b). Sequence specific interaction of the ect1 protein with the long terminal repeat of the human T-lymphotrophic virus type I. *J. Virol.* **65**. 5513.

Gitlin, SD., Dittmer, J., Shin, RC., Brady, JN. (1993). Transcriptional activation of the human T-lymphotrophic virus type I long terminal repeat by functional interaction of tax1 and ets1. *J. virol.* **67**. 7307.

Gluzman, Y. (1981). SV40-transformed simian cells support the replication of early SV40 mutants. *Cell.* **23**. 175.

Goasguen, JE., Dossot, JM., Fardel, O., LeMee, F., LeGall, E., LeBlay, R., RePrise, PY., Cha[eron, J., Fauchet, R. (1993). Expression of the multidrug resistance-associated P-glycoprotein (p-170) in 59 cases of de-novo acute lymphoblastic leukemia: prognostic implications. *Blood.* **81**. 2394.

Goldstein, LJ., Galski, H., Fojo, AT., Willingham, MC., Lai, SL., Gazdar, A., Pirker, R., Green, A., Crist, W., Brodeur, GM., Lieber, M., Cossman, J., Gottesman, MM., Pastan, I. (1989). Expression of a multidrug resistance gene in human cancers. *J. Natl. Cancer. Inst.* **81**. 116.

Goldstein, LJ., Fojo, AT., Ueda, K., Crist, W., Green, A., Brodeur, G., Pastan, I., Gottesman, MM. (1990). Expression of the multidrug resistance, MDR1, gene in neuroblastomas. *J. Clin. Oncol.* **8**. 128.

Gotoh, YL., Sugamura, K., Himuma, Y. (1982). Healthy carriers of a human retrovirus, adult T-cell leukemia virus (ATLV); demonstration by clonal culture of ATLV-carrying T-cells from peripheral blood. *Proc. Natl. Acad. Sci. USA.* **79**. 4780.

Gottesman, MM., Pastan, I. (1988). Resistance to multiple chemotherapeutic agents in human cancer cells. *Trends Parmacol. Sci* **9**. 54.

Gottesman, MM., Pastan, I. (1993a). Biochemistry of multipledrug resistance mediated by the multidrug transporter. *Annu. Rev. Biochem.* **63**. 385.

Gottesman, MM., Currier, S., Bruggemann, E., Lelong, I., Stein, W., Pastan, I. (1993b). Current topics in membranes and transport. *San Siego: academic press.*

Grassmann, R., Dengler, C., Müller-Fleckenstein, I. *et al.* (1989). Transformation to continuos growth of primary human T lymphocytes by human T-cell leukemia virus type I X-region genes transduced by herpesvirus saimiri vector. *Proc. Natl. Acad. Sci. USA.* **86**. 3351.

Grassmann, R., Berchtold, S., Aepinus, C., Ballaun, C., Böhnlein, E., Flickenstein. (1991). In vitro binding of the human T-cell leukemia virus rex proteins to the rex-responsive element of viral transcripts. *J. virol.* **65**. 3721.

Grassmann, R., Berchtold, S., Radant, I. *et al.* (1992). Role of human T-cell leukemia virus type 1 X region proteins in immortalization of primary human lymphocytes in culture. *J. Virol.* **66**. 4570.

Gray, GS., White, M., Bartman, T., Mann, D. (1990). Envelope gene sequences of HTLV-I isolate MT-2 and its comparison to other HTLV-I inolates. *Virology.* **177**. 391.

Gros, P., Fallows, DA., Croop, JM., Housman, DE. (1986a). Chromosome-mediated gene transfer of multidrug resistance. *Mol. Cell Biol.* **6**. 3785.

Gros, P., Croop, J., Housman, DE. (1986b). Mammalian multidrug resistance gene: Complete cDNA sequence indicates strong homology to bacterial transport proteins. *Cell.* **47**. 371.

Gros, P., Ben-Neriah, Y., Croop, JM., Housman, DE. (1986c). Isolation and expression of a complementary DNA that confers multidrug resistance. *Nature.* **323**. 728.

Gius, D., Cao, X., Rauscher, III. *et al.* (1990). Transcriptional activation and repression by fos are independant functions: The C-terminus represses immediate-early gene expression via CArG elements. *Mol. Cell Biol.* **10**. 4243.

Gupta, S., Choong, KH., Tsuruo, T., Gollapudi, S. (1992a). Preferential expression and activity of multidrug resistance gene 1 product (P-glycoprotein), a functionally active efflux pump, in human CD8+ T cells: A role in cytotoxic effector function. *J. Clin. Immunol.* **12**. 451.

Gupta, S., Tsuro, T., Gollapudi, S. (1992b). Expression of multidrug resistant gene-1 (mdr-1) in human T-cell subsets. Regulation by cyclosporin a and role of protein kinase C isoforms. *Adv. Exp. Med. Biol.* **323**. 39.

Haddrick, M., Liu, ZH., Lau, A., Heaphy, S., Cann, AJ. (1996). Production of non-infectious human immunodeficiency virus-like particles which package specifically viral RNA. *J. Virol. Meth.* **61**. 89.

Hall., WW., Takahashi, H., Liu, C. *et al.* (1992). Multiple isolates and characteristics of human T-cell leukemia virus type II. *J. Virol.* **66**. 2456.

Hammes, SR., Greene, WC. (1993). Multiple arginine residues within the basic domain of HTLV-I rex are required for specific RNA binding and function. *Virology.* **193**. 41.

Hanly, SM., Rimsky, LT., Malim, MH., Kim, JH., Hauber, J., Duc Dodon, M., Le, SY., Maizel, JV., Cullen, BR. (1989). Comparative analysis of the HTLV-1 rex and HIV-1 rev trans-regulatory proteins and their RNA response elements. *Genes Dev.* **3**. 1534.

Hart, SM., Ganeshaguru, K., Lyttelton, MPA., Prentice, HG., Hoffbrand, AV., Mehta, AB. (1993). Flow cytometric assessment of multidrug resistance (MDR) phenotype in acute myeloid leukemia. *Leuk. lymphoma.* **11**. 239.

Hart, SM., Ganeshaguru, K., Hoffbrand, AV. *et al.* (1994). Expression of the multidrug resistance associated protein (MRP) in acute leukemia. *Leukemia.* **8**. 2163.

Hattori, T., Uchiyama, T., Toibana, T. *et al.* (1981). Surface phenotype of Japanses adult T-cell leukemia cells characterised by monoclonal antibodies. *Blood.* **58**. 645.

Heder, A., Paca-Uccaralertkun, S., Boros, I. (1991). Mutational analysis of the HTLV-1 trans-activator, Tax. *FEBS lett.* **292**. 210.

Hengen, P. (1994). Long and accurate PCR. *TIBS.* **19**. 341.

Hermine, O., Bouscary, D., Gessain, A., Turlure, P., Leblond, V. *et al.* (1995). Treatment of adult T-cell leukemia-lymphoma with zidivudine and interferon alfa. *New England J. Med.* **332**. 1749.

Hidaka, M., Inoue, J., Yoshida, M., Seiki, M. (1988). Post-transcriptional regulator (rex) of HTLV-1 initiates expression of viral structural proteins but suppresses expression of regulatory proteins. *EMBO J.* **7**. 519.

Higgins, CF., Hyde, SC., Mimmack, MM., Gileadi, U., Gill, DR., Gallagher, MP. (1990). Binding protein-dependent transport systems. *Journal of Bioenergetics and Biomembranes.* **22**. 571.

Higgins, CF., Gottesman, MM. (1992). Is the multidrug transporter a flippase?. *Trends Biochem. Sci.* **17**. 18.

Himes, SR., Coles, LS., Katsikeros, R., Lang, RK., Shannon, MF. (1993). HTLV-1 tax activation of the GM-CSF and G-CSF promoters requires the interaction of NF-kB with other transcription factor families. *Oncogene.* **8**. 3189.

Hino, S. (1990). Maternal-infant transmission of HTLV-1: implications for disease. *Human Retrovirol.* Raven Press, NY. 363.

Hinrichs, SH., Nerenberg, M., Reynolds, RK. *et al.* (1987). A transgenic mouse model for human neurofibromatosis. *Science.* **237**. 1340.

Hinuma, Y., Nagata, K., Hanaoka, M. *et al.* (1981). Antigen in an ATL cell line and detection of antibodies to the antigen in human sera. *Proc. Natl. Acad. Sci. USA.* **78**. 6476.

Hinuma, Y., Komoda, H., Chosa, T. *et al.* (1982). Antibodies to adult T-cell leukemia virus-associated antigen (ATLA) in sera from patients with ATL and controls in Japan: a nation-wide sero-epidemiologic study. *Int. J. Cancer.* **29**. 631.

Hirai, H., Fujisawa, J., Suzuki, T. *et al.* (1992). Transcriptional activator tax of HTLV-I binds to the NF-kB precursor p105. *Oncogene.* **7**. 1737.

Holló, Z., Homolya, L., Davies, CM. *et al.* (1994). Calcein accumulation as a fluorometric functional assay of the multidrug transporter. *Biochim. Biophys. Acta.* **1191**. 384.

Hollsberg, P., Wucherpfennig, K., Ausubel, LJ. *et al.* (1992). Characterisation of HTLV-I in vivo infected T-cell clones. IL-2 independent growth of nontransformed T cells. *J. Immunol.* **148**. 3256.

Hoshino, H., H. Esumi et al. (1983). Establishment and characterisation of 10 cell lines derived from patients with adult T-cell leukemia. *Proc. Natl. Acad. Sci. USA.* **80**. 6061.

Hoshino, H., Shimoyama, M., Miwa, N *et al.* (1983b). Detection of lymphocytes producing a human retrovirus associated with adult T-cell leukemia by syncytia induction assay. *Proc. Natl. Acad. Sci. USA.* **80**. 7337.

Hoyos, B., Ballrd, DW., Böhnlein, E., Siekevitz, M., Greene, WC. (1989). Kappa B specific DNA binding proteins: role in the regulation of human interleukin 2 gene expression. *Science.* **244**. 457.

Ichimaru, M., Ikeda, S., Kinoshita, K., Hino, S., Tsuji, Y. (1991). Mother to child transmission of HTLV-1. *Cancer Detect Prev.* **15**. 177.

Ijichi, S., Matsuda, T., Maruyama, I., Izumihara, T., Kojima, K., Nimura, T., Maruyama, Y., Sonoda, S., Yoshida, A., Osame, M. (1990). Arthritis in a human T lymphotrophic virus type 1 (HTLV-1) carrier. *Ann. Rheum. Dis.* **49**. 718.

Ijichi, S., Izumo, S., Eiraku, N. *et al.* (1993). An autoaggressive process against nystander tissues in HTLV-I-infected individuals: a possible pathomechanism of HAM/TSP. *Med. Hypotheses.* **41**. 542.

Imamura, J., Tsujimoto, A., Ohta, Y., Hirose, S., Shimotohno, K., Miwa, M., Miyoshi, I. (1988). DNA blotting analysis of human retroviruses in cerebrospinal fluid of spastic paraparesis patients; the viruses are identical to human T-cell leukemia virus type I (HTLV-I). *Int. J. Cancer.* **42**. 221.

Inaba, S., Sato, H., Okochi, K. *et al.* (1989). Prevention of transmission of human T-cell lymphotropic virus type I (HTLV-I) through transfustion, by donor screening with antibody to the virus. One year experience. *Transfustion.* **29**. 7

Inoue, J., Itoh, M., Akizawa, T., Toyoshima, H., Yoshida, M. (1991). HTLV-I rex protein accumulates unspliced RNA in the nucleus as well as in the cytoplasm. *Oncogene.* **6**. 1753.

Ishii, K., Yodoi, J., Hanaoka, M. *et al.* (1978). A hypotetraploid human T lymphoid cell line established by cell fusion. *J. Cell. Physiol.* **94**. 93.

Itoyama, Y., Minato, S., Kira, J. *et al.* (1988a). Altered subsets of peripheral blood lymphocytes in patients with HTLV-1 associated myelopathy (HAM). *Neurology.* **38**. 816.

Itoyama, Y., Minato, S., Kira, J. *et al.* (1988b). Spontaneous proliferation of peripheral blood lymphocytes increased in patients with HTLV-I-associated myleopathy. *Neurology.* **38**. 1302.

Iwasaki, Y. (1993). Human T-cell leukemia virus type-I infection and chronic myelopathy. *Brain Pathol.* **3**. 1.

Jacobson, S., Zaninovic, V., Mora, C. *et al.* (1988). Immunological findings in neurological diseases associated with antibodies to HTLV-I; Activated lymphocytes in tropical spastic paraparesis. *Ann. Neurol.* **23**. 196.

Jacobson, S., Gupta, A., Mattsin, D. *et al.* (1990). Immunological studies in tropical spastic paraparesis. *Ann. Neurol.* **27**. 129.

Jeang, KT., Widen, SG., Seemes, OJ., Wilson, SH. (1990). HTLV-I trans-activator protein, Tax, is a trans-repressor of the Human β-polymerase gene. *Science.* **247**. 1082.

References

Jeang, KT., Chiu, R., Santos, E., Kim, SJ. (1991). Induction of the HTLV-I LTR by Jun occurs through the Tax responsive 21 bp elements. *Virology.* **181.** 218.

Johnson, LV., Walsh, ML., Chen, LB. (1980). Localisation of mitochindria in living cells with rhodamine 123. *Proc. Natl. Acad. Sci. USA.* **77.** 990.

Johnshon, RT. (1987). Myleopathies and retroviral infections. *Ann. Neurol.* **21.** 113.

Juliano, RL., Ling, V. (1976). A surface glycoprotein modulating drug permeability in Chinese hamster ovary cell mutants. *Biochim. Biophys. Acta.* **455.** 152.

Kalland, KH., Langhoff, E., Bos, HJ., Gottlinger, H., Haseltine, WA. (1991). Rex dependent nucleolar accumulation of HTLV-I mRNAs. *New Biologist.* **3.** 93.

Kalyanaraman, VS., Sarngadharan, MG., Robert-Guroff, M., Miyoshi, I., Blayney, D., Golde, D., Gallo, RC. (1982). A new subtype of human T-cell leukemia virus (HTLV-11) associated with a T-cell variant of hairy T-cell leukemia. *Science.* **218.** 571.

Kanamori, H., Suzuki, N., Siomi, H. *et al.* (1990). HTLV-I p27 rex stabilises human interleukin 2 receptor a chain mRNA. *EMBO J.* **9.** 4161.

Kaplan, JE., Osame, M., Kubita, H., Igata, A., Nishitani, H., Maeda, Y., Khabbaz, RF., Janssen, RS. (1990). The risk of development of HTLV-I associated myleopathy/tropical spastic paraparesis among persons infected with HTLV-I. *J. AIDS.* **3.** 1096.

Kartner, N., Evernden-Porelle, D., Bradley, G., Ling, V. (1985). Detection of P-glycoprotein in multidrug-resistant cell lines by monoclonal antibodies. *Nature.* **316.** 820.

Kartner, N., Ling, V. (1989). Multidrug resistance in cancer. Sci. Am. **260.** 44.

Kataoka, R., Takehara, N., Iwahara, Y. *et al.* (1990). Transmission of HTLV-I by blood transfusion and its prevention by passive immunization in rabbits. *Blood.* **76.** 1657.

Katamine, S., Moriuchi, R., Yamamoto, T. *et al.* (1994). HTLV-I proviral DNA in umbilical cord of babies born to carrier mothers. *Lancet.* **343.** 1326.

Kato, S., Nishimura, J., Muta, K. *et al.* (1990). Overexpression of P-glycoprotein in adult T-cell leukaemia. *Lancet.* **336.** 573.

Khabbaz, RF., Onorato, ID., Cannon, RO., Hartley, TM., Roberts, B., Hosein, B., Kaplan, JE. (1992). Seroprevalence of HTLV-I and HTLV-II among intravenous drug users and persons in clinics for sexually transmitted diseases. *New Engl. J. Med.* **326.** 375.

Kikukawa, R., Koyanagi, Y., Hirada, S. *et al.* (1986). Differential susceptibility to the aquired immunodeficiency syndrome retrovirus in cloned cells of human leukemic T-cell line Molt-4. *J. Virol.* **57.** 1159.

Kohno, K., Sato, S., Takano, H., Matsuo, K., Kuwano, M. (1989). The direct activation of human multidrug resistance gene (MDR1) by anticancer agents. *Biochem. Biophys. Res. Comm.* **165.** 1415.

Kim, SJ., Kehrl, JH., Burton, J., Tendler, CL., Jeang, KT., Danialpour, D., Thevenin, C., Kim, KY., Sporn, MB., Roberts, AB. (1990). Transactivation of the transforming growth factor $\beta1$ (TGF-$\beta1$) gene by the human T lymphotrophic virus type 1 tax: a potential mechanism for the increased production of TGF-$\beta1$ in adult T-cell leukemia. *J. Exp. Med.* **172.** 121

Kim, JH., Kaufman, PA., Hanly, SM., Rimsky, LT., Greene, WC. (1991). Rex *trans*regulation of human T-cell leukemia virus type II gene expression. *J. virol.* **65.** 405.

Kimata, JT., Ratner, L. (1991). Temporal regulation of viral and cellular gene expression during T-lymphotrophic virus type-1 mediated lymphocyte immortalization. *J. Virol* **65.** 4398.

References

Kimata, JT., Palker, TJ., Ratner, L. (1993). The mitogenic activity of human T-cell leukemia virus type I is T-cell associated and requires the CD2/LFA-3 activation pathway. *J. virol.* **67**. 3134.

Kimata, JT., Wong, FH., Ratner, L. (1994a). CD3-dependant lymphocyte activation by human T cell leukaemia virus type I-producing T cells. *J. Gen. Virol.* **75**. 2433.

Kimata, J. T., Wong, FH., Wang, JJ. and Ratner, L. (1994b). Construction and characterisation of infectious human T-cell leukemia virus type 1 molecular clones. *Virology.* **204**. 656.

Kimata, JT., Wong, FH., Wang, JJ., Ratner, L. (1994). Construction and characterisation of infectious Human T-cell leukemia virus type 1 molecular clones. *Virology.* **204**. 656.

Kimura, I., Tsubota, T., Tada, S. *et al.* (1986). Presence of antibodies against adult T-cell leukemia antigen in the patients with chronic respiratory diseases. *Acta Medica Okayama.* **40**. 281.

Kinoshita, K., Hino, S., Amagasaki, T. *et al.*, (1984). Demonstration of adult T-cell leukemia virus antigen in milk from three seropositive mothers. *Gann. Jpn. J. Cancer Res.* **75**. 103.

Kinoshita, T., M. Shimoyama et al. (1989). Detection of mRNA for the tax1/rex1 gene of HTLV-I in fresh peripheral blood mononuclear cells of ATL patients and viral carriers, using the PCR reaction. *Proc. Natl. Acad. Sci. USA.* **86**. 5620.

Kira, J., Koyanagi, Y., Yamada, T. *et al.* (1991). Increased HTLV-I proviral DNA in HTLV-I associated myelopathy: a quantitative polymerase chain reaction study. *Ann. Neurol.* **29**. 194.

Kira, J., Itoyama, Y., Koyanagi, Y. *et al.* (1992). Presence of HTLV-I proviral DNA in central nervous system of patients with HTLV-Iassociated myelopathy. *Ann. Neurol.* **31**. 39.

Kitajima, I., Yamamoto, K., Sato, K. *et al.* (1991). Detection of HTLV-I proviral DNA and its gene expression in synovial cells in chronic inflammatory arthritis. *J. Clin. Invest.* **88**. 1315.

Komurian, F., Pelloquin, F., De Thé, G. (1981). In vivo genetic variability of human T-cell leukemia virus type I depends more upon geography than upon pathologies. *J. Virol.* **65**. 3770.

Koralnik, IJ., Gessain, A., Klotman, ME. *et al.* (1992). Protein isoforms encoded by the pX region of human T-cell leukemia/lymphotrophic virus type I. *Proc. Natl. Acad. Sci. USA.* **89**. 8813.

Koralnik, IJ., Fullen, J., Franchini, G. (1993). The p12^I, P13^{II} and p30^{II} proteins encoded by human T-cell leukemia virus type-I open reading frames I and II are localised in three different cellular compartments. *J. Virol.* **67**. 4943.

Koralnik, IJ., Mulloy, JC., Andresson, T *et al.* (1995). Mapping of the intramolecular association of the human T-cell leukaemia/lymphotrophic virus type I p12^I and the vacuolar H$^+$ ATPase 16 kDa subunit protein. *J. Gen. Virol.* **76**. 1909.

Koyanagi, Y., Itoyama, Y., Nakamura, N *et al.* (1993). In vivo infection of human T-cell leukemia virus type-I in non-T cells. *Virology.* **196**. 25.

Kozak, M. (1987). An analysis of 5'-noncoding sequences from 699 vertebrate messenger mRNAs. *Nucleic Acid. Res.* **15**. 8125.

Kramer, R., Weber, TK., Arceci, R. *et al.* (1995). Inhibition of N-linked glycosylation of P-glycoprotein by tunicamycin results in a reduced multidrug resistance phenotype. *Br. J. Cancer.* **71**. 670.

Krishnamachary, N., Center, MS. (1993). The MRP gene associated with non-P-glycoprotein multidrug resistance encodes a 190 kDa membrane bound glycoprotein. *Cancer Res.* **53**. 3658.

Kubota, R., Fujiyoshi, T., Izumo, S. *et al.* (1993). Fluctuation of HTLV-I proviral DNA in peripheral blood mononuclear cells of HTLV-I assocoated myelopathy. *J. Neuroimm.* **42**. 147.

References

Kubota, S., Hatanaka, M., Pomerantz, RJ. (1996). Nucleo-cytoplasmic redistribution of the HTLV-I rex protein: alterations by coexpression of the p21^X protein. *Virology*. **220**. 502.

Kuroda, M. J., M. Kannagi, et al. (1992). Inefficient transmission of HTLV-I to Molt-4 cells by cell-free virus and cocultivation. *Intervirology*. **34**. 202.

Kuwazuru, Y., Hanada, S., Furukawa, T. *et al.* (1990a). Expression of P-glycoprotein in adult T-cell leukemia cells. *Blood*. **76**. 2065.

Kuwazuru, Y., Yoshimura, A., Hanada, S. *et al.* (1990b). Expression of the multidrug transporter, P-glycoprotein, in acute leukemia cells and correlation to clinical drug resistance. *Cancer*. **66**. 868.

Kwano, F., Yamaguchi, K., Nishimura, H., Tsuda, H., Takatsuki, K. (1985). Variation in the clinical course of adult T-cell leukemia. *Cancer*. **55**. 851.

LaCoste, J., Petropoulos, L., Pepin, N., Hiscott, JJ. (1995). Constitutive phosphorylation and turnover of I kappa B alpha in human T-cell leukemia virus type I-infected and tax-expressing T cells. *J. Virol.* **69**. 564

Lagrenade, L., Hanchard, B., Fletcher, V., Cranston, B., Blattner, W. (1990). Infective dermatitis of Jamaican children: a marker for HTLV-1 infection. *Lancet*. **336**. 1345.

Lampidis, TJ., Munck, JN., Krishan, A., Tapiero, H. (1985). Reversal of resistance ro rhodamine inadriamycin resistant Friend leukemia cells. *Cancer Res.* **45**. 2626.

Landau, N. R., K. A. Page, et al. (1991). Pseudotyping with human T-cell leukemia virus type I broadens the human immunodeficiency virus host range. *J. Virol.* **65**. 162.

Landshultz, WH., Johnson, PF., McKnight, SL. (1988). The leucine zipper: a theoretical structure common to a new class of DNA binding proteins. *Science*. **240**. 1759.

Le, SY., Shapiro, BA., Chen, JH., Nussinov, R., Maizel, JV. (1991). RNA psudoknots downstream of the frameshift sites of retroviruses. *GATA* **8**. 191.

Lee, KAW., Masson, N. (1993). Transcriptional regulation by CREB and its relatives. *Biochim. Biophys. Acta.* **1174**. 221.

Lee, JS., Paull, K., Alvarez, M., Hose, C., Monks, A. et al. (1994). Rhodamine efflux patterns predict P-glycoprotein substrates in the national cancer insitute drug screen. *Mol. Pharmacology.* **46**. 627.

Leung, K., Nabel, GJ. (1988). HTLV-I transactivator induces interleukin-2 receptor expression through an NF-κB-like factor. *Nature*. **333**. 776.

Liberski, P., Rodgers-Jonson, PEB., Char, G., Piccardo, P., Gibbs, CJ., Gajusek, DC. (1988). HTLV-I like particles in spinal cord cells in Jamaican tropical spastic paraparesis patients. *Ann. Neurol.* **23**. 185.

Lilienbaum, A., Duc Dodon, M., Alexandre, C. *et al.* (1990). Effect of human T-cell leukemia virus type I tax protein on activation of the human vimentin gene . *J. Virol.* **64**. 256.

Lindholm, PF., Marriott, SJ., Gitlin, SD. *et al.* (1990). Induction of nuclear NF-kB DNA binding activity after exposure of lymphoid cells to soluble tax protein. *New Biol.* **2**. 1034.

Lindholm, PF., Reid, RL., Brady, JN. (1992). Extracellular tax$_1$ protein stimulates tumor necrosis factor-β and immunoglobulin kappa light chain expression in lymphoid cells. *J. Virol.* **66**. 1294.

Ling, V., Thompson, LH. (1974). Reduced permeability in CHO cells as a mechanism of resistance to chlchicine. *J. Cell. Physiol.* **83**. 103.

Ling, V., Kartner, N., Sudo, T. *et al.* (1983). The multidrug resistance phenotype in Chinese hamster ovary cells. *Cancer Treat. Rep.* **67**. 869.

Ling, LL., Keohavong, P., Dias, C., Thilly, WG. (1991). Optimization of the polymerase chain reaction with regard to fidelity: modified T7, Taq and Vent DNA polymerases. *PCR Meth. Appl.* **1**. 63.

Luciw, PA. (1996). Human immunodeficiency viruses and their replication. In: *Fields Virology.* **2**. pp1894.

Lundberg, KS., Shoemaker, DD., Adams, MW *et al.* (1991). High-fidelity amplification using a thermostable DNA polymerase isolated from pyrocuccus furiosus. *Gene.* **108**. 1.

Madden, MJ., Morrow, CS., Nakagawa, M., Goldsmith, ME., Fairchild, CR., Cowan, KH. (1993). Identification of 5' and 3' sequences involved in the regulation of transcription of the human mdr1 gene in vivo. *J. Biol. Chem.* **268**. 8290.

Malik, KTA., Even, J., Karpas, A. (1988). Molecular cloning and complete nucleotide sequence of an Adult T cell Leukaemia virus/Human T cell Leukemia virus type-1 (ATLV/HTLV-1) isolate of Caribbean origin: relationship to other members of the ATLV/HTLV-1 subgroup. *J. Gen. Virol.* **69**. 1695.

Malim, MH., Hauber, J., Le, SY. *et al.* (1989). The HIV-1 rev trans-activator acts through a strucured target sequence to activate nuclear export of unspliced viral mRNA. *Nature.* **338**. 254.

Malim, MH., McCarn, DF., Tiley, LS., Cullen, BR. (1991). Mutational definition of the human immunodeficiency virus type-1 rev activation domain. *J. Virol.* **65**. 4248.

Maniatis, T., Kee, SG., Efstraiadis, A., Kafatos, FC. (1976). Amplification and characterization of a β-globin gene synthesized *in vitro.* *Cell.* **8**. 163.

Manns, A., Blattner, WA. (1991). The epidemiology of the human T-cell lymphotrophic virus type I and type II: etiologic role in human disease. *Transfus.* **31**. 68.

Marie, JP., Zittoun, R., Sikic, BL. (1991). Multidrug resistance (mdr1) gene expression in adult acute leukemias: correlations with treatment outcome and in vitro drug sensitivity. *Blood.* **78**. 586.

Marriott, SJ., Boros, I., Duvall, JF., Brady, JN. (1989). Indirect binding of human T-cell leukemia virus type I tax1 to a responsive element in the viral long terminal repeat. *Mol. Cell. Biol.* **9**. 4152.

Marriott, SJ., Lindholm, PF., Brown, KM., Gitlin, SD., Duvall, JF., Randonovich, MF., Brady, JN. (1990). A 36-kilodalton cellular transcription factor mediates an indirect interaction of human T-cell leukemia/lymphoma virus type I tax1 with a response element in the viral long terminal repeat. *Mol. Cell. Biol.* **10**. 4192.

Marriott, SJ., Lindholm, PF., Reid, RL., Brady, JN. (1991). Soluble HTLV-I tax1 protein stimulates proliferation of human peripheral blood lymphocytes. *New Biol.* **3**. 678.

Marriott, SJ., Trinh, D., Brady, JN. (1992). Activation of interleukin 2 receptor alpha expression by extracellular tax protein: a potential role in HTLV-I pathogenesis. *Oncogene.* **7**. 1749.

Maruyama, M., Shibuya, H., Harada, H. *et al.* (1987). Evidence for aberrant activation of the interleukin-2 autocrine loop by HTLV-I-encoded p40^X and T3/Ti complex triggering. *Cell.* **48**. 343.

Matsuoka, M., Hattori, T., Chosa, T. *et al.* (1986). T3 surface molecules on adult T cell leukemia cells are modulated *in vivo.* *Blood.* **67**. 1070.

Matthews, MAH., Markowitz, RB., Dynan, WS. (1992). In vitro activation of transcription by the human T-cell leukemia virus type-I Tax protein. *Mol. Cell. Biol.* **12**. 1986.

Mayer, R., Kartenbeck, J., Buchler, M. *et al.* (1995). Expression of the MRP gene-encoding conjugate export pump in liver and its selective absence from the canalicular membrane in transport-deficient mutant hepatocytes. *J. Cell Biol.* **131**. 137.

McGrath, T., Latoud, C., Arnold, ST. *et al.* (1989). Mechanisms of multidrug resistance in HL60 cells - analysis of resistance associated membrane proteins and levels of mdr gene expression. *Biochem. Pharmacol.* **38**. 3611.

McGuire, KL., Curtiss, VE., Larson, EL., Haseltine, WA. (1993). Influence of human T-cell leukemia virus type-I tax and rex on interleukin-2 gene expression. *J. Virol.* **67**. 1590.

Merl, S., Kloster, B., Moore, J. *et al.* (1984). Efficient transformation of previously activated and dividing T lymphocytes by human T-cell leukemia-lymphoma virus. *Blood.* **64**. 967.

Messing, J., Gronenborn, B., Müller-Hill, B., Hofschnedider, PH. (1977). Filamentous coliphage M13 as a cloning vehivle: Insertion of a *Hind*III fragment of the *lac* regulatory region in M13 replicative form *in vitro*. *Proc. Natl. Acad. Sci. USA.* **74**. 3642.

Michieli, M., Giacca, M., Rento, F. *et al.* (1991). Mdr1 gene amplification in acute lymphoblastic leukemia prior to antileukaemic treatment. *Brit. J. Haematol.* **78**. 288.

Migone, TS., Lin, JX., Creseto, A *et al.* (1995). Constitutively activated Jak-STAT pathway in T-cells transformed with HTLV-I. *Science.* **269**. 79.

Miller, TP., Grogan, TM., Dalton, WS. *et al.* (1991). P-glycoprotein expression in malignant lymphoma and reversal of clinical drug resistance with chemotherapy plus high-dose verapamil. *J. Clin. Oncol.* **9**. 17.

Minato, K., Araki, K., Hanada, S. *et al.* (1991). An interim report of LSG4 treatment for advanced peripheral T-cell lymphoma. *Int. J. Hematol.* **54**. 179.

Mita, S., Sugimoto, M., Nakamura, M. *et al.* (1993). Increased human T lymphotropic virus type-I (HTLV-I) proviral DNA in peripheral blood mononuclear cells and bronchoalveolar lavage cells from Japanese patients with HTLV-I-associated myelopathy. *Am. J. Trop. Med. Hyg.* **48**. 170.

Miyamoto, Y., Yamaguchi, K., Nichimura, H. *et al.* (1985). Familial adult T-cell leukemia. *Cancer.* **55**. 181.

Miyatake, S., Seiki, M., Yoshida, M., Arai, KI. (1988). T-cell activation signals and human T-cell leukemia virus type-I encoded p40x protein activate the mouse granulocyte-macrophage colony stimulation factor gene through a common DNA element. *Mol. Cell. Biol.* **8**. 5581.

Miyoshi, I., Kubonishi, I., Yoshimoto, S. et al. (1981a). Type C virus particles in a cord T-cell line derived by co- cultivating normal human cord leukocytes and human leukaemic T cells. *Nature.* **294**. 770.

Miyoshi, I., Yoshimoto, S., Kubonishi, I. *et al.* (1981b) Transformation of normal human cord-lymphocytes by co-cultivation with a lethally irradiated human T-cell line carrying type-C virus particles. *Gann. Jpn. J. Cancer Res.* **72**. 997.

Miyoshi, I., Taguchi, H., Kubonishi, I. *et al.* (1982). Type C virus producing cell lines derived from adult T cell leukemia. *Gann Monograph on Cancer Res.* **28**. 219.

Mochizuki, M., Watanabe, T., Yamaguchi, K., Takatsuki, K., Shirao, M., Nakashima, S., Mori, S., Araki, S., Miyata, N. (1992). HTLV-1 uvetis: a distinct clinical entity caused by HTLV-1. *Jpn. J. Cancer Res.* **83**. 236.

Mochizuki, M., Tajima, K., Watanabe, T. *et al.* (1994). Human T lymphotrpic virus type I uveitis. *Br. J. Ophthalmol.* **78**. 149.

Molgaard, CA., Eisenman, PA., Ryden, LA., Golbeck, AL. (1989).. Neuro-epidemiology of human T-lymphotrophic virus type-I associated tropical spastic paraparesis. *Neuroepidemiology.* **8**. 109.

Montagne, J., Beraud, C., Crenon, I., Lombard-Platet, G., Gazzolo, L., Sergeant, A., Jalinot, P. (1990). Tax1 induction of the HTLV-I 21 bp enhancer requires cooperation between two cellular binding proteins. *EMBO J.* **9**. 1733.

References

Morgan, O., Rodgers-Johnson, P., Mora, C., Char, G. (1989). HTLV-1 and polymyositis in Jamaica. *Lancet.* (ii). 1184.

Mori, K., H. Sabe, et al. (1987). Expression of a provirus of human T cell leukaemia virus type I by DNA transfection. *J. Gen. Virol.* **68**. 499.

Müller, M., Meijer, C., Zaman, GJR. et al. (1994). Overexpression of the gene encoding the multidrug resistance-associated protein results in increased ATP-dependent glutathione S-conjugate transport. *Proc. Natl. Acad. Sci. USA.* **91**. 13033.

Mulloy, JC., Crowley, RW., Fullen, J. et al. (1996). The human T-cell leukemia/lymphotropic virus type 1 p12(I) protein binds the interleukin-2 receptor beta and gamma(c) chains and affects their expression on the cell surface. *J. Virol.* **70**. 3599.

Murai, K., Tachibana, N., Shioiri, S., Shishime, E., Okayama, A., Ishizaki, J., Tsuda, K., Mueller, N. (1990). Suppression of delayed-type hypersensitivity to PPD and PHA in elderly HTLV-1 carriers. *J. Acquir. Immune Defic. Syndr.* 3. 1006.

Murphy, EL., Figueroa, JP., Gibbs, WN. et al. (1989a). Sexual transmission of human T-lymphotrophic virus. *Ann. Intern. Med.* **111**. 555.

Murphy, EL., Hanchard, B., Figueroa, JP., Gibb, WN., Lofters, WS., Campbell, M., Goedert, JJ., Blattner, WA. (1989b). Modelling the risk of adult T cell leukemia/lymphoma in persons infected with human lymphotropic virus type I. *Int. J. Cancer.* **43**. 250.

Myoshi, I., Kubonishi, I., Yoshimoto, S et al. (1981). Detection of type C virus particles in a cord leukocytes and a human leukemic T-cells. *Nature.* **296**. 770.

Nakajima, T., Aono, H., Hasunuma, T. et al. (1993). Overgrowth of human synovial cells driven by the human T cell leukemia virus I tax gene. *J. clin. Invest.* **92**. 186.

Nam, SH., Kidokoro, M., Shida, H., Hatanaka, M. (1988). Processing of gag precursor polyprotein of HTLV-I by virus encode protease. *J. virol.* **62**. 3718.

Nam, SH., Copeland, TD., Hatanaka, M. et al. (1993). Characterisation of ribosomal frameshifting for expression of pol gene products of human T-cell leukaemia virus type I. *J. Virol.* **67**. 196.

Nerenberg, M., Minor, T., Price, J. et al. (1987). The tat gene of human T-lymphotrophic virus type 1 induces mesenchymal tumors in transgenic mice. *Science.* **237**. 1324.

Nerenberg, M. Minor, T., Price, J. et al. (1991). Transgenic thymocytes are refractory to transformation by the human T-cell leukemia virus type I tax gene. *J. Virol.* **65**. 3349.

Neyfakh, AA. (1988). Use of fluorescent dyes as molecular probes for the study of multidrug resistance. *Exp. Cell Res.* **174**. 168.

Neyfakh, AA., Serpinskaya, AS., Chervonsky, AV et al. (1989). Multidrug resistance phenotype of a sub-population of T-lymphocytes without drug selection. *Exp. Cell. Res.* **185**. 496.

Nicot, C., T. Astier-Gin. et al. (1993). Establishment of HTLV-I-infected cell lines from French, Guianese and West Indian patients and isolation of a proviral clone producing viral particles. *Virus Res.* **30**. 317.

Nishimura, Y., Yamaguchi, K., Kikokawa, T., Takatsuki, K., Imamura, Y., Fujiwara, H. (1989). Prevention of transmission of human T-cell lymphotrophic virus type I by blood transfusion by screening of donors. *Transfusion.* **29**. 372.

Nishimura, M., Adachi, A., Aikiguchi, I. et al. (1990). High ratio of HTLV-I infected cells in HTLV-I associated myelopathy. *Acta Neurol. Scand.* **81**. 209.

Nishioka, K., Maruyama, I., Sato, K. et al. (1989). Chronic inflammatory arthropathy associated with HTLV-1. *Lancet.* i. 441.

References

Nishioka, K., Nakajima, T., Hasunuma, T. *et al.* (1993). Rheumatic manifestation of human leukemic virus infection. *Rheum. Dis. Clin. North Am.* **19**. 489.

Nogae, I., Kohno, K., Kikuchi, J., Kuwano, M., Akiyama, SI. *et al.* (1989). Analysis of structural features of dihydropyridine analogs needed to reverse multidrug resistance and to inhibit photoaffinity labelling of P-glycoprotein. *Biochem. Pharmacol.* **38**. 519.

Nooter, K., Burger, H., Stoter, G. (1995). Multidrug resistance-associated protein (MRP) in haematological malignancies. *Leukaem. Lymph.* **18**. 179.

Nosaka, T., Siomi, H., Adachi, Y., Ishibashi, M., Kubota, S., Maki, M., Hatanaka, M. (1989). Nucleolar targeting signal of human T-cell leukemia virus type I rex encoded protein is essential for cytoplasmic accumulation of unspliced viral mRNA. *Proc. Natl. Acad. Sci. USA.* **86**. 9798.

Nyborg, JK., Matthews, MAH., Yucel, J., Walls, L., Golde, WT., Dynan, WS., Wachsman, W. (1990). Interaction of host cell proteins with the human T-cell leukemia virus type I transcriptional control region. *J. Biol. Chem.* **265**. 8237.

Ohno, R., Masaoka, T., Shirakawa, S. *et al.* (1993). Treatment of adult T-cell leukemia/lymphoma with MST-16, a new oral antitumor drug and a derivative of bis (2,6-dioxopiperazine). The MST-16 Study Group. *Cancer.* **71**. 2217.

Ohshima, K., Kikuchi, K., Masuda. Y. *et al.* (1992). HTLV-1 associated lymphadenopathy. *Cancer.* **69**. 239.

Ohshima, K., Suzumiya, J., Izumo, S. *et al.* (1996). Detection of human T-lymphotrophic virus type-I DNA and mRNA in the lymph nodes; using polymerase chain reaction in situ hybridisation (PCR/ISH) and reverse transcription (RT-PCR/ISH). *Int. J. Cancer.* **66**. 18.

Okamoto, T., Mori, S., Ohno, Y., Tsugane, S., Watanabe, S., Shioyama, M., Tajima, K., Miua, M., Shimotohni, K. (1990). Stochastic analysis of the carcinogenesis of adult T-cell leukemia-lymphoma. *Human Retrovirology.* New York Press, NY. 307.

Orita, S., Saiga, A., Takagi, S. *et al.* (1991). A novel alternatively spliced viral mRNA transcribed in cells infected with human T-cell leukaemia virus type I is mainly responsible for expressing p21^X protein. *FEBS letters.* **295**. 127.

Orita, S., Hironao, K., Aono, Y. *et al.* (1993). p12X mRNA is expressed as a singly spliced pX transcript from defective provirus genomes having a partial deletion of the pol-env region in human T-cell leukemia virus type-1 infected cells. *Nucl. Acid. Res.* **21**. 3799.

Osame, M., Usuku, K., Izumo, S. *et al.* (1986). HTLV-I associated myelopathy, a new clinical identity. *Lancet.* i 1031.

Osame, M. Janessen, R., Kubota, H. *et al.* (1990). Nationwide survey of HTLV-associated myleopathy in Japan: association with blood transfusion. *Ann. Neurol.* **28**. 51.

Paine, E., Gu, R., Ratner, L. (1994). Structure and expression of the human T-cell leukaemia virus type I envelope protein. *Virology.* **199**. 331.

Parker, CE., Daenke, SD., Nightingale, S., Bangham, CRM. (1992). Activated HTLV-I specific cytotoxic T cells are found in healthy seropositives as well as patients with tropical spastic paraparesis. *Virology.* **188**. 628.

Parker, CE., Nightingale, S., Taylor, GP., Weber, J. (1994). Circulating anti-tax cytotoxic lymphocytes from human T-cell leukaemia virus type-I infected poeple with and without tropical spastic paraparesis recognise multiple epitopes simultaneously. *J. Virol.* **68**. 2860.

Paskalis, H., Felber, BK., Pavlakis, GN. (1986). Cis-acting sequences responsible for the transcriptional activation of human T-cell leukemia virus type-I constitute a conditional enhancer. *Proc. Natl. Acad. Sci. USA.* **83**. 6558.

Peden, KW. (1992). Instability of HIV sequence in high copy number plasmids. *J. AIDS.* **5**. 313.

Perini, G., Wagner, S., Green, MR. (1995). Recognition of bZIP proteins by the human T-cell leukaemia virus transactivator Tax. *Nature.* **376.** 602.

Pique, C., Tursz, T., Dokhelar, MC. (1990). Mutations introduced along the HTLV-1 envelope gene result in a non-functional protein: a basis for envelope conservation. *EMBO* **13.** 4243.

Pique, C., Pham, D., Tursz, T., Dokhélar, MC. (1992). Human T-cell leukemia virus type I envelope protein maturation process: requirements for syncyium formation. *J. Virol.* **66.** 906.

Poiesz, BJ., Ruscetti, FW., Gazdar, AF., Bunn, PA., Minna, JD., Gallo, RC. (1980). Detection and isolation of type-C retrovirus particles from fresh and cultured lymphocytes of a patient with cutaneous T-cell lymphoma. *Proc. Natl. Acad. Sci. USA.* **77.** 7415.

Popovic, M., Sarin, PS., Robert-Gurroff, M., Kalyanaraman, VS., Mann, D., Minowada, J., Gallo, RC. (1983a). Isolation and transmission of Human Retrovirus (Human T-Cell Leukemia Virus). *Science* **219.** 856.

Popovic, M., Lange-Wilntzin, G., Sarin, PS. *et al.* (1983b). Transformation of human umbilical coard blood T-cells by human T-cell leukemia lymphoma virus. *Proc. Natl. Acad. Sci. USA.* **80.** 5402.

Popovic, M., Sarngadharan, MG., Read, E., Gallo, RC. (1984). Detection, isolation, and continuos production of cytopathic retroviruses (HTLV-III) from patients with AIDS and pre-AIDS. *Science.* **224,** 497.

Pozzatti, R., Vogel, J., Jay, G. (1990). The human lymphotropic virus type I tax gene can cooperate with the ras oncogene to induce neoplastic transformation of cells. *Mol. Cell. Biol.* **10.** 413.

Quan, L., Wilkinson, M. (1991). DNA fragment purification: Removal of agarose 10 minutes after electrophoresis. *Biotechniques.* **10.** 738.

Raviv, Y., Pollard, HB., Bruggemann, EP., Pastan, I., Gottesman, MM. (1990). Photosensitized labelling of a functional multidrug transporter in living drug-resistant tumor cells. *J. Biol. Chem.* **265.** 3975.

Richardson, JH., Edwards, AJ., Cruickshank, JK. *et al.* (1990). *In vivo* cellular tropism of human T-cell leukemia virus type 1. *J. virol.* **64.** 5682.

Riordan, JR., Ling, V. (1979). Purification of P-glycoprotein from plasma membrane vesicles of Chinese hamster ovary cell mutants with reduced colchicine permeability. *J. Biol. Chem.* **254.** 12701.

Robert-Guroff, M., Nakao, Y., Notake, K. *et al.* (1982). Natural antibodies to human retrovirus HTLV in a cluster of Japanese patients with adult T cell leukemia. *Science.* **215.** 975.

Rohlff, C., Glazer, RI. (1995). Regulation of multidrug resistance through the cAMP and EGF signalling pathways. *Cellular Signalling.* **7.** 431.

Roithmann, S., Pique, C., Le Cesne, A *et al.* (1994). The open reading frame I (orfI)/orfII part of the human T-cell leukemia virus type IX region is dispensable fro p40^{tax}, p27^{rex} or envelope expression. *J. Virol.* **68.** 4914.

Roman, GC., Osame, M. (1988). Identity of HTLV-I associated tropical spastic paraparesis and HTLV-I-associated myelopathy. *Lancet.* **i.** 651.

Roninson, IB. (1992). From amplification to function: The case of the MDR1 gene. *Mutat. Res.* **276.** 151.

Rosen, CA., Terwilliger, E., Dayton, A. *et al.* (1988). Intragenic cis-acting art gene-responsive sequences of the human immunodeficiency virus. *Proc. Natl. Acad. Sci. USA.* **85.** 2071.

Rosenblatt, JD., Gason, JC., Glaspy, J., Bhuta, S. (1987). Relationship between human T-cell leukemia virus-II and atypical hairy cell leukemia: a serologic study of hairy cell leukemia patients. *Leukemia*. 1. 387.

Roth, MJ., Tanese, N., Goff, SP. (1985). Purification and charcterisation of murine retroviral reverse transcriptase expressed in *Escherichia coli*. *J. Biol. Chem*. **260**. 9326.

Rous, P. (1911). A sarcoma of the fowl transmissible by an agent separable from the tumors cells. *J. exp. med*. **13**. 397.

Ruben, SM., Perkins, A., Rosen, CA. (1989). Activation of NF-kB by the HTLV-I trans-activator protein tax requires an additional factor present in lymphoid cells. *New Biol*. 1. 275.

Medappa, KC., McLean, C., Rueckert, RR. (1971). On the structure of Rhinovirus 1A. *Virology*. **44**. 259.

Saida, T., Saida, K., Funauchi, M., Nishiguchi, E., Nakajuma, M., Matsuda, D., Ohta, M., Ohta, K., Nishitani, H., Hatanaka, M. (1988). HTLV-I myelitis: isolation of virus, genomic analysis and infection in neural cell cultures. *Ann. NY. Acad. Sci*. **540**. 636.

Salahuddin, SZ., Markham, PD., Wong-Staalm F. *et al*. (1983). Restricted expression of human T-cell leukemic-lymphoma virus (HTLV) in transformed human umbilical cord blood lymphocytes. *Virology*. **129**. 51.

Sarin, PS., Rodgers-Johnson, P., Sun, DK., Thornton, AH., Morgan, OS., Gibbs, WN., Mora, C., McKhann, G., Gajdusek, DC., Gibbs, C. (1989). Comparison of the human T-cell lymphotrophic virus type-I strains from cerebrospinal fluid of a Jamaican patient with tropical spastic paraparesis with the prototype human T-cell lymphotrophic virus type I. *Proc. Natl. Acad. Sci. USA*. **86**. 2021.

Sato, H., Okichi, K. (1986). Transmission of human T-cell leukemia virus (HTLV-I) by blood transfustion: demonstration of proviral DNA in recipient's blood lymphocytes. *Int. J. Cancer*. **37**. 395.

Sato, H., Preisler, H., Day, R. *et al*. (1990). MDR1 transcript levels as an indication of resistant disease in acute myelogenous leukaemia. *Br. J. Cancer*. **75**. 340.

Sato, k., Maruyama, I., Maruyama, Y *et al*. (1991). Arthritis in patients infected with human T lymphotropic virus type I. Clinical and immunopathologic features. *Arthitis Rheum*. **34**. 714.

Scala, S., Dickstein, B., Regis, J. *et al*. (1995). Bryostatin 1 affects P-glycoprotein phosphorylation but not function in multidrug-resistant human breast cancer cells. *Clin. Cancer Res*. 1. 1581.

Schinkel, AH., Kemp, S., Dolle, M. et al. (1993). N-glycosylation and deletion mutants of the human MDR1 P-glycoprotein. *J. Biol. Chem*. **268**. 18224.

Scotto, KW., Biedler, JL., Melera, PW. (1986). Amplification and expression of genes associated with multidrug resistance in mammalian cells. *Science*. **232**. 751.

Sandler, SG., Fang, CT., Williams, AE. (1991). Human T-cell lymphotropic virus type I and II in transfustion medicine. *Transfusion Med. Rev*. **5**. 93.

Sarkadi, B., Price, EM., Boucher, RC., Germann, UA., Scarborough, GA. (1992). Expression of the human multidrug resistance cDNA in insect cells generates a high activity drug-stimulated membrane ATPase. *J. Biol. Chem*. **267**. 4854.

Schmidt, EV., Christoph, G., Zeller, R., Leder, P. (1990). The cytomegalovirus enhancer: A pan-active control element in transgenic mice. *Mol. Cell. Biol*. **10**. 4406.

Schreck, R., Baeuerle, PA. (1990). NF-κB as inducible transcriptional activator of the ganulocyte-macrophage colony stimulation factor gene. *Mol. Cell Biol*. **10**. 1281.

Seiki, M., Hatton, S., Yoshida, M. (1982). Human T-cell leukemia virus complete cloning of provirus DNA and the unique terminal structure. *Proc. Natl. Acad. Sci. USA*. **79**. 6899.

Seiki, M., Hattoti, S., Hirayama, Y., Yoshida, M. (1983). Human adult T-cell leukemia virus: complete nucleotide sequence of the provirus genome integrated in leukemia cell DNA. *Proc. Natl. Acad. Sci. USA* **80**. 3618.

Seiki, M., Eddy, R., Shows, TB., Yoshida, M. (1984). Nonspecific integration of the HTLV provirus genome into adult T-cell leukemia cells. *Nature.* **309**. 640.

Seiki, M., Inoue, JI., Hidaka, M., Yoshida, M. (1988). Two cis-acting elements responsible for posttranscriptional trans-regulation of gene expression of human T-cell leukemia virus type I. *Proc. Natl. Acad. Sci. USA.* **85**. 7124.

Seiki, M., Hikikoshi, A., Yoshida, M. (1990). The U5 sequence is a cis-acting repressive element for genomic RNA expression of human T-cell leukemia virus type I. *Virology.* **176**. 81.

Shapiro, HM. (1988). In: *Practical flow cytometry.* Alan R. Liss, Inc.

Sharma, S., Rose, D. (1995). Cloning, overexpression, purification and characterisation of the carboxyl-terminal nucleotide binding domain of P-glycoprotein. *J. Biol. Chem.* **270**. 14085.

Shea, TB. (1994). An inexpensive densitometric analysis system using a macintosh computer and a desktop scanner. *Biotechniques.* **16**. 1127.

Shen, DW., Cardarelli, C., Hwang, J., Cornwell, M., Richert, N. *et al.* (1986). Multiple drug-resistant human KB carcinoma cells independently selected for high-level resistance to colchicine, adriamycin, or vinblastine show changes in expression of specific proteins. *J. Biol. Chem.* **261**. 7762.

Shida, H., Tochikura, T., Sato, T. *et al.* (1987). Effect of the recombinant vaccinia viruses that express HTLV-I envelope gene on HTLV-I infection. *EMBO J.* **6**. 3379.

Shimotohno, K., Takahashi, Y., Shimizu, N., Gojobori, T., Golde, DW., Chen, ISY., Miwa, M., Sugimura, T. (1985). Complete nucleotide sequence of an infectious clone of human T-cell leukemia virus type-II: an open reading frame for the protease gene. *Proc Natl. Acad. Sci. USA.* **82**. 3101.

Shimotohno, K., Takano, M., Teruuchi, T., Miwa, M. (1986). Requirement of multiple copies of a 21 bp nucleotide sequence in the U3 regions of human T-cell leukemia virus type-I and type II long terminal repeats for trans-acting activation of transcription. *Proc. Natl. Acad. Sci. USA.* **83**. 8112.

Shimoyama, M. and the lymphoma study group. (1979). Combination chemotherapy with vincristine, cyclophosphamide (Endoxan), presnisolone and adriamycin (VEPA) in advanced adult non-Hodgkin's lymphoid malignancies: Relation between T-cell or non-T-cell phenotype and response. *Jpn. J. Clin. Oncol.* **9(supp)**. 397.

Shimoyama, M. and the lymphoma study group. (1982). Final results of cooperative study of VEPA (vincristine, cyclophosphamide (Endoxan), prenisolone and adriamycin) therapy in advanced non-Hodgkin's lymphoma: Relation between T- or B-cell phenotype and response. *Jpn. J. Clin. Oncol.* **12**. 227.

Shimoyama, M., Ota, K., Kikuchi, M. *et al.* (1988). Chemotherapeutic results and prognostic factors of patients with advanced non-Hodgkin's lymphoma treated with VEPA or VEPA-M. *J. Clin. Oncol.* **6**. 128.

Shimoyama, M. and the lymphoma study group. (1991). Diagnostic criteria and classification of clinical subtypes of adult T-cell leukemia-lymphoma. *Br. J. Haematol.* **79**. 428.

Shimoyama, M. (1992). Treatments of patients with adult T-cell leukemia/lymphoma. Advances in Adult T-cell leukemia and HTLV-1 research. *Japan Scientific Societies Press, Tokyo.* 43.

Shinzato, O., S. Kamihira et al. (1993). Relationship between the anti-HTLV-I antibody level, the number of abnormal lymphocytes and the viral genome dose on HTLV-I infected individuals. *Int. J. Cancer.* **54**. 208.

Shirono, K., Hattori, T., Chosa, T. *et al.* (1989). Profiles of expression of activated cell antigens on peripheral blood and lymph node cells from different clinical stages of adult T cell leukaemia. *Blood.* **73.** 1664.

Sisk, WP., Bradley, JD., Kingsley, D., Patterson, TA. (1992). Deletion of hydrophobic domains of viral glycoporteins increases the level of thier production in *Escherichia coli. Gene.* **112.** 157.

Smith, SD., Shatsky, M., Cohen, PS. *et al.* (1984). Monoclonal antibody and enzymatic profiles of human malignant T-lymphoid cells and derived cell lines. *Cancer Res.* **44.** 5657.

Smith, MR., Greene, WC. (1990). Identification of HTLV-1 tax trans-activator mutants exhibiting novel transcriptional phenotypes. *Genes Dev.* **4.** 1875.

Smith, MR., Greene, WC. (1992). Characterisation of a novel nuclear localisation signal in the HTLV-1 tax transactivator protein. *Virology.* **187.** 316.

Sobue, R., Yamauchi, M., Miyamura, K. et al. (1987). Treatment of adult T-cell leukemia with mega-dose cyclophosphamide and total body irradiation followed by allegeneic bone marrow transplantation. *Bone Marrow Transplant.* **2.** 441.

Sodroski, JG., Rosen, CA., Haseltine, WA. (1984). Transacting transcriptional activation of the long terminal repeat of human T-cell lymphotrophic viruses in infected cells. *Science.* **225.** 381.

Somerfelt, MA., Williams, BP., Clapham, PR., Solomon, E., Goodfellow, PN., Weiss, RA. (1988). Human T cell leukemia viruses use a receptor determined by human chromosome 17. *Science.* **242.** 1557.

Sonada, S. (1990). Genetic and immunologic determinants of HTLV-I associated diseases. *Human Retrovirol. Raven Press Ltd., NY.* 315

Sonneveld, P., Nooter, K. (1990). Reversal of drug resistanec by cyclosporin A in a parient with acute myelocytic leukeamia. *Br. J. Haematol.* **75.** 208.

Sonneveld, P., Durie, BGM., Lokhorst, HM. *et al.* (1992). Modulation of multidrug resistant multiple myeloma by cyclosporin. *Lancet.* **340.** 255.

Spoelstra, EC., Westerhoff, HV., Dekker, H., Lankelma, J. (1992). Kinetics of daunorubicin transport by P-glycoprotein of intact cancer cells. *Eur. J. Biochem.* **207.** 567.

Stuver, SO., Tachibana, N., Okayama, A. *et al.* (1993). Herterosexual transmission of human T-cell leukemia/lymphoma virus type I amoung married couples in southwestern Japan: an initial report of the Miyazaki cohort study. *J. Infect. Dis.* **167.** 57.

Su, IJ., Chang, IC., Cheng, AL. (1991). Expression of growth related genes and drug-resistance genes in HTLV-I-positive and HTLV-I negative post thymic T-cell malignancies. *Annals of oncology.* **2.** 151.

Sugawara, I., Kataoka, I., Morishita, Y. *et al.* (1988). Tissue distribution of P-glycoprotein encoded by a multidrug resistant gene as revealed by a monoclonal antibody, MRK16. *Cancer Res.* **48.** 1929.

Sugimoto, M., Nakashima, H., Wanatabe, S. *et al.* (1987). T-lymphocyte alveolitis in HTLV-1 associated myelopathy. *Lancet.* (ii). 1220.

Sun, SC., Elwood, J., Beraud, C., Greene, WC. (1994). Human T-cell leukemia virus type I Tax activatión of NF-kappa B/Rel involves phosphorylation and degradation of I kappa B alpha and RelA (p65)-mediated induction of the c-rel gene. *Mol. Cell. Biol.* **14.** 7377.

Suzuki, T., Hirai, H., Murakami, T., Yoshida, M. (1995). Tax protein of HTLV-1 destabilizes the complexes of NF-kappa B and- I kappa B alpha and induces nuclear translocation of NF-kappa B for transcriptional activation. *Oncogene.* **10.** 1199.

References

Tajima, K. and the T- and B-cell malignancy study group. (1990). The 4th nation-wide study of adult T-cell leukemia/lymphoma (ATL) in Japan: estimates of risk of ATL and its geographical and clinical features. *Int. J. Cancer.* **45**. 237.

Takahashi, K., Takezaki, T., Oki, T. *et al.* (1991). Inhibitory effect of maternal antibody on mother-to-child transmission of human T-lymphotropic virus type I. *Int. J. Cancer.* **49**. 673.

Take, H., Umemoto, M., Kushuara, K. *et al.* (1993). Transmission routes of HTLV-I: an analysis of 66 families. *Tpn. J. Cancer Res.* **84**. 1265.

Tanaka , YL, Zeng, H., Shiraki, H., Shida, H., Toyawa, H. (1991). Identification of a neutralization epitope on the envelope gp46 antigen of human T-cell leukemia virus type-1 and induction of neutralizing antibody by peptide immunization. *J. Immunol.* **147**. 354.

Tanimura, H., Kohno, K., Sato, S. (1992). The human multidrug resistance 1 promoter has an element that responds to serum starvation. *Biochem. Biophys. res. commun.* **183**. 917.

Tapiero, H., Munck, JN., Fourcade, A., Lamidis, TJ. (1984). Cross resistance to rhodamine 123 in adriamycin and daunorubicin resistant friend leukemia cell varients. *Cancer Res.* **44**. 5544.

Thiebaut, F., Tsuruo, T. Hamada *et al.* (1989). Immunohistochemical localisation in normal tissues of different epitopes in the multidrug transport protein p170: evidence for localization in brain capillaries and crossreacivity of one antibody with a muscle protein. *J. Histochem. Cytochem.* **37**. 159.

Thimmaiah, KN., Horton, JK., Qian, XD. et al. 1990). Structural determinants of phenoxazine type compounds required to modulate the accumulation of vinblastine and vincristine in multidrug-resistant cell lines *Cancer Commun.* **2**. 249.

Timura, K., Mikino, S., Araki, Y. *et al.* (1987). Recombinant interferon β and γ in the treatment of adult T-cell leukemia. *Cancer.* **59**. 1059.

Timura, K., Okayama, A., Koga, K *et al.* (1983). Total body irradiation as a primary treatment for adult T-cell leukemia. *Jpn J. Clin. Oncol.* **13(supp)**. 313.

Theibaut, F., Tsuruo, T., Hamada, H. *et al.* (1987). Cellular localisation of multidrug resistance gene product P-glycoprotein in normal human tissues. *Proc. Natl. Acad. Sci. USA.* **84**. 7734.

Thiebaut, F., Tsuruo, T., Hamada, H., Gottesman, MM., Pastan, I., Willingham, MC. (1989). Immunohistochemical localization in normal tissues of different epitopes in the multidrug transport protein P170: evidence for localization in brain capillaries and cross reactivity of one antibody with a muscle protein. *J. Histochem. cytochem.* **37**. 159.

Tie, F., Adya, N., Greene, WC., Giam, CZ. (1996). Interaction of human T-lymphotrophic virus type 1 tax dimer CREB and the viral 21-base-pair repeat. *J. Virol.* **70**. 8368.

Tournier, LE., Gout, O., Gassain, A. *et al.* (1987). HTLV-I, brain abnormalities on magnetic resonance imaging, and relation with multiple sclerosis. *Lancet.* **2**. 49.

Trent, JM., Callen, DF. (1991). Molecular and Cellular Biology of multiple drug resistance in Tumor cells. *New York: Plenum.* 169.

Tsuchiya, H., Fuji, M., Tanada, Y., Tozawa, H., seiki, M. (1994). Two distinct regions from a functional activation domain of the HTLV-1 trans-activator tax1. *Oncogene.* **9**. 337.

Tsuda, H., Takatsuki, K. (1986). Specific decrease in T3 antigen density in adult T cell leukemia cells: I. Flow cytometric analysis. *Br. J. Cancer.* **50**. 843.

Tsujimoto, A., Nyunoya, H., Morita, T., Sato, T., Shinotohno, K. (1991). Isolation of cDNAs for DNA-binding proteins which specifically bind to a Tax-responsive enhancer element in the long terminal repeat of human T-cell leukemia virus type I. *J. Virol.* **65**. 1420.

Tsuruo, T., Iida, H., Tsukagoshi, S., Sakurai, Y. (1981). Overcoming of voncristine resistance in P388 leukemia in ugh enhanced cytotoxicity of vincristine and vinblastine by verapamil. *Cancer Res.* **41**. 1967.

Twentyman, PR. (1992). Cyclosporins as drug resistance modifiers. *Biochem. Biopharmac.* **43**. 109.

Twentyman, PR., Rhodes, T., Rayner, S. (1994). A comparison of rhodamine 123 accumulation and efflux in cells with P-glycoprotein-mediated and MRP-associated multidrug resistance phenotypes. *Eur. J. Cancer.* **30**. 1360.

Uchiumi, T., Kohno, K., Tanimura, H., Matsuo, K., Sato, S., Uchida, Y., Kuwano, M. (1993). Involvement of protein kinase in environmental stress-induced activation of human multidrug resistance 1 (MDR1) gene promoter. *FEBS lett.* **326**. 11.

Uchiyama, T., Hori, T., Tsudo, M. *et al.* (1985). Interleukin-2 receptor (Tac antigen) expressed on adult T cell laukemia cells. *J. Clin. Invest.* **76**. 446.

Ueda, K., Cardarelli, C., Gottesman, MM., Pastan, T. (1987a). Expression of a full-length cDNA for the human 'MDR1' gene confers resistance to colchicine, doxorubicin, and vinblastine. *Proc. Natl. Acad. Sci. USA.* **84**. 3004.

Ueda, K., Pastan, I., Gottesman, MM. (1987b). Isolation and sequence of the promoter region of the human multidrug-resistance (P-glycoprotein) gene. *J. Biol. Chem.* **262**. 17432.

Ueda, K., Okamura, N., Hirai, M. *et al.* (1992). Human P-glycoprotein transports cortisol, aldosterone and dexamethasone, but not progesterone. *J. Biol. Chem.* **267**. 24248.

Umadome, H., Uchiyama, T., Hori, T. *et al.* (1988). Close association between interleukin-2 receptor mRNA expression and human T cell leukemia/lymphoma virus type I viral RNA expression in short-term cultured leukemic cells from adult T cell leukemia patients. *J. Clin. Invest.* **81**. 52.

Ushima, Y., Furuhara, S., Hattori, S. *et al.* (1981). Chromosome studies in adult T-cell leukemia in Japan: significance of trisomy 7. *Blood.* **58**. 420.

Vieira, J., Messing, J. (1982). The pUC plasmids and M13mp7 derived system for insertion mutagenesis and sequencing with synthetic universal primers. *Gene.* **19**. 259.

Vile, RG., TF. Schulz, Danos, OF. et al. (1991). A murine cell line producing HTLV-I pseudotype virions carrying a selectable marker gene. *Virology.* **180**. 420.

Wagner, S., Green, MR. (1993). HTLV-1 tax protein stimulation of DNA binding of bZIP proteins by enhancing dimerisation. *Science.* **262**. 395.

Waldmann, TA., White, JD., Goldman, CK. *et al.* (1993). The interleukin-2 receptor: a target for monoclonal antibody treatment of human T-cell lymphotrophic virus induced adult T-cell leukemia. *Blood.* **82**. 1701.

Walker, JE., Saraste, M., Runswick, MJ. *et al.* (1982). Distantly related sequences in the a- and b-subunits of ATP synthase, myosin, kinases and other ATP-requiring enzymes and a common nucleotide binding fold. *EMBO J.* **1**. 945.

Watanabe, T., Seiki, M., Yoshida, M. *et al.* (1984). ATLV (Japanese isolated) and HTLV (US isolated) are the same strain of retrovirus. *Virology.* **133**. 238.

Weaver, JL., Ine, PS., Aszalos, A., Schoenlein, PV., Currier, SJ. *et al.* (1991). Laser scanning and confocal microscopy of daunorubicin, doxorubicin and rhodamine 123 in multidrug-resistant cells. *Exp. Cell. Res.* **196**. 323.

Weichselbraun, I., Farrington, GK., Rusche, JR., Böhnlein, E., Hauber, J. (1992). Definition of the human immunodeficiency virus type 1 rev and human T-cell leukemia virus type I rex protein activation domain by functional exchange. *J. Virol.* **66**. 2583.

References

Weiss, A., Wiskocil, RL., Stobo, JD. (1984). The role of T3 surface molecules in the activation of human T cellsL A two-stimulus requirement for IL2 production reflects events occuring at a pre-translational level. *J. Immunol.* **133**. 123.

Wekerle, H., Fierz, W. (1985). T-cell approach to demyelinating diseases. *Springer semin. immunopathol.* **8**. 97.

Wucherpfennig, KW., Höllsberg, P., Richardson, JH. *et al.* (1992). T-cell activation by autologous human T-cell leukemia virus type-I infected T-cell clones. *Proc. Natl. Acad. Sci. USA.* **89**. 2110.

Xu, X., Kang, SH., Heidenreich, O. *et al.* (1995). Constitutive activation of different Jak tyrosine kinases in human T cell leukemia virus type I (HTLV-I) tax protein or virus-transformed cells. *J. Clin. Invest.* **96**. 1548.

Xu, X., Heidenreich, O., Kitajima, I. *et al.* (1996). Constitutively activated JNK is associated with HTLV-I mediated tumorigenesis. *Oncogene.* **13**. 135.

Yamada, K., Morozumi, H., Okamoto, T. (1995). LTR-directed homolgous recombination of full length HIV-1 provirus clone in recA(-) bacteria. *Arch. Virol.* **140**. 1007.

Yamaguchi, K., Takatsuki, K. (1993). Adult T-cell leukaemia-lymphoma. *Baillière's Clin. Haematol.* **6**. 899.

Yang, PH., Cohen, D., Greenburger, LM *et al.* (1990). Differential transport properties of two mdr gene products are distinguished by progesterone. *J. Biol. Chem.* **265**. 10282.

Yanish-Perrun, C., Vieira, J., Messing, J. (1985). Improved M13 phage cloning vectors and host strains: nucleotide sequences of the M13mp18 and pUC19 vectors. *Gene.* **33**. 103.

Yin, MJ., Paulssen, EJ., Seeler, JS., Gaynor, RB. (1995). Protein domains involved in both in vivo and in vitro interactions between human T-cell leukemia virus type I tax and CREB. *J. Virol.* **69**. 3420.

Yodoi, J., Takatsuki, K., Masuda, T. (1974). Two cases of T-cell chronic lymphocytic leukemia in Japan. *New Engl. J. Med.* **290**. 572.

Yoshida, M., Miyoshi, I., Hinuma, Y. (1982). Isolation and characterisation of retrovirus from cell lines of human adult T-cell leukaemia and its implication in the disease. *Proc. Natl. Acad. Sci. USA.* **79**. 2031.

Yoshida, M., Seidi, M., Yamaguchi, K. *et al.* (1984). Monoclonal integration of HTLV in all primary tumors of adult T-cell leukaemia suggests causative role of HTLV in the disease. *Proc. Natl. Acad. Sci. USA.* **81**. 2534

Yoshida, M., Osame, M., Kawai, H. *et al.* (1989). Increased replication of HTLV-I in HTLV-I-associated myelopathy. *Ann. Neurol.* **26**. 331.

Yoshimura, A., Kuwazuru, Y., Sumizawa, T., Ichikawa, M., Ikeda, S. *et al.* (1989). Cytoplasmic orientation and two-domain structure of the multidrug transporter, P-glycoprotein, demonstrated with sequence-specific antibodies. *J. Biol. Chem.* **264**. 16282.

Yoshimura, T., Fujisawa, JI., Yoshida, M. (1990). Multiple cDNA clones encoding nuclear proteins that bind to the tax-dependent enhancer of HTLV-I: All contain a leucine zipper and a basic amino acid domain. *EMBO. J.* **9**. 2537.

Yu, G., Ahmad, S., Aquino, A. *et al.* (1991). Transfection with protein kinase C alpha confers increased multidrug resistance to MCF-7 cells expressing P-glycoprotein. *Cancer Commun.* **3**. 181.

Zack, JA., Cann, AJ., Lugo, JP., Chen, ISY. (1988). HIV-1 production from infected peripheral blood T cells after HTLV induced mitogenic stimulation. *Science.* **240**. 1026.

Zaman, GJR., Versantvoort, CHM., Smit, JJM., Eijdems, WHM., DeHass, M., Smith, AJ., Broxterman, HJ., Mulder, NH., Devries, EGE, Baas, F., Borst, P. (1993). Analysis of the expression

of MRP, the gene for a new putative transmembrane drug transporter, in human multidrug resistant lung cancer cell lines. *Cancer Res.* **53**. 1747.

Zaman, GJR., Flens, MJ., Van-Leusden, MR *et al.* (1994). The human multidrug resistance-associated protein MRP is a plasma membrane drug-efflux pump. *Proc. Natl. Acad. Sci. USA.* **91**. 8822.

Zaman, GJR., Lankelma, J., Tellingen, O. *et al.* (1995). Role of glutathione in the export of compounds from cells by the multidrug-resistance associated protein. *Proc. Natl. Acad. Sci. USA.* **92**. 7690.

Zamora, JM., Pearce, HL., Beck, WT. (1988). Physical-chemical properties shared by compounds that modulate multidrug resistance in human leukemic cells. *Mol. Pharmacol.* **33**. 454.

Zhang, JT., Ling, V. (1991). Study of membrane orientation and glycosylated extracellular loops of mouse P-glycoprotein by in vitro translation. *J. Biol. Chem.* **266**. 18224.

Zhang, F., Riley, J., Gant, TW. (1996). Use of internally controlled reverse transcriptase-polymerase chain reaction for absolute quantitation of individual multidrug resistant gene transcripts in tissue samples. *Electrophoresis.* **17**. 255.

Zhao, LJ., Giam, CZ. (1991). Interaction of the human T-cell lymphotrophic virus type-I (HTLV-1) transcriptional activator tax with cellular factors that bind specifically to the 21 bp repeats in the HTLV-I enhancer. *Proc. Natl. Acad. Sci. USA.* **88**. 11445.

Zhao, LJ., Giam, CZ. (1992). Human T-cell lymphotrophic virus type I (HTLV-I) transcriptional activator, tax, enhances CREB binding to HTLV-1 21 base pair repeats by protein-protein interaction. *Proc. Natl. Acad. Sci. USA.* **89**. 7070.

Zhao, T. M., M. A. Robinson, *et al.* (1995). Characterization of an infectious molecular clone of human T-cell leukemia virus type I. *J. Virol.* **69**. 2024.

Zhou, D., Marie, JP., Suberville, A., Zittoun, R. (1992). Relevance of mdr1 gene expression in acute myeloid leukemia and comparison with different diagnostic methods. *Leukemia.* **6**. 879.

Zhu, Q., Center, MS. (1994). Cloning and sequence analysis of the promoter region of the MRP gene of HL60 cells isolated for resistance to adriamycin. *Cancer Res.* **54**. 4488.